UNIVERSITY OF TECHNOLOGY SYDNEY

Theoretical and experimental work on forward osmosis for the treatment of landfill leachate wastewater

By Ibrar Ibrar

Thesis submitted in fulfillment of the requirements for the degree of

Doctor of Philosophy

under the supervision of Dr Ali Altaee, Dr John L Zhou and Dr Vinh Nguyen

University of Technology Sydney
Faculty of Engineering and Information Technology

February 2023

Certificate of Original Authorship

I, Ibrar Ibrar declare that this thesis, is submitted in fulfilment of the requirements for the award of Doctor of Philosophy, in the School of Civil and Environmental Engineering, Faculty of Engineering and Information Technology at the University of Technology Sydney.

This thesis is wholly my own work unless otherwise referenced or acknowledged. In addition, I certify that all information sources and literature used are indicated in the thesis.

This document has not been submitted for qualifications at any other academic institution.

This research is supported by the Australian Government Research Training Program.

Signature:

Production Note:
Signature removed prior to publication.

Date: February 08/2023

Acknowledgments

To the Lord Almighty, who gave me the opportunity to work on one of the most important resources of the world “water”.

“Allah has created every living thing from water” Al-Quran [24:45]

To Dr. Ali Altaee, without his guidance this Ph.D. would not be possible. Thank you to my co-supervisor Dr. John L Zhou and Dr. Vinh Nguyen for their help and cooperation.

Thanks to the Australian government for providing the RTPS.

We would like to acknowledge the landfill leachate wastewater provided by Omid Sayyar and Hameed from Whyte Gully Resource Centre Wollongong, and Hurstville Golf Centre, Hurstville, New South Wales, Australia.

Publications (All including co-authored)

Ibrar, I., Yadav, S., Altaee, A., Hawari, A., Nguyen, V. & Zhou, J. 2020, 'A novel empirical method for predicting concentration polarization in forward osmosis for single and multicomponent draw solutions', *Desalination*, vol. 494, p. 114668.

Ibrar, I., Yadav, S., Altaee, A., Samal, A.K., Zhou, J.L., Nguyen, T.V. & Ganbat, N. 2020, 'Treatment of biologically treated landfill leachate with forward osmosis: Investigating membrane performance and cleaning protocols', *Science of The Total Environment*, vol. 744, p. 140901.

I. Ibrar, S. Yadav, N. Ganbat, A.K. Samal, A. Altaee, J.L. Zhou, T.V. Nguyen, Feasibility of H2O2 cleaning for forward osmosis membrane treating landfill leachate, Journal of Environmental Management, 294 (2021) 113024

Ibrar, I., Altaee, A., Zhou, J.L., Naji, O. & Khanafer, D. 2019, 'Challenges and potentials of forward osmosis process in the treatment of wastewater', *Critical Reviews in Environmental Science and Technology*, pp. 1-45.

Ibrar, I., Naji, O., Sharif, A., Malekizadeh, A., Alhawari, A., Alanezi, A.A. & Altaee, A. 2019, 'A Review of Fouling Mechanisms, Control Strategies and Real-Time Fouling Monitoring Techniques in Forward Osmosis', *Water*, vol. 11, no. 4, p. 695.

Yadav, S., **Ibrar, I.,** Altaee, A., Samal, A.K., Ghobadi, R. & Zhou, J. 2020, 'Feasibility of brackish water and landfill leachate treatment by GO/MoS2-PVA composite membranes', *Science of The Total Environment*, vol. 745, p. 141088.

Yadav, S., **Ibrar, I**., Bakly, S., Khanafer, D., Altaee, A., Padmanaban, V., Samal, A.K. & Hawari, A.H. 2020, 'Organic Fouling in Forward Osmosis: A Comprehensive Review', *Water*, vol. 12, no. 5, p. 1505.

Yadav, S., Saleem, H., **Ibrar, I**., Naji, O., Hawari, A.A., Alanezi, A.A., Zaidi, S.J., Altaee, A. & Zhou, J. 2020, 'Recent developments in forward osmosis membranes using carbon-based nanomaterials', *Desalination*, vol. 482, p. 114375.

Yadav, S., **Ibrar, I.,** Altaee, A., Déon, S. & Zhou, J. 2020, 'Preparation of novel high permeability and antifouling polysulfone-vanillin membrane', *Desalination*, vol. 496, p. 114759.

Book Chapters (All including co-authored)

SOLAR CO-GENERATION OF ELECTRICITY AND WATER, LARGE SCALE PHOTOVOLTAIC SYSTEMS - Desalination by Forward Osmosis: Failure, Success, and Future Expectations – I Ibrar, Daoud Khanafer, Sudesh Yadav, Salam Bakly¸ Jamshed Ali Khan, and Ali Altaee

Contents

List of Figures

List of Tables

Nomenclature

A	Water permeability constant, m/s.Pa	MNP	Magnetic nanoparticles
AHA	Aldrich Humic Acid	NOM	Natural organic matter
AL	Active layer	PA	Polyamide
B	Solute permeability coefficient, m/s	PES	Polyether sulfone
CECP	Concentrative External polarisation	PRO	Pressure retarded osmosis
BSA	Bovine Serum albumin	PS	Polysulfone
CA	Cellulose acetate	R	Rejection of solute, %
CEOP	Cake enhanced Osmotic pressure	RO	Reverse Osmosis
CFV	Cross flow velocity	RSD	Reverse salt diffusion
CP	Concentration polarisation	S	Membrane structure parameter, µm
ICP	Internal Concentration polarisation	t_s	Support layer thickness μm
CTA	Cellulose triacetate	T	Temperature, K
DICP	Dilutive internal concentration polarisation	TDS	Total dissolved Solids
D	Solute diffusion coefficient m^2/s	TFC	Thin film composite
DS	Draw solution	TOC	Total organic carbon
ECP	External concentration polarisation	UF	Ultrafiltration
EPS	Extra polymeric substances	π	Osmotic pressure, bar
FO	Forward Osmosis	σ	Reflection coefficient
Es	Specific power consumption (kWh/m^3)	n	Pump efficiency

FS	Feed side	τ	Tortuosity of the support layer
ICP	Internal concentration polarisation	ε	Porosity of the support layer
J_s	Salt flux, g/m^2 h	β	Van't Hoff coefficient
J_w	Water flux L/ m^2 h		
k	Mass transfer coefficient, m/s		
K	Salt resistivity, s/m		

Abstract

Forward osmosis (FO) membrane-based desalination has attracted tremendous attention due to its numerous advantages over pressure-driven membrane processes, particularly for treating complex wastewater. However, the process is driven by osmosis or concentration differences between the feed, and the draw solutions are hindered by concentration polarization and fouling. This research investigated the theoretical and experimental work on the forward osmosis process using landfill leachate wastewater. Landfill leachate wastewater can lead to carcinogenic effects, acute toxicity, and genotoxicity among humans if leached into the groundwater or soil. Furthermore, emerging pollutants in the landfill site can contaminate soil, turning it into contaminated land. There are strict regulations regarding the maximum limits of contaminants that must be treated before being disposed of into the environment. In countries such as Australia, the problem is further exacerbated, as long drought years and occasional strong wet spells cause faster dispersion of leachate in the surrounding areas, causing surface and underground contamination. As weather patterns become more unpredictable due to the complex climate change matrix, these leaks may become more severe and frequent. The landfill leachate collected from two sites, Whyte Gully, located in Wollongong, and Hurstville Golf course, located in Hurstville, revealed hazardous contaminants, including radioactive thorium. Successfully, FO was able to reject all the contaminants in the baseline tests. However, it was noticed that traditional chemical cleaning protocols lead to low rejection of some hazardous contaminants (Nickel, Barium, magnesium, to name a few). Therefore, we proposed a novel cleaning protocol for FO membranes fouled by landfill leachate wastewater, which has no impact on membrane rejection, saves energy with in-situ static cleaning, is low cost compared to traditional chemical protocols, can be reused over and over without discharging to the environment and has high efficiency than traditional cleaning protocols such as acid cleaning, base cleaning and cleaning with other chemical agents. In the theoretical part of this thesis, we proposed a new model for measuring concentration polarisation in forward osmosis via empirical and machine learning approaches.

Chapter 1: Introduction

1.1 Research Background

Water scarcity in the coming decades will severely affect society, ecological systems, food security, and environmental sustainability and may pose a significant threat to economic development (Distefano & Kelly 2017). It is predicted that if water is consumed at the current rate, by 2025, two-thirds of the world's population may face water shortages (WWF 2018). Therefore, water use for purposes other than sustenance (industrial processes) is of great concern (Lutchmiah, Verliefde, et al. 2014). Amongst the various methods to address water shortages are desalination, using waterless technologies in industrial processes, water storage in reservoirs, protecting wetlands, and several others. A possible alternative to alleviate global water scarcity is the reclamation and re-use wastewater (Salgot & Folch 2018) using pressure-driven or membrane-based filtration techniques.

Among the many viable wastewater treatment techniques, reverse osmosis (RO) is one of the most effective and widely used technology worldwide (Cath, Childress & Elimelech 2006a; Lee et al. 2010; Volpin et al. 2018). Despite its immense popularity, RO has several drawbacks, such as high operating costs, CO_2 emissions, brine management, irreversible membrane fouling and requirements of extensive pre-treatment (McCutcheon & Elimelech 2006a; Nguyen et al. 2018). Furthermore, RO cannot treat highly saline streams directly and is energy extensive due to high hydraulic pressures (Chung et al. 2012). RO is also not affordable due to its high capital costs (CAPEX) and operational costs (OPEX). Moreover, due to its high-energy consumption, RO can turn the water crisis into an energy crisis (Gilron 2014). Therefore, there is an urgent need to investigate cheaper, less energy-intensive and more sustainable desalination and wastewater treatment processes.

Recently, a new osmotically driven membrane process, forward osmosis (FO), has attracted tremendous interest from researchers and scientists across the globe as one of the promising membrane processes and alternatives to the RO process. The major advantage of FO over other pressure-driven membrane processes is that FO phenomena occur spontaneously and require no hydraulic pressures (Mondal, Field & Wu 2017). While tremendous research has been underway in the field of FO, a very small number of FO publications (since 2010) are on wastewater studies (**Figure 1.1**). Nevertheless, research in this field is still attracting a lot of attention due to the potential in wastewater treatment. Shortcomings of FO include membrane fouling, concentration polarisation, reverse solute diffusion, lack of highly selective membranes, selection of appropriate draw solution and most importantly, the regeneration of the draw solution (Corzo et al. 2017; Korenak et al. 2017; Lutchmiah, Verliefde, et al. 2014; McCutcheon & Elimelech 2006a; McGovern & Lienhard V 2014).

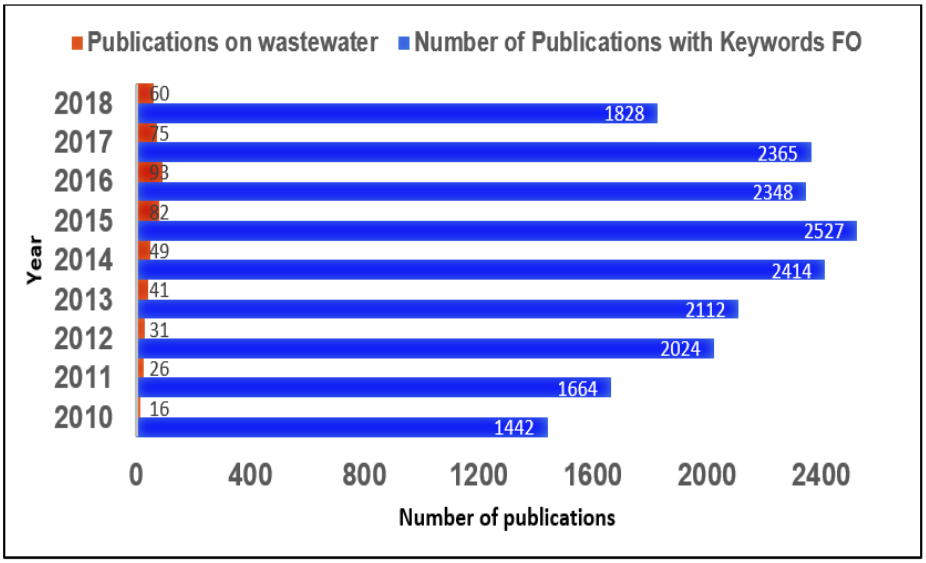

Figure 1.1: Number of FO publications since 2010 (search done using UTS library standard search toolbar)

This research will investigate concentration polarization, fouling and fouling mitigation, and optimizing the FO system for wastewater treatment. In the first part of this research, we reviewed forward osmosis fouling mechanisms, control strategies for fouling, and real-time

fouling monitoring techniques (Ibrar, Naji, et al. 2019; Yadav, Ibrar, Altaee, Déon, et al. 2020). In the second part of this research, FO was reviewed as a potential candidate for wastewater treatment, and its challenges and future potential were discussed (Ibrar, Altaee, et al. 2019). Following the two critical reviews, we proposed a novel empirical method for estimating and predicting concentration polarization levels in the forward osmosis for single and multicomponent draw solutions (Ibrar, Yadav, Altaee, Hawari, et al. 2020). The current work towards completing the objective of the thesis involved fouling and fouling mitigation in forward osmosis. Leachate wastewater was selected as a wastewater feed solution, and fouling and some novel cleaning protocols were investigated for CTA forward osmosis membrane (Ibrar, Yadav, Altaee, Samal, et al. 2020). In the current work, a thin film composite membrane is investigated. Hydrogen peroxide cleaning will be compared with another novel chemical cleaning strategy in long-term forward osmosis experiments. This coming year, the research plan is to work mainly on the draw solution side of forward osmosis, emphasising searching for novel draw solutions and the impact of draw solutions on cleaning protocols.

1.2. Research Gaps and Research Questions

Apart from the review articles in this dissertation, individual chapters address a research gap outlined in the introduction of each chapter. Each review article also had some novelty compared to the contemporary reviews in the area of the forward osmosis process. A brief outline of the research gap is given below.

- Current forward osmosis flux models for estimating concentration polarisation cannot be extended to multicomponent draw solutions since it is hard to calculate the diffusion coefficient of a mixture of draw solutions.
- The impact of physical and chemical cleaning protocols on the rejection performance of the forward osmosis membranes has not been systematically investigated.

- Hydrogen peroxide can damage CTA membranes; however, thin-film composite membranes can withstand hydrogen peroxide for a certain amount of time before breaking down. The extended exposure of thin-film composite membranes to hydrogen peroxide has not been investigated.
- Fouling in forward osmosis is generally considered reversible. However, fouling is generally irreversible during extended fouling tests with wastewater, and chemical cleaning is required. Novel chemical cleaning protocols are lacking in the forward osmosis literature.

The research questions will address these research gaps in the underlying chapters.

- Is it possible to implement a new method for concentration polarisation that can also measure the concentration polarisation for single and multicomponent draw solutions?
- Is fouling reversible in the forward osmosis process when real landfill wastewater is used as feed solution, and whether current cleaning protocols compromise rejection?
- Is it possible to develop a cleaning solution that does not compromise membrane intergry when treating real wastewater with forward osmosis?

1.3. Research Goals and objectives

The first objective of this research was to propose a novel analytical model for estimating concentration polarization levels in the forward osmosis process. The current water flux models are driven by the solution-diffusion theory; they are rather difficult to solve analytically because they depend on the membrane and flow characteristics in the forward osmosis process. For some forward osmosis applications, the mass transfer coefficient or solute resistance to diffusion, particularly with multi-component mixtures in the feed or draw solutions, would be challenging. In this research project, we proposed an alternative new empirical technique to quantify concentration polarization in the forward osmosis process that does not rely on the system's hydrodynamic conditions and flow regime. The developed numerical model is two steps method to measure internal and external concentration polarization using different sodium chloride concentrations for the draw and the feed

solutions. The main advantage of using this model is that it does not require the calculation of mass transfer coefficient and solute resistance to diffusion to determine the permeate flux through the concentration polarization layer. Our results will be compared with two widely used flux models in the literature.

The second objective of this research was to investigate fouling and cleaning protocols in forward osmosis for wastewater treatment. Leachate wastewater was used as a feed solution, and fouling was investigated under different conditions. For flux recovery, the efficiency of physical cleaning was compared with chemical cleaning. Both types of FO membranes are being investigated. The study on the CTA membrane showed that physical cleaning protocols are superior to chemical cleaning protocols in terms of flux recovery and for the sake of membrane integrity. Chemical cleaning with hydrogen peroxide can provide efficient flux recovery but damage CTA and TFC membranes. For the first time, we also investigated the tolerance of TFC membranes towards long-term exposure to hydrogen peroxide.

The third objective of this research is to evaluate a novel chemical cleaning with sodium docusate solution. Docusate is a strong surfactant used as an essential component in ear wax medical treatment. It can potentially treat organic matter and restore water flux in a fouled forward osmosis membrane better than traditional chemical cleaning methods and save energy with static cleaning.

A brief outline of the dissertation is given below.

- Chapter 1 presents the introduction, background and research gaps.
- Chapter 2 is based on the challenges and potentials of forward osmosis in wastewater treatment.
- Chapter 3 presents a review of fouling mechanisms, control strategies and real-time fouling monitoring techniques in forward osmosis. This included a comprehensive review of fouling in the forward osmosis process.
- Chapter 4 presents an empirical method for predicting concentration polarisation in forward osmosis. This included an empirical approach to measure and predict concentration polarisation in forward osmosis.
- Chapter 5 presents the treatment of biologically treated landfill leachate with forward osmosis. This included an investigation of cleaning protocols and fouling.

- Chapter 6 presents the feasibility of H_2O_2 cleaning for forward osmosis membrane treating landfill leachate
- Chapter 7 presents an evaluation of sodium docusate as an efficient, energy saving and reusable cleaning agent for fouled forward osmosis membranes
- Chapter 8 presents the conclusions, recommendations and future work.

Chapter 2 Challenges and potentials of forward osmosis process for the treatment of wastewater

This chapter provides a brief literature review of forward osmosis process for wastewater treatment, draw solutions used in the forward osmosis wastewater treatment applications, forward osmosis membranes, fouling and fouling mitigation methods. This chapter is based on the following publication.

Ibrar, I., Altaee, A., Zhou, J.L., Naji, O. & Khanafer, D. 2019, 'Challenges and potentials of the forward osmosis process in the treatment of wastewater', *Critical Reviews in Environmental Science and Technology*, pp. 1-45.

CRediT authorship contribution statement

Ibrar Ibrar: Conceptualization, Methodology, Writing - original draft. Osama Naji: Methodology, Writing - original draft, Data curation. Ali Altaee: Supervision, Writing - review & editing. John L. Zhou: Supervision, Writing - review & editing. D Khanafer: Visualization, Investigation.

2.1 Forward osmosis process

FO uses an osmotic pressure gradient to permeate water from a solution of low solute concentration (also known as feed solution or FS) through a semipermeable membrane towards a solution of high solute concentration (also known as draw solution or DS). The osmotic pressure is generated by the solution of high solute concentration or draw solution (**Figure 2.1**). On the contrary to the reverse osmosis (RO) process, the FO process uses the osmotic pressure difference ($\Delta\pi$) instead of the hydraulic pressures (ΔP) for freshwater extraction from the feed solution. The hydraulic pressure ΔP is almost zero in the FO process, which negates the need for high-pressure hydraulic pumps and duplex stainless steel tubing required by pressure-driven membrane processes such as reverse osmosis.

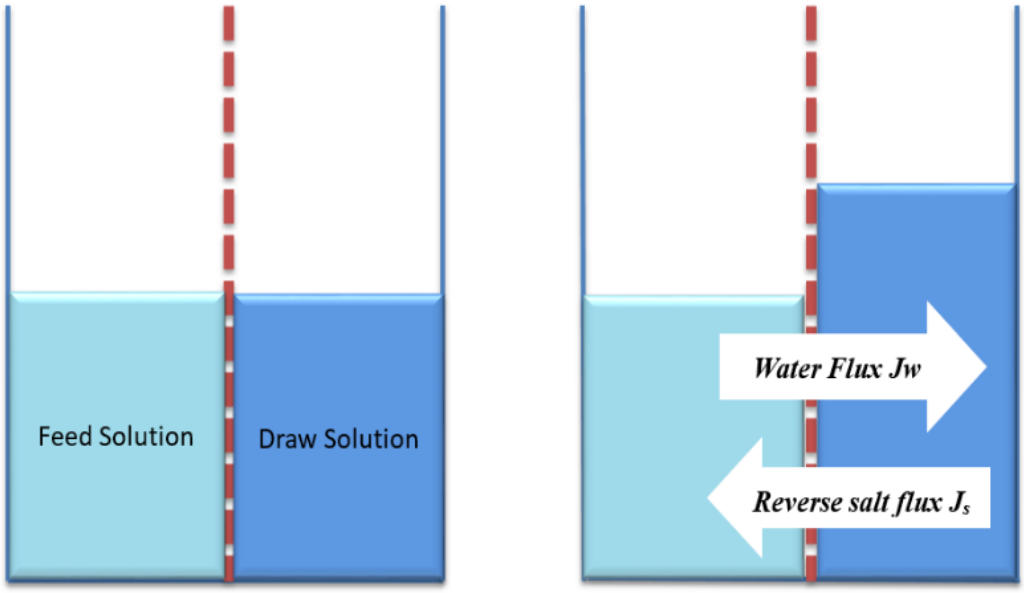

Figure 2.1: The concept of forward osmosis process

The water passage Jw across a membrane is given by

$$Jw = A\ \sigma\ \Delta\pi \qquad [1]$$

Where A ($Lm^{-2}\ h^{-1}\ bar^{-1}$) is the pure water permeability coefficient of the membrane used in the forward osmosis process, and σ is the reflection coefficient, and it is assumed as 1 in FO

experiments due to its high rejection rates. Most commercial FO membranes have a rejection rate of 95-98%. Thus, equation (1) becomes

$$Jw = A\ \Delta\pi \qquad [2]$$

Equation (2) describes water flux across the membrane; however, it over-estimates the water flux by almost 50%. This is mainly because equation (2) neglects the impact of concentration polarisation phenomena across the FO membrane. We will discuss concentration polarisation in detail in the subsequent chapter. Equation (2) can be further simplified. The theoretical water flux in the FO process is driven by the difference of osmotic pressure between the draw solution and feed solution and is given by equation (3).

$$Jw = A(\pi_{db} - \pi_{fb}) \qquad [3]$$

Where π_{db} and π_{fb} are the bulk osmotic pressure of the draw solution and feed solutions, respectively. Experimental water flux in the FO process can be determined analytically by using Equation (4)

$$Jw = \Delta V / A_m \Delta t \qquad [4]$$

ΔV is the change in feed solution volume over time (Δt), and A_m is the effective membrane area (m^2) of the FO membrane. Equation (3) shows that the FO process only relies on the osmotic pressure differences between the feed and the draw solution and the water permeability constant of a membrane. Due to the osmotic pressure gradient, water flows from the feed side to the draw side, diluting the draw solution. An additional step is required to separate the freshwater from the draw side if clean water is desired as the final product.

Along with the water flux across the membrane from the feed to the draw side, there is back diffusion of salt from the draw side to the feed side and is called reverse salt flux as indicted by J_s in **Figure 2.1**. Reverse salt flux is a major issue in the FO process, and it occurs when salt from the draw solution side permeates the feed solution and hence decreases net osmotic pressure across the membrane. In the FO process, the solute diffuses in two directions, or a bidirectional solute flux occurs. Mathematically, the diffusion of solutes through a semipermeable membrane is given by Fick's law

$$Js = B\Delta C \qquad [5]$$

Where ***B*** is the solute permeability coefficient (L/m^{2}h), and ΔC is the solute concentration difference across the membrane. As shown by equation (5), this reverse salt diffusion causes a decrease in the net driving force across the membrane and hence causes a reduction in the water flux from the feed to the draw side. Therefore, an ideal draw solute in the FO process should have osmotic pressure high enough to promote a high water flux across the membrane and smaller reverse salt flux.

FO has wide application to date in seawater desalination and wastewater treatment. Desalination with the FO processes consists of two stages; extraction of freshwater and **dilution of the draw solution** stage and freshwater extraction and regeneration of the **draw solution stage**. At the end of the first stage of the FO process, pure water is not obtained, but a mixture of freshwater and the osmotic agent is the product. For this reason, it is necessary to carry out a separation mechanism to remove the osmotic agent and obtain water suitable for human consumption or reusable for other processes. The quality of the permeate produced by the FO process is close to reverse osmosis and superior to microfiltration and ultrafiltration (Zhang, Jiang & Cui 2017). In wastewater treatment applications, the FO process has tremendous potential. The biggest advantage of FO in treating wastewater is its low fouling propensity. Wastewater has low osmotic pressure than seawater but has a higher fouling propensity. Therefore FO is ideal for treating complex wastewater (Zhao et al. 2012). To cause an optimal water flow in the system, you need a high osmotic potential that exceeds that of the wastewater to be treated. You must also consider that the draw solution is not toxic. It can

be easily recovered once it is concentrated. It also does not deteriorate the osmotic membrane bioreactor if there is a bioreactor in the treatment system. It does not affect the quality of the sludge or the growth of microorganisms. Transport properties will also be significant when choosing a draw solution. For example, large molecules have less diffusivity and filter more slowly through the membrane than small ones. Other factors to take into account are pH and temperature, especially to avoid cases of scaling due to calcium, sulfate, or carbonate precipitation. In the specific case of wastewater as a feed solution to the FO system, certain researchers have proposed magnesium chloride as a draw solution due to its high efficiency and easy recycling by the nanofiltration process.

2.2 Transport phenomena in the FO process, mass transfer, and concentration polarization

Mass transfer operations are characterized by transferring one substance through others on a molecular scale. For instance, when water by evaporation passes from a pool into an air stream that flows over the surface of the water, the molecules of water vapor diffuse through the air molecules at the surface into the mass of the air current, which drags them with it. The mass transfer phenomenon is when a substance that diffuses leaves a place that is highly concentrated to a low concentration due to the concentration difference or gradient. The mass transfer phenomena in the FO process is slightly different from mass transfer in pressure-driven membrane processes, mainly due to the asymmetry of the FO membrane. In an asymmetric membrane, the support layer prevents mixing and dramatically reduces mass transfer (Cath, Childress & Elimelech 2006b). This is the support layer in asymmetric membranes, which hinders mass transfer and leads to a phenomenon known as concentration polarization.

One of the issues in the FO process is the inherent phenomenon of concentration polarization that limit its potential and cause a decrease in the flow of water, contributing to a lower performance of the process. It is an accumulation or decrease of solutes near the surface of the membrane. Since FO asymmetric membranes consist of a dense active layer on top of a porous support layer,

concentration polarization occurs externally at the solution-surface interfaces of the membrane and internally at the porous support layer of the membrane. When the feed flows over the active layer of the membrane, solutes accumulate in the active layer. This accumulation of solutes produces an increase in the feed concentration at the active feed layer interface. This phenomenon is called concentrative external concentration polarization. It occurs when the porous support layer of the membrane faces the draw solution. At the same time, the draw solution is diluted inside the support layer, which leads to dilutive internal concentration polarization. When the draw solution flows over the active layer of the membrane, it is diluted at the draw solution-active layer interface by the permeating water from the feed solution. This phenomenon is called dilutive external concentration polarization. At the same time, the feed solution is concentrated inside the support layer leading to concentrative internal concentration polarization. Both concentration polarization phenomena cause a decrease in the effective osmotic pressure due to:

- An increase in osmotic pressure at the interface of the active layer feed solution leads to concentrative ECP and dilutive ICP. This occurs when the feed solution faces the active layer, and the draw solution faces the support layer, also known as FO mode or the AL-FS mode.
- A decrease in osmotic pressure at the interface of the active layer-draw solution leads to dilutive ECP and concentrative ICP. This occurs when the feed solution faces the support layer, and the draw solution faces the active layer, also known as PRO mode or the AL-DS mode.

With this, lower water flow is obtained than expected, and this phenomenon can be minimized by increasing the speed of the solutions, also termed as cross-flow velocity (liters per minute) and the turbulence on the surface of the membrane.

External concentration polarization affects a thin layer of fluid in contact at the membrane interface. Water and other solutes transported within this thin fluid layer are based only on advection (perpendicular to the membrane surface) and molecular diffusion. Two phenomena are distinguished depending on the orientation of the membrane:

- Suppose the porous support layer of the membrane faces feed. In that case, a polarized layer is established next to the interior of the active dense layer as water and solute propagate and

accumulate in the porous layer. This phenomenon is called concentrative internal concentration polarization.

- When the porous support layer of the membrane faces the draw solution, as the water permeates through the active layer, the draw solution in the porous substructure is diluted. This phenomenon is called dilutive internal concentration polarization.

The effect of internal concentration polarization shows a more severe impact on the reduction of water flux in the FO process than external concentration polarization because there is also an axial flow of a saline solution within the porous layer of the asymmetric membrane. The solutes entering and leaving the porous layer are carried by an advective water flow and direct diffusion. As only a minimal amount of solute can penetrate the active dense layer, reverse diffusion and solute accumulation will occur in the porous layer, contributing to the internal concentration polarization effect. Furthermore, since internal concentration polarization occurs in the porous layer, its effect is not mitigated by altering hydrodynamic conditions such as increasing flow velocity or turbulence (Ibrar, Naji, et al. 2019).

In most FO membrane models, four main parameters are involved. These include the pure water permeability $\boldsymbol{A_w}$ of the membrane, the solute permeability B, and the structural parameter S of the support layer. Additionally, a mass transfer coefficient "k'' and solute resistance to diffusion termed as "K" are required for FO modeling. The value of pure water permeability can be determined through a reverse osmosis test using DI water feed solution. A concentrate/back pressure control valve can adjust trans-membrane pressure. The active layer of the FO membrane is set to face the DI water to avoid membrane deformation. First, the membrane is compacted with maximum hydraulic pressure until the permeate flux reaches a steady state. Following the membrane compaction, the next reading is collected using a range of hydraulic pressures (use pressure range recommended by the manufacturer). The value A_w can be calculated using equation [6].

$$A_w = \frac{J_w}{\Delta P} \qquad [6]$$

The value A_w is reported in $Lm^{-2}h^{-1}bar^{-1}$. The membrane solute permeability can be determined using the same setup using a 2 g/L NaCl feed solution. The test was carried out at different pressures, and the B value can be calculated from the following expression:

$$B = \frac{(1-R_j)}{R_j} exp\left(\frac{-J_w}{k}\right) \quad [7]$$

Where, R_j is the rejection rate of the membrane, and k is the mass transfer coefficient of the rectangular channel.

Lee, Baker & Lonsdale (1981) was the first to introduce a flux model r pressure retarded osmosis (PRO) in the presence of concentration polarisation. PRO performance was predicted from FO and reverse osmosis measurements. Loeb et al. (1997) later described the model of Lee et al.(1981) for the FO process. The following expressions show the effects of internal concentration polarisation and how they relate to water flux and other membrane constants.

$$Concentrative\ ICP: \qquad K = \left(\frac{1}{J_w}\right) \ln \frac{B+A\pi_{D,m}-J_w}{B+A\pi_{F,b}} \quad [8]$$

$$Dilutive\ ICP: \qquad K = \left(\frac{1}{J_w}\right) \ln \frac{B+A\pi_{D,b}}{B+J_w+A\pi_{F,b}} \quad [9]$$

B represents the salt permeability of the active layer, $\pi_{D,\,m}$ is the osmotic pressure of the draw solution at the membrane surface, $\pi_{F,b}$ is the osmotic pressure of the feed solution in bulk, and K represents the solute resistivity to the diffusion within the porous support layer. The value of K is defined by Eq. [10].

$$K = \frac{t.\tau}{D.\epsilon} \quad [10]$$

Here t, τ and ϵ represents the thickness, tortuosity and porosity of the support layer respectively.

2.3 Forward Osmosis Process, the evolution of the current flux model

FO flux models were designed to predict water flux across the membrane (Wang et al. 2014). These models evolved over time to include different physical parameters, reflecting our increased understanding of the phenomenon of osmosis flux in the FO membrane. Lee, Baker & Lonsdale (1981) presented the first model for water flux prediction in pressure-retarded osmosis (PRO) in the presence of concentration polarisation. Several researchers have revised the model and witnessed many improvements over time. McCutcheon & Elimelech (2006a) extended the model of Lee, Baker & Lonsdale (1981) by incorporating the effects of external and internal concentration polarization on flux behaviour. According to the study, water flux in the FO process operating in the PRO mode (active membrane layer faces the draw solution) is given by Equation [11].

$$J_w^{PRO} = A_w \left[\pi_{Db}\, exp\left(\frac{-J_w}{k}\right) - \pi_{Fb} exp\,(J_w K)\right] \qquad [11]$$

For the FO membrane operating in the FO mode (active membrane layer faces the feed solution), water flux is presented by Equation [12].

$$J_w^{FO} = A_w \left[\pi_{Db}\, exp(J_w K) - \pi_{Fb}\, exp\left(-\frac{J_w}{k}\right)\right]$$

[12]

Where J_w is the experimental flux, A_w is the pure water permeability, $\pi_{Db}$and π_{Fb} are the bulk feed osmotic pressure of draw and feed solution, respectively, k is the convective mass transfer coefficient, and K is the salt resistivity. Unfortunately, the proposed model neglects the effects of salt transport and the external mass transfer resistance on the support layer (Nagy 2014). Yip et al. (2011) presented a modified mathematical model to predict water flux in the FO process, including the effects of internal and external concentration polarizations with reverse salt diffusion from the draw to the feed solution. Water flux in the FO process is given by Equations [13] and [14] to express the FO and the PRO operating modes, respectively:

$$J_w^{FO} = A_w \left[\frac{\pi_{Db}\, exp(-J_w K) - \pi_{Fb} exp\left(\frac{J_w}{k}\right)}{1 + \frac{B}{J_w}\left\{exp\left(\frac{J_w}{k}\right) - exp\ -(J_w K)\right\}} \right] \quad [13]$$

$$J_w^{PRO} = A_w \left[\frac{\pi_{Db}\, exp\left(-\frac{J_w}{k}\right) - \pi_{Fb}\ exp(J_w K)}{1 + \frac{B}{J_w}\left\{exp(J_w K) - exp\left(-\frac{J_w}{k}\right)\right\}} \right] \quad [14]$$

Where B is the salt permeability coefficient. Yip's model, however, ignored the mass transfer resistance at the porous support layer. A general resistance in the series mathematical model was developed by Nagy (2014), combining the effects of concentration polarization with the impact of external resistance on the porous support layer (**Figure 2.2**) as given by Equations [15] and [16] for the FO and the PRO operating modes, respectively.

$$J_w^{FO} = A_w \left[\frac{\pi_{Db} \exp\left[-J_w\left(\frac{1}{k_D} + \frac{S}{D_D}\right)\right] - \pi_{Fb} \exp\left(\frac{J_w}{k_F}\right)}{1 + \frac{B}{J_w}\left[\exp\left(\frac{J_w}{k_F}\right) - \exp\left(-J_w\left(\frac{1}{k_D} + \frac{S}{D_D}\right)\right)\right]} \right] \quad [15]$$

$$J_w^{PRO} = A_w \left[\frac{\pi_{Db}\, exp(-\frac{J_w}{k_D}) - \pi_{Fb}\, exp\left[\ J_w(\frac{1}{k_F} + \frac{S}{D_F})\right]}{1 + B/J_w \left\{exp\left[\ J_w(\frac{1}{K_F} + \frac{S}{D_F}) - exp\ (-\frac{J_w}{k_D})\right]\right\}} \right] \quad [16]$$

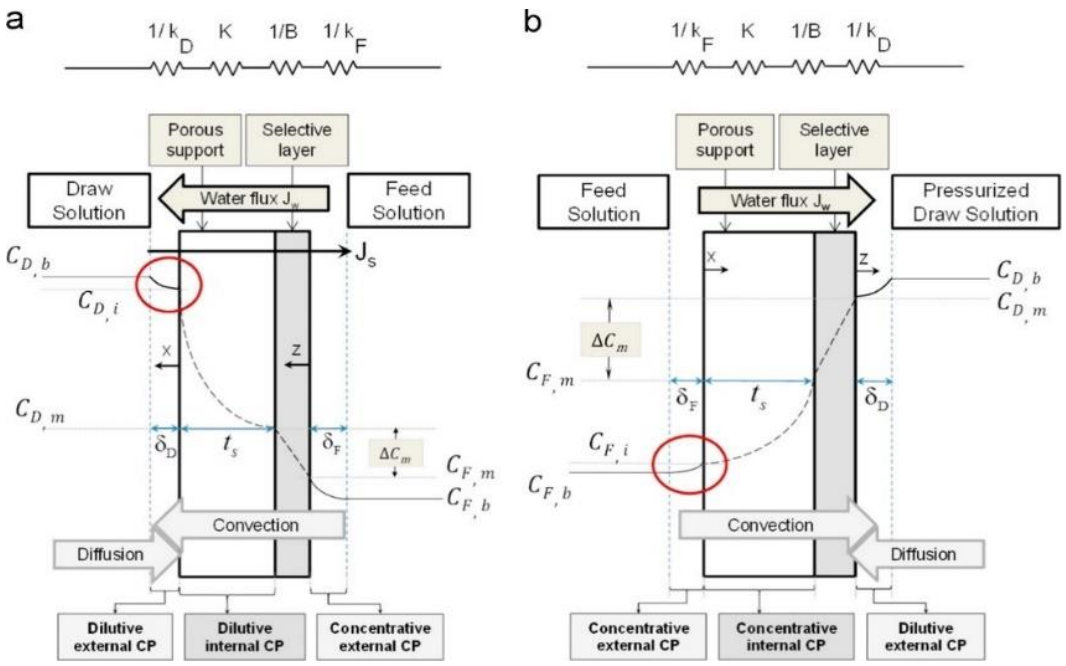

Figure 2.2: Solute Concentration Profiles at steady state across a TFC membrane in (a) FO mode (b) PRO mode. Reprinted from Bui et al. (2015) with permission from Elsevier

Where, S is the membrane structure parameter, and D_D is the diffusion coefficient of the draw solution. Technically, the impact of ECP at the porous support layer is responsible for less than 10 percent water flux decline in the forward osmosis process (Altaee, Zhou, Alanezi, et al. 2017; Bui, Arena & McCutcheon 2015). A recent laboratory-scale study on a flat sheet membrane showed that the effects of CP depend on technical and operating parameters such as type of membrane, solutions concentrations, feed temperature, cross-flow velocity, and membrane orientation (Altaee, Zhou, Alanezi, et al. 2017). Membranes with a denser structure, such as HTI, resist internal mixing, resulting in a severe internal concentration polarization (Hawari, Kamal & Altaee 2016). Such membranes benefit from increasing the cross-flow velocity in reducing the effect of internal concentration polarization (Zhang et al. 2010). The study also revealed that water flux increased, resulting in more intensified ICP, but it was lower at high cross-flow velocities. Therefore, many studies recommended high cross-flow velocity to alleviate the effects of concentration polarization.

In the FO process and the water flux, there is also reverse salt flux from the draw solution to the feed. Reverse salt flux is an intrinsic property of all osmotically driven membrane processes and has adverse effects on membrane performance in the FO process (Phuntsho et al. 2011). The following equation can estimate the reverse salt flux in the FO process (Johnson et al. 2018).

$$J_s = B\left[\frac{C_{Db}\exp\left(-\frac{J_w}{k}\right)-C_{Fb}\exp\left(\frac{J_w S}{D}\right)}{1+\frac{B}{J_w}\left[\exp\left(\frac{J_w S}{D}\right)-\exp\left(-\frac{J_w}{k}\right)\right]}\right] \qquad [17]$$

Where C_{Db} and C_{FB} are the bulk concentrations of the draw and feed solutions, respectively. The reverse salt diffusion has adverse consequences such as decreasing the net driving force across the membrane, increasing the loss of draw solution, contaminating the feed solution (when certain draw solutions are used) and promoting membrane fouling.

2.4 Draw solutions in wastewater treatment applications

Analysis of the FO literature reveals that finding an ideal draw solution and efficient membrane are the main obstacles towards the commercialization of the process (McCutcheon, McGinnis & Elimelech 2005). Despite the wide range of draw solutions, it is still believed that selecting an appropriate draw solution is paramount for an efficient FO process (Cai & Hu 2016). The criteria for an ideal draw solution are high osmotic pressure, low reverse salt diffusion, high diffusion coefficient to reduce ICP, low viscosity to allow easy pumping around the FO system, and ability to regenerate at a competitive cost (Cai and Hu 2016, Johnson, et al. 2018, Phuntsho, et al. 2011). Technically, there is not a single draw solution that meets every criterion of an ideal draw solution. This issue continues confusing a standard draw solution for a specific application such as wastewater treatment. For example, NaCl has been used widely in FO experiments because it has high osmotic pressure, small molecular size, and high diffusion coefficient, but at the same time, it exhibits high reverse salt flux due to its smaller molecular size. On the other hand, draw solutions containing divalent ions such

as $MgSO_4$ and $MgCl_2$ have lower reverse salt flux than NaCl. Still, the presence of divalent magnesium and calcium ions promotes organic fouling by complexation and forming intermolecular bridges among organic molecules. The diffusivity of the draw solution is influenced by other factors such as temperature, viscosity and particle size (Lutchmiah, Verliefde, et al. 2014). According to Ge, Amy & Chung (2017) viscosity of a draw solution is linked to its diffusion coefficient and inversely proportional to the water flux in the FO process. However, high-viscosity hydrogels draw solution exhibits high water flux (Zhang et al. 2015). Hydrogel draw solution requires heat energy for regeneration and freshwater separation, which increases the cost of FO treatment. The economic availability of draw solutions is also a factor in selecting draw solutes. Synthesized draw solutions in the FO studies such as magnetic nanoparticles, polyelectrolytes, zwitterions, and hydroacid complexes have excellent osmotic pressures and low reverse salt flux (Cui et al. 2014; Ge et al. 2012; Lutchmiah, Lauber, et al. 2014; Na, Yang & Lee 2014). Unfortunately, these draw solutions are rather expensive and have an intricate synthesis process, which complicates their commercial application.

Table 2.1 provides information about draw solutions and membranes used to treat various wastewaters. The regeneration process is the most energy-intensive stage in the FO process, but several FO applications successfully eliminated this stage (Ansari et al. 2016; Gwak, Kim & Hong 2018; Kalafatakis et al. 2017; Korenak et al. 2019; Takahashi, Yasukawa & Matsuyama 2016; Zou & He 2016). Ansari et al. (2016) used a real seawater draw solution to recover calcium phosphate from a digested sludge. CTA FO membrane (HTI) was used, and the reported water flux was 6.4 L/m^2h. In this study, the regeneration stage was not required for recovery of the draw solution and hence reduced the energy requirements of the FO process. The problem with indirect desalination is several ethical and environmental guidelines that strict the application of product water. In another study, a flat sheet CTA FO membrane (HTI) was used for fertilizer draw solutions preparation using a treated wastewater feed solution (Zou & He 2016). Although fertilizer draw solution from the FO process is ready for use, it may require dilution before application. Therefore, a source of desalinated

water should be available, which compromises the cost of fertilizer solution. Apart from these applications, FO has recent advancements in industrial applications where the regeneration of the draw solution is eliminated. One recent study suggested crude glycerol and pre-treated hydrolysed wheat straw (PHWS) as potential draw solutions for water recovery and recirculation in biorefineries using the FO process (Kalafatakis et al. 2017). The FO study applied Aquaporin A/S^{TM} membrane, and the reported water flux was 10.5 L/m^2/h and 5.37 L/m^2/h for crude glycerol and PHWS, respectively. Draw solution regeneration was not required as the concentrated glycerol was the draw solution, while biological wastewater effluent was the feed solution. The problem, however, with these draw solutions was the presence of microbial cells, which led to the biofouling of the FO membrane.

Textile dyes draw solution was recently investigated for textile wastewater treatment with Aquaporin A/S FO membrane (Korenak et al. 2019). The regeneration step was eliminated since the draw solution was the dyes from the production line. The major drawback of the dyes draw solution was the high reverse salt flux across the membrane, contaminating the feed solution. Another study used Electroless Nickel plating solution draw solution to recover precious metal ions from PCB (printed circuit board) wastewaters using TFC Porifera membrane (Gwak, Kim & Hong 2018). The FO process successfully concentrated the palladium-based wastewater-stream without the need for regeneration of the draw solution. Although water flux in the FO was relatively high (about 20 L/m^{2}h), membrane scaling was inevitable. Therefore, the disadvantages of using an industrial waste stream as a draw solution negate the advantages of eliminating the regeneration stage in the FO process.

There is a long list of organic and inorganic draw solutions that has been proposed by researchers (Table 2.1) for the treatment of a wide range of wastewaters such as sodium ligno sulphate (SLS) and di-sodium hydrogen phosphate (DHSP) (Achilli, Cath & Childress 2010; Corzo et al. 2017; Lutchmiah, Lauber, et al. 2014; Thiruvenkatachari et al. 2016). Special considerations are given to the compatibility and reliability of the draw solution with the FO membrane and type of wastewater to avoid major technical and operating problems. For

example, researchers used potassium formate and potassium sulfate for boron removal applications. Still, the high pH of the draw solution was not compatible with the operating condition recommended for the CTA FO membrane (Corzo et al. 2017). Researchers also used zwitterions draw solution for wastewater reclamation to reduce reverse salt flux, but it showed drawbacks such as susceptibility to biodegradation and development of biofouling (Lutchmiah, Lauber, et al. 2014). On the other hand, draw solutions containing magnesium and calcium ions are easily rejected by the NF membrane and are more energy-efficient to regenerate, but they promote inorganic scaling (Achilli, Cath & Childress 2010). Furthermore, researchers proposed magnetic nanoparticles as a draw solution because of their high rejection by FO membrane, easy regeneration using a magnetic field, and moderate osmotic pressure, but nanoparticles face problems in scale-up production, agglomeration, intricate synthesis processes, or synthesis can be too expensive (Ling, Wang & Chung 2010). Therefore, magnetic nanoparticles in the draw solution are not practical for large-capacity and commercial applications.

FO process could have a niche market for the treatment of difficult wastewater, such as mining and shale gas wastewater, where conventional treatment processes are less effective (Ge, Amy & Chung 2017; Han, de Wit & Chung 2015; Lee & Kim 2017; Thiruvenkatachari et al. 2016). Experimental work on the FO treatment of shale gas wastewater revealed that reverse salt diffusion is a severe issue due to the formation of irreversible scales on the active layer of the FO membrane. For example, the reverse flux of HCO_3 in the NH_3-CO_2 draw solution chemically reacted with Ca^{2+} ions in the feed to form irreversible $CaCO_3$ scales (**Figure 2.3**) (Lee & Kim 2017).

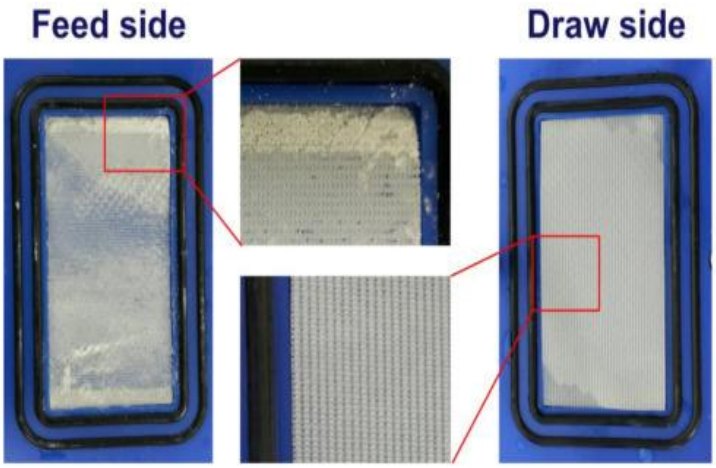

Figure 2.3: Images of the membrane spacers and FO membrane surface after the FO experiment using the NH3-CO2 draw solution to treat a Ca2+-containing feed solution. Reprinted from (Lee & Kim 2017) with permission from Elsevier

Table 2.1: Draw solutions and membranes used in Wastewater treatment studies

Wastewater	**Draw solute**	**Membrane**	**Water flux LMH**	**findings**	**Reference**
WW with heavy metal ions	Hydro acid complex $Na_4[Co(C6H_4O_7)_2]\cdot 2H_2O$ 1M	Lab scale TFC membrane	11	Synthetic, good flux in PRO mode only.	(Cui et al. 2014)
Dye WW	Polyelectrolytes	CA hollow fiber Lab Scale	~ 15 (at 50°C)	High viscosity, Synthetic.	(Ge et al. 2012)
Digested sludge centrate	Real Seawater	CTA HTI	6.4	Phosphorous recovery from sludge. No	(Ansari et al. 2016)

				regeneration required.	
PVC Latex	Synthetic Seawater	CTA-HTI	4.5		(Takahashi, Yasukawa & Matsuyama 2016)
Treated WW	Fertilizers	CTA HTI	4.2	No regeneration	(Zou & He 2016)
Biorefineries WW	PHWS	Flat sheet Biomimetic membrane by Aquaporin A/S	5.37	Microbial cells in DS can lead to biofouling. No regeneration required.	(Kalafatakis et al. 2017)
Biorefineries WW	Undiluted Glycerol	Flat sheet Biomimetic membrane by Aquaporin A/S	10.5	DS can be toxic. No regeneration.	(Kalafatakis et al. 2017)
Textile WW	Green Dye mixture, Blue Dye mixture. NaCl (1M) $MgCl_2$, (1M),	Biomimetic Aquaporin A/S	~ 11.6	High RSF for dye mixtures. No regeneration is required in case of dye mixture DS.	(Korenak et al. 2019)
PCB WW	E'less Ni Plating	TFC	20	DS leads to	(Gwak, Kim &

	solution	Porifera		inorganic scaling. No regeneration required.	Hong 2018)
Medical Radioactive WW	MgCL2 (0.48M). NaCl (0.6M)	TFC PA membrane Porifera	20.4±1.2 to 20.8±2.1	NaCl has a higher rejection for Iodine.	(Lee et al. 2018)
WW plant effluent with antibiotics	1M NaCl without spacer 2M NaCl with spacer	CTA HTI	~13	Same flux for FO and FOwEO (electrochemical oxidation)	(Liu et al. 2015)
Construction WW	NaCl (0.6M)	CTA HTI	7.44	Feed flow rate of 2.9L/min, No spacer and pre-treatment	(Hawari et al. 2018)
Municipal WW	$K_4P_2O_7$, Sodium Polyacrylate, $MgSO_4$	TFC Flat sheet HTI FO 4040 Hollow fiber CTA	9 ~3	TFC flat sheet, $MgSO_4$, Sodium Polyacrylate, and $K_4P_2O_7$ were selected for the demo plant.	(Corzo et al. 2017)
Coal mines WW	SLS, SHMP,	CTA HTI	5.83-6.9	CTA membrane had	(Thiruvenkatachari et al. 2016)

	DHSP			better rejection than the RO membrane.	
Shale gas WW	NH_3-CO_2, NaCl	TFC Porifera	21.4	In-organic scaling in the presence of calcium ions	(Lee & Kim 2017)
Oily WW	Oxalic Acid complexes. NaCl	Lab scale TFC-PES membrane	20-23	In PRO mode oxalic acid had good flux.	(Ge, Amy & Chung 2017)
Emulsified oily WW	1M NaCl	TFC Cellulose acetate butyrate (CAB) Hollow fiber Lab scale	~ 28.2	The experiment was done in the PRO mode. This membrane had excellent oil rejection.	(Han, de Wit & Chung 2015)
Synthetic WW	3M NaCl	TFC-ES HTI	-	Presence of cations in feed aggravates fouling in FO.	(Motsa, Mamba & Verliefde 2018)
Mercury Polluted WW	1M $MgCl_2$, 1M NaCl	TFC HTI	-	Mercury permeation into draw side.	(Wu et al. 2016)
Industrial WW	Glauber Salt 1 to 2M	Low-pressure RO membrane	5.3	Scaling of the membrane due to DS nature.	(Dutta & Nath 2018)

		(Vontron)			
Fracking WW	KAc (4.47 M) NaGly (4.93M) KFor (4.57 M) NaPro(4.60 M) NaCl (4.03 M)	TFC HTI	19.51 to 24.81	Organic DS promote membrane fouling.	(Islam et al. 2019)
Lab WW	Zwitterions	CTA HTI	4.3-4.9	Low RSF but biodegradation of the DS.	(Lutchmiah, Lauber, et al. 2014)
Drilling mud and fracturing WW	NaCl 260g/L	CTA HTI	14	Presence of Humic acid and Fulvic acid in DS.	(Hickenbottom et al. 2013)
Distillery WW	$MgCl_2.6H_2O$	TFC Aquaporin A/S	2.8 to 6.3	Fouling of the membrane	(Singh et al. 2018)
Swine WW	$MgCl_2$ (0.5 M)	CTA HTI	3.12	Nutrient recovery from livestock WW.	(Wu et al. 2018)
Acidic WW	NaCl (2M)	Thin film in-organic Lab scale. (TFI)	69.0	High water flux and good rejection of heavy metals by FO.	(You et al. 2017)
Synthetic wastewater with sludge	NaCl	CTA Flat sheet Lab made	~ 15	Bioinspired surface modification	(Li et al. 2016)

				improved the antifouling abilities of CTA membrane.	
Raw Sewage	1.5 M NaCl	CTA HTI	8	FO-MD	(Xie, Nghiem, et al. 2013a)
Secondary WW Effluent	1M NaCl	CTA HTI	4.5	FO-ED	(Zhang et al. 2013)
Synthetic WW	2M NaCl	TFC HTI	18.6	Sever fouling in the PRO mode.	(Pan et al. 2015)
Olive Mill WW	3.7 M $MgCl_2$	CTA HTI	6.01	The high viscosity of draw solution enhanced DICP.	(Gebreyohannes et al. 2015)
Oil sands produced WW	0.5 M NaCl	Lab-made TFC	18.1	The lab-scale membrane showed good performance than commercial membrane.	(Khorshidi et al. 2016)
High Nutrient	0.2 M Na_3PO_4	TFC HTI	7.09	Less RSD than NaCl	(Nguyen et al. 2016)

sludge					
Synthetic Dye WW	2M NaCl	TFC Lab made	12.01	Cationic dyes show more fouling tendency	(Han et al. 2016)

Until now, there is no standard draw solution for wastewater treatment yet, although NaCl solution has been widely used in laboratory experiments (Table 2.1). As shown in **Figure 2.4**, 49% of the FO studies for wastewater treatment used NaCl draw solution followed by $MgCl_2$ (13%).

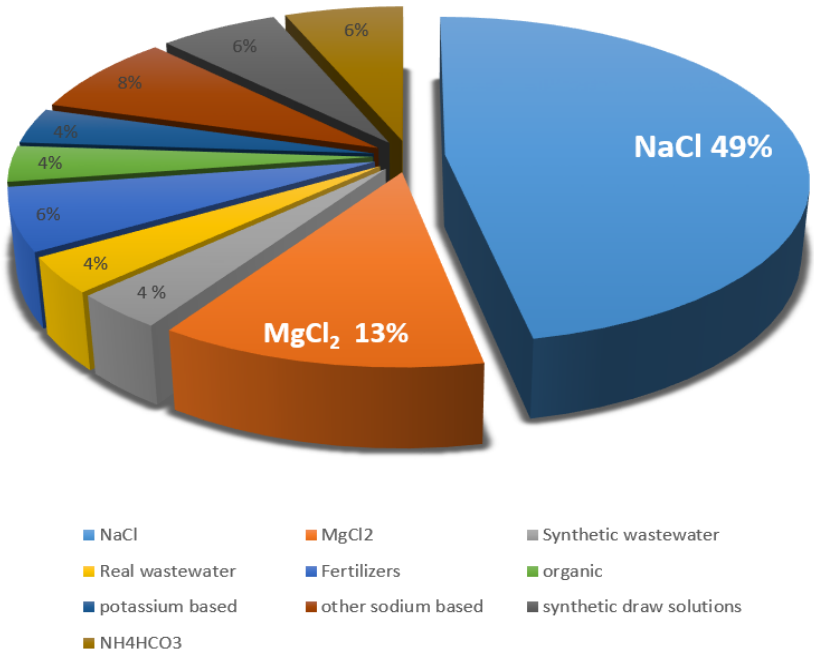

Figure 2.4: Percentages of different draw solutions used in wastewater treatment studies

Future research should focus on suitable membranes for wastewater treatment, which can minimize the back diffusion of salt as well as minimize the bridging effect associated with the back diffusion of divalent ions. NaCl or divalent salts would be perhaps the ideal draw solutions for wastewater treatment applications with such a membrane available.

2.5 FO Membranes

FO membrane plays a critical role in wastewater treatment to minimize fouling. **Figure 2.5** shows the percentage of different types of membranes used in wastewater treatment studies. According to our analysis, 48% of the experimental work used CTA FO membrane to treat wastewater because of its high tolerance to chlorine, insensitive to biological degradation, and low fouling potential (Lv et al. 2017; Thorsen 2004).

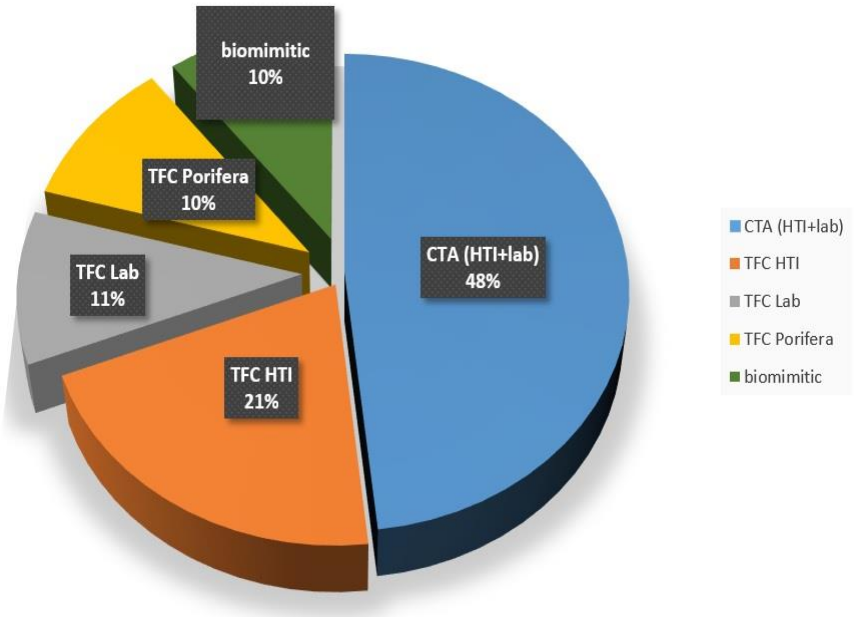

Figure 2.5: Percentage of different FO membranes used in various FO wastewater applications

Despite its numerous advantages, CTA membranes have several shortcomings, such as limited pH tolerance, modest water permeability, and high sodium chloride permeability (Chou et al. 2010; Ren & McCutcheon 2014; Wang, Li & Wang 2018). Commercial CTA membranes were available from Hydration Technology innovation (HTI-USA) and currently from Toyobo Company (Japan) (Nicoll 2013). Toyobo FO membrane is a modification of the RO membrane with a selective layer on the shell side and withstands a maximum hydraulic pressure < 30 bar on the shell side and < 2 bar on the membrane bore side. On the other hand, HTI spiral wound membrane tolerates a maximum pressure of 0.69 bar (10 psi) because of the thinner structural parameter, ~400 μm (Bui, Arena & McCutcheon 2015).

Nowadays, thin-film composite (TFC) FO membranes have become the most competitive membranes for FO because of the higher water permeability than the CTA membranes (Alsvik & Hägg 2013; Ren & McCutcheon 2014). TFC membranes are commercially available from several companies, including Porifera, HTI, and Oasys water Inc., with a high rejection rate for nitrates, silica, and organic compounds (Singh 2006). Unfortunately, TFC membranes are prone to fouling in wastewater treatment due to the high-fouling environment. TFC membranes have limited tolerance to chlorine attack; many studies using complex wastewaters incorporated CTA membrane because it can tolerate up to 1 ppm (part per million) of chlorine residues (Fam et al. 2013; Lu et al. 2017). Additionally, CTA membranes are more resistant to silica and gypsum scaling. In contrast, the presence of a high density of carboxylic acid functional group on the surface of TFC membranes leads to its high fouling propensity (Xie, Tang & Gray 2016).

In addition to fouling of membrane, concentration polarization effects have a detrimental effect on the water flux, especially at the support layer because of the limited hydrodynamic mixing, leading to the severity of internal concentration polarization. Structure parameter (S) of the support layer is a function of the support layer thickness:

$$S = \frac{t_s \tau}{\varepsilon} \qquad [18]$$

Where t_s is the thickness of the support layer, τ is the tortuosity, and ε is the porosity of the support layer. Nowadays, FO membranes are fabricated with a structure parameter ≤ 500 μm (Bui, Arena & McCutcheon 2015). FO membranes with a thinner support layer exhibit higher water flux, but reducing the thickness of the support layer compromises the FO membrane's mechanical integrity. It is also valid to argue that a thinner membrane may have a shorter lifetime, although there is no data available about a pilot FO system operating for 3 years or more (assuming the lifetime of the FO membrane equals that of the RO membrane).

Wastewater treatment, in fact, is a challenging environment that requires a membrane of high fouling resistance. Membrane module configuration plays an essential role in membrane cleaning and fouling reduction. Flat sheet and spiral wound modules require less pre-treatment than hollow fibre modules, and they are also easier to clean up than hollow fiber modules with high packing density (Fritzmann et al. 2007). The main drawbacks of flat sheet FO modules are the low packing density, 70-m^2 per module for Porifera compared to 650 m^2 for Toyobo hollow fiber FO membrane and 16.5 m^2 for HTI spiral wound FO module. Commercial FO modules are available now in a flat sheet (Porifera), spiral wound (HTI and Toray) and hollow fiber (Aquaporin A/S and Toyobo) configuration (Nicoll 2013).

The other challenge that faces the FO process is the cost of the membrane, which is almost ten times more expensive than the RO membrane based on the HTI 16.5 m^2 element costs (Altaee et al. 2014). Unless the cost of the FO membrane is reduced, the technology cannot be considered economically competitive to the existing state-of-the-art RO technology. If the demand for the FO membrane increases, the cost will come down. It is important to mention here that the cost of Toyobo 700 m^2 FO membranes is almost comparable to that of the RO membranes (Altaee, Zhou, Alanezi, et al. 2017). However, Toyobo membranes are less common in laboratory-size experiments and are only available in full-scale modules.

Future research should also focus on developing chlorine resistance membranes to treat wastewater and impaired-quality feed solutions (Lu et al. 2017). Successfully, researchers were able to fabricate a membrane that tolerates up to 1000 mg/L NaOCl using layered double

hydroxide nanoparticles bound on the TFC by a polydopamine-induced immobilization process. The double-layered hydroxide coating serves as a barrier against the chlorine attack and provides enhanced membrane resistance to organic fouling. Such a membrane would be a good fit for wastewater treatment, but the commercial product may take longer to be available. On the other hand, biomimetic membranes made by Aquaporin (Denmark) demonstrated good performance in terms of water flux (Table 1). However, these membranes need further development as they have a shorter life span than polyamide membranes. Research should also focus on the field performance of a full-scale FO membrane rather than the FO membrane coupons in a laboratory size experiment.

2.6 FO pilot-scale applications, energy, and economic aspects

Despite the numerous laboratory size FO experiments, only a few tests on a pilot scale for wastewater treatment (Table 2.2) using the FO process. Scaling up from a laboratory to pilot plant size provides a better perspective and information about the FO process potential and feasibility for wastewater treatment. Several pilot plant tests have been performed to treat various types of wastewater. Oasys water developed the first pilot FO membrane brine concentrator (MBC) for treating high salinity brine streams from oil and gas wastewater (Coday et al. 2014). The draw solution in the FO process was a thermolytic draw solution, which consisted of a mixture of ammonium bicarbonate and ammonium hydroxide dissolved in water. The thermal distillation process was applied to cut the cost of regeneration of the thermolytic draw solution (McGinnis et al. 2013). Due to the elevated concentration of feed solution, water flux was relatively low, 2-3 L/m^2 h, which indicates that a large membrane area is required. The other concern about the FO process for wastewater treatment is the back diffusion of ammonium carbonate across the membrane, which could further contaminate the feed solution (Coday, Almaraz & Cath 2015; Mulder & Mulder 1996). With respect to the energy requirements, a similarly configured open cycle single staged evaporative brine

concentrator (no energy recovery) would need an energy input of 633 kWh/m^3 of thermal energy, which is 2.3 times higher than the energy of 275 kWh/m^3 required in the FO-MBC pilot plant (McGinnis et al. 2013). Therefore, the FO process's justification is the elevated concentration of oil and gas wastewater, which is not suitable for treatment by the thermal or hydraulically driven membrane processes.

Osmotic membrane bioreactor (OMBR) has the potential to reduce the energy consumption of wastewater treatment and generate potable water for direct reuse (Wait 2012). Qin et al. (2010) carried out a pilot-scale FO-MBR study to treat domestic sewage. The pilot study used air scouring at the feed side to mitigate the membrane fouling. Results showed that the OMBR successfully reduced the energy cost of wastewater treatment and provided a stable water flux. The pilot study did not perform any economic analysis but focused only on the performance of the FO process. Cornelissen et al. (2011) extended the pilot study conducted by Qin et al. (2010) by combining the OMBR with the RO process to regenerate the draw solution. Economic analysis of the OMBR-RO system revealed that a water flux of 15 L/m^2h using 0.5M NaCl draw solution would be required for the OMBR system to be economically competitive against a conventional MBR, which is operated at an average 16 L/m^2h water flux. The cost of the draw solution regeneration can also be reduced by choosing a proper RO membrane. For example, coupling the FO process with low-pressure reverse osmosis (LPRO) can reduce the energy consumption of wastewater treatment.

According to one study, the FO-LPRO process consumed energy equal to 1.5 kWh/m^3 when seawater is diluted with a secondary wastewater effluent compared to 4 kWh/m^3 for a high-pressure RO system (Yangali-Quintanilla et al. 2011). The FO-LPRO system for indirect desalination consumes only half of the energy used in the high-pressure RO process and can produce good quality water from impaired feeds. Furthermore, the wastewater pre-treatment should also be included in the total energy requirement for wastewater treatment by the FO process. The capital cost of the OMBR will be higher than that of the MBR due to the additional cost of FO membranes. Currently, the cost of commercial FO membranes varies

from tens of USD to a few hundred USD per square meter (Altaee et al. 2014; Altaee, Zhou, Alanezi, et al. 2017). One of the reasons for the high cost of FO membrane is the low commercial demands, and it is expected to decrease if large capacity FO plants are built. As such, most pilot plant studies did not provide a cost analysis of the FO process.

Table2.2: Overview of pilot studies on forward osmosis for Wastewater Treatment

Feed Water	Membrane material, Module & Configuration	Configuration	Draw Solute	Water Flux L/m^2h	Reference
Pre-treated shale gas produced water	TFC-spiral wound (Oasys water)	FO-Thermal	5.5 M to 6.0 M NH_4HCO_3	2.6 ±0.12	(McGinnis et al. 2013)
Produced water from natural gas processing	Mechanically enhanced Flat sheet CTA module	FO-Thermal	NH_4HCO_3 (3M to 6M)	27.5	(Nelson & Ghosh 2011)
Municipal Wastewater	Aquaporin Inside ,TFC	FO-MF	Seawater Or 2M NaCl	1.1 and 9.1	(Hey et al. 2018)
Domestic sewage	CTA Flat sheet pilot-scale	FO-MBR	0.12M $NaCl+MgSO_4$	3	(Qin et al. 2010)
Wastewater effluent	CTA spiral wound	FO-RO (Closed loop)	Synthetic sea salt (30g/L)	7.8 to 7.5	(Hancock et al. 2013)

Mine impaired water	CTA spiral wound	FDFO-NF	0.95,1.8,2.84 M $(NH_4)_2SO_4$ SOA	5.9,7.5,8.8 respectively	(Phuntsho et al. 2016)
Brackish water	CTA spiral wound FO	FDFO	0.6 to1.0M $(NH_4)_2SO_4$ SOA	1 to 4	(Kim et al. 2015)
Raw Produced water from oil and gas	CTA spiral wound	FO-RO	1M NaCl Brine	3.1	(Maltos et al. 2018)
Drilling wastewater	CTA , Flat sheet spiral wound module	FO-RO Close loop	NaCl	-	(HTI 2011)
Pre-treated Municipal wastewater	CTA flat sheet HTI, Aquaporin Inside TFC	FO with physio-chemical pre-treatment	2M NaCl	13.4 and 12.0 respectively	(Hey et al. 2017)
Pre-treated Municipal wastewater	CTA FO spiral wound	FO	0.5M NaCl	No Data	(Wang, Zheng, et al. 2016)

While these pilot-scale system results are promising, little is known about long-term (greater than one year) fouling propensity and its effects on the efficiency of the FO process when treating complex feeds such as oil and gas wastewater (Coday et al. 2014). Future pilot studies should address the long-term performance of the FO process and the energy consumption for wastewater treatment, including the regeneration process. Furthermore, standard and cost-effective technologies for fouling mitigation should be developed for wastewater reclamation by the FO process, such as air bubbling, reversible flow, and chemical cleaning. Techno-economic studies on the FO treatment of wastewater should be performed, as more information about the feasibility and cost-effectiveness of the FO process is required for comparison purposes with the conventional processes. FO studies should also focus on the advanced treatments of wastewaters, such as NEWater, where the double-barrier can achieve high nitrogen and phosphorus removal in the FO-RO process.

2.7 Conclusions

Forward osmosis has great potential in the field of wastewater treatment; however, challenges such as concentration polarization, ineffective membranes, reverse salt flux, fouling and finding draw solutions that can easily be recycled are the main impediments in its commercialization. FO membranes without a support layer can be the solution for mitigating concentration polarization; however, scaling up such a membrane will take time. In selecting suitable draw solutions for wastewater treatment, NaCl seems the most compatible draw solution with wastewater. Using seawater as a draw solution can eliminate the energy extensive regeneration step in the forward osmosis. On the other hand, industrial waste as a draw solution can eliminate the regeneration process and induce irreversible fouling in the FO system. CTA HTI membranes have been widely used (in wastewater studies) due to its numerous advantages over TFC membranes despite the high rejection rates of TFC membranes. CTA membranes have excellent flux recovery rates and are less prone to fouling compared to TFC membranes. CTA membranes are also more resistant to chlorine compared

to TFC membranes. However, the lower flux of CTA membranes makes it hard for FO to compete economically with the current technologies. Novel TFC membranes with high flux, excellent antifouling and chlorine-resistant properties can be the future of FO wastewater treatment applications.

Chapter 3: A review of Fouling mechanisms, control strategies and fouling mitigation in the FO process

This chapter is based on the following publication.

Ibrar, I., Naji, O., Sharif, A., Malekizadeh, A., Alhawari, A., Alanezi, A.A. & Altaee, A. 2019, 'A Review of Fouling Mechanisms, Control Strategies and Real-Time Fouling Monitoring Techniques in Forward Osmosis', *Water*, vol. 11, no. 4, p. 695.

Author's contributions:

Conceptualization, I.I., A.A. (Ali Altaee), O.N.; writing—original draft preparation, I.I., A.A. (Ali Altaee); writing—review A.S., A.A. (Alaa Alhawari), A.M., A.A.A.; supervision, A.A. (Ali Altaee), A.S., A.A. (Alaa Alhawari).

One of the major issues affecting membrane performance in osmotically driven membrane processes is fouling of the membrane. Membrane fouling occurs when particles or solutes accumulate on a membrane surface or inside the pores of the membranes (Lutchmiah, Verliefde, et al. 2014). These particles block pores, form a cake or gel type layer on the membrane surface and reduce membrane permeability (Roorda 2004). Fouling has several negative impacts on membrane performance, such as inducing its own concentration polarization, weakening the membrane rejection properties, and introducing additional hydraulic resistance (She et al. 2016). Although membrane technologies have advantages over other mature water treatment technologies, membrane fouling is still a major operational problem and needs further investigation (Chun et al. 2017).

Recently, forward osmosis (FO) has emerged as a promising membrane process and alternative to reverse osmosis (RO). FO uses an osmotic pressure gradient to permeate water through a semi-permeable membrane. The major advantage of FO over other pressure-driven membrane processes is that FO phenomena occur spontaneously, without the need for any hydraulic pressures (Mondal, Field & Wu 2017). Pressure-driven processes such as reverse osmosis (RO) and nanofiltration (NF) are driven by the hydraulic pressure gradient across the membrane and hence require high energy for operation. On the other hand, the FO process is driven by the natural osmosis phenomenon across

the membrane, and there is no need for a high-pressure pump. While there has been a rapid surge in the number of publications on the forward osmosis process, half of the papers (2013 to 2018) are dedicated to fouling studies (**Figure 3.1**).

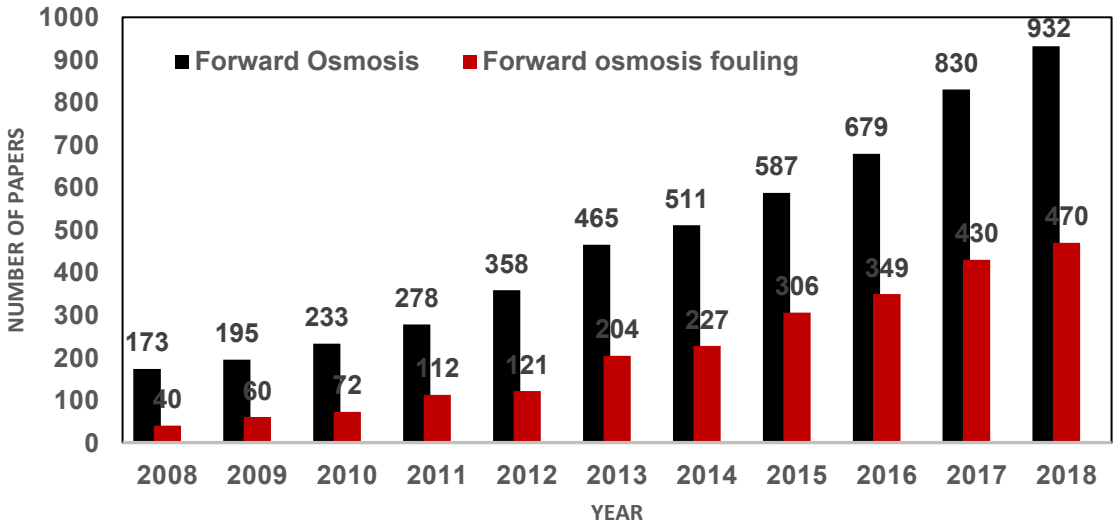

Figure 8.1: Number of publications on forward osmosis and forward osmosis fouling (Search done using Sciencedirect)

Fouling can occur at different locations on the forward osmosis membrane, such as on the active layer, on the surface of the support layer, or inside the support layer. Fouling in osmotically driven membrane processes can be classified into external and internal fouling, depending on the membrane orientation used. In FO mode (when the active layer faces the feed solution), the foulants are deposited on the active layer, leading to the cake-type layer formation. Fouling in this manner is called external fouling (**Figure 3.2a**). The fouling mechanism is more complicated in the PRO mode (when the active layer faces the draw solution). Suppose the size of fouling matters is smaller than the pores of the support layer. In that case, it can penetrate the support layer and be adsorbed on the walls of the support layer or retained by the active layer and deposited on the backside of the active layer. Smaller size foulants enter the support layer and attach to the foulants already deposited on the active layer leading to pore-clogging of the membrane or internal fouling (**Figure 3.2b**). Pore

clogging is the most severe type of fouling and is very hard to clean up (Zhao et al. 2016a). Additionally, the entrapment of foulants in the support layer reduces porosity and enhances internal concentration polarization (ICP) (Korenak et al. 2017).

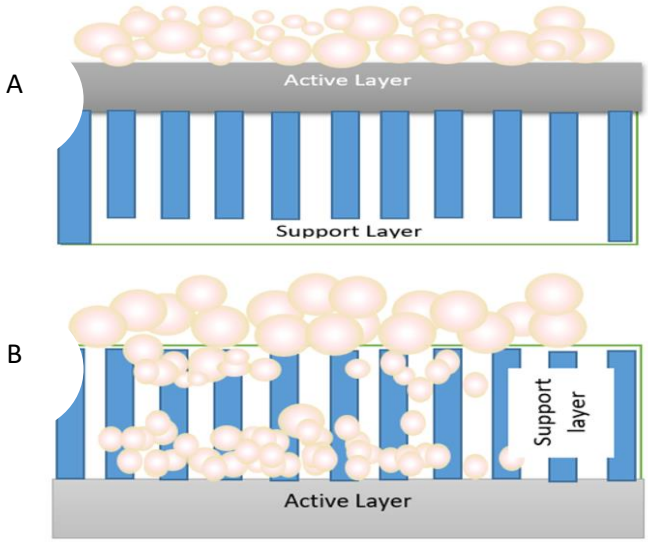

Figure 3.2: External Fouling in the FO mode

A) External Fouling in the FO mode. B). External and internal fouling in the PRO mode

Under severe fouling conditions, more foulants continue to deposit on the outer side of the support layer, leading to both external and internal fouling. If the foulant size is larger than the pore size, the foulant is just deposited on the outer side of the support layer leading to external fouling. External and internal fouling can occur in the PRO mode (active layer facing the draw solution) if the feed water contains a variety of foulants of different sizes. External fouling or surface fouling can be easily controlled via improving feed water characteristics or chemical cleaning (She et al. 2016). Therefore, it is generally more reversible than internal fouling (Arkhangelsky et al. 2012). However, external and internal fouling can be irreversible, depending on feed water characteristics (Jiang, Li & Ladewig 2017).

In this chapter, we will discuss the current trends in the forward osmosis membrane fouling impact of critical flux on fouling, effects of hydrophilicity, charge and morphology on membrane fouling,

coupled effects of concentration polarization and fouling on flux behavior, fouling in osmotic membrane bioreactor and control strategies for fouling and their effectiveness. Finally, this chapter discussed real-time in-situ techniques to monitor membrane fouling with their limitations.

3.1 Mathematical predictive model for fouling in forward osmosis

Hoek & Elimelech (2003) developed a cake enhanced osmotic pressure (CEOP) model for describing flux decline in salt rejecting membranes. The water flux decline in membrane processes depends not only on fouling but also on the driving force (Siddiqui et al. 2018). Mathematically, the water flux "J_w" *can* be expressed by equation [9].

$$J_w = \frac{F}{\mu(R_m+R_c)} \qquad [19]$$

Where F is the osmotic driving force in case of the FO process and hydraulic pressure for RO, μ is the viscosity of the solution, R_m is the resistance of the clean FO membrane and R_c represents the resistance of the cake layer. The osmotic driving force is also proportional to the apparent concentration driving force in the FO and can be divided into four components as shown in Table 3.1. (She et al. 2016).

Table 3.1: components of apparent concentration driving force in FO: Reference (She et al. 2016)

FO mode	**PRO mode**
Effective driving force $(\pi_{ds} - \pi_{fs}) - \Delta P$	Effective driving force $(\pi_{ds} - \pi_{fs}) - \Delta P$
Loss of driving force due to concentrative external concentration polarization $F_{cecp}\left(\pi_{fs} + \frac{J_s}{J_w}\beta R_g T\right)$	Loss of driving force due to concentrative external concentration polarization and concentrative internal polarization $F_{ccp}\left(\pi_{fs} + \frac{J_s}{J_w}\beta R_g T\right)$

Loss of driving force due to dilutive internal concentration polarization and dilutive external concentration polarization	Loss of driving force due to dilutive external concentration polarization
$\boldsymbol{F_{dcp}\left(\pi_{ds}+\frac{J_s}{J_w}\beta R_g T\right)}$	$F_{decp}\left(\pi_{ds}+\frac{J_s}{J_w}\beta R_g T\right)$

Putting the values of F in equation [9], the mathematical equation for flux in the FO mode and the PRO mode is given by equation [18] and equation [19], respectively.

$$J_w^{FO} = \frac{(\pi ds - \pi fs) - \Delta P - F_{cecp}\left(\pi_{fs}+\frac{J_s}{J_w}\beta R_g T\right) - F_{dcp}\left(\pi_{ds}+\frac{J_s}{J_w}\beta R_g T\right)}{\mu(R_m+R_c)} \quad [20]$$

$$J_w^{PRO} = \frac{(\pi ds - \pi fs) - \Delta P - F_{ccp}\left(\pi_{fs}+\frac{J_s}{J_w}\beta R_g T\right) - F_{decp}\left(\pi_{ds}+\frac{J_s}{J_w}\beta R_g T\right)}{\mu(R_m+R_c)} \quad [21]$$

Where F_{cecp}, F_{dcp} are concentration polarization factors for CECP at the active layer side and dilutive CP at the support side in FO mode and F_{ccp}, F_{decp} is concentration polarization factors for concentrative CP at the support layer side and DECP at the active layer side in the PRO mode.

The value of R_m can be measured via RO test by using a foulant free feed solution such as DI water. Alternatively, R_m can be calculated if the pure water permeability constant of the membrane is known:

$$A_w = \frac{1}{\mu R_m} \quad [22]$$

The value of R_m can be estimated by simplifying the osmotic-resistance-filtration model reported for RO (She et al. 2013) for osmotically driven membrane processes (She et al. 2016; Siddiqui et al. 2018). The value of cake layer resistance R_c can be estimated using the Carman-kozeny equation as given below.

$$R_c = \left[\frac{180(1-\epsilon)}{\rho_p d_p^2 \epsilon^3}\right] M_d \quad [23]$$

Where Є is the porosity of the cake layer, ρ_p is the particle density, d_p is the particle diameter and M_d is the mass per membrane unit area of the deposited cake layer. However, for the FO process, finding the value of R_c is hindered by several factors. According to Nagy et al. (2018) modelling the hydraulic resistance of external and internal fouling is challenging mainly due to a number of reasons. Firstly, the hydraulic diameters of foulants are not well described. Secondly, the support layer geometry of the FO membrane is not extensively studied, and it is unknown how much of the support layer will be filled with foulants. Therefore, an alternate model based on one-dimensional transport of salt and water perpendicular to the membrane was proposed by Tow, Rencken & Lienhard (2016). However, this model does not take into account the mechanism of internal fouling such as pore-clogging and can only be applied to foulants with known sizes or one with very large pores (more than 20nm).

3.2 Classification of membrane fouling in forward osmosis

Membrane fouling can be classified into four main categories: biofouling, organic, inorganic (mineral scaling) and colloidal fouling based on the type of foulants. Different types of fouling may occur simultaneously and can influence each other. Interestingly, most of the literature on the forward osmosis fouling studies have used model foulants simulating a single type of fouling condition on the membrane. For instance, if biofouling is investigated as a model foulant, *Pseudomonas aeruginosa PA01 GFP* is used to simulate biofouling conditions on the membrane. Similarly, organic fouling is simulated using alginate as a model organic foulant. It is unclear whether the results of fouling studies using simulating fouling conditions would apply to pilot or commercial applications with real wastewater or high saline water feeds since these waters would contain all the foulant types such as biofoulants, organic foulants, inorganic foulants and colloidal foulants simultaneously. In practice, membrane fouling is caused by a combination of different foulants. The membrane autopsy method can provide useful information about the origin and extent of membrane fouling, distribution of foulants and foulants composition and properties (Gorzalski & Coronell 2014). However, a fundamental understanding of fouling and fouling mechanisms is impossible through membrane autopsy (Jiang, Li & Ladewig 2017). In-situ and real-time fouling

monitoring techniques are vital to understanding fouling mechanism and cleaning strategies efficiency in the forward osmosis.

3.1.1 Biofouling

Biofouling, also known as microbial fouling, involves the deposition of live bacterial cells and the formation and growth of biofilm (Bogler, Lin & Bar-Zeev 2017). In forward osmosis, similar to other membrane processes, accumulation and growth of microorganisms on the surface of the membrane lead to biofouling (Bucs et al. 2016; Shannon et al. 2008; Vrouwenvelder et al. 2008). While other forms of fouling can be controlled with a variety of pre-treatments, biofouling is the most ubiquitous type and difficult to control due to the strong adhesion of bacteria onto the membrane surface and formation of the extracellular polymer matrix (EPS) (O'Toole, Kaplan & Kolter 2000). Biofouling can also lead to pore clogging and assist with other types of fouling such as inorganic fouling. These channelling matters can lead to precipitation of soluble salts and eventually scaling (Abid et al. 2017; Hausman, Gullinkala & Escobar 2009).

To understand biofouling in the FO process, it is important to understand the basic principles of biofilm formation due to bacterial attachment on a microscopic level. Goulter, Gentle & Dykes (2009) describes bacterial attachment to a surface as a two-step model; initial reversible attachment followed by an irreversible attachment. Weak van der Waals forces govern the initial reversible attachment, and it can be easily removed by shear forces such as rinsing or turbulent flow of the surrounding fluid. Still, in some cases, when the bacterial cell and the surface both are negatively charged, some cellular structures overcome the electrostatic repulsion force, resulting in irreversible attachment to the surface. In this case, shear forces such as rinsing or turbulent flow are not sufficient to remove the bacterial attachment; instead, physical or chemical cleaning is required to remove the formation of the bacterial cells. According to Goulter, Gentle & Dykes (2009), due to an excess of carboxyl and phosphate groups located in the cell walls of bacterial cells, the majority of the bacterial cells are negatively charged. Natural organic matter (NOM) or alginate is also negatively charged in aqueous solutions at neutral to high pH (Cornel, Summers & Roberts 1986).

Thus , to prevent adsorption of NOM or alginate on the FO membrane, a strong, negatively charged membrane would be ideal. However, some of these bacterial structures can still overcome the electrostatic repulsion, resulting in irreversible attachment. Therefore a negatively charged membrane may not be sufficient to mitigate biofouling.

Biofouling assessment in FO membrane studies is very limited in applications involving wastewater effluents (Valladares Linares, Li, et al. 2014). Lee et al. (2010) compared fouling behavior in the forward osmosis and the reverse osmosis, but only organic and colloidal model foulants were used in the experiments. A cake enhanced osmotic pressure (CEOP) intensified concentration polarization led to severe flux decline. However, this study only focused on the model organic and colloidal foulants, and biofouling was not discussed. Other studies were limited to silica scaling (or combined inorganic fouling with biofouling (Li et al. 2012; Myint et al. 2010).

Recently, Yoon et al. (2013) investigated the biofouling characteristics of the FO process compared to reverse osmosis using *Pseudomonas aeruginosa PA01 GFP* as model foulant. Results showed that biofouling is less severe in FO than in RO due to lack of hydraulic pressures, but cake enhanced osmotic pressure (CEOP) is more intense in FO compared to RO due to the reverse diffused salt from the draw solution. The cake layer formed by the entrapped foulants on the FO membrane prevents the back diffusion of salt (salt is trapped by the cake layer), thereby increasing osmotic pressure at the membrane surface, leading to a decline in water flux. Although CEOP is also a problem in RO, its effects are less pronounced [22]. The biofilm in the FO process appears to be loosely formed and is thicker than the biofilm in the RO process [25]. This finding also agrees with a previous study by Mi and Elimelech (Mi & Elimelech 2010b) in which a loose structure was reported for the fouling layer in the FO process. The biofouling impact on FO membrane was consistent even with different types of membrane materials or membrane structures. However, this finding does not agree with a previous study conducted by Mi and Elimelech (Mi & Elimelech 2010b), where membrane materials are reported to affect foulant-membrane interactions. The heterogeneous surface of polyamide (PA) membranes makes them more susceptible to foulant adsorption than cellulose acetate (CA) membranes [26]. Generally, it is considered that hydrophilic surfaces are more resistant to bacterial adhesion than hydrophobic surfaces (An & Friedman 1998).

Noting that thin-film composite (TFC) membranes are more hydrophilic than cellulose triacetate (CTA) membranes, under mild fouling conditions, surface heterogeneity becomes a more dominant factor in membrane fouling than surface hydrophilicity (Gu et al. 2013). On the other hand, under severe fouling conditions in the FO process, membrane surface plays a less important role in promoting membrane fouling. According to Yoon et al. (Yoon et al. 2013), combined organic and biofouling leads to a substantial flux decline compared to individual biofouling and organic fouling. Organic fouling caused by organic matter derived from microbial cellular debris can be considered an abiotic biofouling form. In contrast, biofouling is considered a biotic form of organic fouling (Amy 2008b).

3.1.2 Organic Fouling

Wastewater contains different organic macromolecules of organic colloids, which can be either hydrophobic (e.g. humic acids), hydrophilic (e.g. polysaccharides) or transphilic, leading to organic fouling (Chun et al. 2017). Among the different fouling types, organic fouling is perhaps the most poorly understood (Amy 2008a). Most studies on organic fouling have used simulated foulants such as sodium alginate, bovine serum albumin (BSA), Aldrich humic acid, Suwannee River humic acid etc. However, according to Parida and Ng (Parida & Ng 2013) simulated foulants would not be representative of actual foulants in real wastewaters.

Several studies have suggested that humic acid fraction of natural organic matter (NOM) is a major foulant that controls the rate and extent of fouling (Combe et al. 1999; Jones & O'Melia 2000; Yuan & Zydney 1999); while other studies have reported that polysaccharides (hydrophilic fraction) are the main cause of severe fouling in membrane processes (Shon et al. 2006). Humic acid is the portion of humic substances in natural organic matter which is soluble in water at high pH but insoluble at low pH (acidic conditions) [35]. In most FO experiments, model foulants used as humic acid is Aldrich humic acid (AHA). The adsorption of humic acid is enhanced in the presence of divalent calcium ions and reverse solute diffusion (Xie, Nghiem, et al. 2013b); possibly due to

electrostatic shielding by divalent cation [35]. Higher deposition of humic acid was found on the membrane when NaCl was used as draw solution (due to its high reverse salt flux) in comparison to $MgSO_4$, glucose and urea (Xie, Nghiem, et al. 2013b). However, it was concluded that humic acid did not penetrate membrane pores [35, 39]. Therefore, it would be safe to conclude that the humic acid portion of NOM does not control the rate and extent of fouling and is not a major contributor to internal fouling or pore-clogging. On the other hand, it was found that the adsorption tendency of polysaccharides is three times higher than humic acids (Jarusutthirak, Amy & Croué 2002). According to Fan et al. (Fan et al. 2001), the fouling tendency of different fractions in natural organic matter follows the order as shown in **Figure 3.3**.

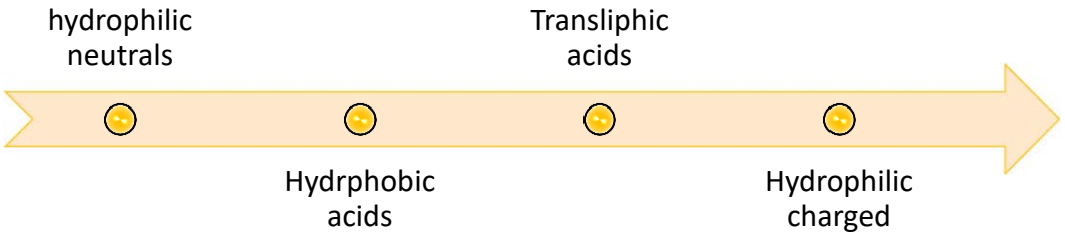

Figure 3.3: Order of fouling potential of fractioned natural organic matter by Fan et al. [33]. hydrophilic neutrals have the highest fouling tendency whereas hydrophilic charged have the lowest amongst these

Mi and Elimelech investigated organic fouling in the forward osmosis process using model organic foulants bovine serum albumin (BSA), sodium alginate and Aldrich humic acid. They observed a strong correlation between organic fouling and molecular adhesion. The strongest molecular interaction was in alginate due to calcium binding, and it formed a cake layer under all hydrodynamic conditions. In contrast, the weakest molecular interaction in BSA enabled it to form a cake layer only under favorable hydrodynamics. The behavior of Aldrich humic acid lied in between BSA and alginate, and no cake layer formation was reported in the FO mode. The study also concluded that before forming a cake layer, fouling is sensitive to intermolecular interactions and hydrodynamic conditions; however, once the cake layer is formed, a strong decline in flux occurs, and a change in hydrodynamic or intermolecular adhesion have little or no effect on the fouling

behavior. Membrane orientation did not affect alginate fouling, and a similar flux decline was observed in the FO and the PRO mode. AHA and BSA foulants had severe flux decline in PRO mode than the FO mode [44]. Parida and Ng (Parida & Ng 2013) reported similar results for strong flux decline in the PRO mode due to organic fouling and less flux decline for FO mode for all organic concentrations in the feed solution tested throughout the whole experimental runs. This again suggests why the FO mode is the most favorable treatment for wastewater treatment.

Lee et al.,(Lee et al. 2010) compared fouling behavior in the FO process and the RO under identical hydrodynamic conditions and feed water chemistries as well as plate and frame cells with identical channel dimensions. Alginate, Suwannee River humic acid (SRHA), and BSA were used as model organic foulants in the experiments representing polysaccharides, natural organic matter, and proteins. There was a significant decline in water flux for alginate and humic acid for the FO experiments, while a lower decline in the water flux was observed for BSA. The decline in the water flux was mainly attributed to the cake enhanced osmotic pressure due to the reverse salt diffusion from the draw solution. The diffused salt is trapped in the cake/gel type layer. It has been proved that a thin fouling layer in salt rejecting membranes may cause significant flux decline through cake-enhanced salt concentration polarization (Hoek & Elimelech 2003). This significant flux decline is not due to the resistance of the cake layer but rather due to enhanced concentration polarization (Lee et al. 2010). This implies that fouling combined with reverse salt diffusion is responsible for significant flux decline. An efficient FO process needs further investigation of ideal draw solute and membranes with better selectivity.

According to Lee et al. (Lee et al. 2010), BSA exhibits lower flux decline due to Homfeister effects, also known as salting in or salting-out effects. Due to this effect, the BSA protein undergoes a structural deformation and allow the protein fouling layer to be removed by shear hydrodynamic conditions. The study also found that fouling in the FO is almost reversible than fouling in the RO, and this is mainly attributed to the loose fouling layer formed in the FO due to the lack of hydraulic pressures.

In order to fully understand organic fouling, further research is needed using real wastewaters, as simulated foulants may not reflect the actual foulants in real wastewater. To understand their impact on flux decline, reverse salt diffusion coupled with cake layer formation needs to be investigated for different draw solutes.

3.1.3 Inorganic Scaling

Inorganic scaling is caused mainly by the retention of sparingly soluble mineral salts such as calcium carbonate, calcium sulphate, barium sulphate, magnesium salts, silica etc. (Fane 2016). When the concentration of these salts in the feed exceed their solubility at higher water recovery rates, precipitation may occur near or on the membrane surface leading to scaling of the membrane surface and flux decline (Fane 2016; Mi & Elimelech 2013). Amongst the various scaling compounds reported in the literature are silica, calcium carbonate, gypsum and calcium sulphate (Choi et al. 2014; Lee & Kim 2017; Mi & Elimelech 2010a, 2013; Xie & Gray 2017; Zhang, Shan & Tang 2016).

Amongst the various inorganic scalants, silica is the most common type of salt that causes scaling in membranes (Mi & Elimelech 2013). Silica is abundant in most natural water resources, has low solubility, and when concentrated beyond its solubility limit of approximately 120mg/L, precipitation may occur, and it forms a hard scale that is difficult to remove (Bush et al. 2018). Typically, silica scaling comprises silica deposition on the membrane surface and the subsequent formation of a silica film through polymerization (Mi & Elimelech 2013).

Several studies have investigated silica scaling in the forward osmosis membrane (Mi & Elimelech 2013; Xie & Gray 2017); but literature on silica scaling and cleaning behavior is rather limited (Li et al. 2012). Mi and Elimelech (Mi & Elimelech 2013) investigated silica scaling and cleaning behavior in the forward osmosis. RO experiments were also conducted in parallel for comparison purposes. Identical flux decline was observed in the FO and RO under similar hydrodynamic conditions, but flux recovery in the FO process was higher than the RO. Membrane material also had an impact on

silica scaling. According to Mi and Elimelech (Mi & Elimelech 2013), cellulose acetate (CA) membranes showed a higher recovery rate than polyamide (PA) membranes. The silica layer on the PA membrane was difficult to remove due to the strong adhesion force between the membrane surface and the silica gel.

A recent publication by Xie and Gray (Xie & Gray 2017) also shows the impact of silica scaling on cellulose triacetate (CTA) and thin-film composite (TFC) membranes. The study concluded that the silica scaling mechanisms on the CTA and TFC membranes were largely different. The CTA membrane was more resistant to silica scaling and exhibited a gradual flux decline compared to the TFC membrane. The TFC membrane is characterized by a high carboxylic acid functional group density, leading to its high fouling propensity (Xie & Gray 2017). Dipoles in carboxylic functional groups allow easy participation in favorable hydrogen bonding interactions (Brück, McCoy & Kilway 2000). The mono-silicic acid interacts with the carboxyl functional group (Si-O bonding) on the TFC membrane surface, followed by silica polymerisation on the membrane surface, leading to a strong flux decline [45]. It is also well known that calcium easily binds with carboxylic acid groups and can accelerate fouling (Li et al. 2012). Membrane surface chemistry also plays a key role in gypsum scaling. Another Study by Xie and Gray (Xie & Gray 2016) concluded that TFC membrane was subject to more severe gypsum scaling compared to CTA membrane. Similar findings were reported by Mi and Elimelech (Mi & Elimelech 2010a), and gypsum scaling of PA membranes was reported to exhibit severe flux decline compared to CA membranes.

Reverse diffusion of draw solutes can also have an impact on membrane scaling. Reverse diffusion of divalent ions such as Mg^{2+} and Ca^{+2} interact with dissolved organic matter present in the feed solution through a bridging effect, significantly affecting cake layer formation and flux decline (Hatziantoniou & Howell 2002; Lee & Elimelech 2006). Lee and Kim (Lee & Kim 2017) investigated calcium carbonate ($CaCO_3$) scaling on the TFC FO membrane by comparing NaCl and NH_3-CO_2 as draw solutes. Using NaCl as a draw solute in the presence of Ca^{2+} ions in the feed solution, water flux did not decline significantly because Na^+ and Cl^- ions do not chemically react with Ca^{2+} ions in the feed. Osmotic backwashing restored the water flux to its original, showing that fouling is reversible when NaCl is used as draw solute. On the other hand, when NH_3-CO_2 was used

as a draw solution, a severe flux decline was observed in the presence of Ca^{2+} in the feed as well as a severe white scaling of $CaCO_3$ was observed on the membrane active layer due to the reverse diffusion of HCO_3^- ions into the feed side. The high selectivity of the TFC membrane prevented the flux of Ca^{2+} ions into the draw side. The HCO_3^- ions chemically react with Ca^{2+} ions to form $CaCO_3$ scaling on the active layer of the membrane.

3.1.4 Colloidal fouling

Colloidal fouling is a persistent problem in many membrane processes and is caused by colloidal particles (Singh & Song 2007). Colloidal particles are small negatively charged particles that are intermediate in size between suspended solids and truly dissolved solids (T. Brunelle 1980). The colloids in feed water often include clay, silica, corrosion products, and bacteria. When concentrated on a membrane surface, these particles lead to poor productivity of the FO system and sometimes salt rejection of the membrane.

Boo et al. (Boo et al. 2012) investigated colloidal fouling in the FO process using a suspension of silica nanoparticles as model colloidal foulants. Results suggested that salt due to reverse diffusion accumulates on the fouling layer formed by the colloidal particles and increases the cake enhanced osmotic pressure, reducing net osmotic driving force and permeate flux. Physical cleaning with high cross-flow velocity restored the flux, which shows that colloidal fouling is reversible in FO; however, when particles aggregate under conditions of high salt concentration due to reverse salt diffusion and high feed solution pH, flux was not recovered.

3.2 Factors affecting FO membrane fouling and performance

3.2.1 The critical flux concept and impact of flux on fouling in forward osmosis

The critical flux concept states that significant membrane fouling occurs when the water flux is above some critical value (Zou et al. 2011) or the permeate flux at which an irreversible deposit on the membrane surface appears (Espinasse, Bacchin & Aimar 2002). In a more general definition, it is the first permeate flux at which fouling becomes noticeable (Bacchin, Aimar & Field 2006). Until now, very few FO publications (**Figure 3.4**) discuss the relationship between critical flux and fouling behavior. Wang et al. (2010) demonstrated that the critical flux concept in pressure-driven membrane processes could also be applied to osmotically driven membrane processes such as the FO process. Wang and his co-workers carried out a direct microscopic observation of the FO process using latex particles as a model foulant. The observations revealed that at a flux of 15 L/m^{2}h, the surface coverage of the membrane by the foulant was negligible. At a flux of 28 L/m^{2}h small amount of coverage appeared on the FO membrane. When the flux value exceeded 41 L/m^{2}h , the surface coverage by the latex particles was drastically increased. This suggested that the critical flux value of the FO process was somewhere close to 28 L/m^{2}h.

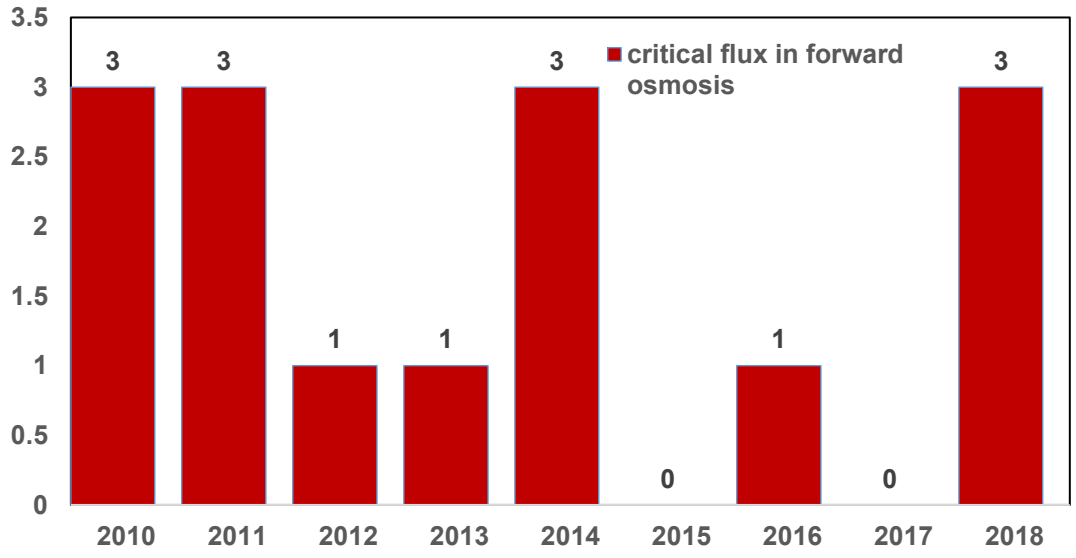

Figure 3.4: Number of papers discussing critical flux in forward osmosis since 2010. Search done on Google scholar database using keywords "critical flux in forward osmosis"

According to Zou et al. (2011), the critical flux value in the FO process decreases when a draw solution containing divalent ions such as MgCl2 is used as a draw solution. On the other hand, when NaCl was used as a draw solution, significant flux decline was not observed for flux as high as 30L/m^2h. Some researchers have associated critical flux value with a critical draw solution concentration (concentration of DS above which significant fouling occurs) (Zou et al. 2011; Zou et al. 2013). Interestingly, while the presence of divalent calcium ions in the feed solution exacerbates fouling, keeping the initial flux value below the critical flux will have a negligible effect on calcium ions on fouling behavior(Liu & Mi 2012).

Feed spacer and membrane orientation also significantly impact critical flux behavior in the FO process (Wang et al. 2010; Zou et al. 2013). Feed spacers are reported to enhance critical flux significantly (Wang et al. 2010). According to Wang and his co-workers (Wang et al. 2010) critical flux was enhanced to about 52 L/m^2h in the presence of feed spacer, whereas in the absence of feed spacers, a critical flux of 28 L/m^2h was observed. In the absence of feed spacer, the membrane will experience a severe external concentration polarization (ECP), which can indirectly promote internal concentration polarization (ICP) and thus lead to a dramatic flux decline (Wang et al. 2010). The high fouling propensity of the membrane in the PRO mode and low fouling propensity in the FO mode can also be explained in terms of critical flux. Significant fouling deposition and water flux decline were observed at a similar baseline water flux in the PRO mode. In contrast, less fouling deposition and stable water flux are achieved in the FO mode (Zou et al. 2013). Similar results were reported by Wang et al. (2010) and Zhao, Zou & Mulcahy (2011). The impact of different spacer designs feed spacer location and the impact of operating parameters on critical flux behavior is still unknown and can be future work on the FO process.

3.2.2 Effects of hydrophilicity, charge and morphology on FO membrane fouling

Generally, if the water contact angle is less than 90^0, the surface is considered hydrophilic, and if the contact angle is greater than 90^0 the surface would be hydrophobic. A contact angle of 0^0 would ideally result in complete hydrophilicity or wetting of the surface. Hydrophilic enhancement of TFC FO membrane is an effective approach to improve FO membrane performance (Park et al. 2018) and resilience against fouling It is generally assumed that increasing hydrophilicity of a membrane will provide more opportunity for water rather than foulants to chemically associate with a membrane surface (Kumar & Ismail 2015). Increasing hydrophilicity of a membrane is preferred over decreasing the thickness because it can selectively increase the water flux without increasing reverse salt flux (Yu et al. 2011). A number of studies have focused on modifying the support layer of the TFC FO membrane by incorporating hydrophilic functionalized nanomaterials such as graphene oxide, carbon nanotubes, titanium dioxide and silica nanoparticles (Park et al. 2018). Some of these studies are listed in Table [3]. One study found that the higher the titanium dioxide loading on Psf-TiO_2 substrate of TFC membrane, the lower the contact angle (high hydrophilicity) and increase porosity (Emadzadeh et al. 2014). However, the higher loading of the nanoparticles compromised the NaCl rejection of the membrane. A more simple way to increase the hydrophilicity of a membrane is by using coatings of hydrophilic polymers like PVA (polyvinyl alcohol). However, to render PVA stable in an aqueous phase, it must be cross-linked with other materials such as glutaraldehyde to reduce its water solubility (Park et al. 2018). Hydrophilic polymers such as PVA, PVP (polyvinyl pyrrolidone), PEG (polyethylene glycol) often act as pore formers and improve the hydrophilicity of membrane surface (Kumar & Ismail 2015)

The surface charge of a membrane also plays a vital role in fouling. Most natural organic matter (NOM), proteins, colloidal particles are negatively charged in an aqueous solution at high pH (Cornel, Summers & Roberts 1986); the presence of negatively charged groups on a membrane surface can electrostatically repel these foulants. However, neutrally charged surfaces with high hydrophilicity are preferred to achieve high resistance to biofouling by both positively and negatively charged foulants (Kumar & Ismail 2015). Some researchers have fabricated hollow fiber FO membranes with a positively charged NF like skin using polyamide-imides (Setiawan et al. 2011). Compared to a neutral membrane, the positively charged membrane provided double

isoelectric points to the salt transfer through the membrane in the FO mode, leading to a lower salt penetration. In contrast, the positively charged surface facilitated salt transportation in the PRO mode.

Table 3.2: Modification of FO membranes to alter hydrophilicity, charge and morphology

Base material	Major factor affecting fouling	Modification	Results	Reference
PVDF nanofiber support	Hydrophilicity and morphology	PVDF Nanofiber support was modified via dip coating and crosslinked with glutaraldehyde.	34.2 LMH flux and improved strength	(Park et al. 2018)
Polysulfone support layer substrate	Hydrophilicity, morphology	A PA layer was formed by interfacial polymerization on top surface of Psf-TiO_2 substrate	Improved water flux	(Emadzadeh et al. 2014)
Polysulfone support layer	Hydrophilicity, surface roughness and charge	Zwitterions incorporation onto the polyamide active layer of forward osmosis membrane	Good antifouling properties, marginal reduction in flux with time.	(Chiao et al. 2019)
Polysulfone support layer	Hydrophilicity	TFC membrane was coated with Polydopamine/ graphene oxide PDA/GO	Enhanced water flux	(Choi et al. 2019)
Polyether sulfone support	Hydrophilicity,	TFC membrane was	These	(Ni & Ge

	charge and morphology	modified using an aniline sulfonate/bisulfonate functionalized polyamide layer formed by interfacial polymerization on support layer.	membranes had more hydrophilic and smoother surfaces, which increases their antifouling abilities. Higher water recovery efficiency and low RSF.	2018)
PA rejection layer	Hydrophilicity and charge	Wheel POM (polyoxometalates) coated silica nanoparticles were incorporated within the PA layer matrix of TFC FO membrane.	Antifouling and high water permeability	(Shakeri et al. 2019)
N/A	Hydrophilicity and modified surface	Prototype Aquaporin based polyamide TFC FO membrane	Good antifouling behavior and water permeability than commercial HTI membrane	(Chun et al. 2018)

Polyether sulfone support	Hydrophilicity and surface	Reduced graphene oxide was coated on the PES support layer	Improved fouling behavior and excellent flux recovery	(Rastgar et al. 2019)
TFC-FO membrane surface	Hydrophilicity and charge	polyamidoamine (PAMAM) dendrimer was grafted on TFC membrane surface via covalent bonds	Robust antifouling capability, electrostatic repulsion improved ammonium ion selectivity.	(Bao et al. 2019)
sulfonated polyethersulfone-polyethersulfone support SPES-PES	Hydrophilicity	A thin active layer was developed using Chitosan through a facile method. The salt rejection was increased by NaOH treatment of the embedded Chitosan.	Membrane showed better permeability than commercial TFC membrane	(Shakeri, Salehi & Rastgar 2017)
PES Support	Hydrophilicity and charge	Molybdenum disulphide MoS_2 coated FO membrane	Higher water flux, low reverse salt flux and good antifouling behavior.	(Li, Sun, et al. 2018)

PES Support	Hydrophilicity	Zwitterion-silver nanocomposite structure was built on the membrane surface	Improved water flux and excellent biofouling resistance	(Qiu & He 2018)
Polysulfone support	Hydrophilicity and charge	Monodisperse surface-charged submicron polystyrene particles were designed, synthesized, and blended into Polysulfone (PSF) support	Increased hydrophilicity and reduction in concentration polarization.	(Zuo et al. 2018)
N/A	Hydrophilicity and reduced membrane roughness	Polydopamine coating on commercial HTI FO membrane	Improved antifouling performance	(Guo et al. 2018)
Polyether sulfone support	Hydrophilicity and smooth surface	Chemically modified TFC FO membrane	Improved resistance against fouling	(Xu & Ge 2018)
Polysulfone support	Hydrophilicity and morphology	Blending sulphonated polyether ketone (SPEK) as substrate material	Increased water flux, reduced membrane thickness, and morphology was changed from finger to	(Han et al. 2012)

			sponge like morphology. 50 LMH flux in PRO mode with DI water as feed solution.	
Polyamide-imide substrate	Charge	Hollow fiber membrane with a positively charged NF like selective layer	Better performance than a neutral membrane in terms of salt transportation and salt penetration	(Setiawan et al. 2011)

Controlling the support layer morphology during membrane fabrication can significantly enhance the performance of FO membrane (Yip et al. 2010). Membrane surface morphology also greatly influences foulant-membrane interaction (Mi & Elimelech 2008). TFC FO membranes fabricated with a sulphonated material in the substrate can exhibit a full sponge (if 50% sulphonated material) or finger-like structure (if less than 50%) (Widjojo et al. 2011). Such membranes have increased hydrophilicity and good flux and antifouling behavior. A full sponge-like structure with good antifouling properties is preferred for the long term stability of the membrane (Widjojo et al. 2011), while a finger-like morphology with large macrovoids has been proved to maximize porosity (Tiraferri et al. 2011).

3.2.3 Other factors limiting membrane performance

Besides fouling the membrane, many other factors limit forward osmosis membrane performance and hence cause a reduction in permeate flux across the semi-permeable membrane. Due to these factors, the water flux is much lower than anticipated based on the osmotic pressure difference between the draw and feed sides and the water permeability coefficient of the membrane. Water flux is of critical importance in all osmotically driven membrane processes, and according to Lay et al. (2012), water flux determines the productivity and, ultimately, the viability of the process. In osmotically driven membrane processes, concentration polarization can take place on both sides of the membrane(McCutcheon & Elimelech 2006a). On the feed side, the solute is concentrated at the membrane surface. This is referred to as concentrative external concentration polarization or CECP. CECP is similar to concentration polarization in pressure-driven membrane processes (Cath, Childress & Elimelech 2006a). On the draw side, the solute is diluted at the membrane surface and is referred to as dilutive external concentration polarization or DECP. In most flux models for FO, the effects of ECP are assumed to be negligible because of low water fluxes, high mass transfers (Lutchmiah, Verliefde, et al. 2014) and no hydraulic pressures (Cath, Childress & Elimelech 2006a). It has been shown that ECP plays a minor role in osmotically driven membrane processes compared to pressure-driven membrane processes and is not the main cause of flux decline in osmotic driven processes (McCutcheon, McGinnis & Elimelech 2006a). ECP effects were ruled out when NaCl dissolved in deionized water was used as feed solution in the study conducted by McCutcheon et al. (McCutcheon, McGinnis & Elimelech 2006a); however, ECP severely impact feeds with high total dissolved solids(Lutchmiah, Verliefde, et al. 2014). Waste from different industries such as food processing, mining operations, oil and gas operations, power plants, landfills, pharmaceutical manufacturing are large sources of total dissolved solids (TDS). According to research by Wang et al. (Wang, Zhang, et al. 2016) the dominant factor for osmotic pressure drop in FO is internal concentration polarization (ICP), however, the effects of ECP can't be ignored when treating high salinity solutions using FO. Therefore, ECP effects should be considered when treating complex feeds such as wastewater.

It is generally known that high crossflow velocities, turbulence or manipulating the water flux can mitigate ECP (Kragl 1997). According to Gruber et al. (Gruber et al. 2011), increased cross-flow

velocities reduce ECP at the membrane, leading to higher permeate flux. Significant ECP is observed on the draw side when cross-flow velocity is less than one meter per second. In contrast, ECP on the feed side is insignificant using realistic cross-flow velocities. Results from the study further revealed that concentrative ECP on the feed side would only become significant when cross flow velocity on the feed side is almost comparable to membrane flux. Simulations done in this study showed that ECP is more significant when low cross flow velocities are used and mass transfer promoting spacers are absent. It must be kept in mind that increasing cross flow velocities entail additional energy consumption (Zhang, Cheng & Yang 2014). Another way to reduce the effects of ECP is by manipulation of flux. But since water flux in FO is already low, the ability to diminish ECP effects by reducing flux is limited (Cath, Childress & Elimelech 2006a).

While ECP can be mitigated by high crossflow velocities and well-designed hydrodynamics, as discussed above, internal concentration polarization or ICP occurs inside the porous support layer in asymmetric membranes and is challenging to mitigate by simply changing cross-flow velocities or hydrodynamics. ECP occurs in both pressure-driven and osmotic-driven membrane processes; on the other hand, ICP is exclusive to FO (Gray, McCutcheon & Elimelech 2006). ICP is considered a major challenge in FO, and it leads to reduce water flux and increased reverse salt diffusion (Lutchmiah, Verliefde, et al. 2014). ICP can be further categorized into concentrative internal concentration polarization or CICP and dilutive internal concentration polarization or DICP.

When the active layer faces the feed solution (AL-FS mode or FO mode), the water permeates through the porous support layer. It dilutes the draw solution inside the support layer, leading to dilutive internal concentration polarization or DICP. At the same time, concentrative ECP is present on the active layer in the FO mode. On the other hand, when the active layer faces the draw solution (AL-DS mode or PRO mode), as water permeates through the membrane, the solutes are concentrated inside the porous support layer giving rise to concentrative internal concentration polarization or CICP. At the same time, dilutive ECP takes place on the active layer.

Several researchers have investigated the use of ultrasound waves to mitigate internal concentration polarization. One such effort was done by Choi et al. (Choi et al. 2018) using frequencies of 25, 45 and 72 KHz over an output power range of 10-70W. Experimental results indicated that ultrasound can only mitigate the adverse effects of ICP but cannot overcome it completely. Another effort using

ultrasound was done by Heikkinen et al. (Heikkinen et al. 2017), in which a novel ultrasound-assisted forward osmosis system was developed. The study demonstrated that sonification effectively mitigated ICP and enhanced water flux (35 LMH with ultrasound and 20 LMH without ultrasound for TFC membrane using sodium sulphate as DS). However, using ultrasound waves had drawbacks in both the works mentioned above. In the first study by Choi et al (Choi et al. 2018) membrane damage was reported at a frequency of 25KHz regardless of the intensity. In the second publication by Heikkinen et al. (Heikkinen et al. 2017) high water flux was accompanied by high reverse salt flux. Several studies have associated high reverse salt flux with membrane damage as well (She et al. 2013; She, Jin & Tang 2012; Wang, Duan, et al. 2016; Xie, Tang & Gray 2016).

Alternatively, the use of spacers has been investigated to overcome ICP effects in the FO. According to Hawari et al. (Hawari, Kamal & Altaee 2016) CICP could be mitigated by using a spacer and increasing feed solution flow rate and DICP is aggravated by increasing draw solution flow rate. Zhang et al. (Zhang, Cheng & Yang 2014) investigated the effect of spacer location to mitigate dilutive ICP without energy input. Results demonstrated that placing the spacer (1mm x 1 mm) in the draw channel with one end of a spacer connected to the membrane can mitigate DICP, and placing a spacer in both the feed and draw channels with one end connected to the membrane can be a method to reduce the effects of CECP and DICP in the FO mode. However, the location of placing spacer seems controversial as another study by Wang et al (Wang, Zhang, et al. 2016) recommends placing a small spacer in contact with the active layer in the feed channel and 2.7 mm away from the support layer in the draw solution channel. However, spacers are reported to induce membrane deformation in FO in the presence of gypsum scaling (Xie, Tang & Gray 2016) and PRO(She et al. 2013) under high pressures while increasing feed solution flow rate leads to a loss in the recovery rate (Jung et al. 2011).

There has been tremendous research done in the field of membrane fabrication to reduce the effects of ICP. These efforts are using double-skinned membranes nanofiber composite membranes, increasing the hydrophilicity of membranes, increasing porosity, reducing the thickness of the support layer or reducing the tortuosity of the support layer (Emadzadeh et al. 2014; Han et al. 2012; Liu & Ng 2015; Puguan et al. 2014; Song, Liu & Sun 2011; Wang, Ong & Chung 2010; Wei et al. 2011; Zhou, Lee & Chung 2014). Several researchers have investigated the use of symmetric FO

membranes in which the support layer is eliminated completely, resulting in no internal concentration polarization (Li, Karanikola, et al. 2018). Porous single-layer graphene oxide membranes also exhibited zero internal concentration polarization and high water flux (3 times higher than cellulose triacetate FO membrane) (Gai & Gong 2014). However, thin membranes exhibit low mechanical strength and may require frequent replacement in the event of damage. Apart from this, most novel membrane fabrication techniques are quite expensive, time-consuming, requires a long time to scale up, and have intricate processes (Zhang, Cheng & Yang 2014); therefore, a simple, effective and efficient way needs to be investigated to minimize ICP in future-forward osmosis applications.

In forward osmosis, water permeates from the feed side to the draw side due to the high osmotic pressure of the draw solution. However, no membrane is perfect, and a small amount of draw solute also diffuses back to the feed side (Phillip, Yong & Elimelech 2010). This phenomenon occurs because of the high concentration difference between the draw solution and the feed solution(Hickenbottom et al. 2013) and is therefore inevitable in the FO process (Zhao et al. 2012). As a result of this reverse salt diffusion, there is a decrease in the net driving force across the membrane and hence reverse salt diffusion is considered a major bottleneck in the FO operation.

Reverse salt diffusion is a unique mass transport phenomenon that can potentially impact FO membrane fouling (Xie, Bar-Zeev, et al. 2015). Wastewater contains a variety of foulants depending on the type of wastewater used. Major foulants in impaired water are microorganisms, organic matter and inorganic matter, which tend to form a fouling/ gel type layer on the membrane surface (Lutchmiah, Verliefde, et al. 2014). Once salt diffuses from the draw side to the feed side, it accumulates on the fouling layer formed on the membrane surface leading to a net reduction in driving force and the permeate flux decline. Lee et al. (Lee et al. 2010) suggest that this reduction in water flux due to reverse salt diffusion is mainly due to a cake-enhanced-osmotic pressure rather than increased resistance of the fouling layer formed on the membrane. Reverses salt diffusion in the FO exacerbates the cake-enhanced osmotic pressure within the fouling layer leading to elevated osmotic pressure on the feed side, as a result of which there is a net reduction in driving force and hence leads to substantial flux decline.

In forward osmosis, reverse salt diffusion is generally attributed to two main factors, the type of draw solution and the selectivity of semi-permeable membrane used. An ideal draw solute for the forward osmosis process should have osmotic pressure high enough to promote a high water flux across the membrane and limit reverse salt diffusion (Nguyen et al. 2018). According to Achilli et al. (Achilli, Cath & Childress 2010) the lowest reverse salt flux is exhibited by draw solutions containing larger-sized hydrated anions such as $MgSO_4$,$KHCO_3$, $NaHCO_3$, Na_2SO4 , $(NH_4)_2SO_4$ and K_2SO_4 , regardless of their paired cations, and reverse salt diffusion through the negatively charged CTA membrane is likely controlled by the hydrated anion size. Based on the solution diffusion mechanism for transport through a semi-permeable FO membrane, it is likely that cations and anions pass through the membrane as a pair to maintain electro-neutrality (Irvine et al. 2013; Yaroshchuk, Bruening & Licón Bernal 2013). However, NH_4HCO_3 showed the highest reverse salt flux despite the larger size ($450x10^{-12}$ m) of HCO_3^- anion and $KHCO_3$ as well as $NaHCO_3$ exhibited the lowest reverse salt flux, which shows that reverse salt flux is not dependent on the size of hydrated anion, or cation, rather overall molecular size of the solute may be a factor. For instance, draw solutions with high molecular size such as TMA-CO_2 (Boo, Khalil & Elimelech 2015) have less reverse salt diffusion than NH3-CO2 and therefore draw solutes with high osmotic pressure. Large molecular sizes need further investigation to minimize reverse salt diffusion issues.

Reverse diffusion is also a crucial factor to consider when the draw solutions containing nitrogen and phosphorous are used as these cause eutrophication in the receiving water environment (Phuntsho et al. 2011). In fertilizer driven forward osmosis by Phuntso et al. (Phuntsho et al. 2011) $(NH_4)_2SO_4$ exhibited the lowest reverse salt flux, whereas NH_4NO_3 showed the highest reverse solute flux amongst the selected fertilizers. The lowest flux of NH_4NO_3 was attributed to the smaller hydrated diameter of both ions. The reverse diffusion of Draw solute also impacts fouling and fouling reversibility in the forward osmosis process. Reverse ionic flux by NaCl is also reported to promote humic acid fouling (Xie, Nghiem, et al. 2013b), and divalent cations such as Ca^{2+} and Mg^{2+} are shown to promote organic fouling in comparison with monovalent such as Na^+ (Zou et al. 2013). Moreover, another study reports that the reverse diffusion of draw solutes (especially divalent cations) can change the feed solution chemistry and promote alginate fouling (She et al. 2012).

Additionally, reverse permeation of divalent cations results in dramatically different biofouling behavior (Xie, Bar-Zeev, et al. 2015).

While fouling in FO is reversible using simple physical cleaning, reverse diffusion of salt can hinder the reversibility (Boo et al. 2012). Therefore, in selecting draw solutes for the forward osmosis, the reverse diffusion of draw solutes into the feed side and the risk of induced fouling should be evaluated (She et al. 2012). Membranes with high selectivity should be coupled with the selected draw solute to reduce reverse salt flux and foul the forward osmosis membrane.

In an effort to reduce reverse salt flux and internal concentration polarization, Zhang et al. (Zhang et al. 2010) investigated a phase inversion process of CA membranes by introducing different casting conditions and coagulant baths. Membrane with ultra-thin selective layer and a fully support layer were fabricated. Amongst the different membranes, double dense layer membrane exhibited the lowest reverse salt flux of about 1gMH, which implies its great suitability for seawater desalination and wastewater treatment. Another novel approach that has recently attracted some attention is assisted forward osmosis, also known as AFO. AFO has been recently investigated and claimed to reduce reverse salt flux (Blandin et al. 2013). Through careful considerations that should be given to keep membrane integrity, AFO seems promising in minimizing reverse salt leakage and enhancing water flux in the forward osmosis process.

3.2.4 Coupled effects of concentration polarization and fouling on flux behavior in forward osmosis

Concentration polarization and fouling are the main factors responsible for flux decline in the FO process. Tang et al. (2010b) systematically investigated the coupled effects of ICP and fouling on flux in the FO process. Results revealed that the stable flux in the FO mode is at the expense of severe initial ICP. In contrast, the PRO mode under fouling conditions is subject to pore-clogging of the support layer, enhancing the effects of ICP, CEOP, and reducing membrane permeability. However, this study did not explore the combined effects of external concentration polarization (ECP) and fouling on flux decline in the FO process. The effects of ECP cannot be ignored in the FO

process when treating high saline streams or feeds with high fouling propensity, such as wastewater. Particularly in the FO mode, the effect of concentrative ECP on the feed side is higher when feeds with high total dissolved solids (TDS) are used (Phuntsho et al. 2013). According to Parida & Ng (2013), in the PRO mode, increasing organic foulants concentration in the feed solution increased external concentration polarization effects at the membrane surface, leading to more severe organic fouling and flux reduction. On the other hand, increasing organic loading in the feed solution had minimal impact on flux decline in the FO mode. In the FO mode, a high cross flow velocity of 50 cm sec^{-1} was used in this study, and hence the effect of ECP was negligible.

Fouling in a broad scope could be caused by cake-enhanced osmotic pressure, concentrative CP on the feed, reverse salt flux, or even the dilution of the draw solution. Information about the type of feed and draw solution should be available in order to understand the reason for water flux. Several lab size FO tests are performed on NaCl draw solution and DI feed water and hence decline in water flux is mainly due to CP. In general, ionic draw solution prepared in the lab, such as NaCl, has very low fouling propensity. Still, ions diffusion across the membrane and reaction with organic and inorganic matters in the feed solution may cause fouling problems. Scaling is also possible when there is an interaction between the components of DS and FS due to diffusion across the membrane. As demonstrated in experimental studies, the membrane charge and surface morphology are responsible for membrane fouling.

Therefore, the best approach to minimize fouling should be through conducting a pilot study to understand the best operating parameters and membrane options. This includes type and concentration of DS, type of FO membrane, recovery rate, pretreatment etc. This approach is similar to pilot studies in commercial RO desalination plants that are carried out before RO plant design and commissioning. Pilot studies will help avoid any major problems and provide skills for troubleshooting. In the case of commercial FO plants, pilot studies are recommended to select the type and concentration of DS, membrane type and any other requirements such as pretreatment.

3.3. Fouling mitigation in the FO process

3.3.1 Fouling and fouling mitigation in osmotic membrane bioreactor (OMBR)

Osmotic membrane bioreactor (OMBR) has recently gained popularity due to its low fouling propensity and ability to produce high-quality water from wastewater (Achilli et al. 2009). However, the performance of OMBR is hampered by fouling. The fouling mechanism in the OMBR is more complicated than the direct FO due to activated sludge's nature as it contains a variety of foulants and microorganisms (Zhang et al. 2012). Long-term investigation of the fouling mechanism in the FO and OMBR revealed that flux decline is more severe in the direct FO than in the OMBR (Sun et al. 2016). The severe flux decline in the direct FO is due to severe organic, inorganic and biofouling (Sun et al. 2018). Short term investigation (7-8 hours) of OMBR operation revealed that reversible and irreversible fouling is absent even with different types and concentrations of draw solutions when the active layer faces the feed solution and the system is operated at low water flux (Cornelissen et al. 2008b). However, it should be pointed out that in the short term operation of the OMBR, there is very little salt accumulation in the bioreactor (Achilli et al. 2009), and membrane fouling in the OMBR is strongly affected by elevation in salinity (Qiu & Ting 2014).

In conventional membrane bioreactors (MBRs), biofouling is a major cause of irreversible membrane fouling in both RO/UF membranes (Cornelissen et al. 2008b). Similarly, amongst the various forms of fouling in the OMBR, biofouling is one of the most challenging issues limiting the feasibility of the OMBR for the treatment of wastewater (Chen et al. 2006). The FO membrane in OMBR is in direct contact with high fouling propensity feeds such as activated sludge or highly complex liquids, making biofouling inevitable (Wang, Zhao, et al. 2016). The high salinity environment further exacerbates biofouling in the OMBR as the growth rate of microorganisms can increase in high saline environments (Wang, Chang & Tang 2016). According to Yuan et al. (2015) the biofouling layer on the FO membrane surface in the OMBR can be divided into three stages. The first stage involves the deposition of EPS (including polysaccharides and proteins) on the membrane surface. In the next stage, the cells are embedded in a EPS matrix and form clusters creating a biofouling layer. Lastly, the cluster of EPS and microorganisms increase dramatically, leading to an increase in the biofouling layer. However, increasing the operating time of the OMBR led to decrease in the growth, and the EPS and microorganisms were easy to detach from the fouling layer [66]. One study revealed that the amount of microorganisms that stick to the membrane surface

can be decreased by increasing the aeration rate, as only those microorganisms that can withstand the high aeration will stick to the membrane surface (Wang, Chang & Tang 2016).

Apart from biofouling, dissolved organic and inorganic contaminants retained in the OMBR leads to membrane fouling (Zhang et al. 2012). Overall flux decline in the OMBR is mainly attributed to biofouling and organic fouling (Bell, Holloway & Cath 2016). A pool of organic substances known as biopolymer clusters (BPC) profoundly affects filtration resistance in MBRs (Wang & Li 2008). Besides organic fouling, when salt accumulates in the OMBR, inorganic scaling is promoted by inorganic minerals, especially in the PRO mode where feed solute also experience a severe concentrative internal concentration polarization (Jin et al. 2011; Mi & Elimelech 2010a).

Compared to conventional MBR, flux in the fouled OMBR can be restored by the osmotic backwashing method (short-term operation 28 days) (Cornelissen et al. 2008b). Long-term operation (70 days), on the other hand, suggests that flux recovery can be significantly lower (10.60 % flux recovery after hydraulic cleaning and 18.54% after chemical cleaning) [61]. Acid cleaning has also proved to be an effective technique to restore the flux in the fouled FO membranes in the OMBR operation (Zhang et al. 2012). For long-term steady flux in the OMBR, air scouring at the feed side of the membrane is very effective (Qin et al. 2010). While flux decline in a direct FO is more severe than in an OMBR, hydraulic and chemical cleaning is more effective in restoring flux in direct FO than OMBR (Sun et al. 2016).

The low water flux is the biggest limiting factor in the OMBR compared to conventional MBR and affects its economic viability (Wang, Chang & Tang 2016). Commercially available membranes such as CTA and TFC FO membranes are not suitable for long-term operation in the OMBR as prolonged exposure to activated sludge can cause biodegradation of these membranes (Luo et al. 2016). This statement is contradicted by another study in which the researchers concluded that FO membranes (CTA and TFC) are suitable for long-term operation of the OMBR and can perform under a variety of activated sludge conditions (Bell, Holloway & Cath 2016). The duration of this study was only 100 days, whereas, in the first study [70], biodegradation of membranes was reported after 7 months of operation. Therefore, it would be safe to conclude that novel membranes materials are required for the long-term operation of OMBR, and commercial FO membranes are not suitable for long-term operation (over seven months).

3.3.2 Fouling mitigation in direct FO

Several studies have reported that fouled FO membranes can be easily cleaned by a simple change in hydrodynamic conditions without using any chemical agents (Coday et al. 2014; Lee et al. 2010; Mi & Elimelech 2010b). Most of these studies have used model foulants and fouling exhibited reversibility by changing hydrodynamic conditions such as high cross-flow velocity flushing with DI water. However, when treating complex feeds such as wastewater, fouling cannot be mitigated by merely changing hydrodynamic conditions and requiring chemical cleaning (Lv et al. 2017; Valladares Linares, Li, Yangali-Quintanilla, et al. 2013). This irreversibility is caused by the presence of divalent calcium and magnesium ions in the feed or the draw solution (Zou et al. 2013). Yoon et al. (Yoon et al. 2013) conducted his study on biofouling in the presence of calcium chloride ($CaCl_2$) and alginate in the feed. The study concluded that physical cleaning was not effective to restore the flux completely and only chemical cleaning with chlorine was able to do complete flux recovery. However, chlorine as a chemical will add extra cost to the FO process, and not all membranes, especially PA membranes, cannot tolerate chlorine attack while CTA membrane is more resistant to chlorine.

Alternatively, a more effective way to limit biofouling in the forward osmosis is phosphate limitation (Kim, Kim, et al. 2014). Phosphate limitation in relation to microbial growth or biofouling has been widely reported in the field of wastewater (Alphenaar et al. 1993; Kasahara, Maeda & Ishikawa 2004; Lehtola et al. 2003). Phosphorus is often present in wastewater in very low concentrations in the form of inorganic phosphates (Karageorgiou, Paschalis & Anastassakis 2007). Removal of phosphate can be achieved with various materials such as activated red mud, fly ash, iron oxide tailings and natural adsorbents (Karageorgiou, Paschalis & Anastassakis 2007; Kim, Kim, et al. 2014; Li et al. 2006; Pradhan et al. 1998). Adsorbents are reported to have lower removal efficiency and high cost (Vasudevan et al. 2008). Chemical precipitation is one of the most common and widely used techniques for phosphate limitation. However, it has several drawbacks, such as disposal problems, high maintenance cost, and the need to neutralise the treated water (Fytianos,

Voudrias & Raikos 1998). Limiting phosphate in the feed water in the FO process can hinder microbial growth and biofilm formation compared to sufficient phosphate conditions (Kim, Kim, et al. 2014).

Several other researchers proposed chemical cleaning protocols for wastewater fouled TFC FO membranes. Wang et al. (Wang et al. 2015) used alkaline cleaning (0.1% NaOH/0.1% SDS mixture) followed by acid cleaning (2 % Citric acid or 0.5 % HCl) and was claimed to be the most effective cleaning protocol. Lv et al. (Lv et al. 2017) tested five different protocols for real wastewater fouled membranes, as shown in Table 3.3. In this study, chemical cleaning with surfactant was the most effective way to restore the flux completely. However, chemical cleaning is not ideal as it entails extra energy consumption, and alternatives should be investigated. Moreover, the effectiveness of chemical cleaning is potentially constrained by the compatibility of membrane material with a chemical agent (Amy 2008a).

Table 3.3: Fouling Control strategies in different Forward Osmosis studies

Fouling Type	Model Foulants/Feed Water	Draw Solution	Membrane	Initial Operating Conditions	Mitigation	Fouling Reversibility	Ref
Biofouling	***Pseudomonas aeruginosa in Synthetic Wastewater***	• 1.3 M NaCl • 1.6 M $MgCl_2$	TFC FO (HTI)	CFV velocity of 8.5cm/s, T 25^{o}C	No data	No data	(Kwan, Bar-Zeev & Elimelech 2015)
Biofouling+organic	Pseudomonas aeruginosa PA01 GFP with 10mM NaCl and 1mM $CaCl_2$ with and without Alginate	• 4M NaCl	CTA (HTI) And TFC	CFV of 4cm/ S and T 25.0±1 °C	Chemical cleaning with chlorine	Reversible with chemical cleaning only	(Yoon et al. 2013)
Biofouling	Chlorella sorokiniana with NaCl and/ or $MgCl_2$	• 0.25 to 2M NaCl stepped up in 30 min interval	CTA	CFV: 22.3cm/S. and 23.0±1 °C AL-DS mode diamond spacer in draw	Feed spacer and high cross flow velocities	Less reversible in the presence of Mg^{2+} ions in feed or draw.	(Zou et al. 2013)

		• $MgCl_2$		channel			
Biofouling and organic, in-organic	• Municipal secondary wastewater • Synthetic municipal wastewater	• 3.6% NaCl for simulating natural seawater DS	CTA (HTI)	Single-phase flow with CFV of 0.04m/s. Bubbly Flow with aeration (0.4 L/min). FS and DS temperature of 35.0± 1 °C	Bubbly Flow method	Bubbly flow could not diminish fouling.	(Du et al. 2017)
Organic	Sodium alginate+50mM NaCl+0.5mM $CaCl_2$	• 4M NaCl	CA membrane HTI. TFC	CFV:8.5 cm/s pH:5.8 20±1°C.	CFV of 21cm/s using 50nM NaCl cleaning solution or DI water for 15 mins or Bubbled DI water for 5 mins	Reversible. Fastest reversibility with bubbled DI water.	(Mi & Elimelech 2010b)
Organic	Bovine Serum Albumin (BSA)+ +Aldrich Humic	• 1.5 or 4M NaCl	CA membrane by HTI	CFV of 8.5cm/s And 20 ± 1 °C	N/A	N/A	(Mi & Elimelech 2008)

	acid+Sodium alginate +50mM NaCl with/ or without $CaCl_2$						
Organic	Soluble algal product	• NaCl • $MgCl_2$ • $CaCl_2$	CTA and TFC	CFV of 5.5cm/s And 25 ^oC	Physical cleaning	Irreversible for CTA. Reversible for TFC	(Li, Ni, et al. 2018)
Organic	Humic acid and alginate	• Red sea salt in DI water	One CTA and TFC from HTI. 2 TFC from Porifera.	CFV of 0.1m/s	High CFV and osmotic backwashing	Reversible	(Blandin et al. 2016)
Organic-inorganic	DI water	• Seawater • RO Brine	CA membrane HTI	CFV of 10.7cm/s 25.0±0.5 °C	None		(Boo, Elimelech & Hong 2013)

Organic-inorganic	Sodium Alginate, BSA and Suwannee River natural organic matter with Synthetic Wastewater	• Seawater • RO BRINE	HTI FO membrane	Cross flow velocity of 10.7cm/s 25.0±0.5 °C	None		(Boo, Elimelech & Hong 2013)
Organic-inorganic	Sodium alginate, BSA and Suwannee River natural organic matter with synthetic wastewater	• 2M NaCl • 5M NaCl	HTI FO	Cross flow velocity of 10.7cm/s 25.0±0.5 °C	1. High Cross flow velocity. 2. Feed spacer. 3. Pulse flow.	Reversible with all three mitigation methods.	(Boo, Elimelech & Hong 2013)
Organic and Colloidal (Separate tests for each)	Sodium Alginate, BSA and Suwannee River Humic acid. Silica with diameter 20nm and 300nm.	• 5 M NaCl • Dextrose	CA membrane by HTI	20 ºC Same initial flux in all fouling tests	High Cross flow velocities without any chemical cleaning	Reversible (cleaning test done with only alginate)	(Lee et al. 2010)
In-organic	$CaSO_4$	• 4M NaCl	CA Flat sheet HTI	CFV 8.0 cm/s 20±2 °C	High cross flow velocity with DI	Reversible	(Choi et al. 2014)

					water		
Colloidal	Silica 10-20nm	• 4M NaCl	CA Flat sheet HTI	CFV 8.0 cm/s 20±2 °C	High cross flow velocity	Partially reversible (75%)	(Choi et al. 2014)
Organic-inorganic-colloidal-biofouling	Oily wastewater	• 2M NaCl	CTA HTI	CFV 8.2 cm/s 25 ºC	High CFV 33 cm/s	Irreversible	(Lv et al. 2017)
Organic-inorganic-colloidal-biofouling	Oily wastewater	• 2M NaCl	CTA HTI	CFV 8.2 cm/s 25 ºC	Osmotic Backwash	95% recovery	(Lv et al. 2017)
Organic-inorganic-colloidal-biofouling	Oily wastewater	• 2M NaCl	CTA HTI	CFV 8.2 cm/s 25 ºC	0.1 % HCl	90% recovery	(Lv et al. 2017)
Organic-inorganic-colloidal-biofouling	Oily wastewater	• 2M NaCl	CTA HTI	CFV 8.2 cm/s 25 ºC	0.1% EDTA	90% recovery	(Lv et al. 2017)
Organic-inorganic-colloidal-biofouling	Oily wastewater	• 2M NaCl	CTA HTI	CFV 8.2 cm/s 25 ºC	0.1% NaClO	85% recovery	(Lv et al. 2017)
Organic-inorganic-colloidal-biofouling	Oily wastewater	• 2M NaCl	CTA HTI	CFV 8.2 cm/s 25 ºC	0.1% surfactant	100% recover	(Lv et al. 2017)

Organic-inorganic-colloidal-biofouling	Drilling wastewater from shale gas	• 260g/L NaCl	CTA HTI	0.3 m/s	Modified osmotic backwash	Reversible	(Achilli et al. 2009)

Fouling in FO can also become irreversible when colloidal particles aggregate under conditions of high salt concentration due to reverse salt diffusion and high feed solution pH (Boo et al. 2012). According to Boo et al. (Boo et al. 2012) in the absence of particle destabilization, colloidal fouling is reversible in the FO process. However, colloidal fouling causes severe flux decline and is harder to clean physically compared to inorganic fouling (Choi et al. 2014). Kim et al. (Kim, Elimelech, et al. 2014) also argue that while individual colloidal and organic fouling exhibits complete reversibility in the FO, combined organic-colloidal fouling shows less reversible behavior, particularly in the presence of Ca^{2+} ions. Fouling due to colloidal particles can be minimized by providing an efficient pre-treatment to feed solution, which guarantees its removal from the feed solution. Ultrafiltration and microfiltration membrane demonstrated high efficiency for removing colloidal particles from feed solutions. Nowadays, many wastewater treatment plants use MBR technology for treatment that warrants the removal of colloidal particles from the treated effluent.

Membrane material also plays a key role in controlling fouling and cleaning behavior in the FO process and the RO because of the foulant-membrane interaction (Mi & Elimelech 2010b). According to Lay et al. (Lay et al. 2012), TFC membranes are more vulnerable to fouling than CTA membranes. PA membranes have higher fouling potential than CA membranes mainly because of vulnerable sites on the PA membranes, which cause more adsorption of foulants (Mi & Elimelech 2010b). The fouling of TFC membranes is exacerbated further in the PRO mode. However, the osmotic backwash technique for cleaning the membrane is surprisingly found to be more effective for TFC than CTA membranes (Lay et al. 2012). Similar findings are also reported in a study by Li et al. (Li et al. 2012) in which physical cleaning was effective in restoring flux of TFC membrane while the CTA membranes exhibited irreversible fouling.

Zhao et al.,(Zhao, Zou & Mulcahy 2011) investigated the effects of membrane orientation on FO performance under no fouling, organic fouling, and inorganic fouling conditions. Results suggested that the selection of membrane orientation is influenced by the composition of feed solution and the concentration degree. When treating complex or high saline streams, FO mode provides a more stable and higher water flux compared to PRO mode. Additionally, lower fouling but high cleaning

efficiency is observed in FO mode. Therefore, the FO mode is preferred for treating complex feeds such as wastewater or high salinity seawater. In contrast, the PRO mode is preferred for a solution with low fouling tendencies such as brackish water desalination. Another study conducted by Jin et al. (Jin et al. 2012) showed that inorganic contaminants were rejected at a much higher rate in the FO mode than in the PRO mode. According to Tang et al. (Tang et al. 2010b), in practical applications such as OMBR, PRO mode is impractical mainly due to the high fouling environment. Therefore, we can claim that FO mode is preferred for wastewater or high saline water treatment.

Feed spacers can also minimize fouling propensity. Zou et al.(Zou et al. 2013) Investigated the use of feed spacers using microalgae *Chlorella sorokiniana* as model foulant. Spacer enhanced initial flux performance and reduced fouling deposition of microalgae on the FO membrane. Spacer thickness also plays a role in minimizing biofilm formation. Thicker spacers are reported to have better performance than thinner spacers. According to a study conducted by Valladares Linares et al.,(Valladares Linares, Bucs, et al. 2014), thicker spacer reduces biofilm's impact on FO membrane performance. However, thicker spacer in the presence of lower cross-flow velocities is reported to promote organic and colloidal fouling and reduce permeate flux (She et al. 2016).

Recently, Gwak and Hong (Gwak & Hong 2017) suggested using an antiscalant–blended draw solution to minimize reverse salt diffusion and FO scaling control. Gypsum was used as a model scalant and an antiscalant blended draw solution containing a mix of NaCl and PAspNa (poly aspartic sodium salt) was examined. Results demonstrated that blended draw solution with antiscalant minimized the loss of draw solute significantly compared to NaCl draw solution, and gypsum scaling was controlled. The problem with adding scale inhibitors is that it will increase the operation costs (Hancock & Cath 2009).

3.3.3 Effectiveness of cleaning strategies for fouled FO membranes

The easiest way to clean fouled FO membranes is by flushing it with DI water using high cross-flow velocity. Some researchers have used 50mM NaCl solution instead of DI water as well, and it was found that both methods (DI water or 50mM NaCl) result in a good water flux recovery (Mi & Elimelech 2010b). Several researchers have used this method for fouling reversibility Table 3.3.

However, when fouling is intense (biofouling, NOM fouling, transparent exopolymer particles fouling), increasing cross-flow velocity is not an effective method to restore the flux, and chemical cleaning is required (Ge, Amy & Chung 2017; Valladares Linares et al. 2012; Yoon et al. 2013). Different researchers use different chemicals for fouled FO membrane listed in Table 3.4 and their properties. However, chemical cleaning can damage the membrane and is not recommended. For instance, TFC membranes, in general, cannot tolerate oxidizing agents such as chlorine or Alconox (Silva, Michel & Borges 2012). Chemical cleaning can also shorten membrane life, have environmental constraints due to waste chemical disposal, and increase operational costs (Park et al. 2014). Apart from these disadvantages, some researchers have claimed that chemical cleaning can only remove or dissolve the cake or gel type fouling layer and not remove foulants inside the membrane pores (Holloway et al. 2007).

Table 3.4: Chemical cleaning agents used in forward osmosis

Chemical	**Reaction**	**Compatibility with membrane material**	**Application in FO literature**
Chlorine or hypochlorite	Oxidation and disinfection	Can damage TFC membrane	(Valladares Linares et al. 2012; Wang et al. 2015; Yoon et al. 2013)
HCl	Solubilisation	Can narrow down the pores through neutralization	(Lv et al. 2017; Wang et al. 2015)
Citric acid	Chelation	Can narrow down the pores through neutralization	(Wang et al. 2015)
Alconox	Oxidation and disinfection	Can damage TFC membranes	(Wang et al. 2015)
NaOH	Hydrolysis and	Can increase pore size	(Wang et al. 2015)

	solubilisation		
Surfactant	Emulsifier, surface conditioner or dispersion	Adsorbs to the membrane surface	(Lv et al. 2017; Wang et al. 2015)
EDTA	Chelation	Can damage TFC	(Lv et al. 2017; Wang et al. 2015)
Alconox+ EDTA	Oxidation, disinfection and chelation	Damages both membranes	(Wang et al. 2015)
Hydrogen per oxide	Oxidation agent	Can damage TFC membranes	None
Sulphuric acid	Solubilisation	Can narrow the pores	None
Phosphoric acid	Chelation	Can narrow the pores	None
Enzyme cleaning	Inhibition of biofilm	N/A	None
Ammonium Biflouride	Solubilisation	Can damage both membranes	None
Na_2EDTA	Chelation	Can damage CTA membrane	(Martinetti, Childress & Cath 2009)
KL733 (King Lee Technologies, chemical)	Powder cleaner	Can scale CTA membrane	(Coday, Almaraz & Cath 2015)

Another popular cleaning method for osmotically driven membrane processes, known as osmotic backwashing, has been used by several researchers in direct FO and OMBR Table 3.4. Osmotic backwashing is a physical cleaning method in which the direction of water flow across the semi-permeable membrane is reversed, thus effectively detaching any foulants attached to the membrane

surface (Holloway et al. 2007). Usually, the draw solution is replaced with DI water, and the water permeation back into the feed side removes foulants attached to the membrane surface. In some studies, the feed solution is replaced with 100g/L NaCl and draw solution with DI water (Martinetti, Childress & Cath 2009). Both streams are circulated for about 20 mins or 30 mins, thereby detaching any foulants deposited on the membrane surface. In severe fouling conditions (oil and gas wastewater), a direct observation over the microscope of osmotically backwashed membrane revealed that loosely bound foulants were effectively removed; however, those sorbed to the membrane surface were not entirely removed by osmotic backwashing(Coday, Almaraz & Cath 2015). Another study by Valladares Linares, Li, Abu-Ghdaib, et al. (2013) used synthetic municipal wastewater as feed revealed that osmotic backwash removed all organic foulants from the membrane surface did not restore the flux completely. Thus, it would be safe to conclude that osmotic backwashing cannot guarantee 100% flux recovery in severe fouling conditions.

Blandin et al. (2016) introduced an extended osmotic backwashing method for fouled FO membranes with alginate, humic acid and calcium chloride model foulants feed solution. Extended osmotic backwashing is carried out for a long duration (1 hour) and high cross-flow velocity. Blandin and his co-workers concluded that extended osmotic backwashing was more efficient than a two-step consecutive osmotic backwashing method. However, the effectiveness of this method with real wastewater fouled membranes has not been tested yet. Arkhangelsky et al. (2012) investigated cleaning protocols for fouled flat sheet and hollow fiber membranes in the PRO mode. Hydraulic backwashing (backwashing with ultrapure water at a pressure of 1 bar) was compared with osmotic backwashing and surface flushing. Amongst these, only hydraulic backwashing restored the flux (75%) for a flat sheet membrane and 100% for hollow fibers.

Air scouring is another effective and widely used technique for fouling mitigation, especially in OMBR (Qin et al. 2010). Cleaning the FO membrane by air scouring with clean water has restored 98% water flux (Yangali-Quintanilla et al. 2011). Air scouring has also proved to be an effective mitigation technique for natural organic matter fouling (90% water flux recovery) (Valladares Linares et al. 2012). For biofouling control, air scouring can mitigate biofilm growth (Cornelissen et al. 2007); however, it grows back rapidly under favorable conditions (D'Haese et al. 2013). Air

scouring is also an expensive cleaning protocol and can be a serious drawback to the economic sustainability of the FO process (Blandin et al. 2016).

Other methods for fouling mitigation includes turbulent promoters such as the pulsed flow method and feed spacers. The pulsed flow method has also been used for fouling control in the FO process (Boo, Elimelech & Hong 2013). However, like flushing with high cross-flow velocity, pulse flow cannot mitigate pore-clogging (Blanpain-Avet et al. 1999).

3.3.4 Fouling mitigation using pretreatment

Cost-effective pre-treatment of wastewater can have numerous benefits such as disinfection, settling of large suspended particles, and removal of suspended solids and low fouling propensity of the feed wastewater after pre-treatment. Pre-treatment of wastewater includes but is not limited to using sand filters, settling and multimedia filters (Hawari et al. 2018), using Ultrasound and UV treatment (Blume & Neis 2004), coagulation-flocculation and flotation (Suarez, Lema & Omil 2009). Using cost-effective pre-treatment for high TDS solutions can help reduce membrane fouling, protect the membrane, and improve FO performance (Hancock, Black & Cath 2012). Rapid sand filters are well known for potable water use, but when it comes to treating wastewater, they have several flaws such as clogging, algae growth and backwashing (Blume & Neis 2004). Settling and multimedia filtration was used in one study conducted by Hawari et al. (2018) to dilate seawater using dewatered construction water in a hybrid Forward osmosis system. The settling method enhanced the flux by 13.5% and multimedia filtration removed most of the particles that would induce fouling.

Coagulation-flocculation and flotation have been used as an effective pre-treatment of hospital wastewater which contains a huge amount of pharmaceutical waste and radioactive compounds (Suarez, Lema & Omil 2009). This method has also been used to pre-treatment industrial effluents before entering municipal waste streams (Jain et al. 2001). However, this method involves using expensive coagulants, and it seems that it is not a cost-effective option if coupled with FO.

Activated carbon pretreatment can be very effective in rejecting most organic micropollutants from wastewater streams (Jamil et al. 2015; McGinnis et al. 2013). We will explore the use of activated carbon and sand filter as a pretreatment in the FO treatment of wastewater in this research.

3.4 In-situ and Real-time Fouling monitoring techniques

A range of in-situ real-time fouling monitoring techniques can be used to understand the mechanism better and fouling layer formation on the FO membrane. These methods include but are not limited to direct observation through the membrane (DOTM), ultrasonic time domain reflectometry (UTDR), nuclear magnetic resonance (NMR), optical coherence tomography (OCT), electrical impedance spectroscopy (EIS) and confocal laser scanning microscopy coupled with multiple fluorescent labelling.

3.4.1 Direct observation over the microscope (DOTM)

Some researchers have used optical microscopy to characterise the membrane's fouling in the forward osmosis process (Liu & Mi 2012; Wang et al. 2010). Direct observation over the membrane (DOTM) is a highly sensitive method to detect fouling deposition on the membrane surface; such small deposition cannot be registered with flux measurement (Zou et al. 2013). The first direct microscopic observation to systematically investigate fouling conducted by Wang et al. (2010) using latex particles as model foulants revealed that foulants usually get trapped in rough surface areas of the membrane, and increasing draw solution concentration increases foulant deposition on the membrane surface. Microscopic observation also revealed that FO mode is more resilient to fouling than the PRO mode, and feed spacers enhance initial and critical flux. The use of feed spacer in enhancing flux was also confirmed by another microscopic observation using model microalgae as foulant (Zou et al. 2013). However, it was found later by another in-situ monitoring study that while spacers can enhance flux, they can hinder the cleaning process as well (Tow, Rencken & Lienhard 2016). In-situ observations also confirmed that the draw solution containing divalent ions promote

severe fouling due to reverse salt flux and makes fouling reversibility more challenging (Zou et al. 2013).

Clearly, DOTM is a very sensitive technique, but its use in the FO is restricted to only transparent membranes or cells with transparent sections. Another limitation of DOTM is its inability to quantify surface coverage of membrane in the FO mode due to the interference from pore structures of the membrane (Zou et al. 2013).

3.4.2 Ultrasonic time-domain reflectometry

Ultrasonic time domain reflectometry (UTDR) is a monitoring technique extensively used in various industrial, medical and military applications (Mairal et al. 1999; Rose, Cho & Ditri 1992). UTDR has been used in reverse osmosis to monitor biofouling (Graf von der Schulenburg et al. 2008; Sim, Suwarno, et al. 2013). This technology has not been used in forward osmosis to the best of our knowledge. UTDR uses sound waves to determine the location of a moving or stationary interface and provides insights into the media's physical characteristics through which the sound waves propagate (Mairal et al. 1999). A possible schematic diagram of UTDR for the FO process is shown below in **Figure 3.5**.

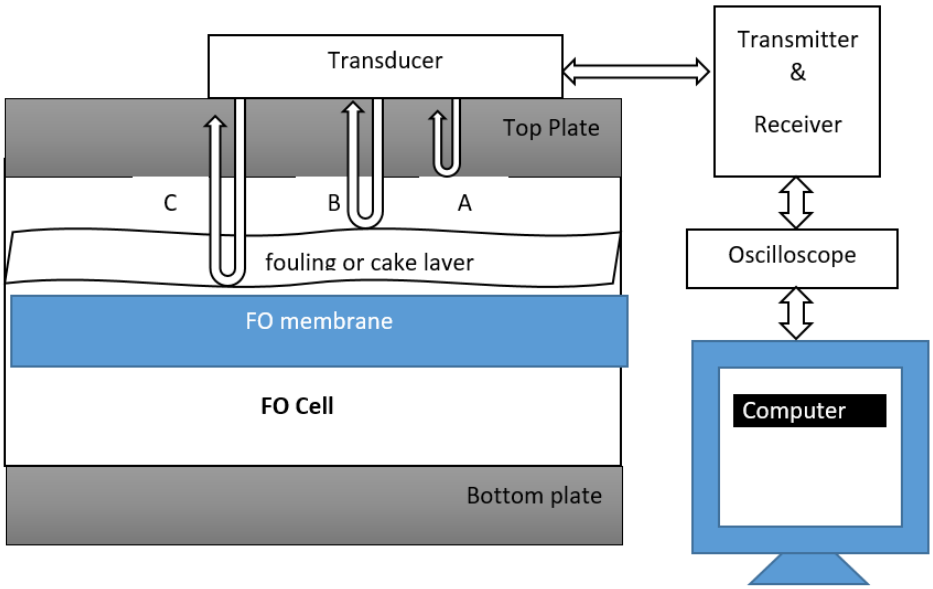

Figure 3.5: Schematic diagram of UTDR modified for the FO process. Modified from (Mairal et al. 1999; Sun, Feng & Lu 2011)

An externally mounted transducer (usually water-immersion) that emits and receives ultrasonic signals is placed in contact with a top plate as shown in **Figure 3.5**. The transducer is usually coupled using commercially available food-grade honey to the top plate (Mairal et al. 1999). The transducer emits ultrasonic waves. There are three interfaces in **Figure 3.5** from which ultrasonic signals are reflected. The top plate and feed solution interface generate echo A, the feed solution and fouling layer interface, generating echo B, and the feed solution and membrane interface, generating echo C. An oscilloscope collects the echo signals. The difference in arrival time represented by ΔT of the echoes is measured. If "c" is the velocity of the ultrasonic wave in the fouling layer, the thickness of the fouling layer ΔS can be calculated using the following equation.

$$\Delta S = 0.5 c \Delta T \qquad [24]$$

Once fouling initiates on the membrane, the acoustic impedance of each interface will change, resulting in a change in the amplitudes of the echoes (Mairal et al. 1999). A change in thickness of

the fouling layer will generate a new echo from the feed solution/fouling layer interface. Similarly, the echo signal will disappear once the membrane is cleaned and the fouling layer diminishes; therefore, UTDR can be a successful and effective technique to assess the effectiveness of cleaning protocols for fouling mitigation as well (Sanderson et al. 2002).

UTDR technique can effectively give us useful insights to monitor fouling layer initiation, fouling layer growth and its removal from the membrane (Sanderson et al. 2002). The limitation of UTDR is that fouling monitoring results may not be precise due to the slight difference in acoustic properties between the interfaces (feed solution/membrane or feed solution/ fouling layer) (Sim, Suwarno, et al. 2013).

3.4.2.1 Nuclear magnetic resonance / Magnetic resonance imaging

Nuclear magnetic resonance (NMR) or magnetic resonance imaging (MRI) can give us insights into biofilm distribution, the impact of hydrodynamics, and the impact of fouling on mass transport (Graf von der Schulenburg et al. 2008). Information about the basic principles of this technology can be found elsewhere (Abragam & Abragam 1961). NMR has several advantages: being non-invasive, the absence of ionizing radiations, freedom to generate 3D samples of the image as a whole, and image non-metallic samples that are optically opaque (Yang et al. 2014). NMR application was used for the first time by Graf von der Schulenburg et al. (2008) to monitor biofouling in spiral wound RO membranes. NMR is also considered a powerful tool for monitoring and analyzing biofouling, the biofilm's spatial distribution, and the impact of flow on hydrodynamics (Creber et al. 2010). Unfortunately, not much literature is available on the application of NMR for fouling studies. This may be because NMR is a very expensive technique Table 3.5, has limited availability and requires experienced operators to operate (Yang et al. 2014). A low cost, mobile solution has also been reported through which measurements are conducted using the earth magnetic field as an external magnetic field (Fridjonsson et al. 2015).

Table 3.5: Cost of Nuclear magnetic resonance / MRI methods. Adapted from (Fridjonsson et al. 2015)

NMR /MRI method	cost
High field (Superconducting)	>1 million Aud
Bench-top (permanent magnet)`	>100k Aud
Mobile (permanent or no magnet)	<10k Aud

3.4.3 Silent Alarm™ Technology

The Silent Alarm™ Technology was designed as an early warning system for membrane fouling and to monitor the performance of the RO plant in real-time (Amin Saad 2004). This would allow RO plant operators to take immediate measures against fouling. This technology can also quantitatively measure fouling via a parameter known as Fouling Monitora (FM). For instance, the FM value of 0-5 % means no fouling occurs on the membrane. In contrast, an FM value of over 20% suggests that extensive irreversible fouling occurs and that membranes may require replacement. However, this technology cannot tell the specific type of fouling on the membrane. Thus, developing an effective strategy for a specific type of fouling control is limited (Nguyen, Roddick & Fan 2012). Until now, this technology has only been applied to study fouling in RO only.

3.4.4 Feed fouling monitor coupled with UTDR

Developed by Taheri and co-workers (Taheri et al. 2015; Taheri et al. 2013), the feed fouling monitor (FFM) is an online flow simulator that gives us useful insights into the fouling propensity of the feed water. The predicted fouling trends for RO based on FFM alone ignore the effects of CEOP on fouling and are found to be slower than actual fouling profiles (Sim et al. 2018). To incorporate the effects of CEOP, Taheri et al. (2013) coupled FFM with UTDR to estimate RO fouling over a

range of applied fluxes using model silica as colloidal foulant. A UF membrane was used for the test as UF membranes are more sensitive to fouling than RO membranes, increasing accuracy. FFM was used to estimate the fouling resistance and porosity of the cake layer, whereas UTDR was incorporated to measure the thickness of the developing fouling layer. This model provided good estimates; however, it can be only applied to colloidal foulant since measuring the thickness of the organic layer is still a challenge for UTDR (Sim et al. 2018).

3.4.5 Optical coherence tomography (OCT)

Optical coherence tomography (OCT) is a relatively new and advanced monitoring technique (Sim et al. 2018), and has been used to monitor real-time fouling in NF/RO membranes. OCT has several advantages, such as high resolution (8 times higher than SEM), doesn't need any signal enhancers or staining of samples, and is used to monitor fouling in low-pressure processes (Park et al. 2019). Since it does not require any sample staining, OCT can be a very efficient tool for in-situ and early detection of biofilm development on membranes (Fortunato et al. 2017; Sim et al. 2018). Recent advances in OCT has made it a very effective technique for assessing the effects of operating conditions and spacer design on membrane fouling (Sim et al. 2018).

3.4.6 Electrical impedance spectroscopy

A more efficient technology, electrical impedance spectroscopy, can be used for fouling monitoring in the FO process. For the first time, EIS was employed by Kavanagh et al. (2009) to monitor fouling in RO. Since that it has been used successfully in various RO studies for fouling monitoring (Ho et al. 2017; Hu et al. 2014; Sim, Wang, et al. 2013). EIS potential to detect inorganic fouling in an osmotically driven flow chamber has also been demonstrated (Kavanagh et al. 2008). The biggest advantage of EIS is its sensitivity to very small changes on the membrane surface (measurements at low frequencies are recommended) and the capability to detect the type of fouling (Cen et al. 2015). The impedance spectra obtained from different types of foulants varies and can indicate the

type of fouling (Cen et al. 2015). Monitoring fouling with EIS in the FO process can be useful research in the future.

3.4.7 Confocal laser scanning microscopy coupled with multiple flouresence labelling

One of the best approaches for in-situ real-time fouling monitoring is coupling confocal laser scanning microscopy (CLSM) with multiple fluorescence labelling [30]. This technique can give us insight into the structure, distribution and function of biofilm constituents on a microscale (Valladares Linares, Bucs, et al. 2014). However, CLSM has some limitations, such as high brightness can cause photo-damage to the specimen, fluorescence saturation, and monochromatic laser (Pawley 2006).

Chapter 4: A novel empirical method for predicting concentration polarization in forward osmosis for single and multicomponent draw solutions

This chapter is based on the following publication.

Ibrar, I., Yadav, S., Altaee, A., Hawari, A., Nguyen, V. & Zhou, J. 2020, 'A novel empirical method for predicting concentration polarization in forward osmosis for single and multicomponent draw solutions', *Desalination*, vol. 494, p. 114668.

Authors contribution:

Ibrar Ibrar: Conceptualization, Methodology, Writing - original draft. Sudesh Yadav: Methodology, Writing - original draft, Data curation. Ali Altaee: Supervision, Writing - review & editing. Alaa Hawari: Visualization, Investigation, reviewing. John L. Zhou: Supervision, Writing - review & editing. Tien Vinh Nguyen: Supervision, Visualization, Investigation.

Abstract

Forward osmosis has gained tremendous attention in the field of desalination and wastewater treatment; however, the process is severely impacted by concentration polarisation and fouling. Concentration polarisation and fouling are key problems hindering the forward osmosis process and potential barriers in commercialisation. In this research, we present emerging findings in the field of the forward osmosis related to concentration polarisation and fouling. Since limited data in the literature exists for the diffusion coefficient of mixed electrolyte or multi-component solutions, which complicates the calculation of mass transfer coefficient and solute resistance to diffusion in the forward osmosis process. Therefore, a novel empirical method based on a limited set of well-defined experiments for evaluating and predicting the concentration polarisation, water flux, and reverse solute flux is presented for single and mixed, or multi-ions draw solutions. The proposed method does not rely on the hydrodynamic conditions and flow regime in the system and provides an

approach to measure and predict concentration polarisation, water flux, and reverse salt flux when the diffusion coefficient of a feed solution (FS) or draw solution (DS) is challenging to determine. Experimental work was carried out with a single, highly soluble sodium chloride (NaCl) DS, and a mixture of NaCl and magnesium sulphate (MgSO4) was used as a selected multicomponent DS. The results showed a 95% to 99% agreement with the experimental data. In the second part of this research, we performed a systematic investigation to evaluate the performance, rejection rate, fouling, cleaning protocols, and impact of physical and chemical cleaning strategies on commercial cellulose triacetate (CTA) membrane performance. The treatment of landfill leachate (LFL) solution was performed in the active layer facing feed solution and support layer facing the draw solution (AL-FS mode), and the active membrane layer facing the draw solution and support layer facing the feed solution (AL-DS mode). Compared to the AL-FS mode, a higher flux for the AL-DS mode was achieved, but membrane fouling was more severe in the latter. In both membrane orientations, the rejection rate of the FO membrane to heavy ions and contaminants in the wastewater was between 93 and 99%. Physical and chemical cleaning strategies were investigated to recover the performance of the FO membrane and to study the impact of cleaning methods on the membrane rejection rate. Physical cleaning with hot water at 35 ºC and osmotic backwashing with 1.5M NaCl demonstrated excellent water flux recovery compared to chemical cleaning. In the chemical cleaning, an optimal concentration of 3 % hydrogen peroxide was determined for 100% flux recovery of the fouled membrane. However, slight membrane damage was achieved at this concentration on the active layer side. Alkaline cleaning at pH 11 was more effective than acid cleaning at pH 4, although both protocols compromised the membrane rejection rate for some toxic ions. A comparison of the membrane long-term performance found that cleaning with osmotic backwashing and hot water were effective methods to restore water flux without comprising the membrane rejection rate. Overall, it was found that physical cleaning protocols are superior to chemical cleaning protocols for the forward osmosis membrane fouled by landfill leachate wastewater.

4.1 Background

4.4.1 A novel empirical method for predicting the concentration polarisation for single and multicomponent draw solutions

Forward osmosis (FO) has gained excellent popularity as a sustainable membrane separation process and a possible alternative to pressure-driven membrane processes (Achilli, Cath & Childress 2009; Chanukya, Patil & Rastogi 2013; McCutcheon, McGinnis & Elimelech 2006b; Nguyen et al. 2018; Straub, Deshmukh & Elimelech 2016; Wang, Goh, et al. 2018). While it has immense potential in wastewater treatment and seawater desalination, a major impediment in its successful commercialization is the inherent problem of concentration polarization (CP) (Altaee, Zhou, Alanezi, et al. 2017; Chanukya, Patil & Rastogi 2013; Heikkinen et al. 2017; Hoek & Elimelech 2003; McCutcheon & Elimelech 2006a; Moody & Kessler 1976; Tan & Ng 2008; Zhang, Cheng & Yang 2014). Unlike pressure-driven membrane processes, the FO process experiences CP on both sides of the membrane (Bui, Arena & McCutcheon 2015; Emadzadeh et al. 2014; Ibrar, Altaee, et al. 2019; Ibrar, Yadav, Altaee, Samal, et al. 2020; Khorshidi et al. 2016; McCutcheon & Elimelech 2006a, 2007; McCutcheon, McGinnis & Elimelech 2006b; Tan & Ng 2008, 2013; Tang et al. 2010b; Wang, Ong & Chung 2010). Although internal CP (ICP) plays a dominant role in flux decline in the FO process, external CP (ECP) effects cannot be overlooked when treating high salinity solutions or when the FO membrane operates at a high water flux (Gruber et al. 2011; Ibrar, Naji, et al. 2019; Wang, Zhang, et al. 2016). It is, therefore, vital to consider the impacts of both external and internal CP in the design and operation of the FO process (Altaee et al. 2014; Yadav, Ibrar, Altaee, Samal, et al. 2020b; Yadav, Saleem, et al. 2020).

The CP is measured in terms of its modulus. The two main parameters used in the FO process for measuring the moduli of external and internal CP are the mass transfer coefficient "k" and the solute resistance to diffusion "K". The most uncertain element in the theoretical determination of CP lies in the determination of the mass transfer coefficient "k" (Sutzkover, Hasson & Semiat 2000b), which is usually estimated from a dimensionless correlation using an appropriate Sherwood relation for the flow regime. Numerous Sherwood relations have been proposed and extensively reviewed in the literature (Lee & Lee 2000; Matthiasson & Sivik 1980; Sutzkover, Hasson & Semiat 2000a; Tan & Ng 2008). Apart from a large number of different relationships in the literature for mass transfer

coefficient and Sherwood relations, most of these relations were developed for mass transfer either in smooth and non-porous systems or were derived from heat transfer-mass transfer analogies (Abdelrasoul et al. 2015). Whist FO membranes are semipermeable and often rough on a microscopic scale. The mass transfer also depends on fluid properties and rate of flow, and if these vary in the direction of flow, so does the mass transfer coefficient (Treybal 1980). Some commercial suppliers of FO membrane modules, such as Porifera, provide limited information about the module (modules are sealed), further complicating finding the mass transfer from Sherwood relations.

The solute resistivity (K), for example, is a function of the membrane characteristics (such as membrane porosity, tortuosity, and thickness), which are not readily available and requires an extensive procedure to determine (McCutcheon & Elimelech 2006a). Most importantly, the K, as well as the mass transfer "k" value, also depends on the value of the diffusion coefficient (D), which is easier to measure for single salt solutions such as sodium chloride (NaCl), potassium chloride (KCl), and magnesium chloride ($MgCl_2$) (Achilli, Cath & Childress 2009; Madsen et al. 2017; McCutcheon & Elimelech 2006a). However, there is limited data available in the literature for the diffusion coefficient of mixed electrolyte solutions except for NaCl and $MgCl_2$ (Holloway et al. 2015). The diffusion coefficient of mixed draw solution (DS) such as seawater or blended (two or more) DSs (Law & Mohammad 2017; Liu et al. 2014; Phuntsho et al. 2012) that often used in the FO applications would be a mix of main diffusivities of individual draw solute and cross diffusivity of both the solution (Medvedev & Shapiro 2005). The co-existence of different species in a DS can also alter the diffusivity of a particular species (Phuntsho et al. 2012). For some DSs, the process becomes more complicated when dilution/suction parameters need to be considered (Tan & Ng 2013). In such instances, finding the value of K would be prone to errors. In addition, the asymmetry of the support structure also causes different diffusion behaviour depending on the direction of flux and ion transport across the FO membrane (Achilli, Cath & Childress 2009). Computer models based on computational fluid dynamics (Gruber et al. 2011) and 2D finite element method (FEM) for predicting FO performance are complex and involve expertise in particular software. Several other new models have been developed recently by researchers, including machine learning models (Jawad, Hawari & Zaidi 2020), temperature/concentration parameter based solution diffusion models (Wang et al. 2019; Wang, Zhang, et al. 2016), and spatial variation model (Lee & Ghaffour 2019).

So far, the current water flux models are exacting methodologies that require a lot of information about the FO membrane and flow characteristics of the filtration system.

Mixed or multicomponent DSs demonstrated excellent performance and were widely used in the FO process (Hamdan et al. 2015; Holloway et al. 2015; Liu et al. 2014; Nguyen et al. 2020). Although several models exist in the literature that addresses the CP for single solutes, the application of these models for quantifying CP in mixed DSs is questionable and non-existent in the literature. The objective of this study is two-fold. Firstly, to develop an empirical method to measure CP profiles in the FO process in both membrane orientations for single and mixed DS. Secondly, the proposed method was validated to predict dilutive and concentrative CP, water flux and reverse salt flux in the FO process for single and mixed DS. The method used in this study does not require information about the flow regime in the FO process and special membrane characteristics (such as structure parameter) to calculate water flux and reverse salt flux. Hence, it can also be extended to ternary quaternary mixtures in osmotically-driven membrane processes.

4.2 Modelling dilutive concentration polarization (CP)

Concentration polarization (CP) in the FO process occurs on both sides of the FO membrane, i.e., the draw and feed sides. Dilutive concentration polarization due to concentration dilution occurs on the DS side, while concentrative concentration polarization occurs on the feed solution side. Dilutive and concentrative CP is taking place simultaneously, making the process of predicting the moduli of concentrative and dilutive concentration polarization in the FO process more complicated. However, the modulus of concentrative CP will be negligible when the feed solution is de-ionized (DI) water. Hence, the modulus of dilutive CP can be separately measured for the AL-DS mode (when the active layer faces the draw solution) for the AL-FS mode (when the active layer faces the feed solution).

According to the modified solution-diffusion model based on film theory, water flux across the FO membrane is given Eq**.** [25].

$$J_w = A_w\,[(\pi_{Db} - \pi_{Fb}) - \Delta P] \qquad [25]$$

where $\boldsymbol{A_w}$ is the pure water permeability coefficient of the FO membrane, $\boldsymbol{\pi_{Db}}$ and $\boldsymbol{\pi_{Fb}}$ are bulk osmotic pressures of the DS and FS (feed solution), respectively, and $\boldsymbol{\Delta P}$ is the transmembrane hydraulic pressure. Eq. [1] calculates the water flux as a function of driving force only based on the concentration difference and is valid only in the absence of CP phenomena. In practice, the flux through an asymmetric FO membrane is far lower than predicted by Eq. [25].

Most commercial FO membranes have a rejection rate of over 90% to ions. It is assumed in this study that the FO membrane is completely selective (complete ion rejection and a reflection coefficient of 1). When the FS is DI water, the osmotic pressure of the feed side will be insignificant, and hence the effect of CP on the feed side is negligible. However, the impact of dilutive CP on the DS side still exists due to the dilution of DS by permeate flow (dilutive external CP) in the AL-DS mode and inside the support layer (SL) in the AL-FS (dilutive internal CP). As such, Eq. [1] can be expressed in terms of dilutive CP at the draw solution side ($\boldsymbol{CP_D}$).

$$J_w = A_w(CP_D\pi_{Db}) - \Delta P] \qquad [26]$$

where $\boldsymbol{CP_D}$ is the dilutive external CP correction factor on the DS side. The osmotic pressure at the membrane surface π_{DM} after correction for the dilution factor can be expressed by Eq. [27].

$$\pi_{DM} = \pi_{Db}CP_D \qquad [27]$$

Substituting Eq. [27] in Eq. [26] yields,

$$J_w = A_w\,(\pi_{DM} - \Delta P) \qquad [28]$$

$$\pi_{DM} = \frac{J_w}{A_w} + \Delta P \qquad [29]$$

Since the FO process is driven by the osmotic pressure gradients across the membrane, the hydraulic pressure in Eq. [29] is equal to zero, $\boldsymbol{\Delta P = 0}$. From Eq. [27] the osmotic pressure difference π_{DM} across the AL can be calculated using experimental water flux and pure water permeability coefficient $\boldsymbol{A_w}$ (Phillip, Yong & Elimelech 2010). Rearranging Eq. [27], the modulus of dilutive CP at the DS membrane interface is given by Eq. [30].

$$CP_D = \frac{\pi_{DM}}{\pi_{Db}} \qquad [30]$$

Experimentally, π_{Db} is calculated as the average osmotic pressure of the inlet and outlet DS, whereas, experimental water flux in the FO process $\boldsymbol{J_{we}}$ is given by Eq. [31]:

$$J_{we} = \frac{(W_t - W_i)}{1000 * A * t} \quad [31]$$

where A is the membrane area, t is the filtration time, and W_t and W_i are weights of permeate at t time and initial time, respectively. In the FO process, the value of $\boldsymbol{CP_D}$ is less than unity due to dilution of the DS, while $\boldsymbol{CP_D}$ value equals unity refers to zero dilutive CP. For a given FO membrane with a known $\boldsymbol{A_w}$ and DI water FS, experimental water flux can be calculated from Eq. [31] then compensated in Eq. [29] to calculate π_{DM}. $\boldsymbol{CP_D}$ can be obtained from Eq. [30]; this process will be repeated for a range of DS concentrations (single or mixed DS) using a DI water FS. **Fig.** 4.1a shows the relationship between J_{we} and $\boldsymbol{CP_D}$ for several DS concentrations (curves replicate experimental data). Practically, the $\boldsymbol{CP_D}$ of any DS within the range of concentrations used in **Fig.** 4.1a can be predicted by knowing water flux (DI water feed or saline feed) in the FO process. **Fig.** 4.1b presents the relationship between the theoretical osmotic pressure π_{Db} and the effective osmotic pressure (π_{DM}) in the FO process for DI water FS. From Fig 4.1a and 4.1b, theoretical water flux in the FO process with DI water feed can be predicted by knowing the bulk osmotic pressure of the DS. From Fig 4.1b, the calculated π_{Db} will be used to predict π_{DM} using regression analysis in the FO process, then theoretical water flux $\boldsymbol{J_{wt}}$ for DI water feed and different DS concentrations can be estimated using Eq. [26].

In general, the modulus of dilutive CP, $\boldsymbol{CP_D}$, of any DS within the range of concentrations in **Fig.** 4.1a can be predicted by knowing the experimental water flux in the FO process. Furthermore, water flux and $\boldsymbol{CP_D}$ in the FO process with DI water feed solution can be theoretically predicted using the relationship between the bulk osmotic pressure $\boldsymbol{\pi_{Db}}$ and $\boldsymbol{\pi_{DM}}$ in **Fig.** 4.1b, then compensating in Eq. [26] to calculate J_w or Eq. [30] to calculate $\boldsymbol{CP_D}$.

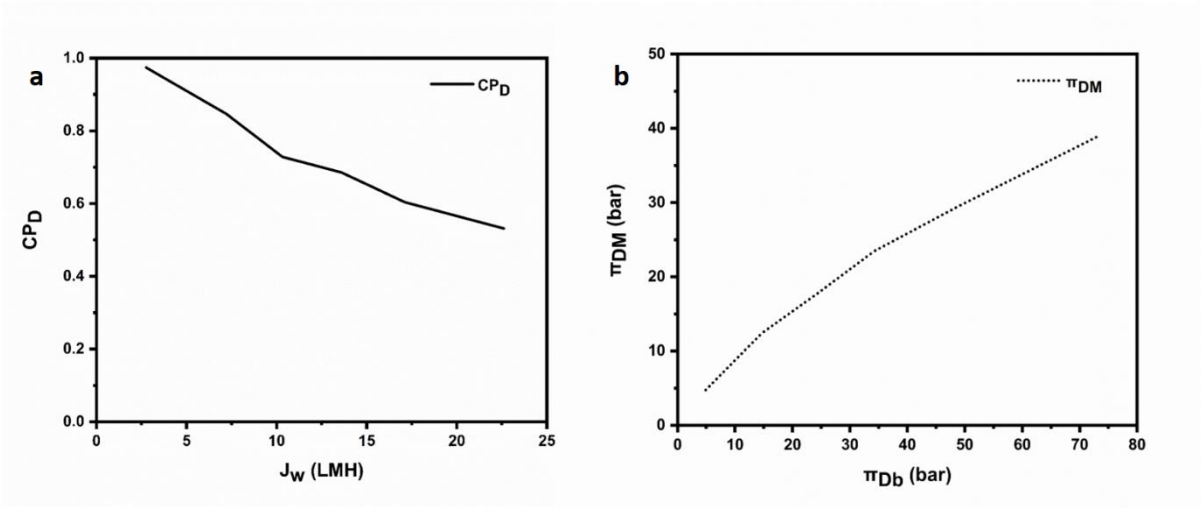

Figure 9.1: Water flux in the FO experiment using DI water FS and NaCl DS. a) Experimental water flux vs. the modulus of CPD. b) A plot of bulk osmotic pressure π_Db against the osmotic pressure at the membrane surface on the DS side π_DM. The concentration of

4.3 Modelling concentrative concentration polarization (CP)

Concentrative and dilutive CP co-occur on the feed and draw sides of the FO membrane. The effect of concentrative CP can be ignored when DI water is the FS but becomes significant as the salinity of FS increases. Two types of FO experiments are required to find out the effects of concentrative and dilutive CP in the FO process. In the first set of experiments, DI water will be the FS [**Fig.4.1**] to calculate a correlation between J_{we} and $\boldsymbol{CP_D}$, as illustrated in section 2.1. In the second set of experiments, the FO process will be performed with different FS and DS salinities to estimate the value of $\boldsymbol{CP_F}$. Eq. [1] calculates water flux in the FO process, using DI water FS. However, Eq. [1] overestimates water flux in the FO process by 50% (Altaee, Zhou, Alhathal Alanezi, et al. 2017). Practically, freshwater transport across the FO membrane dilutes the DS ($\boldsymbol{CP_D}$ on the draw side) and concentrates the FS resulting in a concentrative CP on the feed side ($\boldsymbol{CP_F}$ on the feed side). Experimentally, water flux in the FO process using two solutions of different concentrations is given by the following Eq.:

$$J_w = A_w(\pi_{DM} - \pi_{FM} - \Delta P) \quad [32]$$

$$\Delta\pi = \frac{J_w}{A_w} + \Delta P \quad [33]$$

where, π_{FM} is the osmotic pressure of the FS at the membrane surface, and $\Delta\pi$ is the net osmotic pressure driving force. In Eq. [32], $\Delta \boldsymbol{P}$ can be cancelled since the hydraulic pressure gradient is equal to zero in the FO process. Eq. [32] can be expressed in terms of the moduli of dilutive and concentrative CP for the draw and FS, respectively, as the following:

$$J_w = A_w(CP_D\pi_{Db} - CP_F\pi_{Fb}) \quad [34]$$

where, $\boldsymbol{CP_F}$ represents the modulus of concentrative CP. In Eq. [9], π_{Db} and π_{Fb} are the bulk osmotic pressure of DS and FS, and J_w can be experimentally calculated from Eq. [31]. Once $\boldsymbol{J_{we}}$ is experimentally determined, the modulus of dilutive CP $\boldsymbol{CP_D}$ can be predicted from Fig. 1a from a correlation between experimental water flux $\boldsymbol{J_{we}}$ and the amount of dilution caused by permeating water ($\boldsymbol{CP_D}$). Substituting J_{we}, $\boldsymbol{CP_D}$, π_{Db} and π_{Fb} in Eq. [34] to calculate the modulus of concentrative CP, $\boldsymbol{CP_F}$. Then, the bulk osmotic pressure π_{Fb} will be plotted against the osmotic pressure at the membrane surface (π_{FM}) in Fig. 4.2a and J_{we} will be plotted as a function of π_{FM} in **Fig.** 4.2b. Thus, the theoretical value of water flux in the presence of FS can be predicted based on values of π_{FM} in Fig.4.2b. Mathematically, $\boldsymbol{CP_F}$ is described as the ratio of π_{FM} to π_{Fb} as given by Eq.[35].

$$CP_F = \frac{\pi_{FM}}{\pi_{Fb}} \quad [35]$$

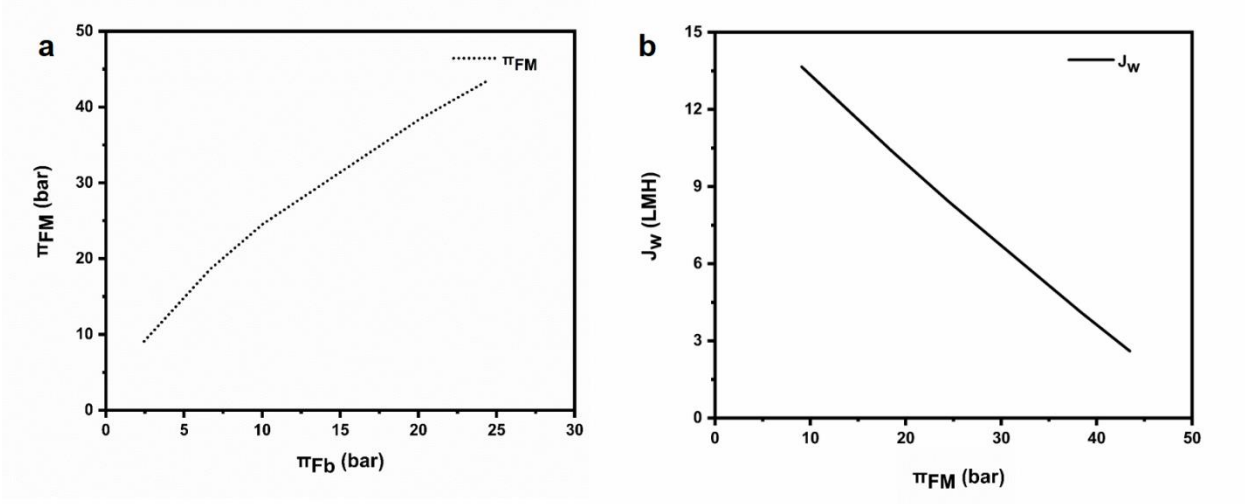

Figure 4.2: Water flux in the FO experiment using NaCl FS and DS

a) A plot of osmotic pressure at the membrane surface π_{FM} and bulk FS osmotic pressure π_{Fb}. **b)** Experimental water flux vs π_{FM}. The concentration of DS is 1M at 20°C, and the concentration of FS ranges from 0.05 to 0.5M at 20°C.

There is also a reverse salt flux (RSF) from the DS to the FS in the FO process, along with the water flux. Ideal FO membrane completely rejects solutes, but in practice, a small amount of the draw solute would transport across the membrane. Mathematically, the salt flux from DS to the FS can be estimated by Eq. [36].

$$J_{st} = B(C_{DM} - C_{FM}) \qquad [36]$$

In Eq. [36] J_{st} is the theoretical RSF, C_{DM} is the concentration of DS at the membrane surface on the DS side, and C_{FM} is the concentration of FS at the membrane surface on the feed side. When DI water is the FS, and all salt in feed is from RSF, Eq. [36] can be modified as:

$$J_{st} = B\left(\frac{\pi_{DM}}{nRT}\right) \qquad [37]$$

Once the osmotic pressure at the membrane surface is determined using Eq. [29], the theoretical RSF can be calculated using Eq. [37] with DI water FS and Eq. [36] for NaCl FS. The experimental RSF was calculated using Eq. [38] for model verification.

$$J_{se} = \frac{V_f C_f - V_i C_i}{A*t} \qquad [38]$$

where V_f and C_f are the final volume and concentration of the FS, respectively, and Vi and Ci are the FS's initial volume and concentration at the start of the FO experiment. A represents the total membrane area, and t is the filtration time of the FO run.

In practice, the water permeability coefficient will be experimentally obtained for a given FO membrane. Then, two steps of experimental work will be carried out to calculate CP_D and CP_F in the FO membrane. The first set of experiments uses DI water FS and saline DS of different concentrations to calculate CP_D in the FO process using the procedure explained in section 4.3. As illustrated, the impact of concentrative CP and dilutive CP will be obtained in the second set of experiments, which uses a range of feed and draw concentrations to calculate CPF in the FO process. To predict water flux in the FO process for a known feed and draw concentrations (within the studied concentrations), π_{FM} will be estimated from Fig. 4.2a using the corresponding values of π_{Fb} to obtain CP_F. Finally, water flux will be estimated from Fig. 4.2b. The reverse salt flux can be obtained using Eq. [37] with DI water feed and Eq. [36] for a saline FS. A schematic diagram of water flux and CP measurements in the FO process is illustrated in **Fig. 4.3.** It should be noted that water flux and reverse salt flux in this method will be directly affected by the testing conditions of the FO process, such as feeds flow rate, the temperature of feed and draw solution, the concentration of feed and draw solution.

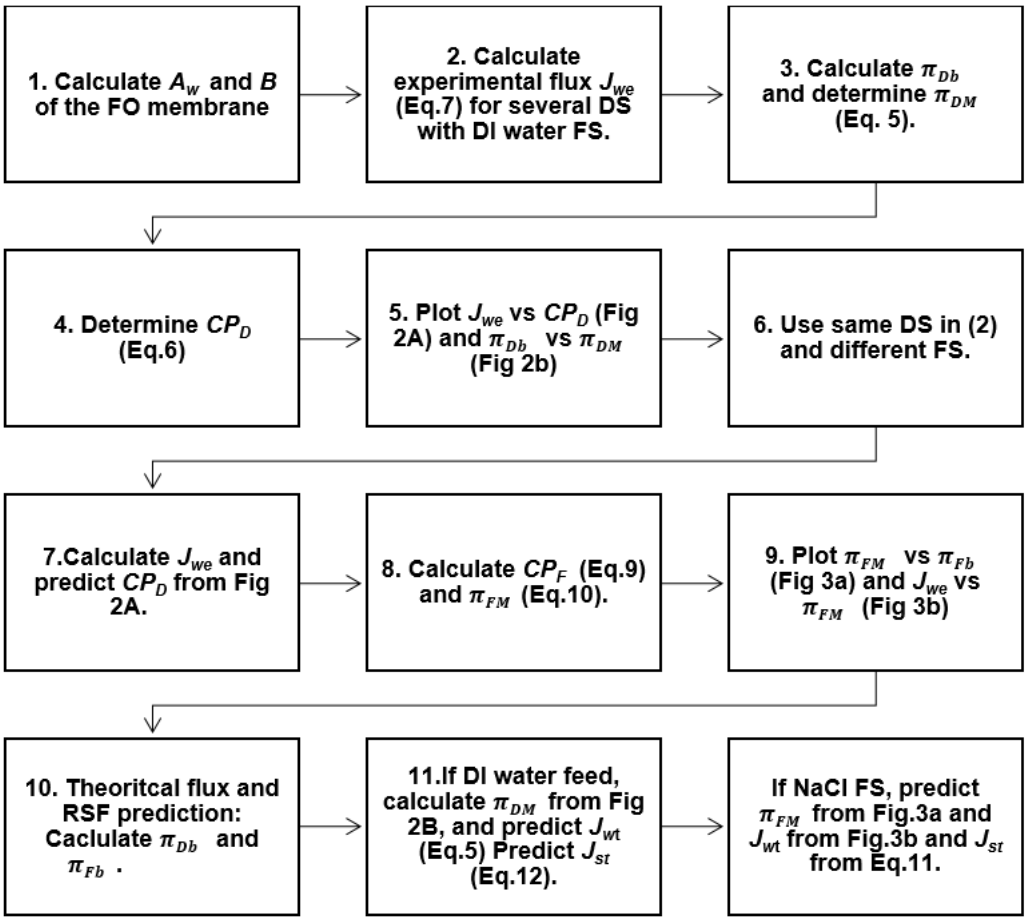

Figure 4.3: Schematic diagram of calculation and prediction of the CP in the FO process

4.4 Methods and Chemicals

4.4.1 Forward osmosis cross-flow system and membrane

A schematic diagram of the laboratory-scale unit is shown in **Fig. 4.4**. The FO cell (CF042D) used in this study was obtained from Sterlitech Corporation (USA) and featured an active membrane area of 42 cm^2 (0.0042 m^2). Two Cole-Parmer Micro-pumps with Console Drive, PEEK (Sterlitech-USA) were used for FS and DS pumping. A panel mount flow meter F-550 (Sterlitech –USA) was used to measure the volumetric flow rate of the FS and the DS. The flow rate was fixed at 2 litres per minute (cross-flow velocity of 36 cm/s) for both the feed and the draw side, and the cell was operated in co-current cross-flow. A digital balance (EK-15KL) connected to a computer was used on the draw side

to record the increase in the weight of the DS. Water flux was calculated from the weight change of the DS. The experiment was operated at an ambient lab temperature of 21 ±1.5 ^{0}C. Immersion circulators (Sterlitech-USA) were used to maintain the temperature of feed and DS when required. A conductivity meter (Hach HQ14d) on both the draw and feed sides was used to record the change in conductivity of the draw and FS.

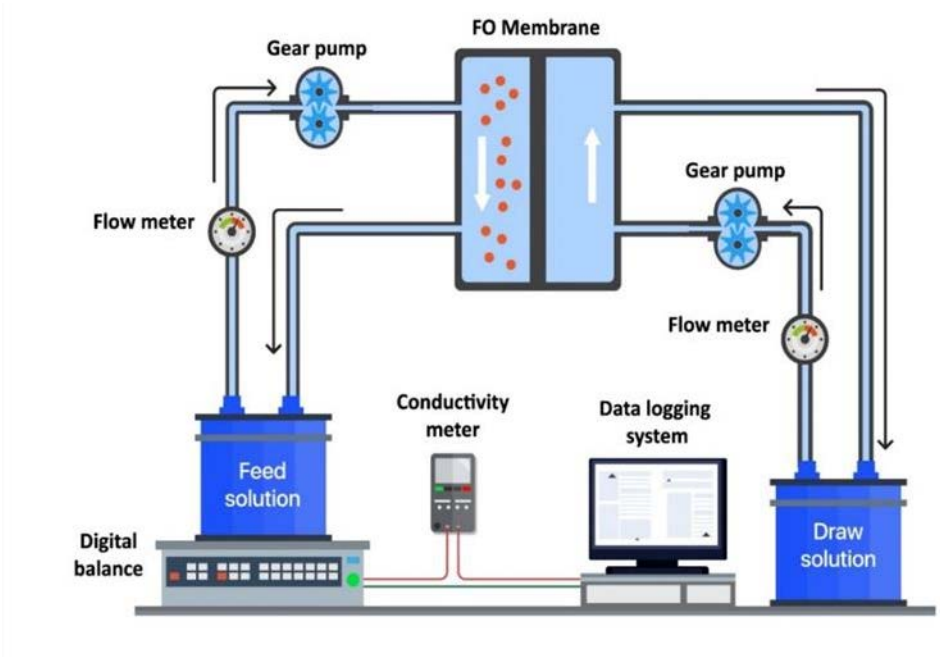

Figure 4.4: Diagram of the lab-scale forward osmosis system. Co-current cross-flow of the feed and DS was used in all the experiments.

This study used a flat sheet cellulose triacetate (CTA) FO membrane "FTSH2O" provided by Sterlitech Corporation and manufactured by Fluid Technology Solutions. The membrane was soaked overnight in DI water to ensure complete wettability. At the beginning of each run, it was flushed with DI water to remove any additives.

4.5 Feed and draw solutions

All chemicals used in experiments were analytical grade obtained from Sigma Aldrich, Australia. NaCl DS was prepared by dissolving an analytical grade NaCl in DI water. Mixed DS was prepared by mixing NaCl solution with $MgSO_4$ (magnesium sulphate, molecular weight 120.37 g/mol). NaCl was used as a major solute and (0.1M) $MgSO_4$ as a minor solute in the solution. Low concentration of $MgSO_4$ was chosen to avoid membrane fouling due to divalent ions, which may have an impact on CP. Depending on the objective of experiments, the FS used in this study was either DI water or NaCl solution with concentrations ranging 0.05M to 0.5M. The osmotic pressure of all solutions was calculated by the Van't Hoff Eq.:

$$\pi = iCRT \qquad [39]$$

where i= number of ions produced during dissociation of solute, R is the universal gas constant (0.0820 L atm $mol^{-1}K^{-1}$), C is the molar concentration of the solute (mole/L), and T is the absolute temperature (kelvin).

4.5.1 Experimental protocol

Two types of experiments were carried out to measure the effects of CP in the FO process in both the AL-DS and the AL-FS orientation. The first set of experiments used DI water FS and single salt NaCl DS with concentrations between 0.1M and 1.5M to measure the DS side's dilutive CP (CPD). In the second set of experiments, DI water FS was replaced with NaCl FS to measure the effects of concentrative CP ($\boldsymbol{CP_F}$). The concentration of FS was from 0.05M to 0.5M NaCl. After each run, the membrane was rinsed with DI water at a 2.8 LPM flow rate (cross-flow velocity of 51 cm/s) for at least 30 minutes to remove any salts accumulated from a previous test. A similar protocol was used for mixed salt experiments, except that a constant 0.1M $MgSO_4$ was added to the corresponding NaCl DS. Each experiment was conducted at least 2 times, and the average results were reported in this study.

4.6 Results and Discussions

4.6.1 Membrane intrinsic properties

The pure water permeability A_w and salt permeability B was determined through a cross-flow RO (reverse osmosis) setup. Primarily, we need the value of A_w and B for modelling in this study. The A_w value used in the calculation in this study was 0.58 $Lm^{-2}h^{-1}bar^{-1}$. The membrane B value used in the prediction of RSF was 0.32±0.05 $Lm^{-2}h^{-1}$. These values are comparable to those previously reported for this membrane (Madsen et al. 2017).

4.6.2 Quantification of CP for mixed DS

CP is usually measured in terms of its modulus. The dilutive concentration polarization modulus is defined as the ratio of the osmotic pressure of the DS at the membrane surface to the bulk osmotic pressure of DS [Eq. 30]. According to the previous mass transfer models in the literature [12], the dilutive CP modulus is usually less than 1, and the concentrative CP modulus is greater than 1. To measure the effect of CP_D and CP_F, NaCl was used as a DS, and FS was DI water in the first set of experiments. In the next set of experiments, FS was replaced with 0.05M to 0.5M NaCl solution to calculate the values of CP_F.

4.6.3 AL-DS mode: Quantification of CP_D NaCl DS-DI water FS

In the AL-DS mode, experimental water flux, J_{we} and experimental RSF J_{se} curves (calculated with different DS concentrations from Eq. [31] and Eq. [38]) are presented in Fig. 4.5a as a function of the net osmotic driving force. Water flux is presented on the primary y-axis, whereas RSF is presented on the secondary y-axis. The concentrations of DS were 0.1, 0.3M, 0.5M, 0.7M, 1M, and 1.5M NaCl, while DI water was the FS to minimize the effect of concentrative CP, i.e., $CP_F \approx 0$. As the DS concentration increased gradually from 0.1 to 1.5M, water flux in the FO process increased.

The concentration of NaCl in the FS due to reverse salt flux (RSF) was measured at the end of the FO experiments and found to be very low (<100 mg/L) to have a significant effect on the osmotic pressure of the FS. The osmotic pressure at the membrane AL surface π_{DM} was obtained from Eq. [29] and is presented in Fig. 4b as a function of the osmotic pressure of bulk draw solution. The value of π_{DM} represents the actual osmotic pressure at the membrane surface responsible for the water transport across the FO membrane. The osmotic pressure π_{DM} was divided by the osmotic pressure of the bulk draw solution to obtain the $\boldsymbol{CP_D}$ modulus using Eq. [30]. The values of $\boldsymbol{CP_D}$ were calculated for each DS concentration and are presented as a function of the experimental permeate flux in Fig. 4.5c and as a function of NaCl draw solution concentration in Fig. 4.5d.

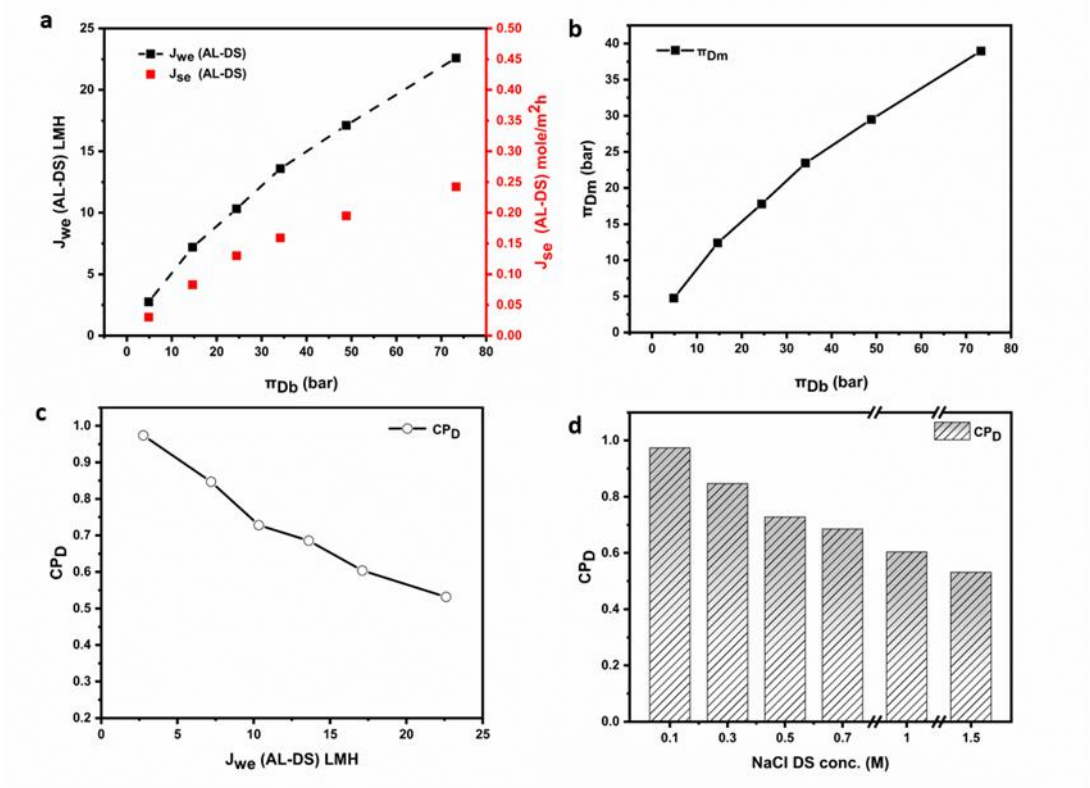

Figure 4.5: Quantifying dilutive concentration polarisation in the FO process for AL-DS mode with

(a) Plot of experimental water flux J_{we} and experimental RSF J_{se} against the bulk osmotic pressure π_{Db}, (b) Plot of osmotic pressure at the membrane surface π_{DM} against bulk DS osmotic pressure π_{Db} (c) A plot of dilutive CP modulus $\boldsymbol{CP_D}$ as a function of experimental water flux J_{we} (d) A plot of dilutive CP modulus $\boldsymbol{CP_D}$ as a function of NaCl DS concentration.

Results in Fig. 4.5c and Fig.4.5d show that the $\boldsymbol{CP_D}$ became severer (farther from unity) with increasing the concentration of DS and increased water flux. In other words, the value of $\boldsymbol{CP_D}$ is strongly dependent on water flux (Achilli, Cath & Childress 2009). Higher DS concentrations result in higher permeation flux, hence creating a higher degree of dilution of the DS on the surface of the AL. For example, the most severe $\boldsymbol{CP_D}$ was 0.52 for 1.5M NaCl DS, indicating that the osmotic pressure of DS at the membrane surface is almost half of that in bulk DS. Therefore, at higher water flux, the effects of dilutive external CP can become a limiting factor in the FO process (Chanukya, Patil & Rastogi 2013; Yip & Elimelech 2011). At very low water fluxes and DS concentration such as 0.1M, the effects of $\boldsymbol{CP_D}$ is almost negligible ($\pi_{DM} \approx \pi_{Db}$).

4.6.4 AL-DS mode: Quantification of CP_F NaCl DS-NaCl FS

When the feed solution in the FO process is DI water, the osmotic pressure at the FS side of the membrane will be negligible, and the relationship between J_{we} and $\boldsymbol{CP_D}$ is illustrated in Fig. 4.5c. For the FO process with a saline FS, additional information should be available to calculate the $\boldsymbol{CP_F}$ in the FO process. NaCl concentrations between 0.05 and 0.5M were FS in the FO process to measure the concentrative CP, $\boldsymbol{CP_F}$, in the FO membrane at 1M NaCl. The FO process was performed in the AL-DS mode to study the moduli of $\boldsymbol{C_{PF}}$ and the $\boldsymbol{C_{PD}}$. The two CPs act simultaneously on the FO membrane leading to a reduction in the experimental permeate flux J_{we} (Fig. 4.6a). As shown in Fig.4,6a, water flux increased with increasing the net osmotic pressure $\Delta\pi$. The modulus of $\boldsymbol{C_{PD}}$ can be obtained from the correlation between J_{we} and $\boldsymbol{C_{PD}}$ from Fig. 4.5c, which shows water flux at different osmotic pressure gradients. In effect, the dilutive CP is mainly caused by water flux permeating across the membrane, diluting the concentration of the DS at the boundary layer. Compensating in Eq. [35] to obtain the modulus of $\boldsymbol{C_{PF}}$ at different water flux, and results are shown in Fig. 4.6b. As the concentration of FS increases, water flux and the modulus of $\boldsymbol{CP_D}$ decrease. In other words, as $J_{we} \rightarrow 0$ the modulus of $\boldsymbol{CP_D}$ is approaching 1 (Phuntsho et al. 2012).

At low FS concentration, $\boldsymbol{CP_D}$ will be more substantial while the role of $\boldsymbol{CP_F}$ will be insignificant (McCutcheon & Elimelech 2006b) and this explains the levelling of the modulus of $\boldsymbol{CP_F}$ at lower FS

concentration (Fig. 4.6b). The modulus of $\boldsymbol{CP_F}$ increases exponentially as the water flux increases and vice versa. Once the value of $\boldsymbol{CP_F}$ is available, the value of π_{FM} can be found from Eq. [35]. The correlation between π_{FM} and π_{Fb} is presented in Fig. 4.6c and experimental water flux (J_{we}) and π_{FM} is presented in Fig. 17d. The modulus of $\boldsymbol{CP_F}$ at any point can also be obtained from the slope of the line in Fig. 17c between π_{FM} and π_{Fb}. As the concentration of FS increases, the osmotic pressure at the membrane surface also increases (Fig. 4.6c), leading to a reduction in the osmotic driving force due to the severe $\boldsymbol{CP_F}$.

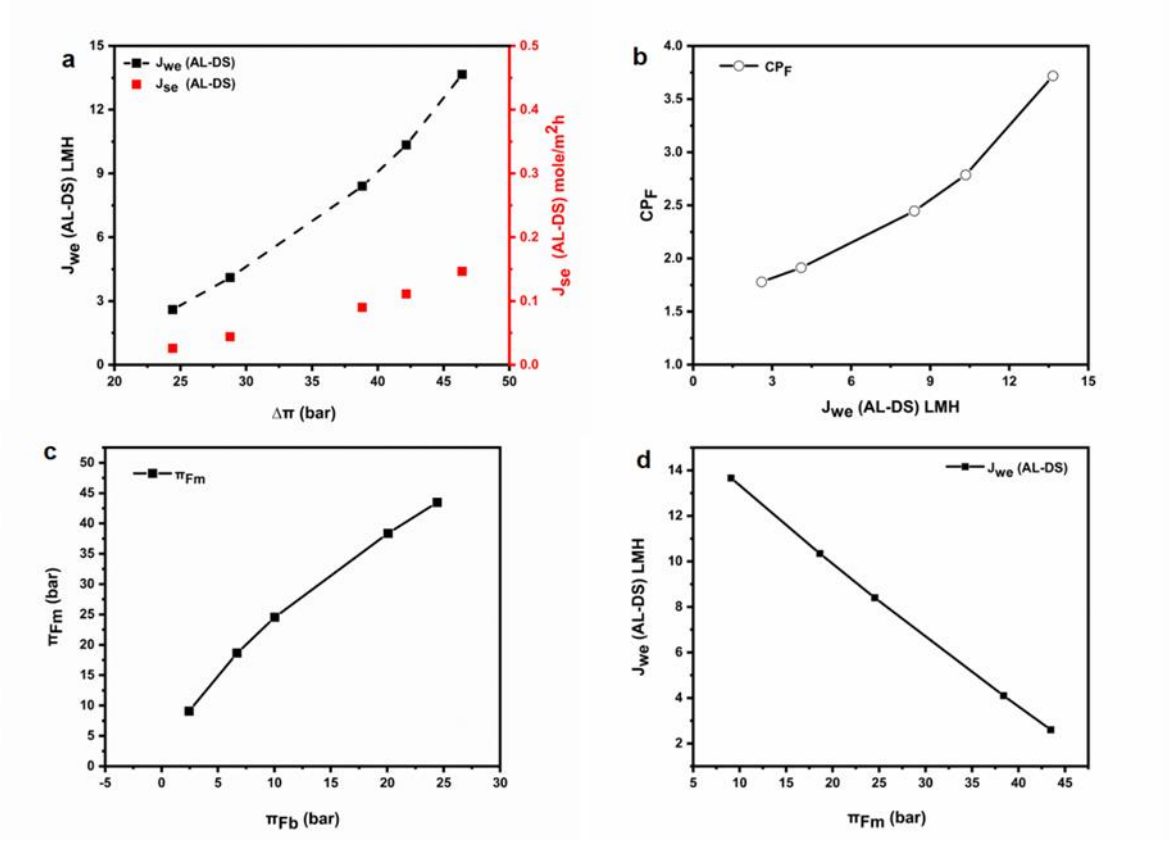

Figure 4.6: Quantifying concentrative concentration polarisation in the FO process for AL-DS mode with NaCl feed solution (0.05 to 0.5M) and NaCl DS (1M)

(a) Plot of experimental water flux J_{we} and experimental RSF J_{se} against the bulk osmotic pressure (b) Plot of concentrative CP modulus $\boldsymbol{CP_F}$ against experimental water flux J_{we} (c) Plot of osmotic pressure at the membrane surface on the feed side π_{FM} as a function of π_{Fb} (d). A plot of experimental water flux J_{we} as a function of osmotic pressure at the membrane surface on the feed side π_{FM}.

The correlations in Fig. 4.6c and Fig.4.6d can also be employed to predict theoretical water flux for different feed solution concentrations once the theoretical value of π_{FM} is available. These relations will be used to predict the theoretical water flux in the FO process for different feed solution concentrations using regression analysis.

4.6.5 AL-FS mode: Quantification of CP_D NaCl DS-DI water FS

When the FO membrane is operated in the AL-FS orientation, $\boldsymbol{CP_D}$ occurs inside the SL while $\boldsymbol{CP_F}$ is on the AL side. In the case of DI water FS, the $\boldsymbol{CP_F}$ values are insignificant due to the negligible osmotic pressure on the FS side (π_{Fb}=0.08 bar for 100ppm NaCl). Water permeates inside the SL and dilutes the DS, leading to a dilutive CP inside the SL. Initial tests were performed with DS concentrations ranging from 0.1M to 1.5M, and the water flux and RSF curves as a function of the osmotic driving force are presented in **Fig.** 4.7a. Water flux in the AL-FS mode is less than that in the AL-DS mode for the same driving force due to severe CPD inside the SL. As the boundary layer exists now inside the SL, it is difficult to mitigate it using a cross-flow velocity of 36 cm.sec^{-1} in our study. The RSF in the AL-FS mode was also lowered compared to the AL-DS mode. The numerical value of π_{DM} was calculated according to Eq. [29] and is presented as a function of the DS osmotic pressure (Fig. 4.7b). $\boldsymbol{CP_D}$ was calculated from Eq. [30] and plotted against the experimental water flux in Fig. 4.7c and the concentration of the DS in Fig. 4.7d.

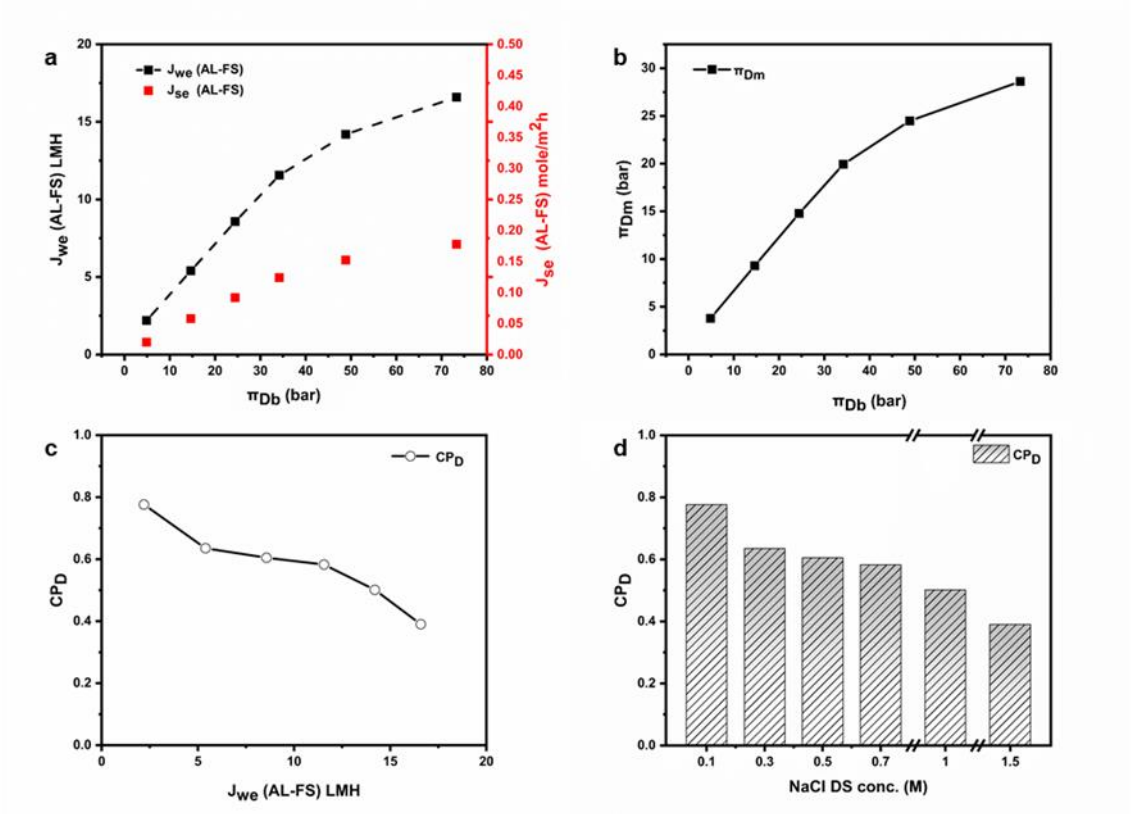

Figure 4.7 Performance of FO membrane in the AL-FS mode with single salt DS

a) Water flux and RSF in the FO mode with single salt NaCl solution as a function of the osmotic driving force,(b) Plot of osmotic pressure at the membrane surface π_{DM} as a function of bulk NaCl DS osmotic pressure π_{Db} (c) Plot of dilutive CP $\boldsymbol{CP_D}$ against the experimental water flux, (d) Dilutive CP $\boldsymbol{CP_D}$ as a function of NaCl DS concentration.

As the concentration of DS increases, $\boldsymbol{CP_D}$ tends to be farther away from the value of 1, depicting its severity. However, from 0.3M to 1M, an increase in DS concentration and water flux decreases the modulus by a tiny percentage (**Fig.** 4.7b and **Fig.** 4.7c, a flatter curve for the modulus). This phenomenon also is known as the ICP self-compensation effect (Tang et al. 2010b), means that an increase in ICP or CPD compromises any increase in DS concentration or driving force. Above 1M, the increase in the ICP becomes more severe, as marked by a greater increase in the modulus of $\boldsymbol{CP_D}$ for 1.5M DS. This severity makes the experimental water flux highly non-linear at high DS, as depicted in Fig.4.7a.

4.6.6 AL-FS mode: Quantification of CP_F NaCl DS-NaCl FS

In order to measure the concentrative CP modulus, $\boldsymbol{CP_F}$, FS was replaced with 0.05 to 0.5M NaCl, and the concentration of DS was 1M NaCl. The experimental permeate flux J_{we} and experimental RSF J_{se} as a function of osmotic driving force are presented in Fig. 4.8a. Both the water flux and RSF were lowered in the AL-FS orientation compared to the AL-DS. The $\boldsymbol{CP_D}$ was predicted from Fig. 4.7c and the $\boldsymbol{CP_F}$ was calculated from Eq. [35]. The $\boldsymbol{CP_F}$ as a function of experimental water flux is presented in Fig. 4.8b. Compared to the AL-DS mode, severe dilutive CP resulted in a smaller water flux when the membrane operated in the AL-FS mode. Once $\boldsymbol{CP_F}$ is determined the value of π_{FM} can be found using Eq.[35]. Fig. 19c presents the correlation between π_{FM} and π_{Fb}. For any concentration of FS (within the range of 0.05 to 0.5M) and 1M DS, the value of π_{FM} can be estimated from Fig. 4.8c. Finally, Fig. 4.8d can be used to predict theoretical water flux with any FS concentration from 0.05M NaCl to 0.50M NaCl and 1M DS.

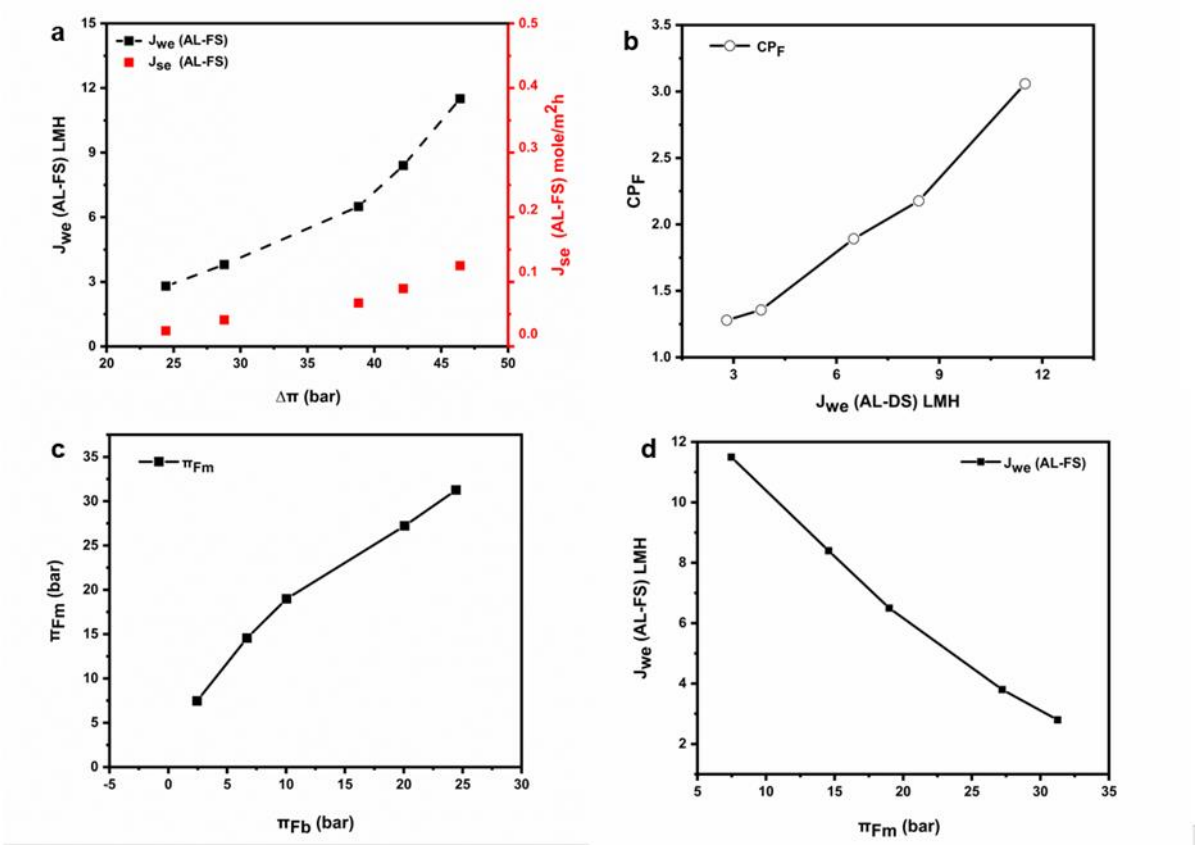

Figure 4.8: Performance of FO membrane in AL-FS mode with 1M NaCl DS and 0.05M to 0.5M NaCl FS

(a) Plot of experimental water flux and RSF against bulk osmotic pressure, (b) Plot of concentrative CP $\boldsymbol{CP_F}$ against experimental water flux (c) Plot of bulk FS osmotic pressure π_{Fb} against osmotic pressure at the membrane surface π_{FM}. d. Correlation between experimental water flux and osmotic pressure at the membrane surface π_{FM}.

4.6.7 Quantification of CP for mixture DS

The osmotic pressure of a solution is affected by adding a second solute to the solution (Hamdan et al. 2015). The addition of multivalent ions to a solution also affects the structure of the solvent (Hribar et al. 2002). It has been demonstrated that water structure is ordered by small or multivalent ions and disordered by large or monovalent ions (Hribar et al. 2002). On the one hand, multivalent ions such as Mg^{2+} and SO_4^{-2} will tend to order the solvent structure. On the other hand, large monovalent ions such as Na^{+} will try to disorder the water structure in mixed draw solution experiments. The ions effect on the water can also be explained by a competition between ion-water interactions (Collins 1997). Small ions of high charge density bind to water molecules strongly, whereas, there is weak binding between large monovalent ions and water molecules relative to the strength of water-water interaction in the bulk solution (Collins 1997). Thus, different CP behaviour is expected for mixed solutions. To investigate the CP moduli in mixed DS, a 0.1M $MgSO_4$ was added to the corresponding NaCl DS of concentrations ranging from 0.1M to 1.5M. The CPs were investigated in both the AL-DS and the AL-FS mode using DI water and NaCl salt ranging from 0.05 to 0.5M as a FS.

4.6.8 AL-DS mode: Quantification of CP_D mixture DS-DI water FS

Fig. 4.9a shows the experimental water flux J_{we}, and RSF J_{se} as a function of the osmotic driving force for DI water FS and NaCl solution (0.1 to 1.5M) + 0.1$MgSO_4$ DS. The osmotic driving force increased slightly with the increase of the concentration of mixture DS, yet the average water flux

for the DS was slightly less than that for NaCl DS only. The slight decrease in the water flux for a mixture DS can be attributed to the swelling of the cellulose acetate polymer in the presence of divalent magnesium cation (Kesting 1965). The presence of $MgSO_4$ in the DS might cause swelling of the AL, making it slightly less permeable to water molecules (Wong et al. 2012b). Compared to a single NaCl DS, RSF decreased in the FO process with a mixture DS. Similar results with a mixed DS for reducing the RSF has been reported in previous studies (Holloway et al. 2015). The decrease in the RSF can be simply attributed to the larger molecular size of the $MgSO_4$ and the smaller diffusivities of the Mg^{2+} and SO_4^{-2} ions. The co-existence of mixed solutions also affect the diffusivity of the species in the mixed draw solutions mainly because of the main diffusivities (flux of a component with its concentration gradient) and cross diffusivities (flux of a component with the gradients of all other components in the mixed DS) that arise from mixing the two solutions. The net value of a diffusion coefficient in a multicomponent DS will be the result of interaction between all species in that solution. For binary mixtures such as NaCl+$MgSO_4$, there is limited data available from the literature for the mutual diffusion coefficient value. Even if such data is available in the literature, they are valid only for the experimental conditions for that particular experiment or study and invalid outside the experimental conditions. The dilutive effects of $\boldsymbol{CP_D}$ in the AL-DS mode leads to a substantial decrease in the bulk osmotic pressure. The osmotic pressure at the membrane surface π_{DM} was calculated using Eq. [29] and plotted as a bulk DS osmotic pressure function in **Fig.** 4.9b. The modulus of $\boldsymbol{CP_D}$ was calculated from Eq. [30] and plotted as a function of experimental water flux J_{we} (**Fig.** 4.9c) and function of the DS concentration (**Fig.** 4.9d).

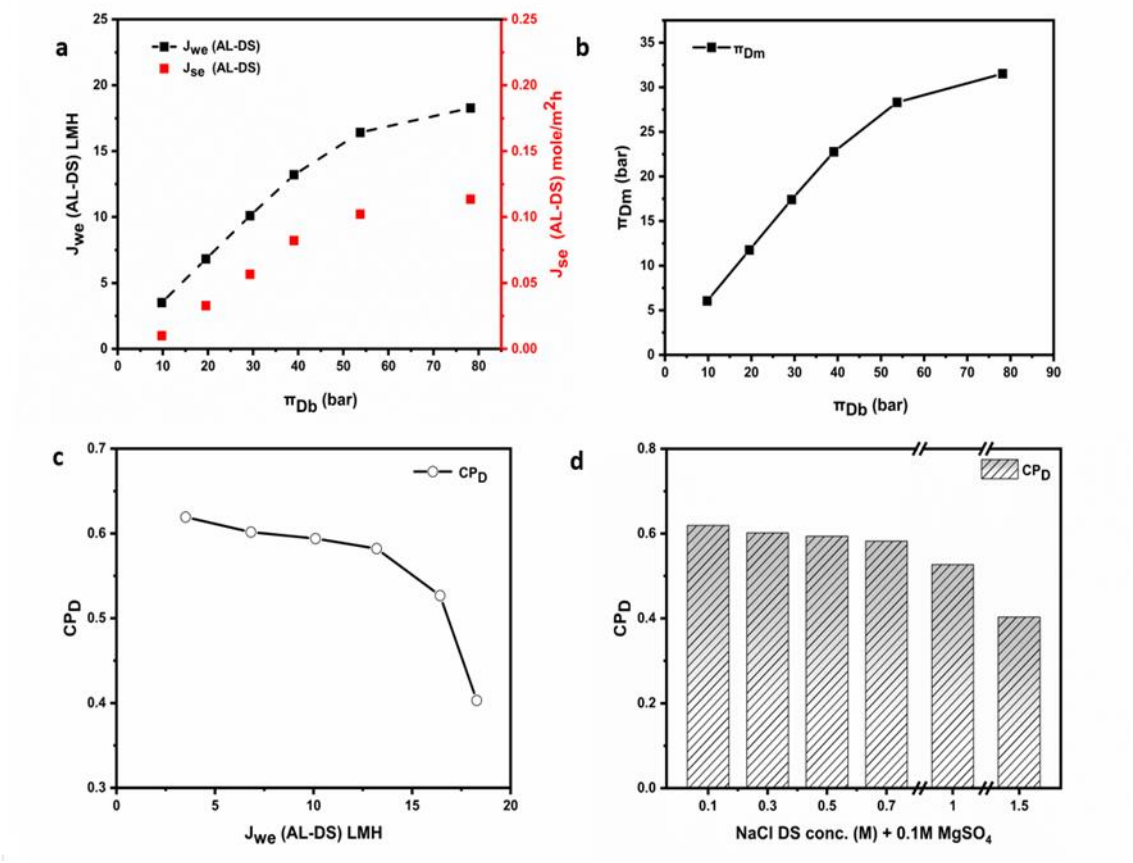

Figure 4.9: Quantifying dilutive concentration polarisation in the FO process for AL-DS mode with DI water feed solution

(a) Plot of experimental water flux J_{we} and RSF J_{se} against the bulk osmotic pressure, (b) Plot of osmotic pressure at the membrane surface π_{DM} against bulk osmotic pressure π_{Db}, (c) Plot of dilutive CP modulus as a function of experimental water flux, (d) CP modulus against NaCl (0.3 to 1.5M) +0.1$MgSO_4$ draw solution concentration.

The results revealed that CPD for a mixed DS was more severe compared to a single DS. This can be attributed to the fact that the concentration of divalent ions on the membrane AL (DS side) increased more abruptly (due to their lower diffusivities), leading to a higher concentration on the membrane surface (Déon et al. 2013). Table 4.1 shows the value of $\boldsymbol{CP_D}$ and osmotic pressure values for NaCl and mixture DS. The osmotic pressure drop due to the dilution of DS, i.e. $\pi_{Db} - \pi_{DM}$, of a mixture DS is approximately 6 bar higher than that for NaCl draw solution.

Table 4.1: Osmotic pressure values and CPD for single NaCl (1M) and mixed DS (1M+0.1M)

DS	Concentration	π_{Db}	π_{DM}	$\pi_{Db} - \pi_{DM}$	CP_D
NaCl	1M	48.86 bar	29.50 bar	19.36 bar	0.60
NaCl+$MgSO_4$	1M+0.1M	53.75 bar	28.31 bar	25.44 bar	0.53

4.6.9 AL-DS mode: Quantification of CP_F mixture DS-NaCl FS

To calculate the modulus of concentrative polarization, $\boldsymbol{CP_F}$, a mixture DS of 1M NaCl + 0.1M $MgSO_4$, was the DS, and NaCl in a concentration ranging from 0.05 to 0.5M was the FS. The experimental water flux J_{we} and RSF J_{se} as a function of the osmotic driving force are presented in **Fig.** 4.10a. The $\boldsymbol{CP_F}$ is plotted against the experimental water flux in **Fig.** 4.10b. The $\boldsymbol{CP_F}$ for a mixture DS ranged from 1.08 to 3.30 (Table 4.2). Water flux is slightly lowered in mixture DS tests leading to a relatively smaller concentration of the FS inside the SL. The RSF of the DS was also smaller in the case of mixture DS tests, which further reduced the impact of RSF on concentrative ICP. The plot of $\boldsymbol{CP_F}$ as a function of the osmotic driving force shows an exponential relationship (Fig 4.10b). The osmotic pressure at the membrane surface on the feed side π_{FM} was calculated from Eq. [35] and plotted against the osmotic pressure of FS (**Fig.** 4.10c). **Fig.** 4.10d shows that experimental water flux declined (almost linearly) with increasing the values of π_{FM}.

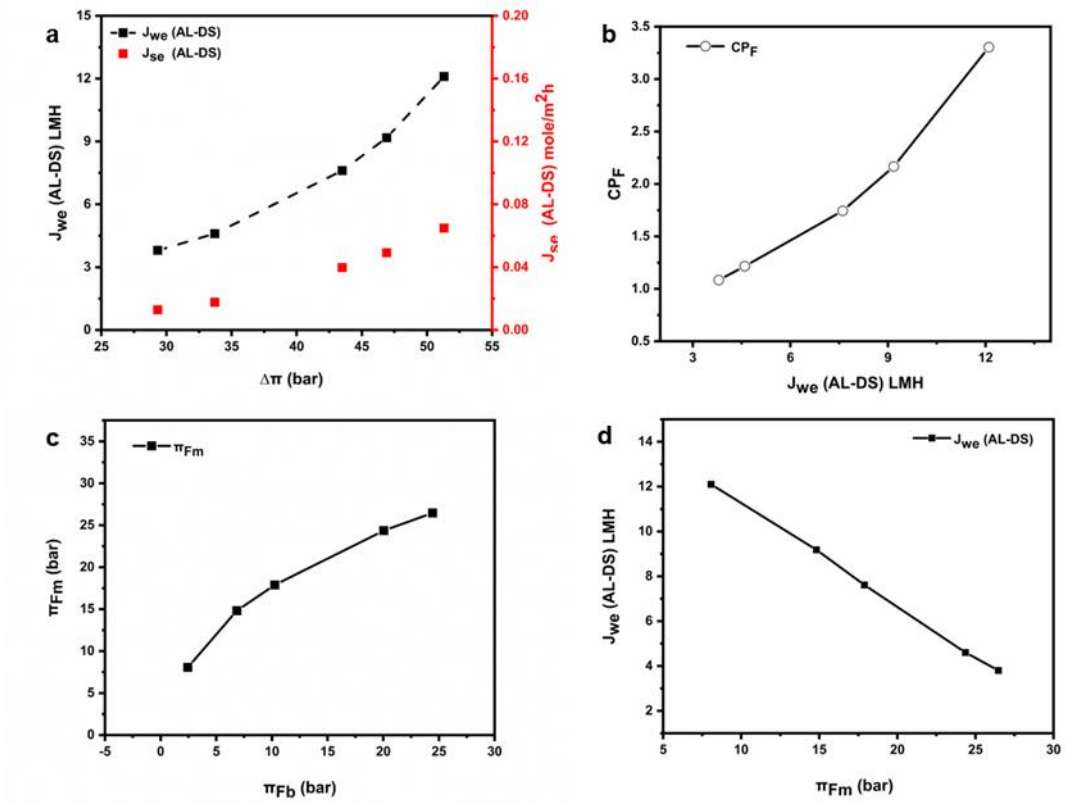

Figure 4.10: Performance of FO membrane in AL-DS mode with mixed DS

a) Plot of experimental water flux and RSF against bulk osmotic pressure, (b) Plot of concentrative CP $\boldsymbol{CP_F}$ against experimental water flux, (c) Plot of bulk feed osmotic pressure π_{Fb} against osmotic pressure at the membrane surface π_{FM}, (d). Correlation between experimental water flux and osmotic pressure at the membrane surface π_{FM}.

Table 4.2: CP moduli for various feed solution concentration with 1M NaCl + 0.1M MgSO4 DS (AL-DS mode)

DS Concentration	Feed solution NaCl	CP_D (from Fig 9c)	CP_F (Eq.12)
1M NaCl + 0.1MgSO$_4$	0.05M	0.54	3.30
1M NaCl + 0.1MgSO$_4$	0.14M	0.57	2.17
1M NaCl + 0.1MgSO$_4$	0.21M	0.58	1.74
1M NaCl + 0.1MgSO$_4$	0.41M	0.60	1.22

1M NaCl + 0.1MgSO$_4$	0.50M	0.61	1.08

4.6.10 AL-FS mode: Quantification of CP_D mixture DS-DI water FS

When a mixture DS of NaCl (0.3-1.5M) + 0.1M $MgSO_4$ is placed against the SL, and DI water FS is against the AL, the experimental water flux J_{we} and RSF J_{se} as a function of osmotic driving force are presented in **Fig.** 4.11a. The π_{DM} value was calculated using Eq. [29] and is plotted against the osmotic pressure of DS in **Fig.** 4.12b. The mixture DS is diluted inside the SL, leading to a dilutive internal CP. The modulus of $\boldsymbol{CP_D}$ was calculated from Eq. [30] and is presented in **Fig.** 4.11c as a function of experimental flux J_{we} and as a function of DS concentration in **Fig.** 4.11d. As shown in Fig 4.11a and 4.11c, as the water flux increases due to the increase in the concentration of DS, the effect of $\boldsymbol{CP_D}$ becomes more substantial. Interestingly, results showed an insignificant difference in the $\boldsymbol{CP_D}$ in the FO tests with NaCl and NaCl + $MgSO_4$ DS. For instance, for 1.5M NaCl+0.1$MgSO_4$, the value of $\boldsymbol{CP_D}$ was 0.37 compared to 0.39 for NaCl DS. Overall, the $\boldsymbol{CP_D}$ values for the mixture DS was between 0.37 and 0.58 for the range of concentrations in **Fig.** 4.11d.

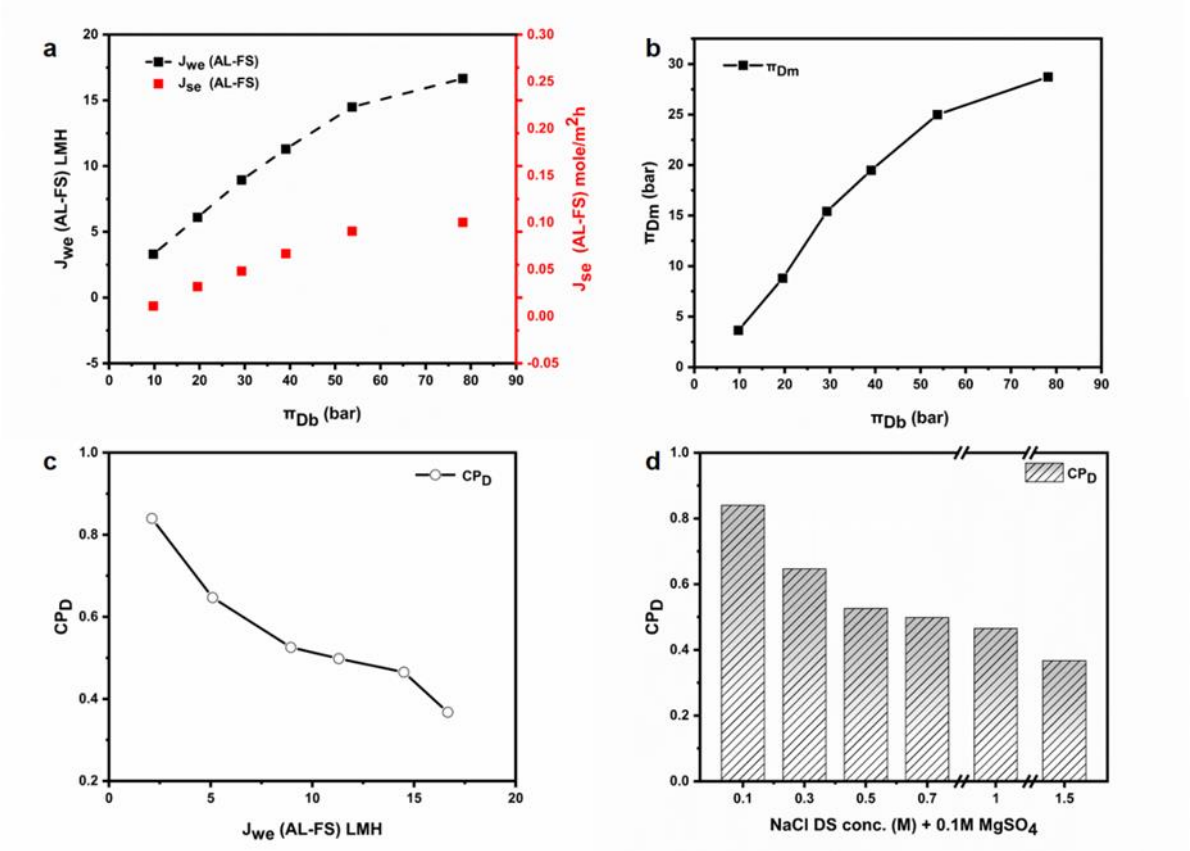

Figure 4.11: Quantifying dilutive concentration polarisation in the FO process for AL-FS mode with DI water feed solution

(a) Plot of experimental water flux J_{we} and RSF J_{se} against the bulk osmotic pressure (b) Plot of osmotic pressure at the membrane surface π_{DM} against bulk osmotic pressure π_{Db} (c) Plot of dilutive CP modulus as a function of experimental water flux. d). CP modulus against NaCl (0.3 to 1.5M) +0.1$MgSO_4$ draw solution concentration.

4.6.11 AL-FS mode: Quantification CP_F mixture DS-DI water FS

When the FS was replaced with NaCl 0.05M to 0.5M in the AL-FS mode, and a mixture DS was against the SL, the concentrative external CP, $\boldsymbol{CP_F}$, develops on the AL side of the membrane and dilutive internal CP, $\boldsymbol{CP_D}$, on the DS side. Water flux, J_{we}, and RSF, J_{se}, were plotted as a function of

the osmotic driving force (**Fig.** 4.12a). The lowest RSF amongst all the experiments is achieved in the AL-FS mode with a mixture DS. The moduli of $\boldsymbol{CP_D}$ and $\boldsymbol{CP_F}$ are presented in Table 4.2. The $\boldsymbol{CP_F}$ values ranged from 1.18 to 3.27 for the FS concentration of 0.05 to 0.5M. The plot of $\boldsymbol{CP_F}$ as a function of experimental water flux J_{we} is Presented in **Fig.** 4.12b. $\boldsymbol{CP_F}$ can also be predicted at from the slope of the plot between the π_{FM} and π_{Fb} in **Fig.** 4.12c. The value of π_{FM} can also be predicted from **Fig.** 4.12c for any feed solution osmotic pressure. Furthermore, the value of theoretical water flux in the FO process for any FS within the range of FS and DS concentrations can be predicted from **Fig.** 4.12d for the same range of draw solutions.

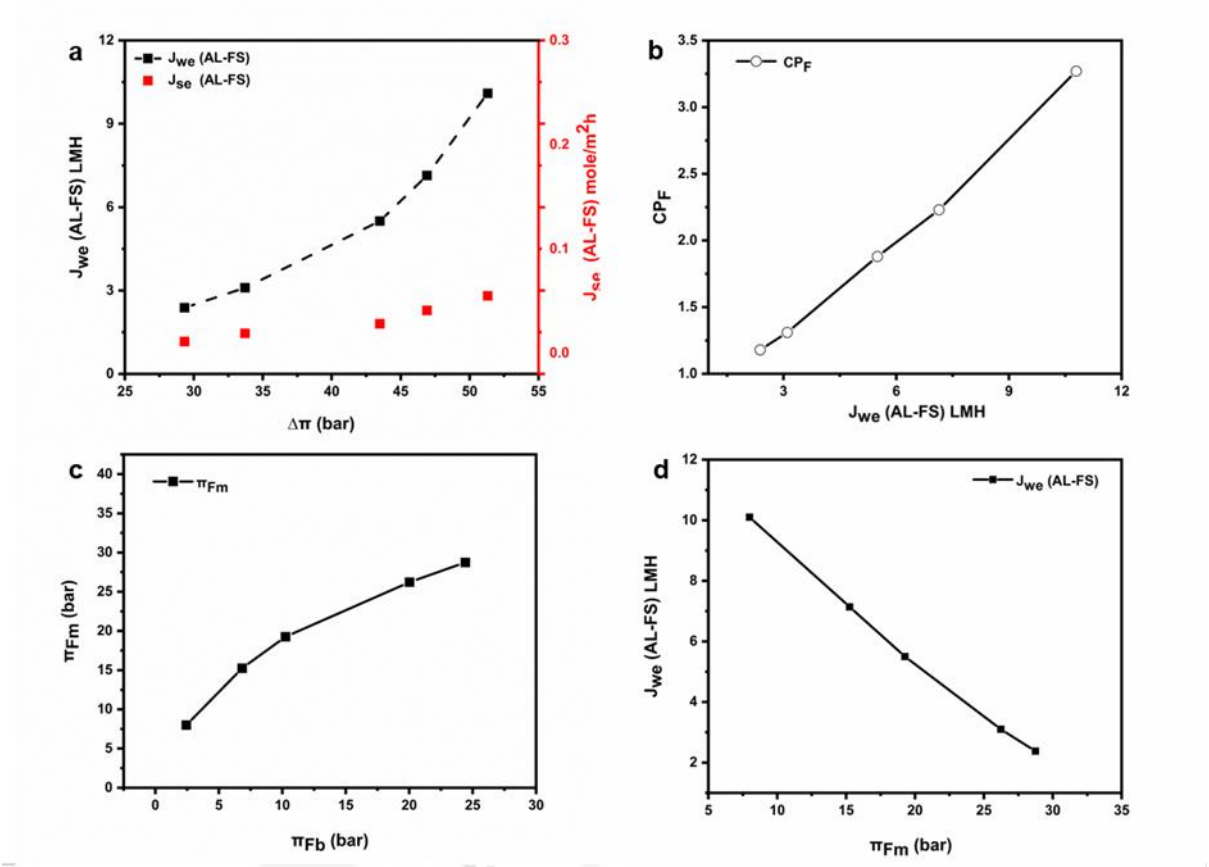

Figure 4.12: Performance of FO membrane in AL-FS mode with mixture DS and 0.05 to 0.5M NaCl FS

(a) Plot of experimental water flux and RSF against bulk osmotic pressure, (b) Plot of concentrative CP against experimental water flux, (c) Plot of bulk feed osmotic pressure π_{Fb} against osmotic pressure at the membrane surface π_{FM}, (d). Correlation between experimental water flux and osmotic pressure at the membrane surface.

Table 4.3: Moduli of dilutive and concentrative CP for various feed solution concentration with 1M NaCl + 0.1M MgSO4 DS (AL-FS mode)

DS Concentration	Feed solution NaCl	CP_D (from Fig 11c)	CP_F (Eq.12)
1M NaCl + 0.1MgSO$_4$	0.05M	0.47	3.27
1M NaCl + 0.1MgSO$_4$	0.14M	0.51	2.23
1M NaCl + 0.1MgSO$_4$	0.21M	0.53	1.88
1M NaCl + 0.1MgSO$_4$	0.41M	0.59	1.31
1M NaCl + 0.1MgSO$_4$	0.50M	0.61	1.18

Table 4.3 shows that the $\boldsymbol{CP_D}$ values in the AL-FS mode are more severe than the $\boldsymbol{CP_D}$ in the AL-DS mode. This is mainly because the $\boldsymbol{CP_D}$ in the AL-FS occurs inside the SL and cannot be mitigated by the high cross-flow velocities in this study.

4.6.12 Prediction of water flux, CP and RSF

It is possible to estimate theoretical water flux $\boldsymbol{J_{wt}}$ in the FO process with a DI water FS and NaCl DS (concentrations 0.1M-1.5M in this study), using the empirical data from the FO experiments. First, π_{Db} can be calculated to predict π_{DM} from the correlation between the two, then $\boldsymbol{J_{wt}}$ will be obtained from Eq. [26] using the predicted π_{DM} value. To do this, several draw solution concentrations between 0.1M and 1.5M (0.4, 0.6, 0.8, 1, 1.2, 1.3, and 1.4M) were considered for water flux prediction in the FO process using a DI water feed solution. For each DS concentration, π_{Db} was calculated to obtain π_{DM} and they are substituted in Eq. [26] to obtain $\boldsymbol{J_{wt}}$. Experimental water flux was also determined for all draw solutions (0.4, 0.5, 0.6, 0.8, 1.2, and 1.4M NaCl DS for single DS and 0.1M MgsO$_4$ was added to each for mixed DS) and compared with the $\boldsymbol{J_{wt}}$ for both NaCl and mixture DS in the AL-DS and the AL-FS modes (**Fig.** 4.13a and **Fig.**4.13b). The results

show an excellent agreement between J_{wt} and J_{we} for all draw solution concentrations, with an error of less than 5%. The CP_D for the investigated draw solutions can be predicted from Eq. [30].

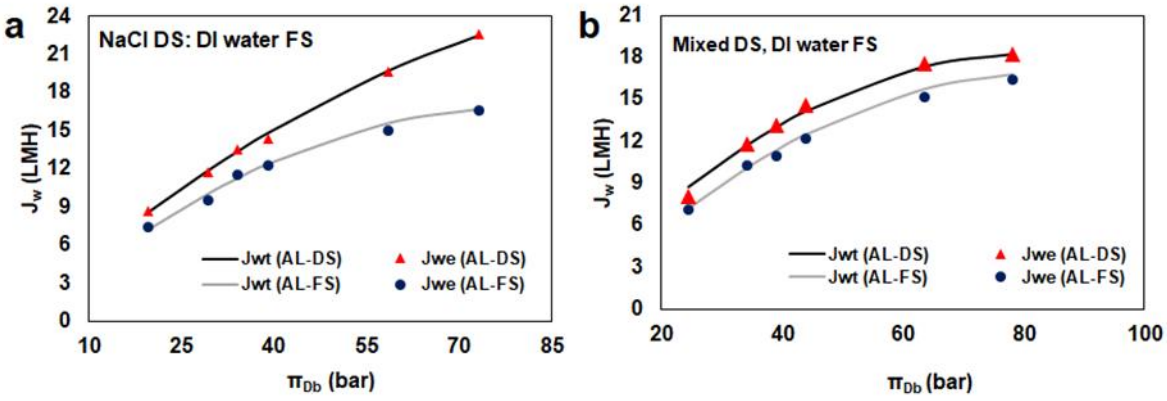

Figure 4.13: Theoretical flux prediction based on the correlations between empirical data

(12a) 0.4M to 1.4M NaCl DS and DI water FS in AL-DS and AL-FS mode, and (12b) Mixed DS with DI water feed in the AL-DS and AL-FS mode.

The excellent agreement between theoretical and experimental water flux J_{we} and J_{wt} shows the reliability of the proposed model to predict water flux in the FO process using empirical data. Compared to the previous models, water flux in the FO membrane can be determined with less information about the membrane and flow characteristics in the FO process. However, the feed solution in the FO process is often saline water, which leads to internal concentration polarization. This issue will be covered in the following section of the study.

For the FO process with a saline feed solution, additional information about the correlation between π_{FM} and J_{we} should be available to predict the J_{wt} and CP_F in the FO process with a saline FS. Initially π_{Fb} and π_{Db} were calculated as an average of the inlet and the outlet concentration of the feed and draw solutions. DS used was 1M NaCl DS experiments and 1M+0.1M $MgSO_4$ in mixed DS experiments. For each FS concentration, the osmotic pressure π_{Fb} was determined as the average inlet and outlet FS osmotic pressure and then the value of π_{FM} was obtained from the correlations with π_{Fb} . The value of J_{wt} was then predicted for NaCl and mixture DS using the correlations between J_{we} and π_{FM} as shown in **Fig**. 4.14a and 4.14b, respectively. The percentage error ranged from 4% to 5% for the experimental and theoretical values. The values of π_{FM} and J_{wt} was

compensated in Eq. [8a] to obtain the value of π_{DM}. Furthermore, $\boldsymbol{CP_F}$ can be predicted from Eq. [35] and $\boldsymbol{CP_D}$ from Eq. [30].

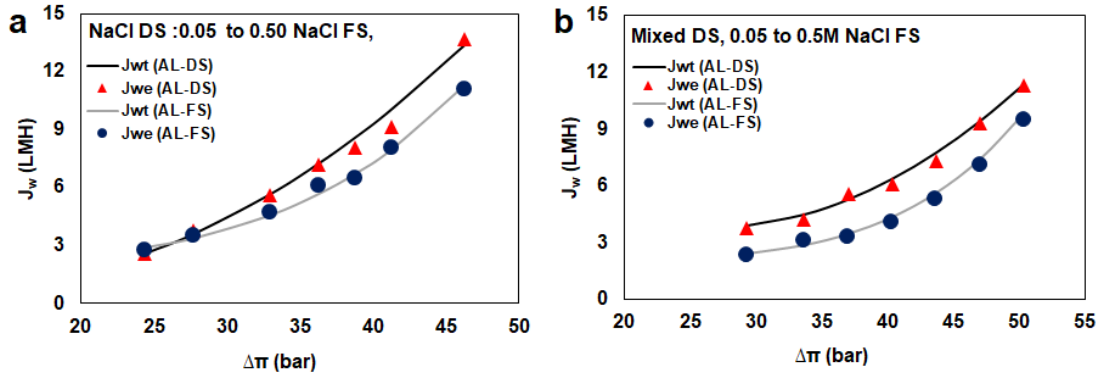

Figure 4.14: Prediction of theoretical water flux with NaCl feed solution (3g/L to 29.5g/L) in the AL-FS and the AL-DS mode

(a) Plot of theoretical and experimental water flux as a function of the osmotic driving force for single NaCl DS 1M and FS of 3g/L, 9g/L, 12g/L, 15g/L,19g/L,25.20g/L and 29.20g/L NaCl solution in the AL-FS and the AL-DS mode (b) Plot of theoretical and experimental water flux with 1M NaCl+0.1M $MgSO_4$ DS and FS of 4g/L, 8g/L,12g/L,16g/L, 20g/L, 24g/L and 29.20g/L NaCl in the AL-FS and the AL-DS mode. All prediction was based on empirical data.

From **Fig.**4.15a and 41.5b, the proposed model can provide a good estimation of theoretical water flux for any FS within the range of experimental data. For instance, $\boldsymbol{J_{wt}}$, $\boldsymbol{CP_F}$, *and* $\boldsymbol{CP_D}$ of any NaCl FS from 0.05 M-0.5M can be estimated using the methodology in this study. Apart from predicting the parameters above, the theoretical RSF $\boldsymbol{J_{st}}$ in the FO process can also be predicted since the value of solute concentrations at the membrane surface $\mathbf{C_{Dm}}$ and $\mathbf{C_{Fm}}$ can be determined easily once the value of π_{DM} and π_{FM} is available. The theoretical RSF can then be predicted from Eq.[36]. The experimental RSF was determined from Eq. [10]. The theoretical and experimental RSF are compared in **Fig.**4.15a &4.15b for NaCl and a mixture DS, respectively; results showed less than 10% error between the theoretical and experimental values. As evident from **Fig.**41.5a and **Fig.** 4.15b, the model can provide a good estimation of the RSF based on the solute concentration profiles

at the membrane surface. The error was slightly larger in the RSF prediction for mixed DS compared to the single NaCl DS.

The proposed empirical model can provide solute concentration profiles of the FO membrane and quantify CP in the FO process. Most importantly, this model does not rely on hydrodynamic relations such as Reynold and Sherwood relations and the solute resistance to diffusion "K" value.

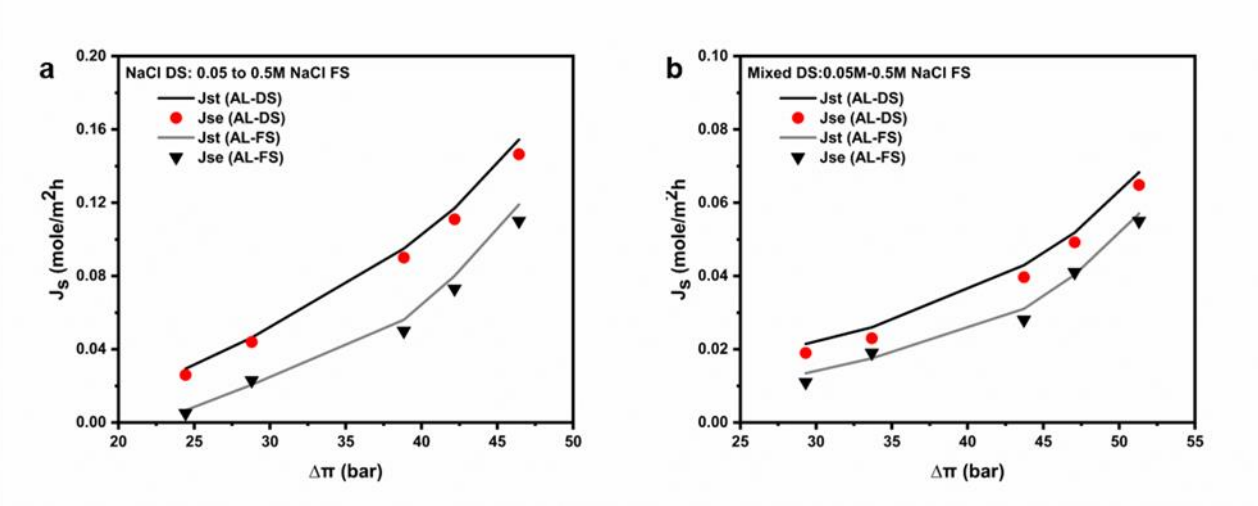

Figure 4.15: Comparison of theoretical RSF Jst and experimental RSF Jse

(a) For 1M NaCl DS and 0.05 to 0.5M NaCl FS, (b) For 1M NaCl+0.1M $MgSO_4$ DS and 0.05M to 0.5M NaCl FS.

4.7 Conclusion

The moduli of CPs' in the FO process require a large amount of information to calculate. The existing models can predict the experimental flux in the FO process. Still, they become more demanding when a mixture of draw solutions is used or lack of information about the FO modules due to propriety issues. Therefore, the solute resistivity "*K*" and mass transfer coefficient "*k*" value are hard to determine for a forward osmosis system. The empirical model in this study can provide an alternative solution for predicting water flux in the FO process. The model demonstrated an

excellent capability to predict CP and water flux in the FO process with 95-99% agreement with experimental values and without obtaining experimental parameters such as K and k. The model can be particularly helpful in the FO processes using a mixture of draw solutions. In a multicomponent draw solution, the diffusion coefficient is hardly available in the literature and ions move at a distinct rate within the film layer; therefore, it is impossible to define an effective diffusivity of the mixture. The model in this study only relies on a set of experimental data to measure CP and predict performance, such as Flux, CP, and RSF. It can also be extended to ternary and quaternary mixtures of DSs as well as commercial spiral wound modules.

Chapter 5: Treatment of biologically treated landfill leachate wastewater with forward osmosis: investigating membrane performance and cleaning protocols

This chapter is based on the following publication.

Ibrar, I., Yadav, S., Altaee, A., Samal, A.K., Zhou, J.L., Nguyen, T.V. & Ganbat, N. 2020, 'Treatment of biologically treated landfill leachate with forward osmosis: Investigating membrane performance and cleaning protocols', *Science of The Total Environment*, vol. 744, p. 140901.

Authors contributions:

Ibrar Ibrar: Conceptualization, Methodology, Writing - original draft. Sudesh Yadav: Methodology, Writing - original draft, Data curation. Ali Altaee: Supervision, Writing - review & editing. Akshaya K. Samal: Visualization, Investigation. John L. Zhou: Supervision, Writing - review & editing. Tien Vinh Nguyen: Visualization, Investigation. Namuun Ganbat: Visualization, Investigation.

Abstract

Sanitary landfills are an attractive and preferred method for the ultimate disposal of municipal and industrial wastes (Renou et al. 2008b). Over the years, landfill sites have transformed from open dumps to highly engineered facilities to minimize the adverse impacts on the environment (Calace et al. 2001a; Calace et al. 2001b; Nguyen & Min 2020). Despite the remarkable developments in improving the landfill facilities, these sites still generate undesirable leachate water, which is a source of environmental pollutants containing pharmaceuticals, organic wastes, radioactive elements, and many other contaminants (Ali et al. 2018; Ferraz et al. 2014; Först et al. 1989; Götz 1986; Kang, Shin & Park 2002; Schwarzbauer et al. 2002; Slack, Gronow & Voulvoulis 2004). Untreated leachate, therefore, poses hazards to the surrounding environment and requires competent treatment methods.

Forward osmosis is an emerging osmotically driven membrane process for the treatment of a wide variety of wastewaters, with potential advantages over other conventional methods (Achilli et al. 2009; Alphenaar et al. 1993; Awad et al. 2019; Bell, Holloway & Cath 2016; Boo, Elimelech & Hong 2013; Ibrar, Altaee, et al. 2019; Kim, Li & Ghaffour 2020; Linares et al. 2016; Yadav, Saleem, et al. 2020). Recently, the advancements in the FO technology have also enabled it to treat challenging feeds such as landfill leachate (LFL) wastewater (Aftab et al. 2019; Iskander, Novak & He 2018; Zhou et al. 2017). The potential of the FO process for treating LFL seems promising as biological and chemical processes treatment may not be sufficient for discharging the leachate to a sewer facility. FO treatment aims to reduce the volume of hazardous leachate wastewater before treatment by chemical/physical processes to remove or extract heavy metal ions. The concentrate can also be fed directly to an anaerobic treatment system (Ansari et al. 2017). NaCl draw solution can be treated by RO (reverse osmosis) or NF (nanofiltration) processes for regeneration and freshwater recovery. However, the main challenge is that LFL is laden with high organic, colloidal, and inorganic materials, which can promote severe irreversible membrane fouling in membrane processes such as the FO membrane.

Previous studies studying the impact of membrane orientation on the performance of the FO process suggested that membrane fouling was lower when the dense active layer was facing the feed solution and the support layer faces the draw solution (AL-FS or FO mode) (Tang et al. 2010b) compared to

when the active layer faces the draw solution, and the support layer faces the feed solution or AL-DS mode. The majority of the literature recommended the AL-FS mode for the treatment of challenging wastewater due to its advantages such as low fouling tendency, stable water flux and higher flux recovery after membrane cleaning (Yadav, Ibrar, Bakly, et al. 2020). The selection of membrane orientation is also influenced by other factors such as the composition and concentration of feed solution (Zhao, Zou & Mulcahy 2011). There are several concerns regarding the practical applications of the AL-FS mode, such as swelling/de-swelling of the support layer and change in the membrane structural parameter may occur when the ionic strength of the draw solution is high (Wong et al. 2012a). Furthermore, the water flux in the AL-FS mode is lower than that in the AL-DS mode (Thabit et al. 2019) as the former suffer from severe dilutive internal concentration polarization (Cornelissen et al. 2008a; Tang et al. 2010b). Operating the FO membrane in the AL-DS mode causes pore-clogging and rapid flux decline, particularly when the feed solution has a high fouling tendency coupled with a draw solution of high concentration, resulting in an initial water flux exceeding the critical flux. However, using a low concentration draw solution keeps water flux below the critical flux, and water flux in the AL-DS orientation follows a similar trend as the baseline water flux (Tang et al. 2010a). Therefore, more water recovery is achievable in the AL-DS mode. Water flux recovery after cleaning in the AL-DS mode is also lower than that in the AL-FS mode due to pore-clogging in the former. However, if the size of the majority of the fouling materials is larger than the pores of the support layer, fouling in the CTA membrane operating in the AL-DS mode would be a surface phenomenon, even on the support layer side (Mazlan et al. 2016). Developing effective cleaning methods is a key for fouling mitigation, knowing that the fouling in the AL-DS mode could be hydraulically or chemically reversible. As such, higher water flux can be achieved in the FO process, leading to efficient dewatering of the wastewater with excellent permeate quality that is ready for discharge. The diluted draw solution can be treated by reverse osmosis or nanofiltration processes for regeneration and freshwater recovery. Furthermore, the AL-DS orientation is necessary to investigate along the AL-FS as it can give insights to the impact of membrane orientation on FO performance with different wastewater feeds. Despite the wealth of literature on the applications of the FO process in wastewater treatment, there is no systematic investigation on the impact of the membrane orientation on the performance of the FO process in

terms of membrane performance, rejection of contaminants, and cleaning protocols for LFL treatment.

The objective of this study was two-fold, firstly, to evaluate the performance of the CTA FO membrane in AL-FS and AL-DS orientations and determine the best operating mode and fouling reversibility for the treatment of landfill leachate wastewater. The second objective of this study was to determine the advantages of physical membrane cleaning protocols over chemical cleaning protocols for the fouled FO membrane. In the physical cleaning, we investigated flushing with DI water at high cross-flow velocity, cleaning with hot water (35 ^{o}C), and osmotic backwashing methods. Hot water, in particular, can be a new environmentally friendly way for mitigating membrane fouling without compromising membrane integrity compared to chemical cleaning. The study also investigated the effectiveness of different chemical agents on the recovery of water flux and the rejection rate of the fouled FO membrane. Three types of chemical cleaning agents were selected for membrane cleaning. Hydrogen peroxide (H_2O_2) is a green oxidant, which has an excellent potential to oxidize organic and inorganic foulants effectively (Al-Amoudi & Lovitt 2007). The performance of the H_2O_2 was compared with the commonly used acid and base cleaning methods. Three acid and base cleaning methods were performed, acid cleaning at pH 4, base cleaning at pH 11, and sequential acid-base cleaning (15 mins acid cleaning followed by 15 mins base cleaning) for comparison purposes.

5.1 Introduction

This study presents systematic investigations to evaluate the performance, rejection rate, fouling, cleaning protocols, and impact of physical and chemical cleaning strategies on commercial cellulose triacetate (CTA) membrane performance. The treatment of landfill leachate (LFL) solution was performed in the active layer facing feed solution and support layer facing the draw solution (AL-FS mode), and the active membrane layer facing the draw solution and support layer facing the feed solution (AL-DS mode). Compared to the AL-FS mode, a higher flux for the AL-DS mode was achieved, but membrane fouling was more severe in the latter. In both membrane orientations, the rejection rate of the FO membrane to heavy ions and contaminants in the wastewater was between 93 and 99%. Physical and chemical cleaning strategies were investigated to recover the performance of the FO membrane and to study the impact of cleaning methods on the membrane rejection rate.

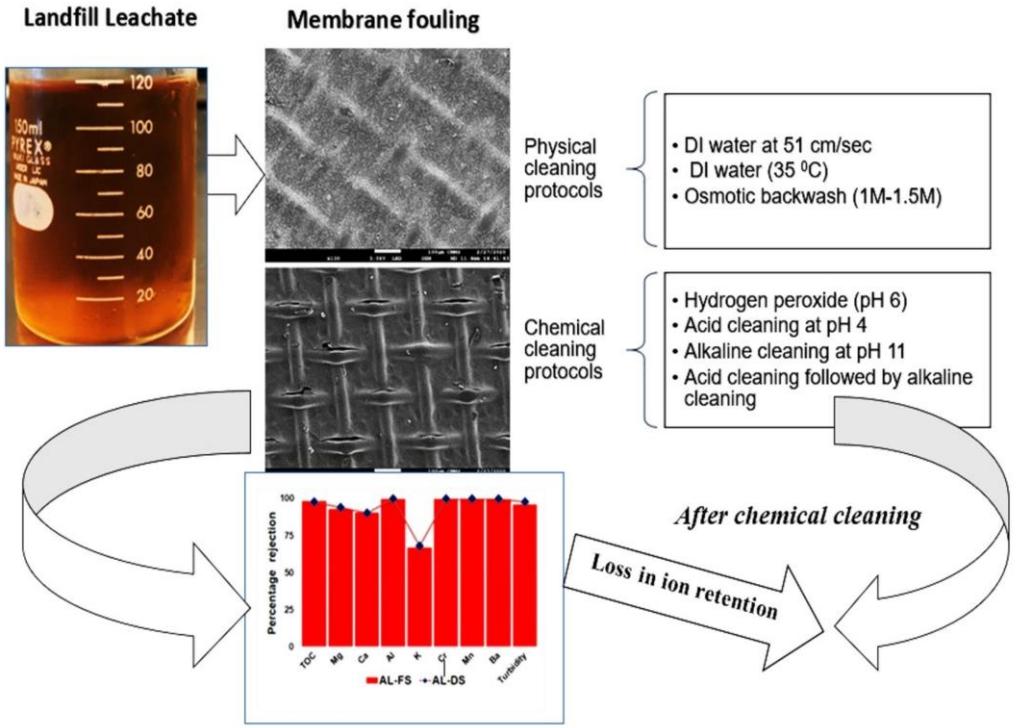

Physical cleaning with hot water at 35 ºC and osmotic backwashing with 1.5M NaCl demonstrated excellent water flux recovery compared to chemical cleaning. In the chemical cleaning, an optimal concentration of 3 % hydrogen peroxide was determined for 100% flux recovery of the fouled membrane. However, slight membrane damage was achieved at this concentration on the active layer side. Alkaline cleaning at pH 11 was more effective than acid cleaning at pH 4, although both protocols compromised the membrane rejection rate for some toxic ions. A comparison of the membrane's long-term performance found that cleaning with osmotic backwashing and hot water was an effective method to restore water flux without comprising the membrane rejection rate. Overall, it was found that physical cleaning protocols are superior to chemical cleaning protocols for the forward osmosis membrane fouled by landfill leachate wastewater.

5.2 Materials and methods

5.2.1 Landfill leachate wastewater and chemical reagents

Biologically treated LFL (landfill leachate) samples were collected from Whyte Gully landfill site in New South Wales, Australia. This landfill site collects all the city waste from the Wollongong council area except for building and demolition wastes. The leachate samples were collected in two 25 L polyethylene containers (one time) and stored in a refrigerator at 4 ºC before using, without dilution, in the FO experiments. All chemical reagents (analytical grade sodium chloride (NaCl) and hydrogen peroxide (H_2O_2) solution 30 % (w/w)) were procured from Sigma Aldrich, Australia. The draw solution in the FO experiments was NaCl solution of 0.6M concentration. A 30% w/w H_2O_2 solution was diluted to 3% w/w and used for the chemical cleaning experiments. Acid cleaning was conducted using an aqueous HCl solution at pH 4, and alkaline cleaning was done using an aqueous NaOH solution at pH 11.

5.2.2 Forward osmosis membrane

The FO membrane used in this study was the cellulose triacetate (CTA) membrane manufactured by Fluid Technology Solution (FTS) and purchased from Sterlitech Corporation, USA. This membrane was selected because it has been widely used for several wastewater studies and has excellent stability in harsh wastewater environments due to its high chlorine tolerance, low reverse salt flux, and good water flux (Phuntsho et al. 2013; Wu et al. 2018). Before using the membrane, it was soaked in DI water overnight at laboratory temperature (21±3 ^{o}C) to ensure complete wettability. At the beginning of each new experiment, the virgin FO membrane was washed with DI water for an hour.

5.2.3 FO experimental setup and operating conditions

The forward osmosis lab-scale cross-flow filtration unit used in this study is presented in **Figure 5.1**. The FO cell (CF042D) was purchased from Sterlitech Corporation, USA. This cell features an active membrane area of 42 cm^2 with two symmetric flow channels, holding a volume of 17ml on each draw and feed solution side. Feed and draw solutions were circulated at 2 litters per minute (LPM) or cross-flow velocity of 36 $cm.sec^{-1}$ in a co-current flow arrangement using two gear pumps (Longerpumps). The rationale for using this high cross-flow was to minimize the impact of external concentration polarization (ECP) on the water flux. The volumetric flow rate of the feed and draw solutions was measured using panel mount flow meters (FF-550 Sterlitech).

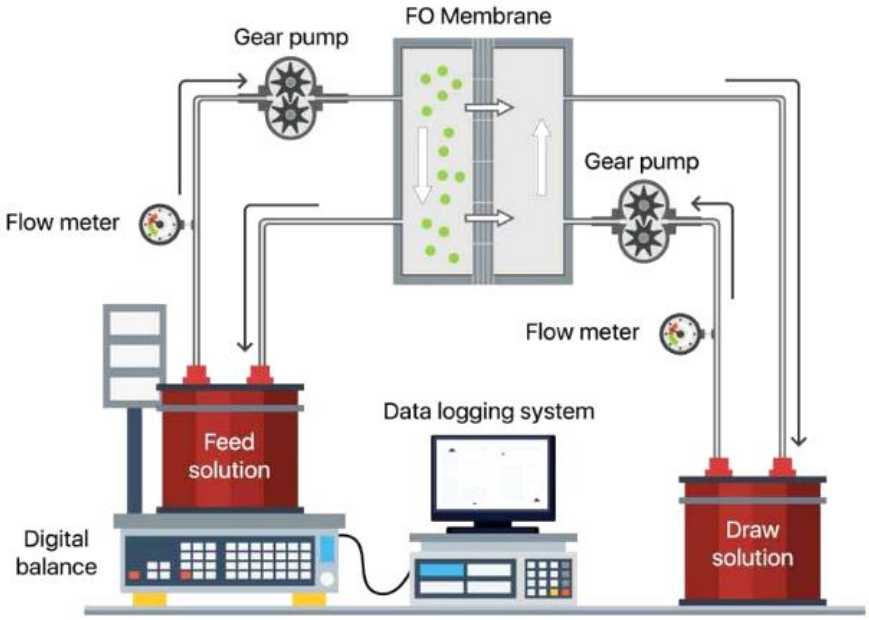

Figure 10.1: Laboratory-scale forward osmosis crossflow filtration unit

A digital balance (A&D EK-15KL) connected to a digital logging system (HP 470 laptop) was used on the feed solution side to monitor change in the weight of the feed solution with respect to time. The change in the weight of the feed solution was converted to water flux using equation 39.

$$J_w = \frac{(\Delta V)}{A*t} \qquad [39]$$

where ΔV is the volume of permeated water over time, A is the membrane area (0.0042 m^2), and t is the filtration time. All the experiments were conducted at ambient laboratory temperatures of 21±3 ^oC. The change in conductivity of the feed was recorded using a conductivity meter (LAQUA). The turbidity of all samples (n=3) was measured with a turbidity meter (Hach 2100P).

5.2.4 Experimental methodology

A previously soaked CTA membrane was mounted in the FO cell for each experimental cycle. The membrane was initially flushed and stabilized with DI water for one hour to ensure a stable permeate flux. In the next step, 500 mL of landfill leachate (from the collected refrigerated sample) and 0.6M

NaCl were pumped into the FO unit as the feed and draw solutions. Fouling experiments lasted 4 hours (240 minutes) to avoid the compaction of the fouling layer, which becomes harder to remove in longer filtration cycles (Al-Amoudi & Lovitt 2007). At the end of the fouling tests, the membrane was flushed with DI water for one minute on the leachate solution side to ensure that the remaining leachate in the feed channel does not compromise the cleaning efficiency of the suggested method. The membrane was cleaned physically or chemically for 30 mins following the following cleaning protocols listed in **Figure 5.2**. It should be noted that air scouring was not investigated as a cleaning protocol in this study mainly because it is energy-intensive. Additionally, a recent study Kim, Li & Ghaffour (2020) revealed that air scouring was not an efficient method to recover the water flux of the fouled FO membrane.

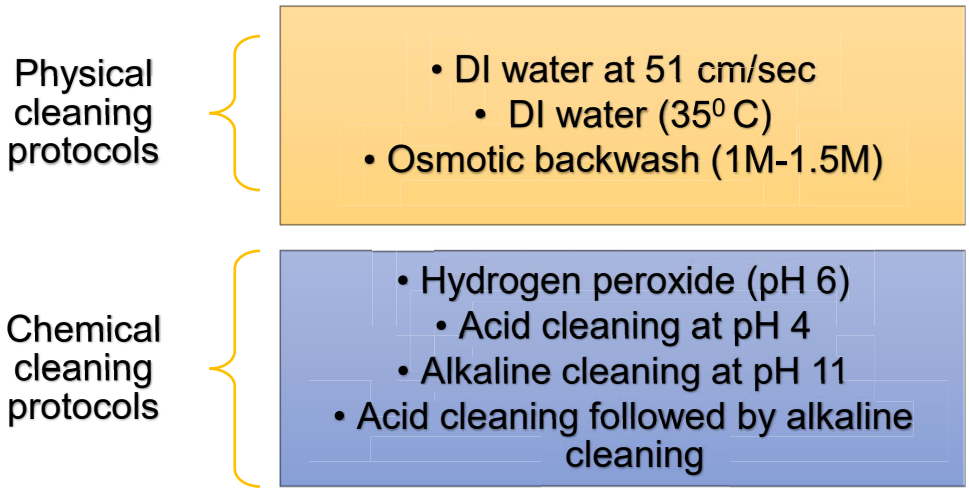

Figure 5.2: Cleaning protocols used in this study in both membrane orientations

Cleaning with chemical solutions was only employed on the fouled side of the membrane, whereas the other side of the FO membrane was flushed with DI water. Following the cleaning protocols, another test was performed with a new LFL solution and 0.6M NaCl draw solution. The water flux recovery (FR) was calculated by equation [40].

$$FR = \frac{J_c}{J_f} * 100 \qquad [40]$$

Where J_f is the average water flux of the fouled membrane for the whole cycle before cleaning and J_c is the average water flux of the membrane for the whole cycle after employing a physical or chemical cleaning protocol.

The physical cleaning methods were performed for four consecutive runs on the FO membrane in both membrane orientations to evaluate the efficiency of the physical cleaning protocols in the long-term operation of the FO process. Each FO run was 240 mins followed by 1 min flush with DI water and 30 mins cleaning with a hot DI water (35 ºC) or osmotic backwashing method. Only physical cleaning protocols were employed in the long-term tests to evaluate the efficiency of the cleaning process over time. Each experiment was repeated at least 3 times, and the average values were reported in this study.

5.2.5 Surface characterization of FO membrane

Field emission scanning electron microscopy (FE-SEM) was used to analyse the membrane morphology. FE-SEM images were taken for virgin, fouled, and cleaned membranes. In addition, Fourier transformation infrared spectroscopy (FT-IR) analysis was carried out for the same membranes.

5.2.6 Characteristics of the LFL wastewater

The leachate samples analysis (n=3) was accomplished by inductively coupled plasma mass spectroscopy (ICP-MS) and X-ray fluorescence (XRF) and is presented in Table 5.1. The leachate has a light brownish colour, indicating a high presence of organic materials (Humic and Fulvic acids). The conductivity of the raw leachate was 12.10 mS/cm and had a total dissolved solid of 5.5 g/L. The average zeta potential (n=3) analysed through the Malvern zeta analyser was highly negative, with a value of -15.6mV indicating strong repulsion between the foulants in the LFL. The XRF analysis revealed the presence of silica at an elevated concentration, which may contribute to

irreversible membrane fouling of the FO membrane in the presence of divalent calcium and magnesium ions (ICP-MS).

Table 5.1: Main characteristics of LFL wastewater collected from Whyte Gully resource centre, New South Wales

Parameter	Value	Unit
Zeta potential	-15.6	mV
Turbidity	34	NTU
Colour	Light brown	
Appearance	Small granules/particulates	
pH	7.82	-
Conductivity	12.10	ms/cm
TDS	5550	mg/L
TOC	149.2±5	mg/L
TC	204±5	mg/L
IC	27.6±3	mg/L
Mg	82.23±5	mg/L
Ca	66±5	mg/L
K	429±5	mg/L
Al	0.08	mg/L
Cr	0.08	mg/L
Mn	0.04	mg/L
Ba^{2+}	0.34	mg/L
Pb	0.006	mg/L
Si *	1717±88	ppm
Ag *	47±7	ppm

Th *	12±3	ppm
P *	54±29	ppm
S *	265±19	ppm

* XRF Analysis

Furthermore, divalent calcium ions can increase the fouling rate of humic acids on the membrane surface (Al-Amoudi & Lovitt 2007). The XRF analyser also indicated a low concentration of Thorium ions in the LFL. The total organic carbon (TOC), the total carbon, and inorganic carbon (IC) were measured with a TOC analyser (Shimadzu Corporation, Japan).

5.3 Results and discussions

5.3.1 Membrane characterization

A reverse osmosis (RO) test was performed to determine membrane water and salt permeability coefficients, A_w and B, respectively.

5.3.2 FO treatment of LFL wastewater

The size distribution of particulates in the LFL wastewater was analysed by the Malvern particle analyser. The average diameter of the particles in the LFL is 10 μm with a polydispersity index (PDI) value of 0.802, representing multiple particle size populations such as 2~4nm and 60~90nm. The average size of the contaminants in the range (60~90nm) is much bigger than the mean pore size of the support layer of the CTA membrane; hence more surface fouling phenomena is expected in the AL-DS. Figure 5.3a presents the performance of the CTA membrane treating LFL solution in the AL-FS and the AL-DS mode. The water flux obtained from the fouling experiments is divided by a normalization factor to give the normalized water flux (Mi and Elimelech 2008). The decline in the water flux is only attributed to the fouling of the FO membrane. The initial water flux in the AL-FS mode is around 7.38±0.3 LMH, and after four hours, it drops to 6.1±0.3 LMH, recording a 17% decline in the water flux. The feed water recovery reached 68% at the end of the filtration cycle. The AL-FS mode shows a stable and steady performance. Membrane fouling led to a slight decrease in the permeation flux, about 17%, over 4 hours of the filtration process (**Figure 5.3a**). The deposition of foulants in the AL-FS mode is presented in Figure 5.3b, and the AL-DS in Figure 5.3c. Overall, the average water flux in the AL-FS mode was 6.60±0.3 LMH.

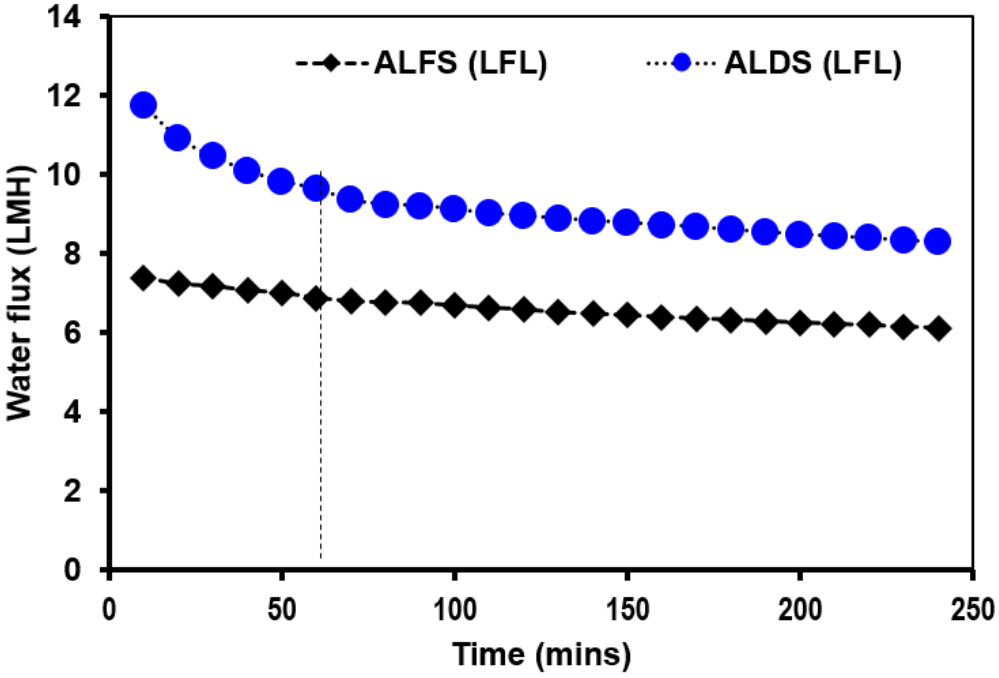
ALFS (LFL)
ALDS (LFL)
Water flux (LMH)
Time (mins)
0
2
4
6
8
10
12
14
0
50
100
150
200
250

a.

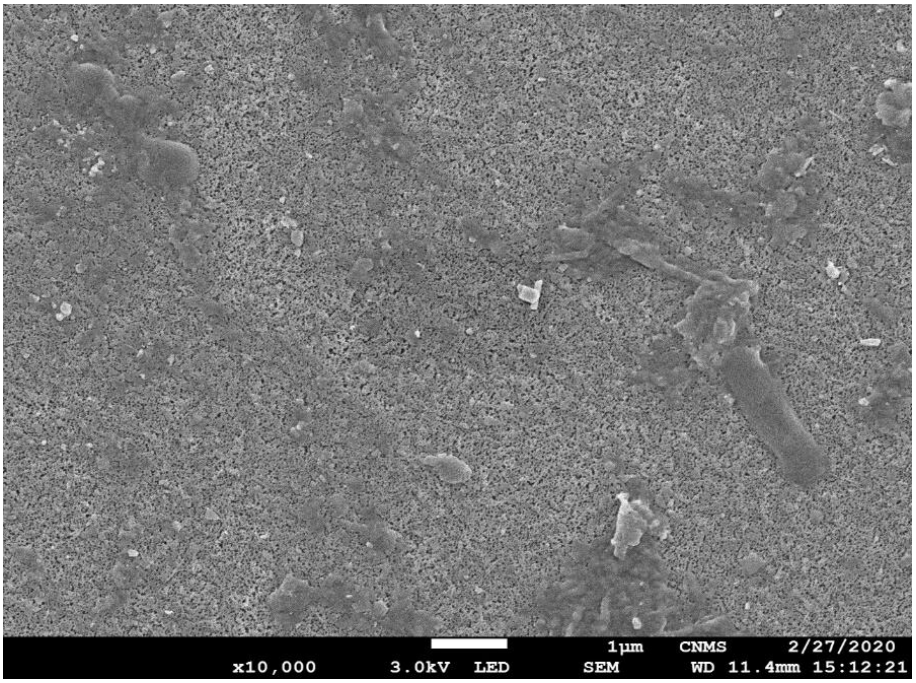
x10,000
3.0kV
LED
1µm
SEM
CNMS
2/27/2020
WD 11.4mm 15:12:21

b.

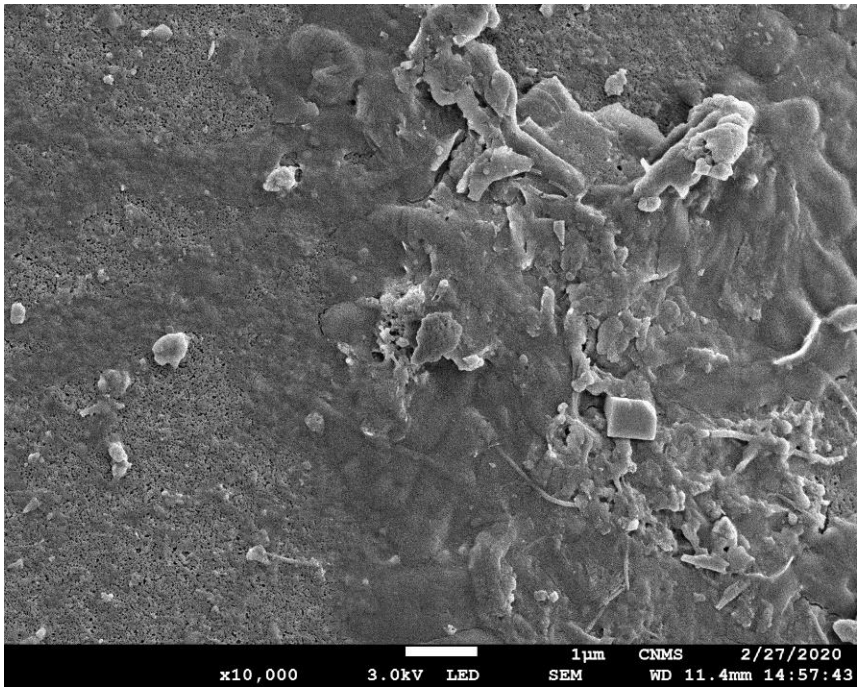

c.

Figure 5.3: Water flux in the AL-DS mode and the AL-FS with LFL feed

a). Water flux in the AL-DS mode and the AL-FS with LFL feed, b) fouling in the AL-FS mode on the active layer of the FO membrane, c) fouling in the AL-DS mode on the support layer of the membrane.

Experiments showed that the water flux and the feed water recovery in the AL-DS are higher than in the AL-FS orientation in the FO process for LFL treatment. The results agree with previous studies by (Vu et al. 2018) using seawater draw solution for treating digested sludge concentrate and Xie, Price, et al. (2013) study for rejection of trace organic contaminants. The initial water flux in the AL-DS mode was 11.72±0.7 LMH, which is higher than that in the AL-FS mode, which is attributed to the lower dilutive concentration polarization in the AL-DS mode. The feed water recovery in the AL-DS orientation reached 71.68% by the end of the filtration cycle. The higher hydrophilicity of the membrane support layer compared to the active layer also contributed to the high water flux and the water recovery in the AL-DS mode. There was a sharp decline in the water flux at the first hour of the filtration, and that could be attributed to the higher initial water flux, leading to a rapid

dilution of the draw solution. The other reason for the rapid decline in the initial water flux could be due to the membrane fouling caused by the accumulation and deposition of foulants inside the membrane support layer due to particulates in the range of 2~4nm. The low shear force effect on the foulants inside the porous support and the absence of the ICP self-compensation effect in AL-DS orientation also contributed to the decline of water flux (Mi & Elimelech 2010c; Tang et al. 2010a). After the first hour of the filtration process, a steady decline in the water flux continued to the end of the experiment to record 25% decrease compared to the initial water flux. At this stage, the reduction in the water flux mainly occurred due to a cake layer fouling.

Analyzing the foulants size by Malvern analyser revealed that most of the foulants have a larger diameter (in the range 60~90nm) than the pore size of the support layer. Therefore, it is likely that a large amount of fouling on the support layer is surface fouling. Accordingly, large-size foulants that could not enter the support layer were deposited on the outer surface of the support layer, leading to a cake layer formation on the porous support layer. Overall, an average flux of 9.17±0.7 LMH was achieved in the AL-DS mode. Figures 5.3b and 5.3c present the membrane fouling in the AL-DS and the AL-FS mode, respectively. An irregular fouling layer was observed in the AL-DS mode and looks more severe than a uniform cake layer in the AL-FS mode. The fouling appears to be combined organic, colloidal and inorganic scaling.

The difference in water flux between the two modes could also be attributed to the electrostatic interaction between the membrane surface and the contaminant (Zhao et al. 2016b; Zheng et al. 2015). The support layer of the CTA membrane is more negatively charged than the active layer, leading to a greater electrostatic repulsion between the membrane surface and the foulants in the landfill leachate. As a result, higher initial water flux is obtained in the AL-DS orientation compared to the AL-FS orientation.

Figure.5.4. presents the rejection performance of the FO membrane for different ions, TOC, total carbon (TC), and turbidity. The overall TOC and turbidity rejection of the FO membrane in both membrane orientation was about 99±1% and 100%, respectively. The low concentration of calcium ions did not affect the rejection rate of TOC in this study. The high rejection of heavy metal ions in the FO process was due to the lack of hydraulic pressure and the size exclusion or the sieving mechanism. Since the FO process operates under zero hydraulic pressure, the effect of convective

flow on the metal ion transport is negligible (Cui et al. 2014). The rejection of multivalent ions such as Ca^{2+} and Mg^{2+} was higher than that of monovalent cations such as K^{+}. Multivalent ions rejection by the membrane was higher than that of monovalent ions due to the higher valency charge. Typical FO membranes have a negative surface charge at neutral pH, which explains the higher rejections of multivalent of negative charge. For barium ions, the rejection rate by CTA membrane is between 94 and 96%, which is lower than that of other divalent ions (Guide 2007). For a positively charged membrane, such sequence would be $CaCl_2$ > NaCl > Na_2SO_4; for a negatively charged membrane, the normal sequence is Na_2SO_4 > NaCl > $CaCl_2$. According to Tansel et al. (2006), ions with smaller crystal radii and larger hydrated radii hold their hydration shells more strongly; hence they are highly rejected by the membrane and, therefore, the higher rejection of Ca^{2+} and Mg^{2+} was higher than K^{+}. The highest rejection for Ni ions (not detectable) and Pb (>99%) in both AL-FS and AL-DS mode could be due to the largest hydrated radii amongst all the pollutants. Interestingly, the effect of membrane orientation had a minor impact on the rejection of the micropollutants in this study, which could be due to the similar composition of the active and support layer material.

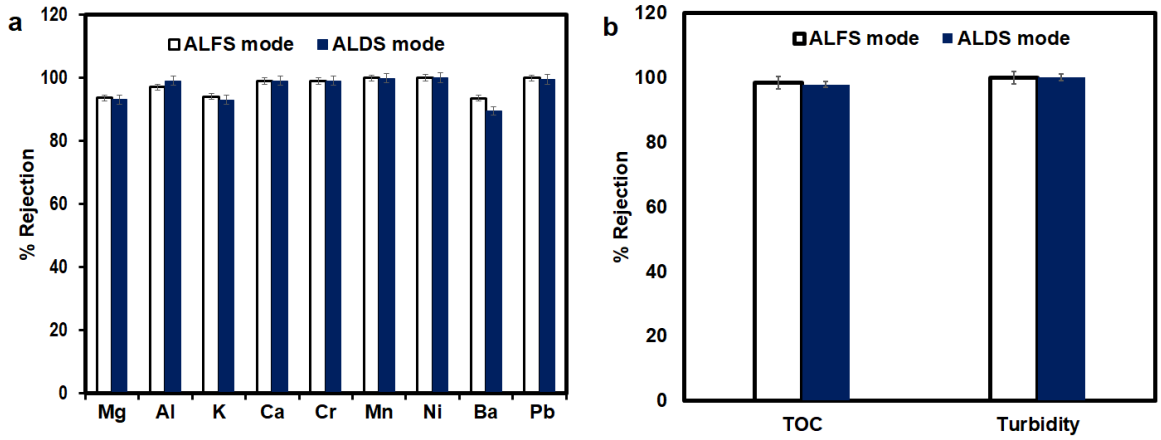

Figure 5.4: Rejection of CTA FO membrane in AL-FS and AL-DS mode analysed by ICP-MS

a). Rejection of CTA FO membrane in AL-FS and AL-DS mode analysed by ICP-MS, b). Rejection of CTA FO membrane for TOC and turbidity analysed by TOC analyser and Turbidity meter. * The amount of Ni was not detectable in the permeate solution and therefore almost 100% rejection for Ni for the FO membrane.

5.4 Comparison of physical and chemical cleaning protocols

In this study, the FO membrane was fouled with LFL wastewater for four hours and then cleaned by physical or chemical protocols for 30 mins. **Figure 5.5a** and **5.5b show** the FR for each cleaning protocol. The SEM images of the virgin and fouled membranes are presented in Fig 5c. Overall, the FR is higher in the AL-FS mode than the AL-DS for both physical and chemical cleaning, as the fouling on the active layer is mainly external fouling compared to the combination of external & internal fouling in the porous support layer. In the physical cleaning, hot DI water at 35 ^{o}C was a very effective method for the membrane cleaning, restoring 97% of the water flux in the AL-FS orientation and 89% in the AL-DS mode. The average water flux and recovery rate after hot water cleaning was 6.40±0.1 LMH and 66%, respectively, in the AL-FS mode, and 8.16±0.3 LMH and 70%, respectively, in the AL-DS mode. The probable reason for the high FR may be the introduction of thermal shock to the fouling layer, which disintegrated or cracked the fouling layer; consequently, it was quickly removed by flushing with water at 36cm.sec^{-1} crossflow velocity (**Figure 5.5c**).

Interestingly, the solubility of some foulants (such as silica) attached to the active layer or inside the porous support layer increases with the increase in temperature, facilitating the removal by hot water. Furthermore, the temperature is among the factors that affect cleaning efficiency, and better cleaning efficiency could be achieved at elevated temperatures between 35 and 50 ^{o}C. However, Madaeni & Samieirad (2010) state that 35 ^{o}C is the optimum temperature for a complete water flux recovery in the reverse osmosis membrane fouled by wastewater. A further increase in temperature up to 45^{o}C does not affect flux recovery. In the AL-DS mode, almost 89% of the flux was reversible with hot water cleaning compared to 76% by flushing with DI water at a high crossflow velocity of 51cm.sec^{-1}. The high shear stress with DI water flushing could only remove some large-size foulants in the AL-DS mode compared to hot water, which can dissolve some organic matter inside the porous layer, making them easily removable (Camilleri-Rumbau et al. 2016). In the AL-DS mode,

the hot water can slightly increase the membrane's pore size, leading to a better cleaning efficiency for internal fouling or pore-clogging. The visual observations of the membrane from the SEM analysis (Fig 31c) indicate a great resemblance to the virgin membrane in the AL-FS orientation as well as AL-DS orientation. In the AL-DS mode, the membrane displayed a slight cake layer, indicating the presence of some fouling materials. It is probably the reason for a smaller water flux recovery than the AL-FS orientation. In contrary to hot water cleaning, chemical cleaning is more expensive and generates chemical wastewater. Overall, hot water cleaning can efficiently clean the membrane in both the AL-FS and the AL-DS modes.

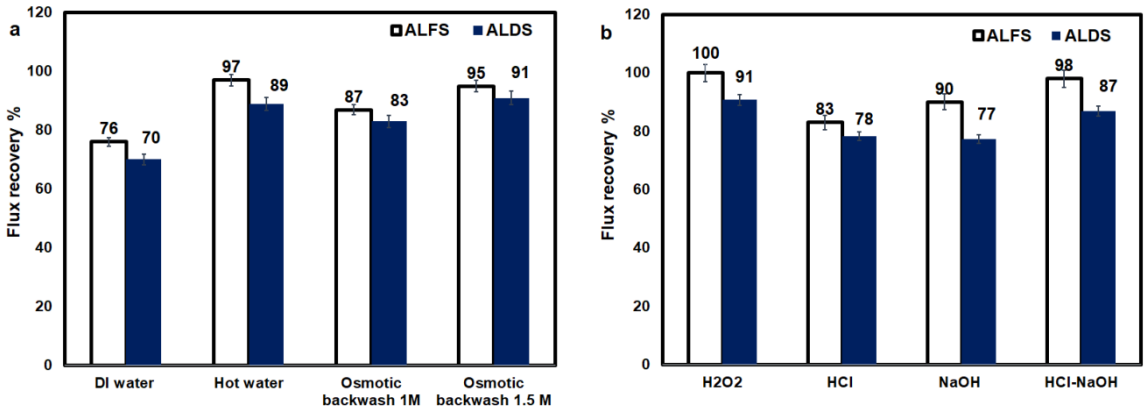

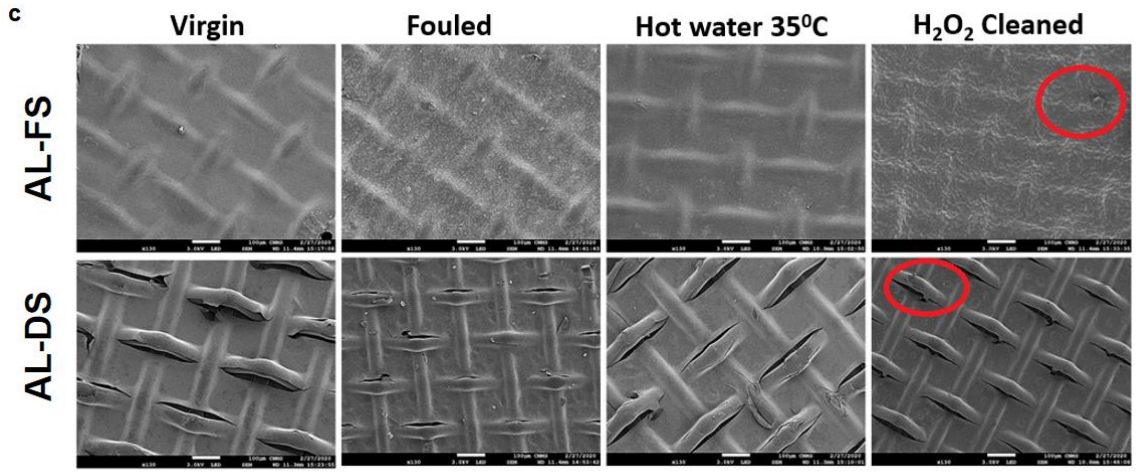

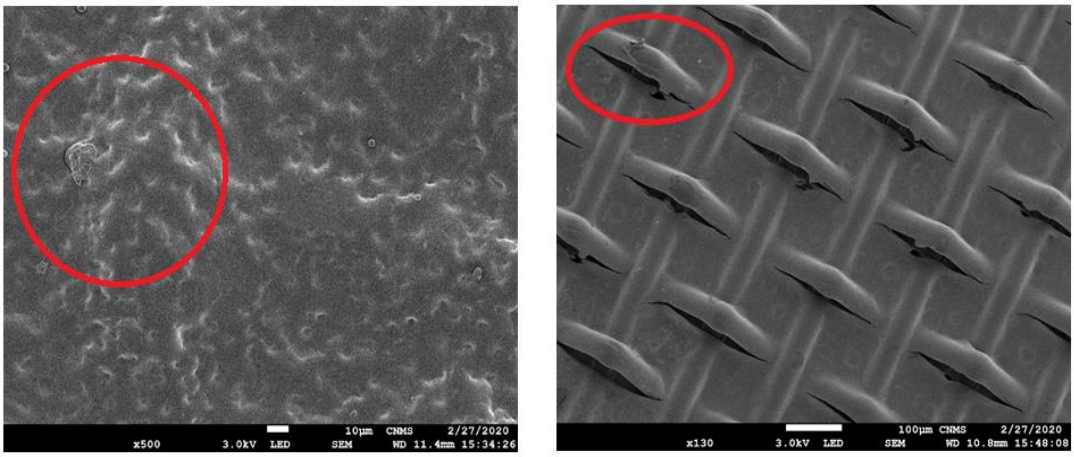

Figure 5.5: Comparison of physical and chemical cleaning protocols for CTA FO membrane

a). Physical cleaning protocols (DI water at 51cm.sec^{-1}, Hot water 35 ^{o}C, osmotic backwashing 1M, and 1.5M) in AL-FS and AL-DS mode. b). Chemical cleaning protocols (100mL/L H_2O_2, 0.05M HCl at Ph 4, 0.05M NaOH at pH 11, and sequential cleaning, which was 0.05M HCl at pH 4 followed by 0.05M NaOH at pH 11) in AL-FS mode and AL-DS. c). FE-SEM images of the virgin membrane, fouled membrane, hot water 35 ^{o}C cleaned, and H_2O_2 cleaned membrane, (a) AL-FS mode (b) AL-DS mode. The red circle in H_2O_2 cleaned membrane illustrates a slight peeling of the membrane layer due to chemical cleaning. D) Damage on the active layer by hydrogen peroxide cleaning, a). On the active layer in the AL-FS mode. b). Slight peeling of the support layer in the AL-DS mode.

Further investigation was attempted to evaluate the efficiency of osmotic backwashing for cleaning the fouled CTA membrane. Osmotic backwashing is an effective technique to restore the water flux of the fouled CTA membrane by colloidal and combined colloidal and organic materials (Kim, Elimelech, et al. 2014). Initially, osmotic backwashing was conducted with 1M NaCl draw solution, and it was able to recover 83% of the water flux (average flux of 7.61±0.3 LMH and feed water recovery of 65 %) in the AL-DS mode and 87% in the AL-FS mode (average flux of 5.74±0.2 LMH and feed water recovery of 59%). When the concentration of the draw solution increased to 1.5M, water flux was high enough to backwash and detach foulants, recovering 95% of the water flux in

the AL-FS mode (average flux of 6.27±0.2 LMH and feed water recovery of 64 %) and 91% in the AL-DS mode (average flux of 8.34±0.1 LMH feed water recovery of 71%). In the short-term filtration process over 4 hours, the efficiency of the osmotic backwashing with 1.5M NaCl was as effective as hot water cleaning. It is worth mentioning that after osmotic backwashing, the draw solution side of the membrane was flushed with DI water for one minute before performing the next run.

In addition to the physical cleaning methods, chemical cleaning was investigated to clean the CTA membrane, and results were compared with the physical cleaning methods (hot water 35 ^{o}C and osmotic backwashing). Chemical cleaning was investigated using hydrogen peroxide (100mL of 30% H2O2 diluted with DI water to a final volume of 1L), acid cleaning by HCl at pH 4, and alkaline cleaning by NaOH at pH 11. Chemical agents were circulated on the fouled side of the FO membrane and DI water on the other side of the FO membrane. Using a low concentration of H_2O_2 (50ml/L or 50mL of 30% H2O2 diluted by pure water to a final volume of 1L) could not achieve enough water flux recovery in this study. Hence, 100ml/L concentration was chosen for final cleaning. Hydrogen peroxide (H_2O_2) was found more effective than acid and alkaline solution for cleaning the CTA membrane. Practically, H_2O_2 can break down the organic fouling layer via the oxidation of chemical functional groups (Liu & Mi 2014) and reduce fouling materials' adhesion to the membrane surface. Although H_2O_2 has no significant environmental concerns, it could compromise the integrity of the CTA FO membrane, particularly when it contacts the FO membrane active layer. The flux recovery of hydrogen peroxide solution with different concentrations is listed in Table 5.2. A smaller concentration of 50ml/L was initially used for chemical cleaning, which failed; hence, it was optimized to 100ml/L for better flux recovery.

Table 5.2: Flux recovery of fouled membrane after H2O2 cleaning with different concentrations

Membrane orientation	H_2O_2 Concentration	Flux recovery %
AL-FS	50ml/L	75
AL-FS	100ml/L	102
AL-DS	50ml/L	62
AL-DS	100ml/L	91

In the AL-FS mode, the results revealed that the pure water flux after H_2O_2 cleaning was slightly higher (average flux of 6.74LMH and 67% feed water recovery) than that in the virgin CTA membrane indicating slight damage to the membrane active layer (Figure 5.5d). In the AL-DS mode, 91% (average flux of 8.34±0.2 LMH and 71% feed water recovery) water flux recovery was achieved, indicating a potential application of the H_2O_2 for recovering the water flux when fouling occurs on the support layer side. Slight peeling of the support layer, however, was detected by the SEM analysis (Figure 5.5d) after the H_2O_2 cleaning, and this could have a detrimental impact on the long-term performance of the membrane. The higher FR with H_2O_2 in the AL-DS could be attributed to its ability to enter the pores of the support layer, increasing the pore diameter by removing absorbed foulants, resulting in an increase in the permeate flux (Mohammadi, Madaeni & Moghadam 2003).

Cleaning with an HCl solution was selected as it does not cause degradation of organic matters, which can lead to a subsequent fouling layer if cleaned by other acids such as nitric acid or sulphuric acid (Madaeni & Samieirad 2010). Acid cleaning at pH 4 using 0.05M HCl restored around 83% (average water flux of 5.47LMH and feed water recovery of 56%) of the water flux in the AL-FS and 78% (average flux of 7.15LMH and feed water recovery of 61%) in the AL-DS orientation. Acid cleaning can hydrolyze organic foulants and solubilize inorganic foulants (Zondervan & Roffel 2007). However, acid cleaning was less effective than alkaline cleaning at pH 11 on both membrane

operating modes. At high pH (pH 11), the functional groups of most foulants would be deprotonated, and hence facilitating the repulsion of fouling materials during the cleaning process (Wang et al. 2015).

Cleaning at high pH with NaOH was more effective due to the excellent efficiency of the alkaline solution in the cleaning and removal of organic materials compared to the acid solution (Madaeni & Samieirad 2010), while acid cleaning is more effective in the removal of metal ions from the membrane surface (Gan et al. 1999). Therefore, a two-step sequential cleaning with an acid solution at pH 4 for 15 mins, followed by the alkaline solution at pH 11 for another 15 mins, was the most effective method of restoring the membrane performance in both membrane orientations. Sequential cleaning with an acid solution for 15 minutes, followed by an alkaline solution for 15 minutes, resulted in 98% (average flux of 6.46±0.1 LMH and feed water recovery of 66%) and 87% (average flux of 7.97± 0.2 LMH and feed water recovery of 68%) water flux recovery in the AL-FS and AL-DS mode, respectively. The results suggest that sequential cleaning with acid and base effectively removed organic and inorganic foulant in the fouled CTA membrane. It should be noted that no DI water rinsing was performed between acid and alkaline cleaning. Generally, any sequence of acid followed by alkaline or alkaline followed by acid cleaning is an effective approach for removing organic and inorganic foulants deposited on the membrane surface.

Figure 5.5 shows there are no advantages offered by chemical cleaning over the physical cleaning methods. Chemical cleaning also requires soaking the membrane after chemical cleaning and recirculating DI water to remove the chemicals before the membrane is ready for reuse. Based on the experimental results, hot water and osmotic backwashing methods outperformed the chemical cleaning methods, apart from H_2O_2 cleaning method. The latter method recovered the entire water flux in the AL-FS mode, but it damaged the active layer of the membrane, as shown in the SEM image. In the AL-DS, H_2O_2 method resulted in slight damage to the membrane support layer, leading to severe consequences over time. Therefore, long-term filtration processes were performed on a fouled membrane using hot water at 35 ^{o}C and osmotic backwashing with 1.5M NaCl as the preferred cleaning methods.

5.4.1 Impact of cleaning protocols on membrane rejection performance

The experimental work investigated the rejection rate of the FO membrane to evaluate the impact of different cleaning methods on membrane performance (**Figure 5.6**). In the physical cleaning protocols, the membrane rejection was investigated only for hot water cleaning experiments since high cross-flow velocity and osmotic backwashing methods have no adverse impact on the membrane surface chemistry. Since hot water may slightly increase the membrane pore size, the rejection rate of the FO membrane could drop after the cleaning. Experimental work studied the rejection rate of the FO membrane after cleaning with hot water in both membrane orientations, and the ICP-MS analyzed the samples. Apart from a slight reduction in the retention of Mg^{2+} ions, the rejection rate of most metal ions was not affected after cleaning with hot water in the AL-FS mode and AL-DS mode, suggesting there was no deterioration in the membrane performance. Hence, cleaning with hot water at 35 ^{o}C did not compromise the performance of the FO membrane.

In the chemical cleaning, oxidation of the membrane active layer by the H_2O_2 caused a loss in the rejection rate of Mg^{2+} in the AL-FS mode, indicating a slight change in the properties of the membrane active layer. Most importantly, retention of toxic Ni ions decreased dramatically to almost 60±1% in the AL-FS and 68±1% in the AL-DS orientation.

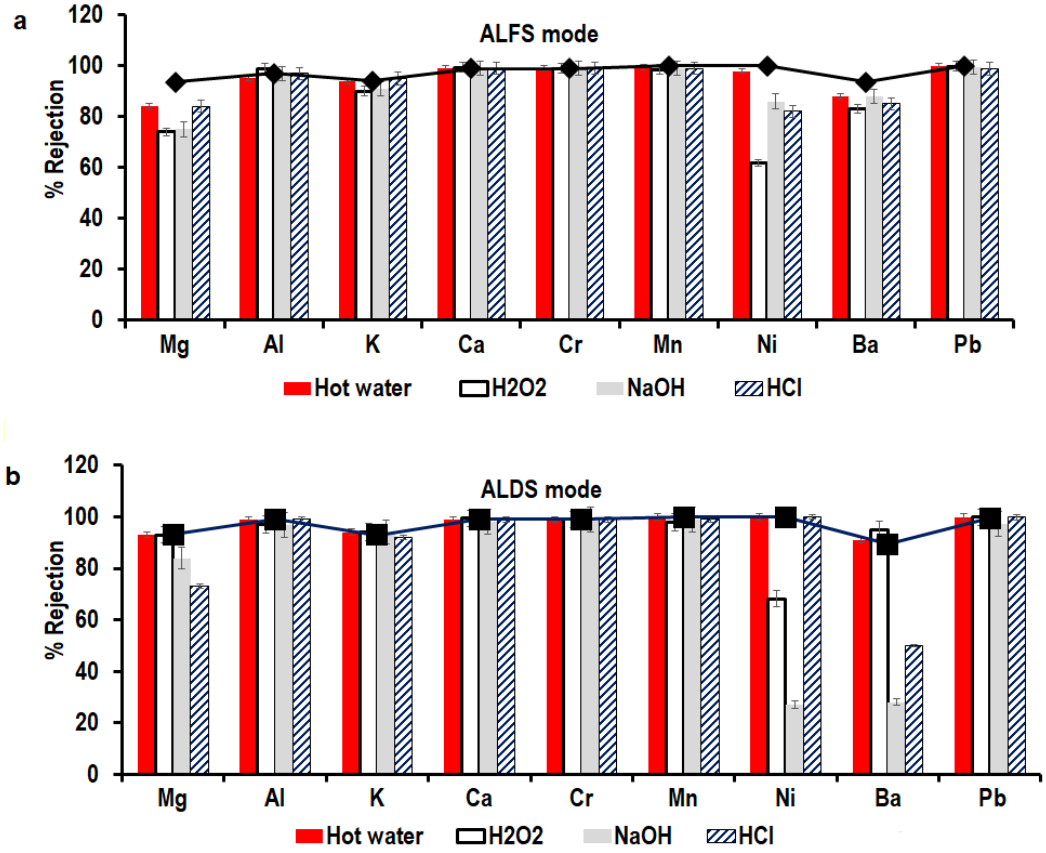

Figure 5.6: Impact of physical and chemical cleaning protocols on pollutants rejection in the AL-FS

a). Impact of physical and chemical cleaning protocols on pollutants rejection in the AL-FS. b). Impact of physical and chemical cleaning protocols on pollutant rejection in the AL-DS. Physical cleaning protocols included Hot water cleaning at 35 ^{o}C. Chemical cleaning protocols were 100ml/L H_2O_2, 0.05M HCl cleaning at pH 4, and in 0.05M NaOH at pH 11. For Ni rejection, no column or zero rejection represents Ni was not detected in the samples.

Cleaning with NaOH solution at pH 11 affected the ion rejection rate of the FO membrane in both orientations, particularly for Ni^{2+} and Ba^{2+} ions. In the AL-FS mode, Ni^{2+} ions rejection decreased to 60±2% compared to the virgin membrane performance, whereas, in the AL-DS mode, it declined to almost 20±2%. The rejection rate of Ba^{2+} ions was similar to the virgin membrane in the AL-FS

mode; however, in the AL-DS, it declined after cleaning with the NaOH solution. Two main factors cause the decrease in the rejection of ions after the cleaning with NaOH. Firstly, the alkaline solution makes the membrane's pores more open, hence reducing ions retention, which the virgin membrane would otherwise reject. Secondly, pH can change the charge on the membrane surface and affect ions' rejection (Hagmeyer & Gimbel 1998; Ozaki, Sharma & Saktaywin 2002). Cleaning with HCl solution at pH 4 decreased the rejection of the FO membrane for Ba^{2+} ions in the AL-DS mode and a slight decrease in retention of Mg^{2+} ions in the AL-FS mode. The rejection rate of the rest of the metal ions was not affected. Acid cleaning generally narrows down the membrane's pore size, increasing ion retention (Wang et al. 2015).

Although chemical cleaning methods were efficient for restoring water flux in the FO membrane, there is a possibility of membrane damage after chemical cleaning. H_2O_2 cleaning, for example, led to the deterioration of the membrane active layer, and the result was a reduced ions rejection rate after the cleaning process. Other methods, such as acid and alkaline cleaning, may cause irreversible membrane damage at extreme pH's and generate a wastewater by-product. Physical methods, therefore, would be recommended for membrane cleaning since they have a low impact on the environment. Cleaning with hot water at 35 ºC and osmosis backwash methods have great potential as alternative methods for cleaning at the end of the LFL filtration process. It is suggested to use a source of waste heat to heat the cleaning solution to 35oC to reduce the membrane cleaning cost by this method.

5.4.2 Analysis of the fouled and cleaned membrane by FT-IR

The fouled and cleaned membranes with hot water 35 ºC, and H_2O_2 were analysed by FT-IR, and the spectra were compared with the FT-IR of the virgin membrane is presented in **Figure 5.7**. The stretching vibrations of the carbonyl groups of the CTA membrane show a peak around 1745 cm^{-1}. Compared to the AL-FS mode, the FT-IR of the AL-DS mode shows severe attenuation in this band region. A clear change in the FT-IR spectrum is observed in the fouled membranes. Compared to the virgin FO membrane, the FT-IR of the fouled membrane is attenuated by the coating of the foulants in the band 4000-3300 cm^{-1}. The foulants in this band are mainly irreversible and are not removed by

hot water cleaning or H_2O_2 in both the AL-FS and the AL-DS due to organic foulants (Dean 1999; Wei et al. 2010), which contributed to the irreversible membrane fouling. The cleaning of the active layer with H_2O_2 diminishes the peak at 1500 cm^{-1}, indicating slight membrane damage. However, this peak was still present when the H_2O_2 was used for the support layer cleaning in the AL-DS mode. The bands at wavenumber 1000-1500 cm^{-1} also show severe attenuation in the AL-DS compared to the AL-FS mode. The fouling in this band is also irreversible, as confirmed by the FT-IR of cleaned membranes.

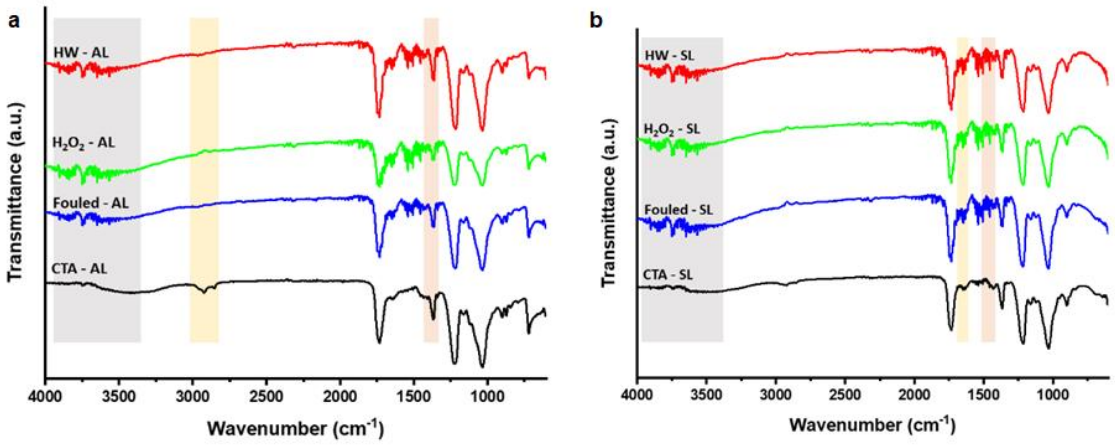

Figure 5.7: FT-IR spectra of the virgin, fouled, and cleaned membrane

a) Active layer of the FO membrane in the AL-FS mode b) Support layer of the FO membrane in the AL-DS mode. Hot water cleaning (HW).

5.4.3 The efficiency of physical cleaning protocols over multiple cycles

The experimental work evaluated the efficiency of the osmotic backwashing method and hot water cleaning over multiple cycles. Shorter filtration cycles were chosen as previous studies found that the fouling layer becomes compact and is hard to remove in longer filtration cycles (Al-Amoudi & Lovitt 2007). Osmotic backwashing with 1.5M NaCl was conducted for three consecutive filtration cycles after an initial fouling test. As presented in **Figure 5.8**, osmotic backwashing was very effective in recovering up to 95%, 92, and 91% of the water flux in the second, third, and fourth

cycle, respectively, in the AL-FS mode. The high water flux recovery was due to the nature of external fouling and the smooth surface of the membrane active layer, which shows resistance against fouling over multiple cycles. The osmotic backwash efficiency declined dramatically after the second cycle in the AL-DS mode. The water flux recovery was 90%, 73%, and 68% for filtration cycles 2, 3, and 4, respectively. The reason for this is attributed to the membrane orientation during the cleaning test, which is the AL-DS mode when the membrane filtration cycle is on the AL-FS mode. Such operating mode, i.e., AL-DS, generates high permeate flow to flush off foulants from the membrane surface. On the contrary, when the membrane was in the AL-DS mode, the osmotic backwash was performed in the AL-FS mode, which is renowned for its low permeation flow that was not enough to clean the membrane. Therefore, osmotic backwashing with 1.5M draw solution was not effective in the long term when the FO membrane was in the AL-DS mode. For instance, a higher draw solution concentration, 3M, might generate enough backwash flux to recover the flux in the AL-DS mode over multiple cycles.

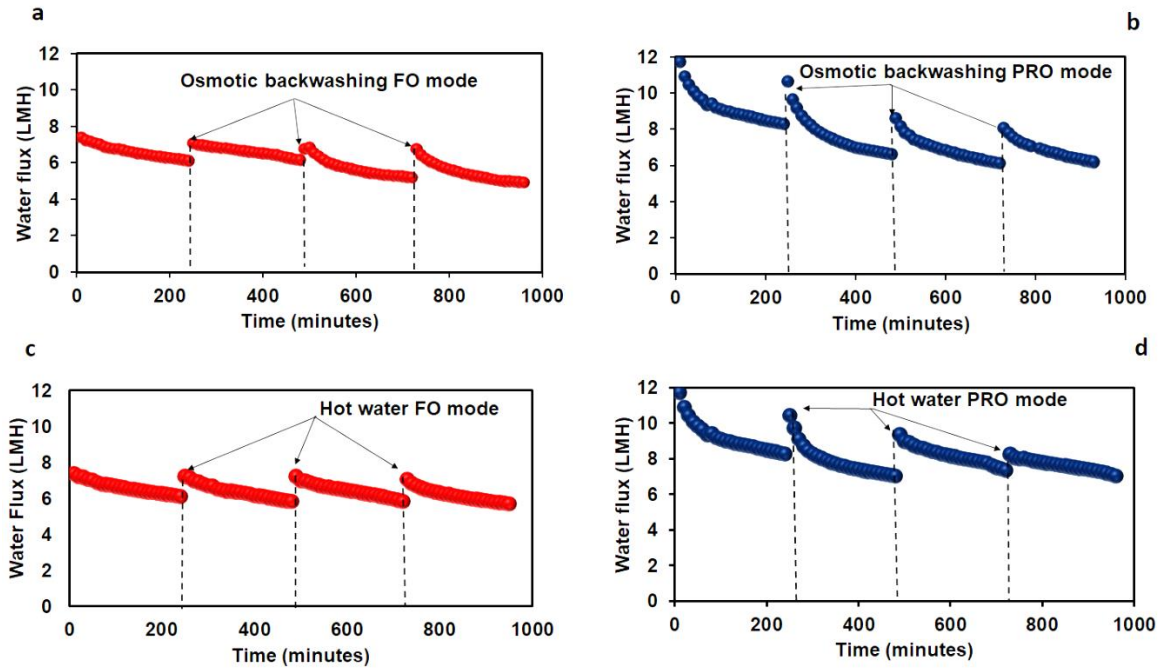

Figure 5.8: Physical cleaning protocols employed over four cycles of FO operation

a) Osmotic backwashing with 1.5M NaCl in the AL-FS mode, b) Osmotic backwashing with 1.5M NaCl in the AL-DS mode. c) Hot water 35 ºC cleaning in the AL-FS mode, d) Hot water 35 ºC cleaning in the AL-DS mode.

When the fouled membrane was cleaned by hot water at 35 ºC, the FR was remarkable in the AL-FS mode. After the second run, a 97% FR was achieved, followed by a similar 97% in the third run and declined to only 95% in the fourth cycle. In the AL-DS mode, the FR after the initial fouling run was 88%, followed by 79% in the next filtration cycle. The FR was 73% compared to 68% in the fourth cycle with osmotic backwashing. Compared to the AL-FS orientation, fouling was not ultimately hydraulically reversible with hot water flushing over multiple cycles in the AL-DS orientation. Increasing the cleaning duration can recover the water flux over multiple filtration cycles in the AL-DS mode with hot water cleaning. Physical cleaning method with hot water or osmotic backwash demonstrated higher FR and maintained the integrity of the FO membrane compared to chemical cleaning protocols used in this study. Therefore, hot water is recommended with the FO operating in the AL-FS mode to ensure high water recovery over time and to avoid chemical use.

5.5 Conclusions

The present study revealed the potential of the FO process for the treatment of landfill leachate and the removal of metal ion contaminants. The efficiency of the FO process was strongly related to the membrane operating mode. In contrast, the long-term performance of the FO process was highly dependent on the cleaning methods for the removal of various contaminants from the membrane surface. Membrane orientation significantly impacts the water flux, and it was higher when the membrane was in the AL-DS mode. But the latter operating mode resulted in more recalcitrant membrane fouling compared to the AL-FS mode. The fouled FO membrane was cleaned using several physical and chemical techniques. Physical cleaning by DI water was ineffective in restoring the water flux. Still, hot DI water at 35 oC and osmotic backwash with 1.5M NaCl solution achieved higher water flux recovery. Chemical cleaning with H_2O_2 was more efficient than acid and alkaline

solutions, although it caused severe membrane damage when landfill leachate faced the FO membrane active layer. The rejection rate of metal ions was lower after cleaning with the H_2O_2 solution. The experimental study suggests that physical cleaning methods with hot water and osmotic backwash are preferable over chemical cleaning methods due to their efficiency in restoring the water flux without generating chemical wastes. Furthermore, long-term experiments showed that cleaning with hot water at 35 ^oC was slightly more effective than cleaning with the osmotic backwash with 1.5 M NaCl, especially when the membrane operated in the AL-DS mode. The results demonstrated the feasibility of the FO process for the treatment of leachate wastewater without the need to change the FO membrane after washing with hot water or osmotic backwashing with NaCl solution.

Chapter 6: Feasibility of H_2O_2 cleaning for forward osmosis membrane treating landfill leachate

This chapter is based on the following publication.

I. **Ibrar**, S. Yadav, N. Ganbat, A.K. Samal, A. Altaee, J.L. Zhou, T.V. Nguyen, Feasibility of H2O2 cleaning for forward osmosis membrane treating landfill leachate, Journal of Environmental Management, 294 (2021) 113024

Authors contribution:

Ibrar Ibrar: Conceptualization, Methodology, Writing – original draft. Sudesh Yadav: Methodology, Writing – original draft, Data curation. Namuun Ganbat: Visualization, Investigation, Ali Altaee: Supervision, Writing – review & editing. Akshaya K. Samal: Visualization, Investigation. John L. Zhou: Supervision, Writing – review & editing. Tien Vinh Nguyen: Visualization, Investigation.

Abstract

This study reports landfill leachate treatment by the forward osmosis (FO) process using hydrogen peroxide (H_2O_2) for membrane cleaning. Although chemical cleaning is an effective method for fouling control, it could compromise membrane integrity. Thus, understanding the impact of chemical cleaning on the forward osmosis membrane is essential to improving the membrane performance and lifespan. Preliminary results revealed a flux recovery of 98% in the AL-FS mode (active layer facing feed solution) and 90% in the AL-DS (draw solution faces active layer) using 30% H_2O_2 solution diluted to 3% by pure water. The experimental work investigated the effects of chemical cleaning on the polyamide active and polysulfone support layers since the FO membrane

could operate in both orientations. Results revealed that polysulfone support layer was more sensitive to H_2O_2 damage than the polyamide active at a neutral pH. The extended exposure of thin-film composite (TFC) FO membrane to H_2O_2 was investigated, and the active layer tolerated H_2O_2 for 72 hours and the support layer for only 40 hours. Extended operation of the TFC FO membrane in the AL-FS based on a combination of physical (hydraulic flushing with DI water) and H_2O_2 was reported, and chemical cleaning with H_2O_2 could still recover 92% of the flux.

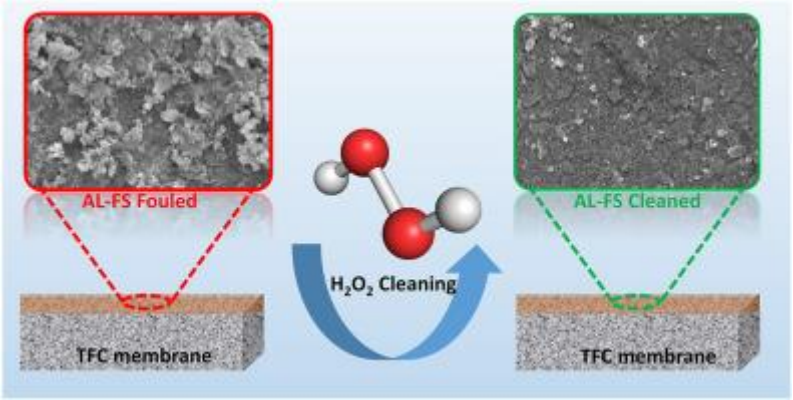

Graphical abstract

6.1 Introduction

Sanitary landfills are considered an effective way to dispose of solid waste (Atmaca 2009; Renou et al. 2008a). Comparative studies revealed that the sanitary landfill method is the most economic method of eliminating solid urban waste (Renou et al. 2008b). Despite being effective, these landfill sites generate undesirable and hazardous leachate wastewater when rainwater percolates through the dumping site. The landfill leachate wastewater is regarded as a serious environmental threat due to the existence of various hazardous organic and inorganic compounds (Danley-Thomson et al. 2020; Ghanbari et al. 2020; Reshadi, Bazargan & McKay 2020). The disposal of landfill leachate wastewater is a challenging problem that the municipal waste management industry has encountered. The composition of landfill leachate varies from site to site (Abbas et al. 2009; Renou et al. 2008a), making the treatment process of landfill leachate a formidable challenge. If not appropriately treated,

landfill leachate can contaminate groundwater and surface water; therefore, it requires an efficient treatment process.

Currently, biological treatments (e.g. aerobic, anaerobic, physical/chemical) and membrane processes (nanofiltration and reverse osmosis), or a combination of different processes (Marttinen et al. 2002; Rautenbach & Mellis 1994; Trebouet et al. 2001) are the dominant processes for landfill leachate treatment. Biological processes are usually used to treat leachate because they are simple and economical (Peng 2017). However, authority's stricter environmental regulations make biological processes incompetent, as they cannot satisfy the specifications required for discharge. In recent years, a significant increase in pressure-driven membrane technologies has been noticed compared to biological treatment methods (Bhol et al. 2021; Renou et al. 2008a). Among membrane processes, reverse osmosis (RO) (43 RO plants) and nanofiltration (NF) treatment of landfill leachate have been widely used worldwide (Trebouet et al. 2001). However, membrane fouling and large concentrate generation are critical issues in the RO process (Renou et al. 2008a), and the NF membrane exhibits low permeability. For instance, Li, Wichmann & Heine (2009) studied the tertiary treatment of landfill wastewater using thin-film composite (TFC) RO membranes, achieving a water flux of 6.5 Lm^2h^{-1} with a 53.4% recovery rate; however, membrane fouling resulted in a complete loss of permeability after two weeks. The RO technology also demands intensive pre-treatment of the FS and membrane cleaning to overcome fouling (Renou et al. 2008a) and is therefore not considered affordable. In another study, a composite graphene-oxide (GO) NF membrane was used for landfill leachate treatment. Although an 86.5% to 99.8% rejection rate was achieved, low membrane permeability (6.93 to 2.05 LMH) was a significant challenge (Yadav, Ibrar, Altaee, Samal, et al. 2020a).

Forward osmosis (FO) is an alternative membrane technology for reducing the volume of landfill leachate wastewater (Ibrar, Yadav, Altaee, Hawari, et al. 2020; Ibrar, Yadav, Altaee, Samal, et al. 2020; Yadav, Saleem, et al. 2020) and freshwater recovery (Iskander, Novak & He 2019). In the FO, a concentrated DS will extract freshwater from landfill leachate for volume reduction. Then, the diluted DS will either be treated for freshwater water production or safe discharge. Membrane fouling control and cleaning strategies will inevitably achieve a high recovery rate for a successful FO treatment. Dong et al. (2014)) used a cellulose triacetate (CTA) membrane to treat MBR

(membrane bioreactor) landfill wastewater; however, membrane chemical cleaning was unavoidable. Chemical cleaning was conducted using Alconox as a cleaning agent; however, Alconox is only feasible for CTA membranes and detrimental to TFC membranes (Wang et al. 2015). Aftab et al. (2019) used 0.1M NaOH to clean a CTA FO membrane treating landfill wastewater due to physical cleaning failure to restore water flux. Previous studies on the FO process for landfill leachate treatment demonstrated that H_2O_2 could be an alternative to acid and alkaline cleaning of the membrane, but CTA membrane damage was observed on the active and support layers after the H_2O_2 cleaning (Ibrar, Yadav, Altaee, Samal, et al. 2020).

Compared to CTA membranes, thin-film composite (TFC) FO membranes are broadly employed in desalination and wastewater treatment systems because of the high permeation water flux and rejection of ions. Also, CTA membranes are sensitive to oxidants and operate within a narrow pH range (Farooque, Al-Amoudi & Numata 1999). In contrast, TFC membranes are relatively tolerant of oxidant damage and tolerate a pH range from 2 to 12. H_2O_2 is environmentally safe, and it can efficiently remove foulants (almost 100%) from the membrane surface, compared to chemical cleanings such as citric acid, hydrochloric acid (HCl), sodium hydroxide (NaOH), sodium dodecyl sulphate (SDS), and disodium ethylenediaminetetraacetate (Ibrar, Yadav, Altaee, Samal, et al. 2020; Wang et al. 2017). Other oxidizing agents such as sodium hypochlorite (NaOCl) can react with organics, generating halogenated by-products that are potentially more toxic to the environment (Cai et al. 2016; Li et al. 2019).

This study applied the FO process for landfill leachate treatment using an H_2O_2 cleaning agent. The polyamide and polysulfone (PSf) support layer of TFC FO membrane tolerance to long-term exposure to H2O2 was experimentally investigated for the first time. There is no systematic study that has reported the tolerance of TFC FO membrane over an extended period to H_2O_2. Firstly, the TFC membrane performance was investigated for the dewatering of landfill leachate in the AL-FS (leachate feed against the active layer) and the AL-DS (DS against the active layer). Secondly, in separate experiments, the TFC membrane tolerance to H_2O_2 was investigated for the active polyamide layer and the PSf support layer in the long term. At the end of the experiments, a 4-day continuous operation with H2O2 cleaning was performed to calculate the permeation flux and the membrane rejection rate.

6.2 Materials

6.2.1 Leachate sampling and chemicals

The landfill leachate samples were procured from the Hurstville Golf course located at Peakhurst, Sydney, Australia, and employed as an FS (FS). The DS (DS) was 0.6 M NaCl simulating the osmotic pressure of real seawater. In a long filtration test, the DS was 1M NaCl solution to avoid a significant dilution of the DS. Analytical grade H_2O_2 (30% w/w) was purchased from Merck Millipore, and was used as a cleaning agent in all the fouling experiments.

6.2.2 FO membrane

In the FO tests, this study used a TFC (thin-film composite) membrane, Toray Chemical (South Korea). This membrane consists of an active polyamide layer and a PSf porous support layer (Nguyen et al. 2019). To ensure complete wetting, the virgin membranes were placed in DI water for at least 24 hours before using in the experiments.

6.2.3 FO laboratory setup and experimental methodology

A schematic diagram of the FO cell termed CF042D by the manufacturer (Sterlitech Corporation, USA) can be found in our previous study (Ibrar, Yadav, Altaee, Hawari, et al. 2020). The cell features a membrane area of 42 cm^2. The feed and DS were pumped using two gear pumps at a rate of 2 Litres/minute. Two- flow meters (FF-550) were connected to the FO cell to monitor the feed and DS flow rate. The FS was placed on a balance (EK-15L) connected to a computer that recorded the weight change in the FS. The data obtained from the computer (grams) was converted to the volume (V), and the water flux was calculated using equation 1.

$$J_w = \frac{(\Delta V)}{A*t}$$

(1)

In equation 1 ΔV represents the volumetric change of the FS, A is the membrane area, and t is the time for the FO run. The reverse salt flux (RSF) was determined using equation 2.

$$Js = \frac{V_f C_f - V_i C_i}{A * t} \quad (2)$$

In equation 2, V_f and V_i are the final and initial volumes of the FS, respectively, C_f and C_i are the final and initial concentrations of the FS, respectively, A is the effective membrane area, and t is the filtration time. A conductivity metre obtained from LAQUA was used to record the change in the FS's conductivity, and a turbidity meter (Hach 2100P) was used for all turbidity measurements. Equation 3 was used to measure the pollutant rejection.

$$R = 1 - \frac{\frac{C_d V_d}{V_p}}{C_f} \quad (3)$$

In equation 3, C_d (ppm) is the concentration of the pollutants in the DS, V_d (L) represents the final volume of the DS, V_P (L) is the volume of the freshwater that permeated from the FS to the DS side, and C_f (ppm) is the initial pollutants concentration in the FS. The concentration of all the pollutants was measured using inductively coupled mass spectroscopy (ICP-MS).

6.2.4 FO fouling and cleaning experiments

A virgin pre-soaked TFC membrane was flushed with DI water for 30 minutes to remove any impurities and mounted in the FO filtration unit. Fouling studies were conducted in two membrane modes, the AL-FS and the AL-DS orientation. Initial runs were conducted using deionized water (DI) feed and 0.6M NaCl DS to obtain a normalisation factor for normalised flux. Following this, the FS was replaced with landfill leachate and the DS with a fresh 0.6 M NaCl DS. Short-term tests lasted four hours per cycle. After each cycle, the membrane was cleaned with a 30% H_2O_2 solution diluted with pure water to 3% on the fouled side and DI water on the other side. The landfill leachate wastewater has a neutral pH of 7.52 (Table 6.1), and hence no pH adjustments were made to the H_2O_2 solution in all experiments. Additionally, the primary aim of using H_2O_2 was to avoid by-products or generate a secondary chemical waste stream. Adding acid or bases to the H_2O_2 may generate reaction by-products, making the process less environmentally friendly.

Long filtration tests were performed in the AL-FS, each cycle lasting 24 hours. Instead of a 0.6 M NaCl, a 1 M NaCl solution was the DS to avoid significant dilution of the NaCl DS. The FS and DS were changed after every 24 hours at the beginning of the new cycle. Cleaning in long-term

experiments was conducted every 24 hours, using DI water for the first few cycles and then with H_2O_2 to compare their efficiencies. The recovered water flux of the FO membrane was obtained mathematically using equation 4.

$$FR = \frac{J_c}{J_f} * 100 \quad (4)$$

J_f denotes the average flux of a fouled membrane over a complete period, while J_c denotes the flux of the membrane after cleaning.

6.2.5 Membrane tolerance tests for hydrogen peroxide

Active exposure tests were conducted to test the membrane tolerance to H_2O_2 oxidation. A pre-soaked TFC membrane was mounted on the FO cell to calculate the pure water flux and RSF as baseline results. DI water was used to wash the membrane for about 30 minutes to remove any accumulated salt. Then, the FS was changed to the H_2O_2 (50 ml/L of 30% solution diluted with 1 L of DI water) while DI water was on the other side to prevent membrane dehydration. The solution was circulated continuously and periodically stopped to record the pure water flux and RSF to compare them against the baseline values. The pure water flux and RSF were recorded after 1 hour and periodically after every 4 hours. The membranes were considered damaged when there was a substantial variation in water transport or solute transport compared to the virgin membrane. Each trial was done twice to confirm the findings. The maximum dose of H_2O_2 the membrane could withstand was calculated using equation 5.

$$D_{max} = C * t_{max} \quad (5)$$

D_{max} (ppm-h) is the maximum dose of H_2O_2 the membrane could withstand before critical performance loss occurred (Ling et al. 2017), C is H_2O_2 concentration, and t_{max} is the maximum time the membrane could withstand the oxidant. Membrane specimens were dried (24 hours) then analysis and evaluated through microscopic analysis.

6.2.6 Characterisation of FO membrane

A Thermo Scientific Nicolet 6700 FT-IR spectrometer was used to perform Fourier transform infrared (FT-IR) analysis to study the characterisation of virgin and long-term exposed membranes to H_2O_2 over the range of 500–4000 cm^{-1}. All membranes were dried before characterisation, and each scan was averaged from 50 scans. Microscopic analysis of the membrane morphology was conducted using field emission scanning electron microscopy (FE-SEM).

6.2.7 Characteristics of the landfill leachate wastewater

Inductively coupled plasma spectroscopy (Agilent Technologies ICP-MS 7900) was employed to analyse the landfill leachate wastewater. All the samples were collected from the landfill leachate containers with a plastic syringe. The colour of the leachate was a strong yellowish-brown, representing refractory compounds in the leachate formed by high concentrations of humic acids, fulvic acids, and hydrophilic fractions (Ibrahim & Yaser 2019; Marañón et al. 2010). The presence of iron can lead to inorganic fouling that might contribute to irreversible fouling. The pH and conductivity were measured with a meter supplied by AQUA. The humic acids were negatively charged at the measured pH. The landfill leachate's TOC (total organic carbon) values were measured using a TOC analyser (Shimadzu Corporation, Japan).

Table 6.1: Analysis of the landfill FS using ICP-MS

Parameter	Value	Unit
Turbidity	35	NTU
Colour	Brown (yellowy)	
Apparent particles	Small particulates	
pH	7.52	-
Conductivity	12100	$\mu s.cm^{-1}$
Total dissolved solids	4500	mgL^{-1}
Total organic carbon	145.1±5	mgL^{-1}
Ammonia	<0.5	mgL^{-1}
Total suspended solids	27-117	mgL^{-1}
Total Iron	3.5-5.2	mgL^{-1}
Magnesium	95.3±5	mgL^{-1}
Calcium	126±5	mgL^{-1}
Potassium	47.87	mgL^{-1}

The wastewater treatment plant supplied the values of ammonia, total suspended solids, and total iron.

6.3 Results and discussions

6.3.1. Forward osmosis performance during short-term filtration

To determine the best membrane orientation for dewatering the landfill leachate, initial short-term filtration tests were conducted to analyse the TFC membranes' performance in the AL-DS and AL-FS modes (Figure S.1) using a 0.6M NaCl DS (simulating seawater osmotic pressure) and landfill leachate FS. All water flux data were normalized to account for water flux decline due to membrane fouling. All the flux data reported here was normalized to avoid the impact of dilution of the DS. Initial tests indicated that the membrane water flux in the AL-DS orientation was more than the AL-FS, which agrees with previous work [14]. This is mainly due to the lower impact of dilutive internal concentration polarisation in the AL-DS (Fig. 6.1a). An average flux of 18.85±1 LMH over four hours was obtained in the AL-FS orientation, with 305 mL of freshwater extracted from the landfill leachate wastewater to the DS (Fig. 6.1b). The initial flux decline over time in the AL-FS mode was very small. The TFC membrane exhibited stable flux in this orientation. The steady water flux decline in the AL-FS mode could be attributed to the low water flux that reduced the foulants convection to the smooth, active layer. In contrast, a much higher initial water flux (24 ±1 LMH) was obtained in the AL-DS orientation, followed by a rapid decline to 20 LMH in the first 75 minutes. The water flux then levelled out after 2 hours, following a trend similar to that in the AL-FS mode. The rapid flux decline in the AL-DS orientation compared to the AL-FS mode can also be attributed to the larger pore size of the support layer and higher water flux that encouraged the convection of foulants in the landfill leachate wastewater to the membrane surface, leading to severe pore blockage by fouling materials. The overall higher water flux in this orientation also agrees with the finding in our previous study on landfill leachate wastewater with CTA membrane, where the AL-DS mode exhibited a higher water flux than the AL-FS mode (Ibrar, Yadav, Altaee, Samal, et al. 2020). The membrane material would impact the flux behaviour in the two membrane modes.

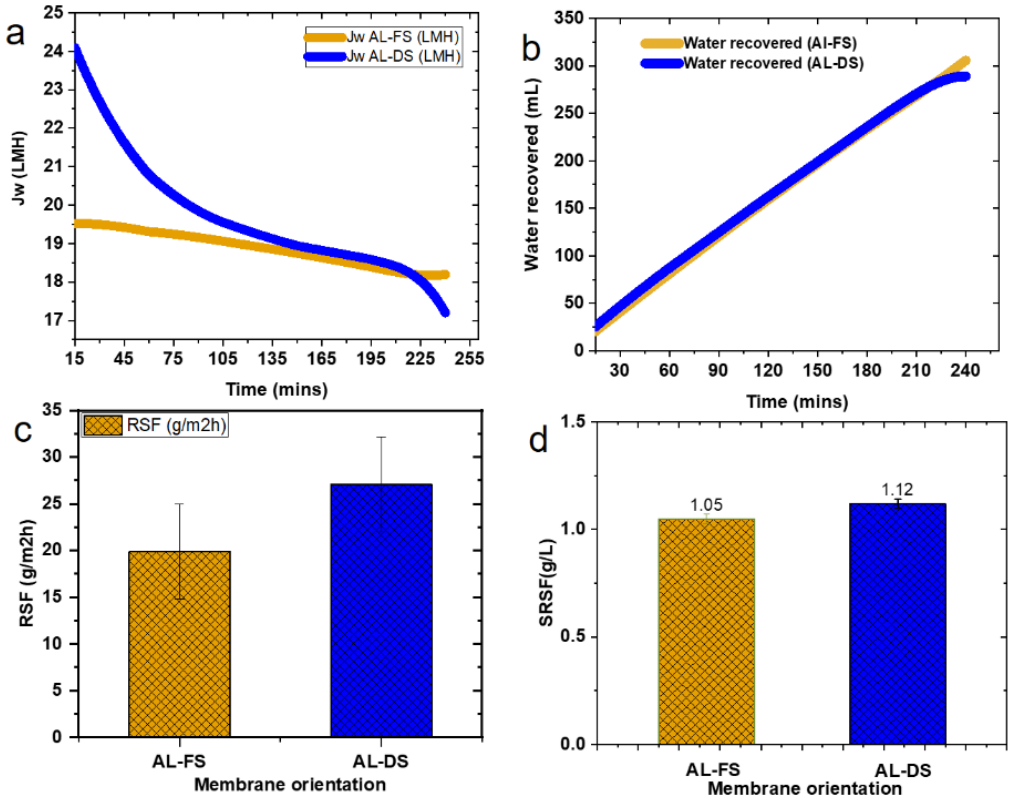

Figure 6.1: (a) Plot water flux against time in the AL-FS orientation and the AL-DS orientation using 0. 6M NaCl DS and DI water FS **(b)** Volume of water recovered in the AL-FS and the AL-DS mode as a function of time **(c)** RSF in the AL-FS mode and the AL-DS mode. **(d)** Specific RSF in the AL-FS and the AL-DS mode.

To determine the best membrane orientation for dewatering the landfill leachate, initial short-terms filtration tests were conducted to analyse the TFC membranes' performance in the AL-DS and AL-FS modes using a 0.6M NaCl DS (simulating seawater osmotic pressure) and landfill leachate FS. The fouling mechanisms in the AL-FS and AL-DS modes were analysed using the experimental data by plotting t/V vs V Fig. 6.2 to evaluate whether fouling was mainly because of the pore-blocking or cake formation mechanism (Wang & Tarabara 2008). For the AL-FS mode, the curves in Fig. 6.2a show linear lines with a correlation coefficient almost equal to 1, indicating that the cake layer in this orientation was the main cause of the small decline in the flux over time. The FE-SEM analysis of the fouled active layer also revealed the cake layer, as presented in Fig. 6.2b. The cake layer in the AL-FS orientation from the FE-SEM looks homogenous with a couple of cracks in the membrane. The cracks are due to the process of drying the membrane before the FE-SEM analysis. The straight

line in the plot (Fig 6.2a) indicates a homogenous cake layer formation. The homogeneity of the cake layer was probably due to the interactions between humic substances or polysaccharides with proteins in the landfill leachate wastewater (Kim, Elimelech, et al. 2014). It can be hypothesized that the cake layer acts as a pre-filter, protecting the membrane from materials with high fouling propensity in the landfill leachate wastewater (Di Bella & Di Trapani 2019; Kochkodan, Johnson & Hilal 2014). This will ease cleaning the AL of the membrane and hence facilitate a high flux recovery. However, the cake layer can also promote some foulants adsorption on the membrane surface, which will be harder to remove by physical cleaning.

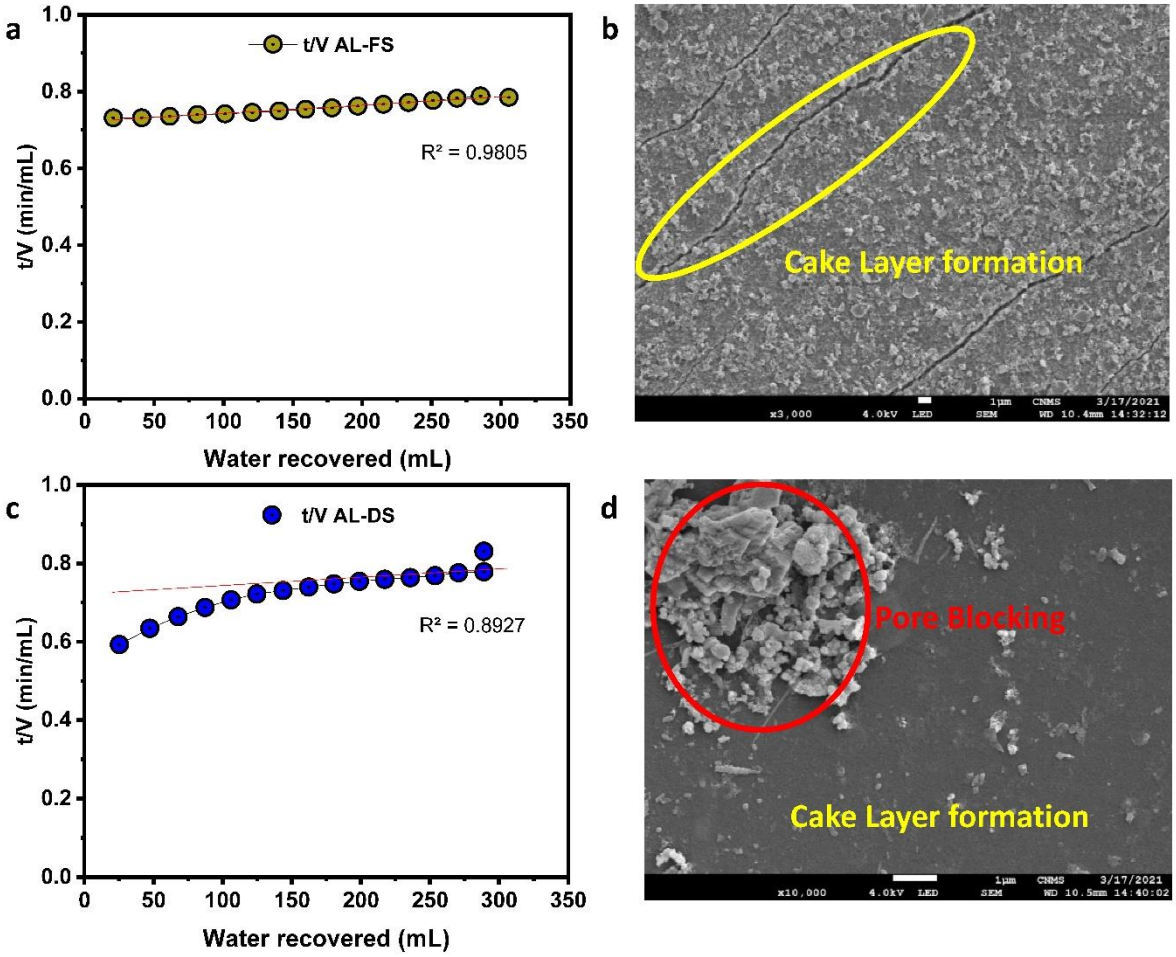

Figure 6.2: **(a)** Plot of volume (V) of water recovered against time/volume (min/mL) for the AL-FS **(b)** FE-SEM of the fouled active layer after four hours of filtration **(c)** Plot of volume (V) against time/volume (min/mL) for the AL-DS mode. **(d)** FE-SEM of the fouled support layer after four hours of filtration.

Compared to the AL-FS mode, the AL-DS mode water flux decline shows a curved line, indicating pore-blocking at the early stages of filtration, which is also evident from Fig S.3.1a the water flux declined rapidly in the first 75 minutes. The line seems to level out at the later experiment stages, showing that the flux decline shifted from pore-plugging to the cake layer. The results again agree with Fig 6.1a, where the AL-DS water flux was stable. The FE-SEM of the fouled support layer is presented in Fig. 6.2d; the red circle indicates large-sized fouling materials attached to the smaller foulants trapped inside the support layer. These foulants are possibly a combination of macromolecular (such as humic and fulvic acids, which are the major contributors to the organic fouling on the membrane) and soluble metal ions in the leachate wastewater (Mi & Elimelech 2010b).

The fouled membranes in both orientations were further examined through FT-IR spectroscopy to get some qualitative information about the foulants in the landfill leachate wastewater attached to the membrane surface. A visible change can be observed in the FT-IR of the fouled membrane (Fig. 6.3). Fig. 6.3a and 6.3b presented the FT-IR of pristine membrane and fouled membrane in the AL-FS orientation, respectively, and the FT-IR of the pristine membrane and the fouled membrane is presented in Fig 6.3c and 6.3d for the AL-DS mode. In the AL-FS mode, the FT-IR of the fouled membrane shows a small peak at the wavenumber 3749 cm^{-1}. This can be attributed to the clay particles (aluminium silicate) present in the landfill leachate wastewater. The clay particles were also visible in the landfill leachate wastewater. The band marked in the range 1520-1550 cm-1. The peaks at 1481 and 1489 cm-1 represent secondary amide and indicate fouling due to proteins(Delaunay et al. 2008). The intensity at these bands shows a decrease in intensity compared to the pristine membrane. To gain more insights into the FT-IR of the foulants on the FO membrane, the fouled membrane spectra were subtracted from the pristine membrane spectra to get the spectra of the foulants only on the membrane surface. Spectral subtraction is frequently employed to isolate the spectral features of a component or physical change in the sample (Lin, Liu & Hao 2001). The spectra of the foulants are presented in Fig. 1b for the AL-FS orientation treatment of the landfill.

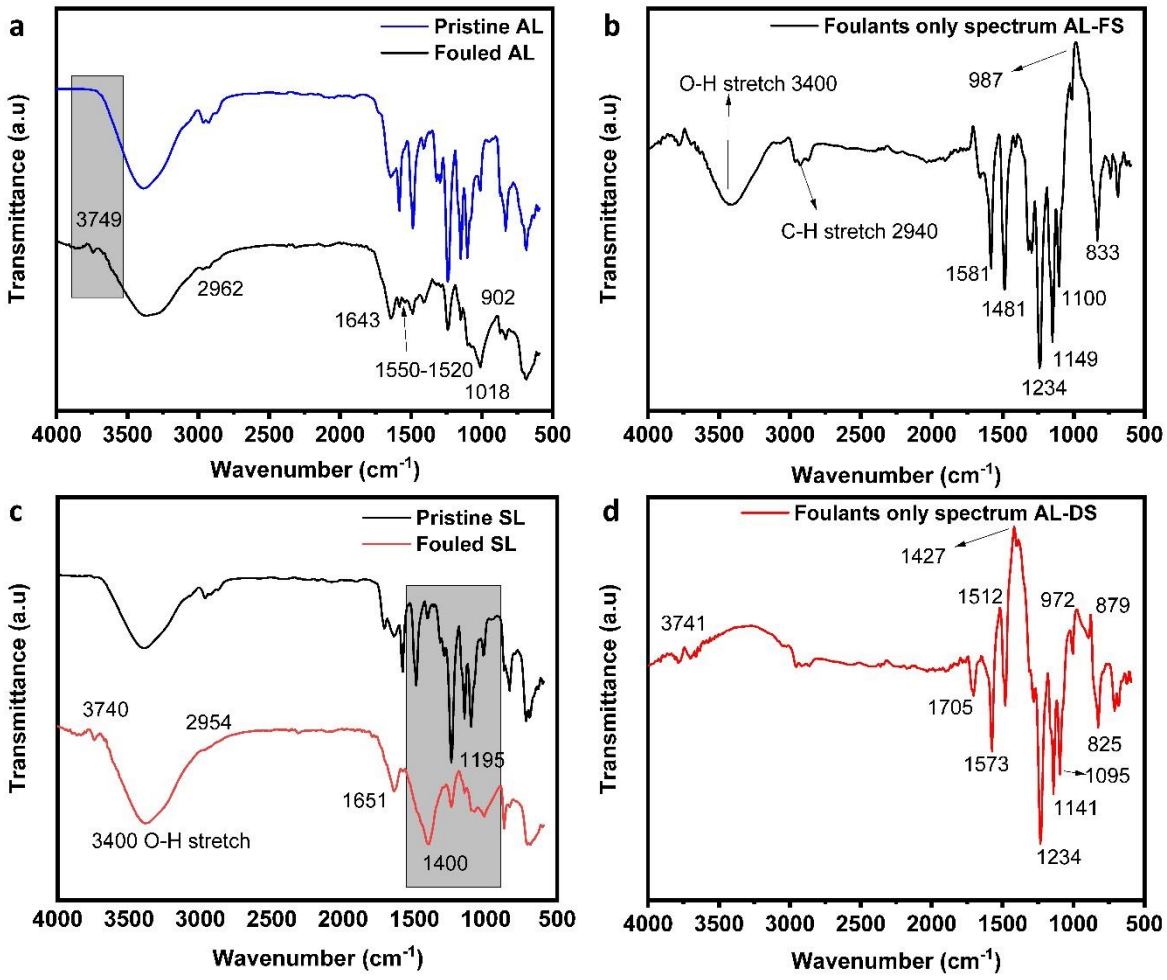

Figure 11.3: FT-IR of the pristine active layer and fouled membrane operating in AL-FS orientation

(a) FT-IR of the pristine active layer and fouled membrane operating in AL-FS orientation **(b)** FT-IR of the fouled active layer in the AL-FS orientation **(c)** FT-IR of the pristine support and fouled support layer of the membrane **(d)** FT-IR of the fouled support layer in the AL-DS mode.

The peak in the band 2940 cm^{-1} (Fig 6.3b) indicates silica fouling (Nataraj et al. 2008). Silica fouling in the FO process can contribute to irreversible fouling (especially in the presence of divalent calcium and magnesium ions), as it is stubborn and hard to clean by physical cleaning methods such as hydraulic flushing. The peak at 1100 cm^{-1} is an indicator of the alcohol group. The FT-IR of the fouled FO membrane in the AL-DS orientation is presented in Fig. 6.3c and 6.3d. Fig. 6.3c compares the pristine membrane's spectrum with the fouled membrane, whereas Fig. 6.3d shows only the foulants spectrum. The band at 3400 cm^{-1} is attributed to the O-H groups. The AL-DS spectrum also

shows the presence of clay particles (3741 $cm^{-1)}$ and silica fouling (2962 cm^{-1}). The bands in Fig. 1d from 1427-1600 are indicators of aromatic compounds. The sharp peak at 1427 usually shows calcium carbonate scaling ($CaCO_3$) (Lee & Kim 2009) due to Ca ions in the landfill leachate wastewater. The peak at this band is more intense when the FO membrane operates in the AL-DS orientation compared to the AL-FS. This implies that Ca ions have more fouling propensity in the AL-FS mode than the AL-DS mode. Both the AL-FS and the AL-DS fouled membrane showed similar peaks at 1234 cm^{-1}, associated with the carboxyl and ester group and primary and secondary amines (Croué et al. 2003; Kurtoğlu Akkaya & Bilgili 2020).

6.3.2 Tolerance of FO membrane to H_2O_2 in extended exposure

A pre-soaked virgin TFC membrane was exposed to H_2O_2 at the cleaning concentration (50 ml/L) with the active layer facing the H_2O_2 solution, and DI water was circulated on the other side to avoid membrane dehydration. The concentration of H_2O_2 solution was chosen based on the previous studies (Ibrar, Yadav, Altaee, Hawari, et al. 2020; Wang et al. 2017). Similar tests were conducted with the support layer against the H_2O_2 solution and DI water on the AL (active layer) side. After 24 hours, the H_2O_2 solution-DI water test was stopped, the membrane was cleaned with DI water (to flush out the H_2O_2), and a pure water flux and RSF were measured in the FO membrane using a 0.6M NaCl DS and DI water FS. The water flux and RSF were recorded every 4 hours during the experiment and presented in Fig. 6.4a and 6.4b. For the AL-FS orientation and the H_2O_2 facing the active layer, no major changes in the pure water flux and RSF were noticed until 72 hours. After 72 hours, the pure water flux of the TFC membrane using 0.6M NaCl DS and DI water reached 118 LMH (a fivefold increase compared to the baseline), demonstrating substantial damage to the membrane. Moreover, the RSF declined significantly at the breakdown point due to AL damage, and hence most of the water permeated across the membrane. This may also be a sign of membrane ageing due to the long exposure to oxidants (Benavente & Vázquez 2004). Similar results of membrane damage after 72 hours of H_2O_2 exposure were reported by Abejón, Garea & Irabien (2013) for PA (polyamide) reverse osmosis membranes. However, the concentration of H_2O_2 was very high (35% w/w of aqueous H_2O_2 solution).

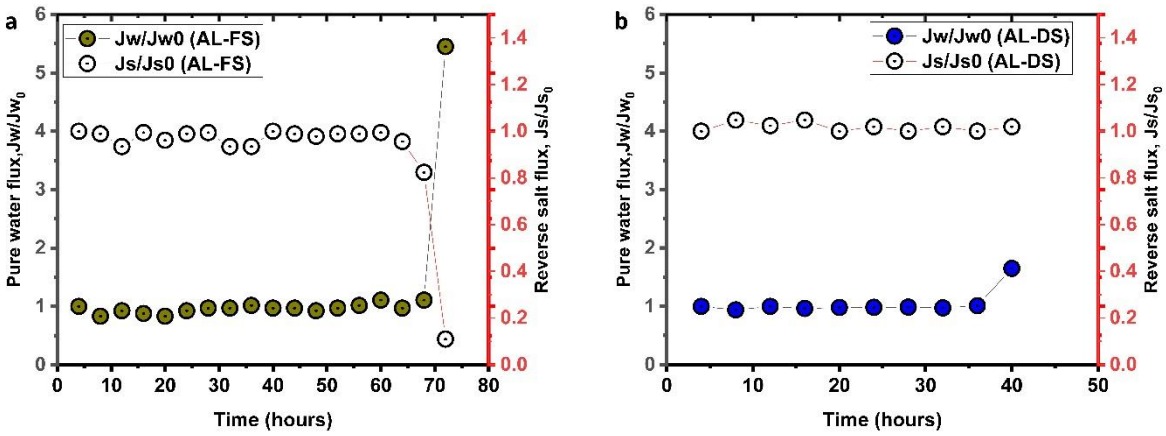

Figure 6.4: Pure water flux and RSF recorded during the exposure tests

(a) Pure water flux and RSF recorded during the exposure tests, **(b)** Pure water flux and RSF recorded during the 40 hours of exposure.

The support layer of the FO membrane tolerated the H_2O_2 concentration for 40 hours only before a significant change in performance was recorded. After 40 hours, the FO experiments showed a threefold increase in the pure water flux and no substantial change in the RSF than the virgin membrane. Most membrane manufacturers report oxidant exposure in terms of maximum tolerance dosage value or D_{max} (Abejón, Garea & Irabien 2013). The maximum H_2O_2 the membrane could withstand was calculated using the equation [5]. Table 2 lists the maximum dosage calculated for the AL and the support layer (SL). All values were calculated at neutral pH. The polysulfone SL of the TFC membrane could tolerate the 3% concentration for only 40 hours during long-term exposure. A threefold increase in the pure water flux was recorded only after 40 hours of operation.

Table 6.2: Maximum dose values of hydrogen peroxide for the active layer and the support layer

Membrane Orientation	D_{max}	t_{max}	C
AL	3,600,000 ppm-h	72 hours	50,000 mg/L
SL	2,00,000 ppm-h	40 hours	50,000 mg/L

6.3.4. Characterization of the damaged membranes by FT-IR and FE-SEM

The exposed membranes exhibited significant changes in the transport properties, a sign of membrane performance deterioration. The degradation of the membranes was further confirmed by FT-IR analysis since no studies are available which describes the oxidative damage of the FO membrane by FT-IR analysis. The pristine and exposed membranes were analysed through FT-IR spectroscopy to study the surface chemistry of the exposed membranes. Both the polyamide AL and the PSf SL FT-IR analysis were conducted and are presented for the active layer (Fig. 6.5a and 6.5 b) and the support layer (Fig. 6.5c and 6.5d).

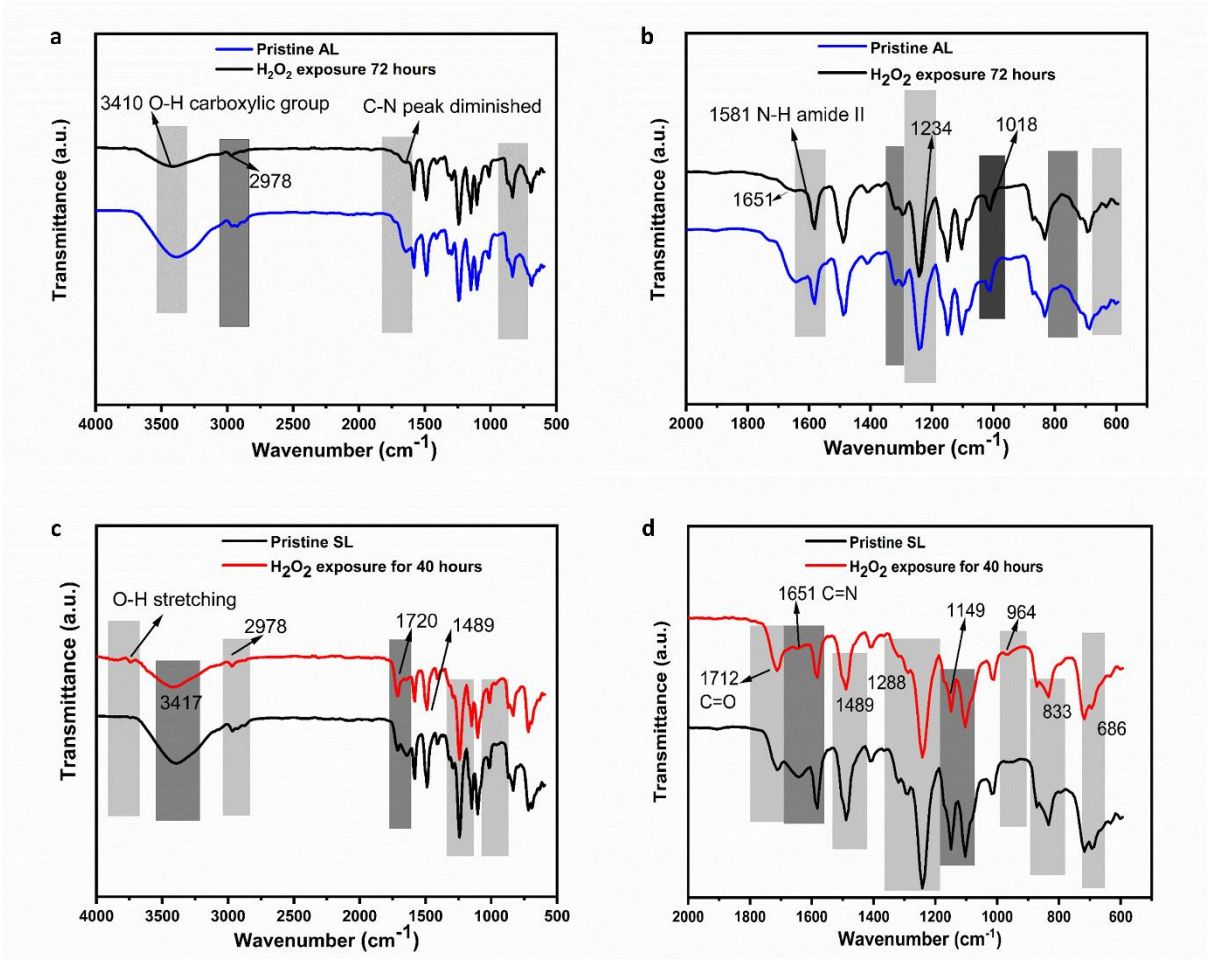

Figure 6.5: FT-IR of the pristine active layer and exposed active layer of the membrane for 72 hours ranging from 4000 to 500 cm-1

(a) FT-IR of the pristine active layer and exposed active layer of the membrane for 72 hours ranging from 4000 to 500 cm^{-1} **(b)** FT-IR of the pristine and exposed active layer of the membrane for 72

hours ranging from 2000 to 500 cm^{-1} **(c)** FT-IR of the pristine support and exposed support layer of the membrane for 42 hours ranging from 4000 to 500 cm^{-1} **(d)** FT-IR of the pristine and exposed support layer of the membrane for 40 hours ranging from 2000 to 500 cm^{-1}.

The most obvious disturbance in the spectra for the exposed AL was the suppression of the peak intensity at 3400 cm^{-1}, indicating the O-H suppression (strong broad) of the carboxylic group in the exposed membrane for 72 hours (Fig 6.5a). Similar peak suppression was observed for the PSf SL exposed for 40 hours (Fig 6.5c). The ring suppression in these bands might cause poor membrane performance in both orientations after continuous exposure to H_2O_2. There was no change at the peak at wave number 3750 (O-H stretching alcohol) for the AL, but suppression was visible in the SL at the same peak. For the damaged membranes, peak suppression was observed at around 3000 cm^{-1}, as marked by the N-H stretching (amine salt) for both the AL and the SL. Antony et al. (2010) reported similar results for oxidant-damaged polyamide RO membranes. Minor suppression was also noticed for the O=C=O band at around 2300 cm^{-1}. Significant stretching in the C=C band at around 1690 cm^{-1} indicates a change in the hydrogen bonding behaviour for the AL. Suppression was visible for this peak for the SL, suggesting a change in the hydrogen bonding behaviour for both the AL and the SL and indicating poor membrane performance. A more visible spectrum for the FT-IR analysis from wavenumber 2000–5000 cm^{-1} is provided in Fig. 6.5b and Fig. 6.5d for the AL and SL, respectively. At 1542 (N-H amide II), the peak stands for the N-H plane bending (Antony et al. 2010). Stretching was observed for the peak at 1664, indicating C=O stretching for the AL. This peak is usually identified as amide I mode (Kwon et al. 2017). Stretching was noticed at this band for the AL, as marked in Fig. 3b. Contrary to that observed for chlorine-damaged RO membranes, the peak shifts in the AL for the N-H group were lesser than the stretching of the C=O group. In general, H_2O_2 is known for its reducing and oxidizing properties (Bienert, Schjoerring & Jahn 2006). For instance, H_2O_2 can oxidize the hydroxyl (-OH) group to the carbonyl ($R_2C=O$) group (Sadri et al. 2014). Overall, it can be summarised that the oxidation of the membrane in the long exposure tests leads to damage of the polar functional (hydroxyl, carbonyl and amide) groups of the membrane.

The exposed membranes to H_2O_2 were further examined through FE-SEM analysis. The FE-SEM of the pristine active layer of the TFC membrane (Fig. 4a and 4b). The FE-SEM of the exposed active layer for 72 hours is also presented (Fig. 4c and 4d). The active layer after the prolonged exposure

to H_2O_2 appears to have scratches, possibly due to handling of the membrane in preparation for FE-SEM analysis (Fig. 4c). However, no visible damage is noticeable. At higher magnification (Fig. 4d), there is a considerable difference between the virgin and exposed membrane morphologies.

The FE-SEM of the pristine support layer (Fig. 6.6e and 6.6f) and exposed the support layer to H_2O_2 (Fig. 6.6g and 6.6h) were also examined. Compared to the AL, the SL FE-SEM shows clear visible signs of damage. Thus, the chemical cleaning of the SL with H_2O_2 is not recommended in the long term. Although there was no significant change in the water flux or RSF after 24 hours, the FE-SEM of the support layer after 24 hours indicates cracks, indicating a change in the membrane morphology after 24 hours of exposure.

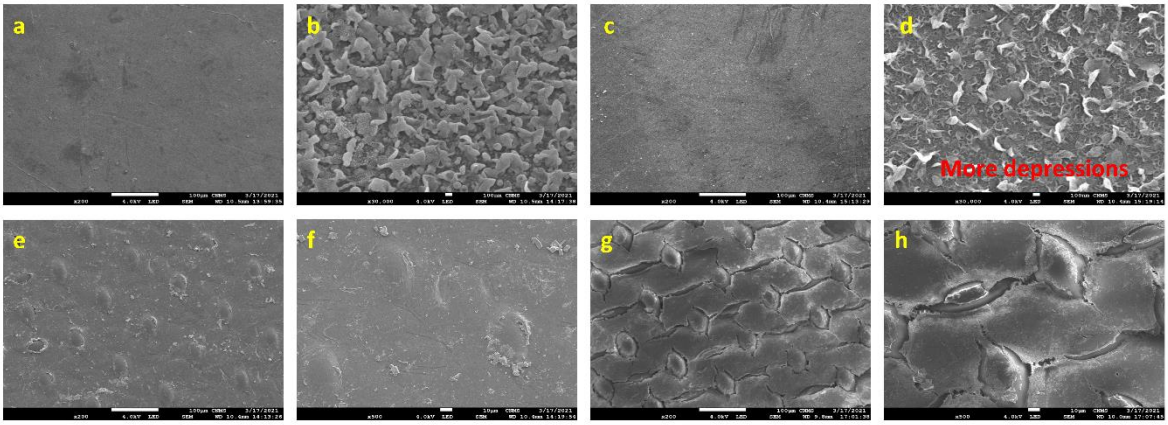

Figure 6.6: FE-SEM of the pristine active layer at 100 µm

Figure 6.6 FE-SEM of the **(a)** pristine active layer at 100 µm; **(b)** pristine active layer at 100 nm**; (c)** exposed active layer toward H_2O_2 for 72 hours at 100 µm; **(d)** exposed active layer against H_2O_2 at 100 nm; **(e)** pristine support layer at 100 µm; **(f)** pristine support layer at 10 µm; **(g)** exposed support layer toward H_2O_2 for 40 hours at 100 µm; and **(h)** exposed support layer towards H_2O_2 at 10 µm.

6.3.5. Impact of membrane orientation on flux recovery

Laboratory tests were performed in both the membrane modes in consecutive cycles using a 0.6M NaCl DS to determine the best orientation for water reclamation from the landfill leachate. A cleaning cycle with H_2O_2 was conducted after each four-hour filtration cycle with landfill leachate. Table 6.3 and Fig. 6.7 show the flux recovery after each AL-DS and AL-FS filtration cycle. After the first filtration cycle, water flux recovery when the membrane AL against the landfill leachate feed was 97.7±1 %. Then, the membrane was cleaned with H_2O_2 for 30 minutes and tested for landfill leachate filtration in another four-hour cycle to determine the impact of H_2O_2 cleaning in consecutive cycles. For the next three filtration cycles, the water flux recovery was 96.97±1 %, 92.9 %, and 84.95±1 %, respectively. The higher water flux recovery is due to the smooth surface of the active layer. It is also observed that there was no significant change in the RSF compared to the baseline RSF test. The AL-DS water flux recovery was 92±1% in the first cycle, followed by approximately 68±1% for cycle 2, 66±1% for cycle 3, and 61% for cycle 4. Based on the TFC membrane performance, the AL-FS can be selected as the best orientation for landfill leachate dewatering under a long operating time.

Table 6.3: Flux recovery percentage in two membrane modes

Membrane orientation	**Recovery Cycle-1 (%)**	**Recovery Cycle-2 (%)**	**Recovery Cycle-3 (%)**	**Recovery Cycle-4 (%)**
AL-FS	97.74	96.97	92.9	84.95
AL-DS	92	68	66	61

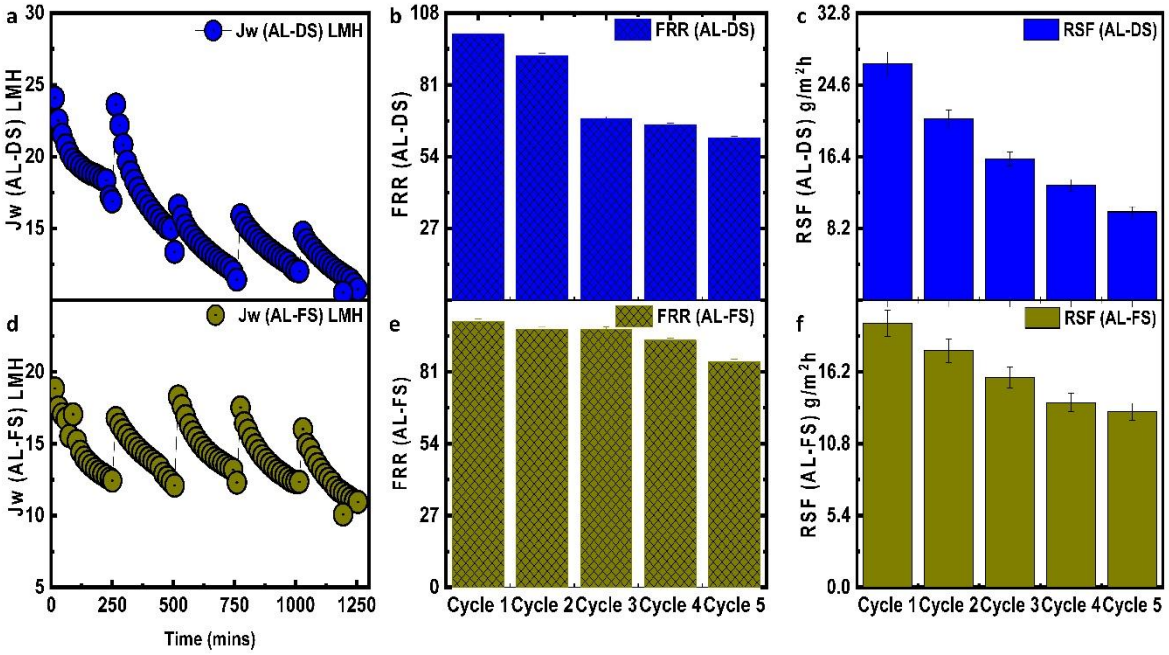

Figure 6.7: Permeation flux in the AL-DS AND AL-FS for five cycles

(a) Permeation flux in the AL-DS for five cycles **(b)** Flux recovery rate (FRR) in the AL-DS for five cycles after the initial baseline cycle **(c)** Plot of RSF in the AL-DS mode for the five cycles of filtration **(d)** AL-FS water flux in five cycles **(b)** AL-FS water flux recovery rate (FRR) for four cycles **(d)** Plot of RSF in the AL-DS for the four cycles of filtration.

The cleaning efficiency of the H_2O_2 cleaning for the AL-FS and the AL-DS orientation can be further elucidated by comparing the FT-IR of the pristine, fouled membrane by landfill leachate and cleaned membrane by H_2O_2. The band at 3749 cm^{-1} might be attributed to aluminosilicate, which is still present in the spectrum of the cleaned membrane with H_2O_2 in the AL-FS and the AL-DS mode. In principle, aluminosilicate or clay is resistant to chemical cleaning attacks, high temperatures, and pressures (Armstrong, Gallego & Chesters 2009), and therefore H_2O_2 could not effectively remove the clay foulants. Interestingly, there is no difference in the intensity for this band in the AL-FS and the AL-DS mode. Proper pretreatment of the landfill leachate wastewater can eliminate clay particles or other colloids that may contribute to irreversible fouling on the membrane surface. The bands in the range 1520-1550 cm^{-1} and the peaks at 1481 and 1489 cm^{-1} for protein fouling in the cleaned membrane spectrum show great resemblance to the pristine membrane.

Results imply that H_2O_2 can be effectively employed for membrane cleaning fouled with a wide range of organic matters. Previous studies have also demonstrated that H_2O_2 can provide better cleaning efficiency than acid or alkaline cleaning. For instance, for PSf membranes fouled by glutamic acid wastewater, cleaning with H_2O_2 achieved higher water flux recovery than HCl and sodium hydroxide (NaOH) (Li et al. 2005). Also, for CTA membrane fouled by landfill wastewater, H_2O_2 cleaning was more effective than HCl cleaning and alkaline cleaning at pH 11 (Ibrar, Yadav, Altaee, Samal, et al. 2020). Other polysaccharides foulants (1034 cm^{-1}) are also effectively removed by the H_2O_2. The band at 1243 cm^{-1} (C-O-C stretching) for the cleaned membrane is identical in intensity to the pristine membrane. The peaks in this region are usually of phosphate groups (P=O from phosphate or C-O-P, P-O-P) associated with nucleic acids (Liu, Chang & Defersha 2015; Schmitt & Flemming 1998). Other organic foulants (833 cm^{-1} to 686 cm^{-1}) are also effectively removed by the H_2O_2 as evident from the FT-IR in both the membrane orientations.

H_2O_2 is a green and cost-effective oxidising agent used to clean fouled wastewater membranes without generating secondary by-products. H_2O_2 oxidises the foulants on the fouled membrane to carbon dioxide and water (Li et al. 2005). However, cleaning by H_2O_2 alone is a slow reaction. The high content of some organic refractory compounds (Huang et al. 2020) or inorganic foulants (in this study) cannot be effectively removed at the used concentration and time.

6.3.6 Forward osmosis membrane performance in long filtration

While H_2O_2 can damage the membrane in long-term exposure, combining physical cleaning with an H2O2 chemical cleaning protocol is feasible for efficient FO operation. This will minimize the requirements for frequent membrane cleaning, reduce the damages associated with chemical cleaning, membrane integrity, and membrane lifetime, and reduce operational costs associated with chemical cleaning. Hence, long-term filtration tests were conducted using DI water physical cleaning and H_2O_2 chemical cleaning. After the initial two cycles, physical cleaning with DI water was done, and H_2O_2 was employed only in the last filtration cycle (Fig.6.8). It is noteworthy that all values of permeation flux were normalized to avoid the impact of dilution.

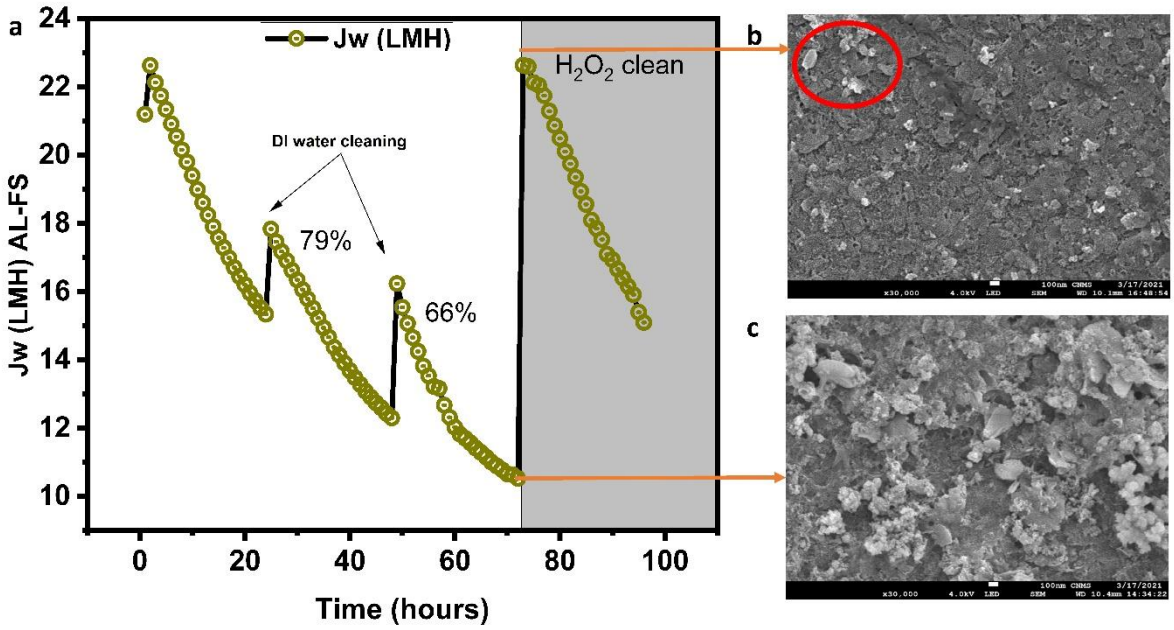

Figure 6.8: Permeation flux in the AL-FS during long-term experiments, each cycle was 24 hours

(a) Permeation flux in the AL-FS during long-term experiments, each cycle was 24 hours (**b)** FE-SEM analysis of the fouled membrane after the 72 hours filtration, (**c)** FE-SEM analysis of the membrane after cleaning with H2O2 after the 72 hours of filtration.

Since fouling in the AL-FS filtration style is governed by the cake layer, introducing some turbulence can dislodge fouling materials from the membrane surface. Physical cleaning at elevated cross-flow velocity (51 cm.sec^{-1}) was employed after each FO filtration cycle of 24-hour length. To avoid significant changes in the concentrations of the FS and DS, both were replenished after each 24-hour cycle. The high turbulence induced by physical cleaning with DI water only restored 79 ±1% (first cycle) and 66 ±1 % (second cycle) of the average water flux, indicating that some fouling materials were strongly attached to the membrane surface. This can be probably due to inorganic foulants such as silica foulants, which in the existence of Ca or Mg ions are stubbornly attached to the membrane and require chemical cleaning. It can also be assumed that physical cleaning could remove large-size fouling materials from the membrane surface, leaving the smaller and stubborn fouling matters. After 72 hours of FO filtration, H_2O_2 cleaning was employed, which restored 92 ± 2 % of the average flux. The FE-SEM of the fouled membrane before 72 hours of filtration is shown in Fig. 6.8b. After 72 hours of filtration by H_2O_2 (Fig. 6.8c), the cleaned membrane showed some

irreversible fouling (red circle), which is still attached to the membrane surface. This seems like inorganic scaling, which is inevitable due to the complex nature of landfill leachate wastewater. In this study, the inorganic scaling on the membrane is mainly caused by the clay particles (3741 $cm^{-1)}$ and silica fouling (2962 cm^{-1}), as presented earlier in the FT-IR. It is evident from the FE-SEM and FT-IR analysis that H_2O_2 concentration and duration were insufficient to remove the irreversible inorganic scaling of the membrane effectively. Proper pretreatment of landfill leachate wastewater can be another effective way to control inorganic fouling. Also, antiscalant blended DS or lowering FS pH would reduce inorganic scaling in long-term FO operations (Zhang, She, et al. 2017).

The TFC membrane achieved efficient rejection for total organic carbon (98 %) and turbidity of 99.5% as presented in Fig. S.6. The rejection of divalent calcium and magnesium ions was higher than that of monovalent potassium. This can be attributed to the larger hydrated radii and smaller crystal radii of calcium and magnesium ions compared to the potassium ion (Tansel et al. 2006). Generally, it is important to consider inorganic scaling when selecting proper cleaning protocols. Since flushing with DI water combined with H_2O_2 cleaning was not completely effective for removing inorganic scaling, the osmotic backwash method could be coupled with H_2O_2 and proven effective (Ibrar, Yadav, Altaee, Samal, et al. 2020). Future research should investigate combining the osmotic backwashing method with the H_2O_2 method to clean organic and inorganic foulants as an environmentally friendly method.

6.4. Conclusions

FO can be a viable alternative for dewatering landfill leachate; it can efficiently reject contaminants in landfill leachate wastewater. In short-term filtration cycles, cleaning with H_2O_2 proved an efficient cleaning protocol in the AL-FS filtration style. However, only 70% of the average flux could be restored in the AL-DS filtration style. This study also explored long-term exposure of TFC membrane to H_2O_2 cleaning. The AL of the FO membrane could tolerate the cleaning concentration in this study for almost 72 hours, whereas the support layer could only tolerate it for about 40 hours. The AL and the SL were damaged after the long-term exposure, as confirmed from the FT-IR and

FE-SEM analysis. For efficient FO operation, physical cleaning protocols such as DI water flushing or osmotic backwashing techniques should be combined with chemical cleaning with H_2O_2 to avoid compromising the membrane integrity. Future studies should test the forward osmosis membrane's tolerance to other cleaning agents or wastewater laden with chemicals. Additionally, novel chemical cleaning protocols should be investigated to clean the membrane without compromising integrity.

Chapter 7: Sodium docusate as an efficient, energy-saving and reusable cleaning agent for fouled forward osmosis membranes

Author contributions

Ibrar Ibrar: Conceptualization, Methodology, Data curation, Visualization, Investigation, Formal analysis, Writing – original draft. Sudesh Yadav: Formal analysis. Ali Altaee: Supervision, Project administration, Resources, Funding acquisition, Validation, Writing – review & editing. Akshaya K. Samal: Formal analysis, Javad Safae: Formal analysis. John Zhou: Formal analysis. Senthilmurugan Subbiah, Graeme Millar and Priyamjeet Deeka: Formal analysis.

Abstract

Membrane cleaning is critical for economic and scientific reasons in wastewater treatment systems. Docusate sodium or sodium docusate is used as a laxative agent and in cerumen (ear wax) removal ear drops. Docusate penetrates the hard ear wax, making it softer and easier to remove. The same principle can be applied to hardened fouling layers on the membrane surface. Once softened, the foulants can be easily flushed with water. In this study, we evaluated the efficiency of docusate sodium for cleaning fouled forward osmosis membranes with real landfill leachate wastewater. A remarkable (99%) water flux recovery was achieved using docusate at a small concentration of only 0.1% for 30 minutes. Furthermore, docusate can also effectively restore flux with static cleaning. From an economic and energy-saving perspective, static cleaning without circulating the docusate can almost achieve the same cleaning efficiency as kinetic cleaning for fouled forward osmosis membranes. Since pumping energy is a major contributor to the overall energy of the forward osmosis system, it can be minimized to a certain degree by using a static cleaning approach and can bring good energy savings when using larger membrane areas. Docusate is more environmentally friendly than acid or alkaline solutions from an environmental perspective. Furthermore, the cleaning

solution can be reused for several cycles without discarding it due to the surfactant properties of docusate.

7.1 Introduction

Forward osmosis technology or FO is generally considered a low fouling process due to the lack of hydraulic pressure, compared to the traditional pressure-driven membrane processes such as RO (reverse osmosis) and NF (nanofiltration); however, membrane fouling is still one of the major issues in the FO process. Fouling in the FO process hinders process efficiency, deteriorates membrane performance, and increases operational costs. Although several efforts can be made to minimize membrane fouling, it is still inevitable. To maintain continuous operation of the process, periodic cleaning employing physical or chemical cleaning of the membrane is unavoidable when concentrating wastewater with the FO process. Physical cleaning detaches weakly bonded cake layers from the membrane surface, but it does not remove all the fouling layers (Weerasekara, Choo & Lee 2014). Several recent studies have proved that physical cleaning protocols are often not enough to restore the performance of the FO membrane when treating wastewaters (Valladares Linares et al. 2012; Yoon et al. 2013), and chemical cleaning may be the ultimate solution. Traditionally, acid cleaning, alkaline cleaning, cleaning with surfactants, and cleaning with oxidizing agents such as hydrogen peroxide or sodium hypochlorite have been investigated for FO membranes fouled by wastewater. The choice of appropriate chemical protocol is usually tailored to the feedwater or determined by trial and error (Van der Bruggen, Mänttäri & Nyström 2008), whereas, sometimes chosen without any theoretical justification (Regula et al. 2014).

Traditional chemical cleaning protocols have several drawbacks. Traditional chemical cleaning agents can induce change in the membrane surface properties, which in turn may influence the separation performance of FO membranes, especially when treating hazardous wastewaters such as landfill leachate (Ibrar, Yadav, Altaee, Samal, et al. 2020; Ibrar et al. 2021). For instance, a caustic cleaning environment increases membrane pore size, leads to a low rejection of neutral and hydrophobic contaminants, pore opening (Mänttäri et al. 1999; Simon et al. 2013; Simon, Price &

Nghiem 2012), low rejection of magnesium, sodium and chloride ions, and swelling of the active layer (Wadekar et al. 2019). Caustic or acid cleaning also requires high or low pH, respectively, exceeding the manufacturers recommended pH windows for some membranes such as cellulose triacetate membranes (CTA). Acid cleaning also impacts sulphate rejections (Wadekar et al. 2019). When subjected to other cleaning agents such as hypochlorite, microscopic-level chain scission of the polymer components leads in a gradual loss of mechanical strength of the membranes (Arkhangelsky et al. 2007) besides the formation of hazardous and toxic halogenated by-products (Wang, Ding, et al. 2018; Xie, de Lannoy, et al. 2015). Furthermore, rupture of the C–S bond and changes in macroscopic membrane properties has been reported after hypochlorite cleaning (Arkhangelsky, Kuzmenko & Gitis 2007). Cleaning with detergents such as Alconox is compatible only with CTA membrane, whereas detrimental to TFC membranes (Wang et al. 2015). Table 7.1 (adapted from our previous work (Ibrar, Naji, et al. 2019)) lists the different cleaning protocols and their impact on different types of for forward osmosis membranes. In most cases, when the manufacturer recommended chemical cleaning protocol is followed, it is compatible with the membrane but may damage the other components of the system, such as feed spacers, due to the harsh environment (D'souza & Mawson 2005; Regula et al. 2014).

Table 7.1 Chemical cleaning protocols employed in forward osmosis

Cleaning agent	Mechanism of action	Impact on membrane	Reference
NaOCl	Oxidation and disinfection	Oxidative damage of TFC and CTA membranes	(Valladares Linares et al. 2012; Wang et al. 2015; Yoon et al. 2013)
Acids	Solubilization and chelation	Narrowing of pores	(Lv et al. 2017; Wang et al. 2015)
Alconox (detergent)	Oxidation and disinfection	Oxidation of TFC membranes	(Wang et al. 2015)

Sodium hydroxide (NaOH)	Hydrolysis and solubilization	Can increase pore size leading to lower rejection of contaminants	(Wang et al. 2015)
Surfactant	Dispersion and emulsification	Can lead to pore-plugging	(Lv et al. 2017; Wang et al. 2015)
EDTA	Chelation	Can damage TFC membrane	(Lv et al. 2017; Wang et al. 2015)
Alconox+ EDTA	Oxidation, disinfection and chelation	May damage both CTA and TFC membranes	(Wang et al. 2015)
Hydrogen per oxide	Oxidation agent	Damage to both CTA and TFC membrane	(Ibrar, Yadav, Altaee, Samal, et al. 2020; Ibrar et al. 2021)
Na_2EDTA	Chelation	May damage CTA membranes	(Martinetti, Childress & Cath 2009)

While a tremendous number of FO publications have focused on new membrane development, hybrid FO processes, novel FO draw solutions, draw solutions recovery and modelling of the FO process, there is no development focussing on the fundamental issue of membrane cleaning for continuous FO operation. With this, we report the feasibility of dioctyl sodium sulfosuccinate **($C_{20}H_{37}NaO_7S$)** or docusate sodium as a cleaning agent for FO membranes fouled with landfill leachate as characteristic wastewater. Docusate is an anionic surfactant that acts as an excellent dispersive and wetting agent used for cerumen (ear wax) removal or stool softener where it penetrates the hard symptomatic cerumen or faecal mass by making it softer and breaking it up (Meehan et al. 2002), therefore, enabling easy removal. Using this concept, we can hypothesize that docusate sodium can penetrate hard fouling layers making, dispersing it, and making it softer,

enabling easy flushing or removal from the membrane surface with normal cross-flow. Compared to the traditional surfactants used in chemical cleaning, the critical micelle concentration (CMC) value of docusate is only 0.02% (w/v) (Chambliss et al. 1981). Docusate is miscible in both organic and aqueous solutions because it contains both hydrophilic and hydrophobic groups. Furthermore, docusate sodium, a surfactant, produces foam and bubbles even in small concentrations. Chemical foam cleaning and bubbly methods have been an effective way for cleaning fouled membranes with the added advantage of reducing cleaning time compared to traditional chemical cleaning agents (Gahleitner et al. 2014; Zhang, Ding, et al. 2017). As a result, cleaning and downtime could be reduced for more efficient desalination and industrial processes. Docusate can also be used for the in-situ static cleaning of the membrane without circulation, in other words, static cleaning. Static cleaning can reduce pumping energy cost of the system, and provide some energy savings in the long-run for a desalination system.

This research investigates sodium docusate as a novel membrane cleaning agent since it can significantly reduce surface tension even at extremely low concentrations compared to other surfactants. We report the flux recovery of fouled FO membrane after cleaning (kinetic and static) with docusate in the FO mode (when the feed solution faces the support layer and draw faces the active layer) and the PRO mode (when the draw solution faces the active layer, and feed the support layer). To minimize the impact on the environment, the cleaning solution was reused for the whole cycle of FO operation. The impact of docusate on the rejection performance is also provided in detail. Furthermore, insights are provided into the energy saving that can be possible with using docusate as a cleaning agent.

7.2 Materials and methods

7.2.1 Feed and Draw solution

The biologically treated landfill leachate wastewater was collected from Hurstville Golf Centre, Sydney, Australia and used as FS (feed solution). This landfill site was used until the early 1980s when it was shut down, capped, and turned into a golf course. The landfill wastewater was stored in

a refrigerator to avoid any change in composition. Details analysis for heavy metals and contaminants of the wastewater was conducted using ICPMS (inductively coupled plasma mass spectroscopy) and presented in the previous chapter. The draw solution used in this study was NaCl (sodium chloride) of concentration 1 M (molar). Higher draw solution concentration was used in this study compared to 0.5M in our previous work (Ibrar, Yadav, Altaee, Samal, et al. 2020; Ibrar et al. 2021) to simulate harsh fouling conditions.

7.2.2 Chemical cleaning agent

Sodium docusate was procured from Sigma Aldrich, Australia, as a cleaning agent. Cleaning solutions prepared were of concentration ranging from 0.1% to 0.3% by dissolving the appropriate amount in DI water and mixed with a magnetic stirrer for at least 30 minutes. Figure 7.1 presents the chemical structure of docusate with the headgroup ion having a negative charge, thus representing an anionic surfactant. Table 7.2 lists the properties of docusate sodium with a surface tension of 28.7 dyne/cm for 0.1% solution and a topological Polar surface area of 118 Å².

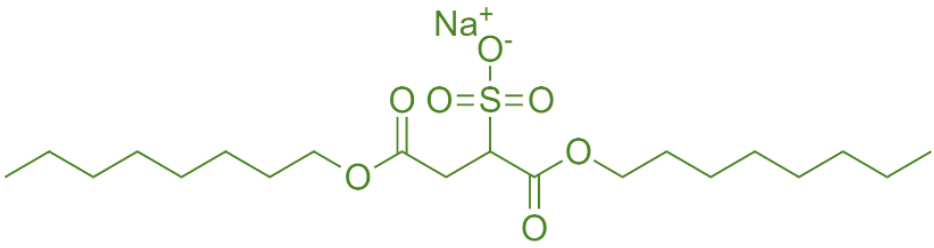

Figure 12.1 Chemical structure of sodium docusate

Table 7.2 Properties of sodium docusate

IUPAC name	**Dioctyl sodium sulfosuccinate**
Appearance	White waxy
Molecular formula	$C_{20}H_{37}NaO_7S$
Molecular weight (g/mol)	444.6

Surface tension (dynes/cm)	28.7 for 0.1% solution
Common uses	Surfactant, wetting agent, and solubilizer
Number of Hydrogen Bond Acceptors	7
Topological Polar Surface Area	118 Å²

7.2.3 Membrane and experimental setup

The FO membrane made from cellulose triacetate (CTA) was procured from Sterlitech, USA. The membrane was soaked in DI water for 24 hours to ensure complete wetting and was then immersed in the FO cell (CF042D) obtained from Sterlitech Corporation. The FO lab-scale setup used in this study was similar to our previous publication (Ibrar, Yadav, Altaee, Hawari, et al. 2020). The FS and DS were circulated at 1.8 Litres per minute, representing a cross-flow velocity of 33 cm.sec^{-1} at ambient laboratory temperature of 25 ±2 °C. The FS was placed on a scale, and the change in the weight of the feed solution over time was converted into the water flux as given by Eq. (1).

$$J_w = \frac{(\Delta W/1000)}{A_m * t} \qquad (1)$$

Where ΔW represents the change in weight of the FS recorded with a digital computer, A_m is the membrane area (0.0042 m^2) and t is the duration of the experimental run. The experimental RSF (reverse solute flux) of NaCl was calculated using Eq. (2).

$$J_s = \frac{(V_f C_f - V_i C_i)}{A_m * t} \qquad (2)$$

Where V_f and V_i are the final and initial volumes of the FS, and C_f and C_i are the initial and final concentration of the FS respectively after the end of the FO experimental run. The change in concentrations was recorded through a conductivity meter obtained from Laqua.

7.2.4 Experimental protocol

Experiments were conducted both in the FO and PRO modes to assess membrane orientation's impact on flux recovery. A previously soaked CTA membrane was installed in the FO system and flushed with DI water for at least one hour on both sides. The FS and DS were then replaced with landfill leachate (500 mL) and 1M NaCl (500 mL) and circulated for 16 hours for initial baseline performance of the membrane with the landfill leachate. After the initial baseline run, the membrane was rinsed with DI water for one minute and then cleaned with different concentrations of sodium docusate for 15 to 30 minutes, depending on the objective of each experiment (Fig.7.2). Subsequently, the membrane was washed with DI water again to remove any docusate. After each cleaning cycle, the FS and DS were replaced with the fresh ones, and the experiment was conducted again. Each experimental run lasted for three cycles. At the end of the third cycle, the samples were collected from the DS side for ICPMS analysis, and the membrane was cleaned with docusate to be analysed later by FT-IR and FE-SEM. The water flux recovery was calculated using Eq. (3) for two consecutive cycles.

$$WFR = \frac{J_{wf}}{J_{wc}} * 100 \qquad (3)$$

Where J_{wf} is the average water flux (LMH) of the fouled membrane for the whole 16 hours cycle, and J_{wc} represents the average water flux (LMH) of the cleaned membrane for the whole cycle.

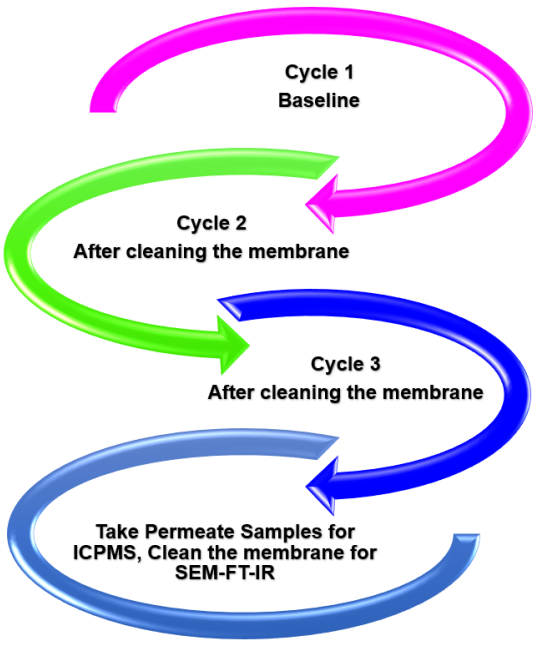

Figure 7.2: Experimental protocol followed in this study

7.2.5 Procedure for static cleaning

Static cleaning was performed with the FO system filled with the sodium docusate solution on the feed solution side. A close valve was used in the circulating loop of the feed solution near the FO cell to maintain the docusate intact with the membrane. To avoid pressure build-up in the system, the flow rate was lowered to 0.1 LPM, and the cleaning solution was pumped till the system was filled with the docusate. After the desired contact time, the membrane was flushed with DI water for 5 mins to remove the docusate from the system.

7.2.6 Membrane characterisation

The membrane morphology was studied using field emission scanning electron microscopy (FE-SEM). FE-SEM images of virgin, fouled, and cleansed membranes were taken. In addition, the same membranes were subjected to Fourier transformation infrared spectroscopy (FT-IR) investigation for functional group analysis.

7.2.7 Membrane rejection and wastewater analysis

ICPMS (Inductively coupled plasma spectroscopy) analysis was conducted to analyse the wastewater samples of the landfill leachate. To measure the impact of sodium docusate on rejection, additional ICPMS tests were done for permeate samples after cleaning with docusate and compared with the baseline.

7.3 Results and Discussions

7.3.1 Mechanism of Action of sodium docusate

Sodium docusate is an anionic surfactant used as a laxative and used in ear drops to clear the ear canal if it is blocked by cerumen (ear wax). It softens the hardened stool or cerumen by penetrating it

initially and then dispersing it. The cleaning mechanism could be implemented for fouled membranes treatment. The cleaning of sodium docusate initially involves the formation of micelles around the foulants in the wastewater, followed by the transfer of the foulants from the membrane surface to the bulk feed solution. When docusate is applied for the cleaning protocol, the micelles are formed, and the formed micelles then break down partially to bind the foulants and cover the membrane surface (Naim, Levitsky & Gitis 2012). In the next step, the binding of the micelles to the foulants causes displacement of the foulants from the CTA membrane, and, eventually, the surfactant occupies the membrane surface, including the spots liberated by the foulants. Once the surfactant occupies the membrane surface, the membrane becomes more hydrophilic. After cleaning, the presence of anionic surfactant molecules on the membrane surface may also lead to an increased repulsion between the membrane surface and negatively charged organic foulants in the landfill leachate wastewater (Masse et al. 2015). However, care should be taken because if the cleaning time and concentration of docusate are not optimised, the occupation of the membrane surface by docusate can act as an adsorption site for micelles leading to fouling.

7.3.2 Influence of concentration and time of SD on flux recovery

7.3.2.1 FO mode with kinetic cleaning

Baseline experiments with landfill leachate feed solution and 1M NaCl draw solutions with all the pristine membranes are presented in **Fig. S.1a** for the FO mode. Due to the osmotic pressure gradient generated across the CTA membrane, the water permeation naturally occurs from the feed to the draw solution without any external hydraulic pressure. Our initial tests were conducted using LFL as the FS and 1M NaCl DS for 16 hours in the FO mode, followed by a 30-minute cleaning of the fouled membrane with DI water at a high cross-flow velocity of 0.36 $cm.sec^{-1}$. The results revealed that the shear force generated by the high cross-flow velocity was insufficient to restore the permeability of the fouled membrane, with only 65 % of the average flux of the FO membrane restored. The lower flux recovery with DI water flushing agrees with previous studies on landfill leachate wastewater (Iskander et al. 2017). A new set of experiments were conducted for three consecutive cycles, and cleaning with docusate was conducted starting with 0.1% of docusate

concentration. The cleaning solution was circulated (kinetic cleaning) for only 15 minutes. **Fig.7.3a** presents the flux profiles for the two cycles after cleaning with reference to the baseline cycle, and **Fig. 7.3b** shows the flux recovery. To eliminate the effects of DS dilution on flux decline, all flux data was normalised using the same procedure as our previous work (Ibrar, Yadav, Altaee, Samal, et al. 2020; Ibrar et al. 2021) and reported here. An initial flux of 9.42 ±2 LMH and average flux of 4.26 ±0.5 LMH was observed in the baseline cycle with LFL solution for the pristine membrane. After the first cleaning cycle, there was an excellent flux recovery of 98% (average flux of 4.20 ±0.5); however, it dropped to 93% after the second cleaning cycle (average flux of 3.97±0.5) for the last cycle. Since 15 minutes cleaning was not enough for complete flux recovery in a consecutive cycle, the cleaning time was increased to 30 minutes for the same concentration. The results are presented in **Fig.7.3c and Fig.7.3d.**

The cleaning with 30 minutes restored almost 99% of flux in the consecutive cycles. To minimize the downtime for the system, the higher concentration of 0.2 % was tested again to check whether the cleaning duration could be reduced to 15 minutes only **(Fig.7.3e and Fig.7.3f).** However, increasing the concentration to 0.2% and cleaning for 15 minutes had lower FR than the 0.1% for 15 minutes and 30 minutes. The higher concentrations of docusate might promote pore plugging of the FO membrane and lower the water flux recovery. Other studies have also reported severe concentration polarisation and pore-blocking with higher concentrations of surfactant solutions (Al-Amoudi & Lovitt 2007; Ochando-Pulido, Victor-Ortega & Martínez-Ferez 2015). Higher concentrations of docusate also create more foam which can be problematic in practical applications. A higher concentration of docusate can, therefore, not be an effective remedy, as it can enhance fouling due to micelles pore blocking. Ideally, testing should be investigated starting from lower concentrations.

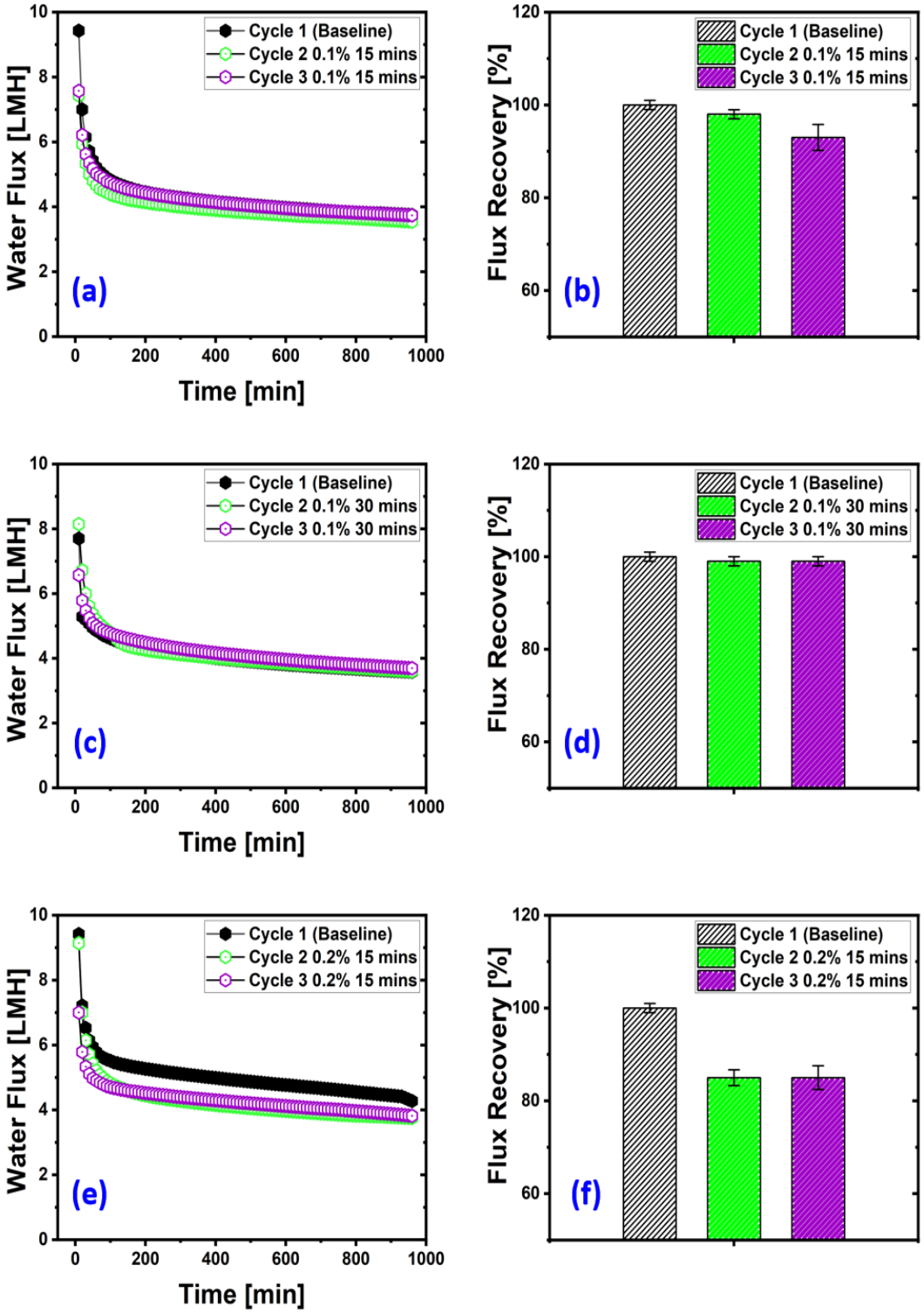

Figure 7.3: Water flux profiles and flux recovery for different concentrations and time

a) Water flux profiles in three cycles with 0.1 percent cleaning for 15 minutes, b) Water flux profiles in three cycles with 0.1 percent cleaning for 30 minutes, c) Water flux profiles in three cycles with 0.2 percent cleaning for 15 minutes.

7.3.2.2 PRO mode with kinetic cleaning

A similar protocol to the FO mode tests was maintained for the PRO tests to investigate the influence of concentration and time on FR. Initial tests in the PRO mode were conducted with the LFL solution and 1M NaCl DS, and cleaning was done with DI water at high cross-flow velocity. However, this cleaning method resulted in only 53% of the average water flux being restored for the fouled FO membrane. Subsequently, a new membrane was installed, and tests were done for three cycles circulating docusate at a concentration of 0.1 percent for only 15 minutes cleaning time (**Fig. 7.4**). An average flux of 4.88 ±2 LMH was obtained for the baseline experiments in the PRO mode. This was slightly higher than the average flux of the baseline experiments in the FO mode. Following the baseline experiments in the PRO mode, cleaning was performed after cycle 1 and cycle 2, respectively, and the FR is reported in **Fig.7.4b.** The FR achieved was 88% after the second cycle and declined to 85% after the third filtration cycle. In the next set of experiments with a new membrane installed in the FO system, cleaning with docusate was conducted with the same concentration but for a duration of 30 minutes (**Fig. 7.4c**). The prolonged contact time of the cleaning solution exacerbated the FR for the same concentration, with 69% FR in cycle 2 and only 64% in cycle 3 (**Fig.7.4d**). The cleaning concentration was stepped up to 0.2%, and new experiments were conducted to analyse whether it could recover more flux compared to the 0.1%. The flux profiles are shown in **Fig.7.4e.** The increased concentration of 0.2% led to a FR of 78% and 75% in the second and third cycles, respectively, as presented in **Fig.7.4f.** Increasing the duration of the 0.2% in the PRO mode also had a similar effect on FR (**Fig.7.4g and 7.4h**) as 0.1%, and longer duration and higher concentration is therefore not recommended in the PRO mode.

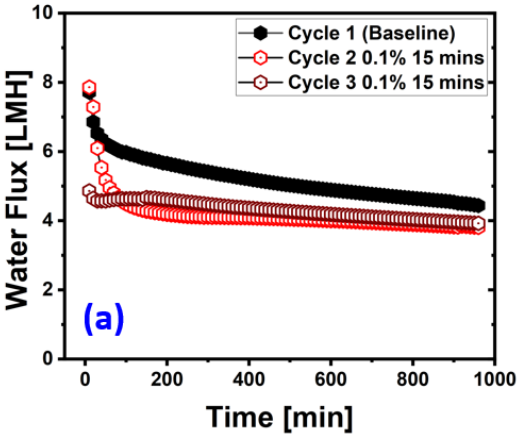
Cycle 1 (Baseline)
Cycle 2 0.1% 15 mins
Cycle 3 0.1% 15 mins
Water Flux [LMH]
Time [min]
(a)

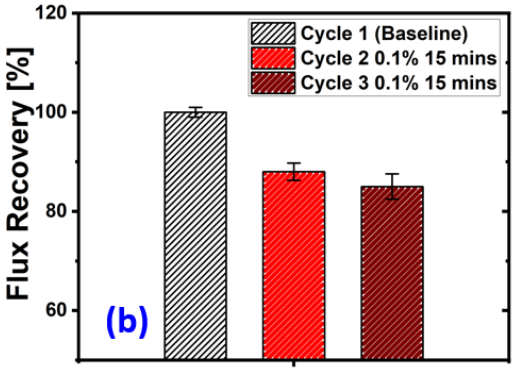
Cycle 1 (Baseline)
Cycle 2 0.1% 15 mins
Cycle 3 0.1% 15 mins
Flux Recovery [%]
(b)

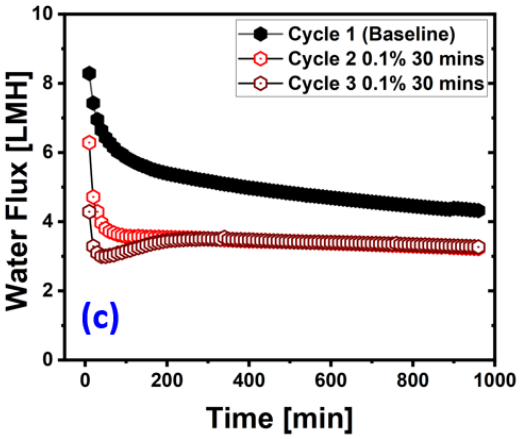
Cycle 1 (Baseline)
Cycle 2 0.1% 30 mins
Cycle 3 0.1% 30 mins
Water Flux [LMH]
Time [min]
(c)

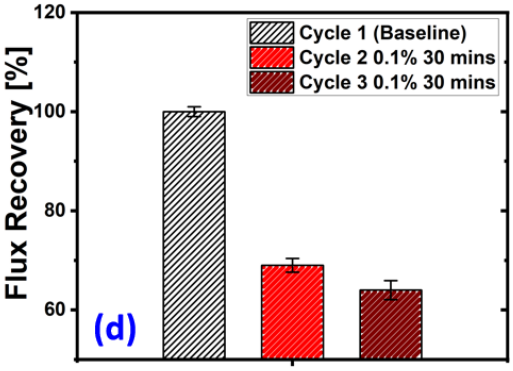
Cycle 1 (Baseline)
Cycle 2 0.1% 30 mins
Cycle 3 0.1% 30 mins
Flux Recovery [%]
(d)

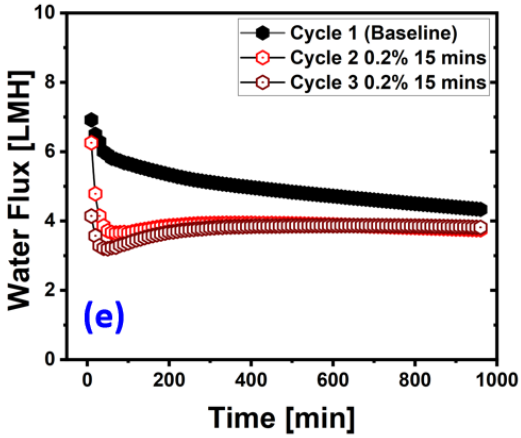
Cycle 1 (Baseline)
Cycle 2 0.2% 15 mins
Cycle 3 0.2% 15 mins
Water Flux [LMH]
Time [min]
(e)

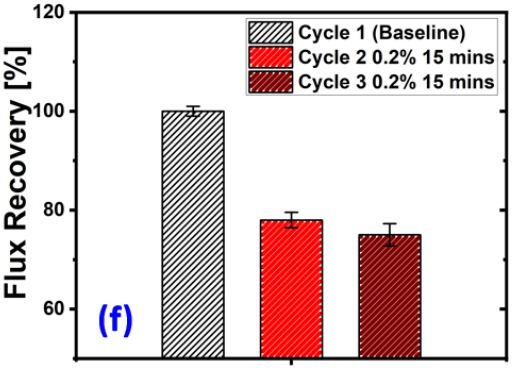
Cycle 1 (Baseline)
Cycle 2 0.2% 15 mins
Cycle 3 0.2% 15 mins
Flux Recovery [%]
(f)

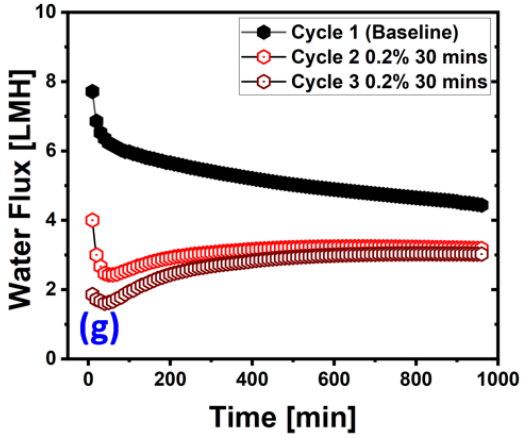
Cycle 1 (Baseline)
Cycle 2 0.2% 30 mins
Cycle 3 0.2% 30 mins
Water Flux [LMH]
Time [min]
(g)

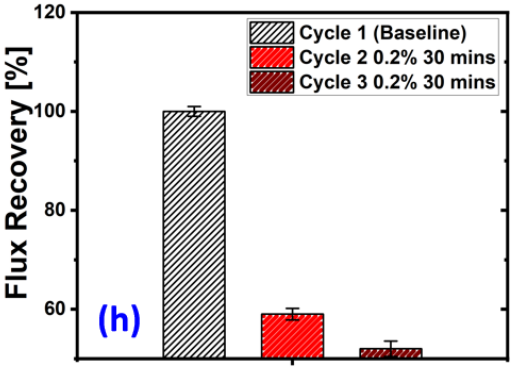
Cycle 1 (Baseline)
Cycle 2 0.2% 30 mins
Cycle 3 0.2% 30 mins
Flux Recovery [%]
(h)

Figure 7.4: Water flux profiles and flux recovery for different concentrations and time

a) Water flux profiles in three cycles with 0.1 percent cleaning for 15 minutes, b) Water flux profiles in three cycles with 0.1 percent cleaning for 30 minutes, c) Water flux profiles in three cycles with 0.2 percent cleaning for 15 minutes.

7.3.2.3 FO mode and PRO mode with static cleaning

Previous studies on surfactant cleaning have revealed that the circulation of a cleaning solution accelerates surfactant transport to the membrane surface and facilitates micelle pore blocking (Naim, Levitsky & Gitis 2012). Cleaning without circulation can also have benefits such as reducing the energy consumption of pumping the cleaning solutions. The best concentration from the kinetic cleaning was chosen for static cleaning experiments, 0.1% for the FO and the PRO mode. The duration for static cleaning was determined through trial and error by starting from 15 minutes of contact time. The static cleaning was investigated for 15 minutes, 30 minutes and one hour for the FO and the PRO mode, respectively. Among these experimental runs, the static cleaning for 30 minutes had superior flux recovery for both the FO and PRO modes, as shown in **Fig.7.5.** A snapshot of the static cleaning of the FO membrane in the FO mode is presented in **Fig.7.5a**, and the clean FO membrane in the FO mode is presented in **Fig.7.5b**. The FO cell was placed sidewise with the milky docusate foam is visible on the top part of the cell. In the FO mode, the flux profiles for three cycles are presented in Fig.7.5c and the FR in Fig.7.5d. An FR of 95% and 93% were achieved for cycle 2 and cycle 3, respectively. Additional tests were conducted for static cleaning in the FO mode, and the membrane was soaked for an additional one hour in DI water after 30 mins docusate static cleaning. The flux recovery was slightly higher (97% cycle 1 and 93% cycle 2). However, additional soaking will entail extra downtime for the system, and the flux recovery is not as high compared to the 30 mins static cleaning.

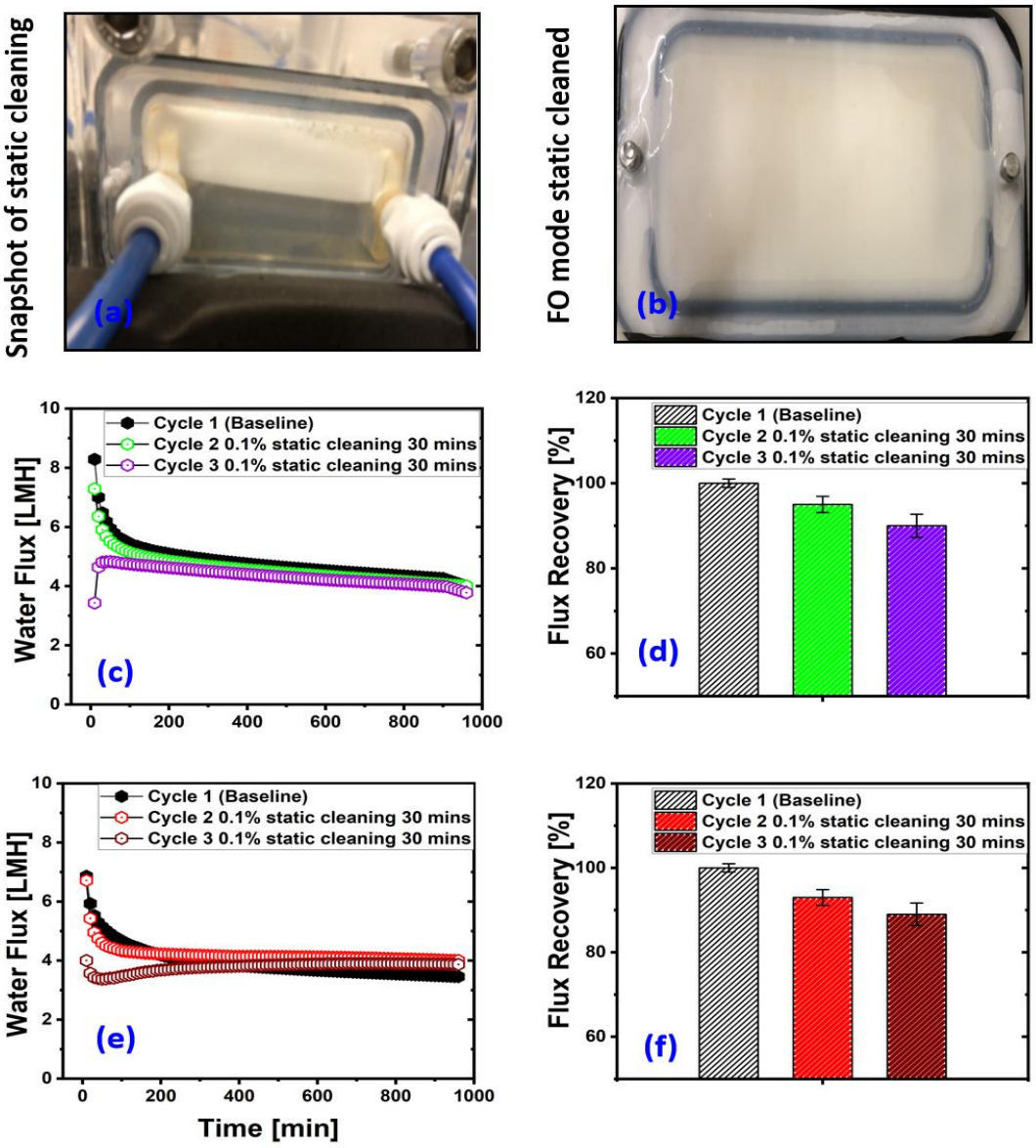

Figure 7.5: Water flux profiles and flux recovery for different concentrations and time with static cleaning a) FO cell profile in static cleaning, b) clean FO membrane after 30 mins static cleaning, c) Water flux profiles in three cycles with 0.1 percent cleaning for 30 mins in the FO mode, d)flux recovery with 0.1 percent cleaning for 30 mins in the FO mode, e) Water flux profiles in three cycles with 0.1 percent cleaning for 30 mins in the PRO mode, f) Flux recovery in three cycles with 0.1 percent cleaning for 30 mins in the PRO mode

Compared to the FO mode, in the PRO mode, a good flux recovery of 92% was achieved after the first cleaning cycle and then declined to 90% after the second cleaning cycle. Additional tests were conducted and the membrane was soaked in one hour in DI water after static cleaning in the PRO mode. This improved the flux recovery to 94% in cycle 2 after the first cleaning and 91% in cycle 3. Soaking DI water may facilitate cleaning the pores in the support layer and promote further flux recovery.

7.4 FE-SEM and contact angle

The fouled and cleaned membranes were further analysed by contact angle (Table 7.3) and the morphological changes were observed through FE-SEM analysis (Figure 4). The contact angle for the kinetic and static cleaned membranes (Table 7.3) was lowered due to the docusate cleaning, implying more hydrophilicity of the FO membrane after cleaning with the docusate solution compared to the pristine membrane. The contact angle for the static cleaned was slightly lower than the kinetic cleaned, probably due to the residual docusate on the membrane surface. A similar trend was observed in the PRO mode, with the static cleaned membrane having a slightly higher contact angle than the kinetic cleaned. The SEM analysis (Figure 7.6) of the pristine, fouled and cleaned membranes can give useful qualitative information about the pristine membrane, the nature of the fouling and the efficiency of docusate cleaning. The cleaned membrane in the FO mode shows great resemblance with the pristine membranes (Figure 7.6a to 7.6h), proving the efficiency of the docusate with kinetic as well as static cleaning. In the PRO mode, the SEM of the fouled and cleaned membranes are also compared with those of pristine membranes (Fig.7.6i to 7.6o). The cleaned membrane shows a little surface conditioning, probably due to the docusate. The static cleaned membrane also shows a good resemblance with the pristine membrane (Fig.7.6o).

Table 7.3: Contact angle for pristine, fouled and cleaned membranes

Membrane Surface/Mode of operation	Contact angle (°)

Pristine active layer	68.16('<Energy issues in Desalination processes . Critical Review , R. Semiat.pdf>')('<Energy issues in Desalination processes . Critical Review , R. Semiat.pdf>')('<Energy issues in Desalination processes . Critical Review , R. Semiat.pdf>')('<Energy issues in Desalination processes . Critical Review , R. Semiat.pdf>')
Fouled active layer	70.23
Kinetic cleaned FO mode	64.57
Static cleaned FO mode	63.22
Pristine support layer	52.31
Fouled PRO mode	57.35
Kinetic cleaned PRO mode	53.17
Static cleaned PRO mode	55.13

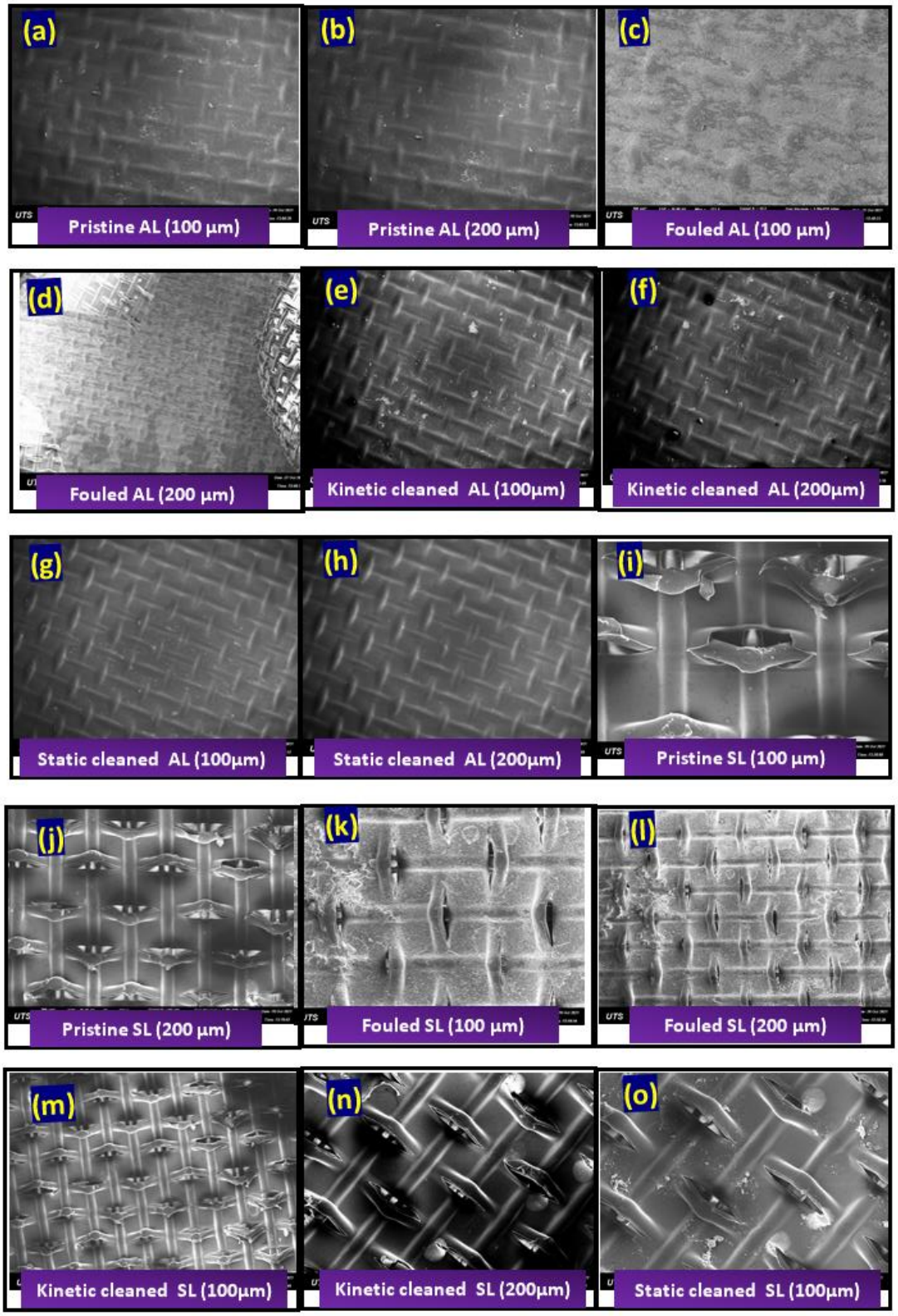

Figure 7.6: SEM images of pristine, fouled and cleaned membranes in the FO and the PRO mode

a) pristine membrane in the FO mode at 100 µm, b) pristine membrane in the FO mode at 200 µm, c) fouled membrane in the FO mode at 100 µm, d) fouled membrane in the FO mode at 200 µm, e) kinetic cleaned membrane in the FO mode at 100 µm, f) kinetic cleaned membrane in the FO mode at 200 µm, g) static cleaned membrane in the FO mode at 100 µm, h) static cleaned membrane in the FO mode at 200 µm, i) pristine membrane in the PRO mode at 100 µm, j) pristine membrane in the PRO mode at 200 µm, k) fouled membrane in the PRO mode at 100 µm, l) fouled membrane in the PRO mode at 200 µm, m) kinetic cleaned membrane in the PRO mode at 100 µm, n) kinetic cleaned membrane in the PRO mode at 200 µm, o) static cleaned membrane in the PRO mode at 100 µm. All membranes were flushed with DI water after cleaning with docusate for five minutes.

7.5 FT-IR Analysis

The cleaning efficacy of the docusate cleaning was evaluated using FTIR analysis, which compared the characterisation of cleaned and fouled membranes to that of virgin membrane. The cleaned membrane with 0.1% for 30 mins static and kinetic cleaned in the FO mode, and 0.1 % for 15 mins and 30 mins with kinetic and static cleaning in the PRO mode respectively were reported only, since these concentrations and durations had exhibited the best performance. The FT-IR spectrum of the docusate is also presented to assess whether any docusate was adsorbed onto the cleaned membrane. **Fig.7.7a** and **Fig.7.7b** presents the FT-IR of docusate, pristine, fouled and cleaned membranes for the FO and the PRO mode, respectively. The majority of the bands in the FT-IR of the fouled membrane in the FO and the PRO mode may be attributed to organic foulants showing that organic fouling is the primary issue when treating landfill leachate wastewater. The FT-IR of the fouled membrane in the FO mode and the PRO mode shows a visible diminishing of the peak at 1735, usually attributed to the fatty acids fouling (Levitsky et al. 2011). The band stretching at wavenumber 1643 in the FO and the PRO mode may indicate protein fouling (Yadav, Ibrar, Altaee, Déon, et al. 2020).

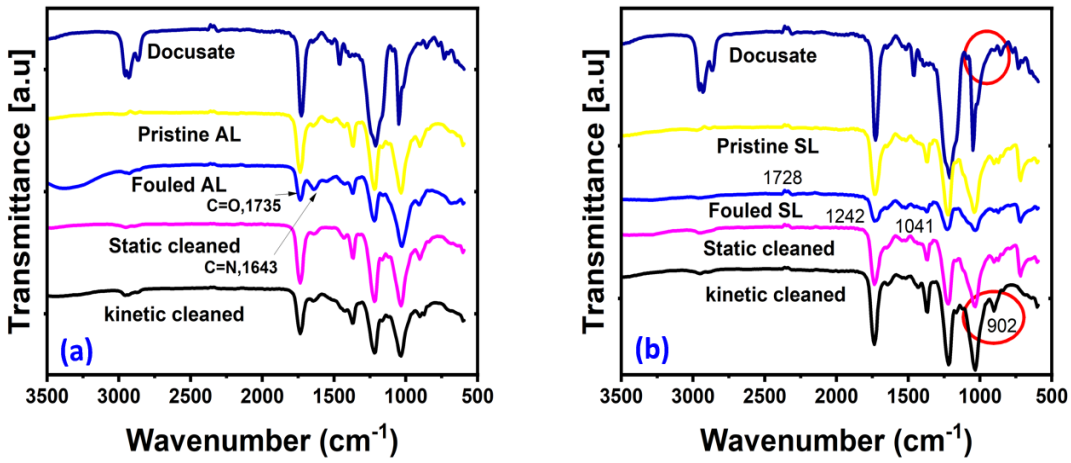

Fig.7.7. FT-IR of docusate, pristine, fouled and cleaned membranes ,a) for the FO ,b) the PRO mode

The FT-IR of the cleaned membranes in both the FO and the PRO mode shows a remarkable resemblance with the pristine membrane, implying cleaning with docusate was effective. The docusate adsorption to the membrane is visible for the wavenumber 902 cm^{-1} in the PRO mode with kinetic cleaning. This band is absent in the pristine membrane, indicating that docusate might cause pore plugging in the PRO mode. Similarly, the static cleaned membrane shows more resemblance to the pristine membrane for the FO mode than the kinetic cleaned.

7.6 Energy savings due to static cleaning

Fouling and energy consumption are directly connected to each other. A higher degree of membrane fouling may lead to higher energy consumption by cleaning the FO membrane at high cross-flow rates or pumping chemical cleaning solutions. A major proportion of FO energy is consumed in the reconcentration of the draw solution for reuse, and the rest is consumed by pumping the feed and the draw solutions. The FO process in this study for dewatering landfill leachate does not involve DS regeneration. The majority of energy utilised is pumping the feed solution and the draw solution, and the additional pumping energy is for the chemical cleaning during the cleaning of the fouled membrane. Though it is claimed that physical cleaning protocols recover most of the FO flux recovery with low energy input, it is not supported by a systematic investigation (Zou et al. 2016), and on the other hand, chemical cleaning consumes more energy than physical cleaning, particularly

in the treatment of landfill leachate (Iskander et al. 2017). The pumping energy of the FO system for the landfill leachate wastewater in this study can be estimated using Equation (4).

$$E = \frac{P_{FS}Q_{FS}+P_pQ_p}{\eta Q_P} \qquad (4)$$

where P_{FS} and P_p represents the hydraulic pressure of the landfill leachate wastewater (bars) and permeate water, Q_{FS} and Q_p indicates the flow rate of the FS and the permeate and η represents the pump efficiency, assumed to be 0.85. The baseline tests in the FO mode consumed an average of 0.024 ±0.01 kWh/m^3. It should be noted that higher energy may be required with lower DS concentration, such as 0.6M or seawater DS. The kinetic cleaning in the FO process consumed an average of 0.0011 ±0.001 kWh/m^3 per cleaning cycle. The kinetic cleaning was conducted at the same cross-flow velocity as the baseline tests, as higher cross-flow velocities would require more energy. Since excellent FR was achieved in the static mode and FO mode, static cleaning would help save energy during the cleaning procedure (a saving of 0.0011 kWh/m^3) for each cycle of chemical cleaning.

7.7 Conclusions

Sodium docusate was evaluated as a novel cleaning agent for fouled forward osmosis membrane. Although forward osmosis is considered a low fouling process compared to reverse osmosis, the process is still subjected to irreversible fouling, particularly when treating real wastewater with high organic content, such as landfill leachate, for longer durations. Traditional cleaning agents such as alkaline cleaning and acid cleaning, although beneficial, cannot be suitable for all types of membranes or compatible with the types of wastewater. High flux recovery was achieved in the FO mode with kinetic as well as static cleaning. In the PRO mode, the performance of the docusate was

also satisfactory; however, care might be taken as docusate can enhance pore-plugging in the PRO mode if circulated for a long time. Using static cleaning, a proportion of pumping energy can be saved, bringing long-term benefits for commercial projects using docusate as a cleaning agent.

Chapter 8 Conclusions and recommendations for future work

This research investigated concentration polarisation and fouling in the FO process, using landfill leachate wastewater as the feed and NaCl draw solutions. The moduli of CPs' in the FO process require a large amount of information to calculate. The existing models can predict the experimental flux in the FO process. Still, they become more demanding when a mixture of draw solutions is used or lack of information about the FO modules due to propriety issues. Therefore, the solute resistivity "*K*" and mass transfer coefficient "*k*" value are hard to determine for a forward osmosis system. The empirical model in this study can provide an alternative solution for predicting water flux in the FO process. The model demonstrated an excellent capability to predict CP and water flux in the FO process with 95-99% agreement with experimental values and without obtaining experimental parameters such as *K* and *k*. The model can be particularly helpful in the FO processes using a mixture of draw solutions. In a multicomponent draw solution, the diffusion coefficient is hardly available in the literature and ions move at a distinct rate within the film layer; therefore, it is impossible to define an effective diffusivity of the mixture. The model in this study only relies on a set of experimental data to measure CP and predict performance, such as Flux, CP, and RSF. It can also be extended to ternary and quaternary mixtures of DSs as well as commercial spiral wound modules.

The present researchrevealed the potential of the FO process for the treatment of landfill leachate and the removal of metal ion contaminants. The efficiency of the FO process was strongly related to the membrane operating mode. In contrast, the long-term performance of the FO process was highly dependent on the cleaning methods for removing various contaminants from the membrane surface. Membrane orientation significantly impacts the water flux, which was higher when the membrane was in the AL-DS mode. But the latter operating mode resulted in more recalcitrant membrane fouling than the AL-FS mode. The fouled FO membrane was cleaned using several physical and chemical techniques. Physical cleaning by DI water was ineffective in restoring the water flux. Still, hot DI water at 35 oC and osmotic backwash with 1.5M NaCl solution achieved higher water flux recovery. Chemical cleaning with H_2O_2 was more efficient than acid and alkaline solutions, although

it caused severe membrane damage when landfill leachate faced the FO membrane active layer. The rejection rate of metal ions was lower after cleaning with the H_2O_2 solution. Experimental study suggests that physical cleaning methods with hot water and osmotic backwash are preferable over chemical cleaning methods due to their efficiency in restoring the water flux without generating chemical wastes. Furthermore, long-term experiments showed that cleaning with hot water at 35 ^oC was slightly more effective than cleaning with an osmotic backwash with 1.5 M NaCl, especially when the membrane operated in the AL-DS mode. The results demonstrated the FO process's feasibility for treating leachate wastewater without the need to change the FO membrane after washing with hot water or osmotic backwashing with NaCl solution.

FO can be a viable alternative for dewatering landfill leachate; it can efficiently reject contaminants in landfill leachate wastewater. In short-term filtration cycles, cleaning with H_2O_2 proved an efficient cleaning protocol in the AL-FS filtration style. However, only 70% of the average flux could be restored in the AL-DS filtration style. This study also explored the long-term exposure of TFC membrane to H_2O_2 cleaning. The AL of the FO membrane could tolerate the cleaning concentration in this study for almost 72 hours, whereas the support layer could only tolerate it for about 40 hours. The AL and the SL were damaged after the long-term exposure, as confirmed by the FT-IR and FE-SEM analysis. For efficient FO operation, physical cleaning protocols such as DI water flushing or osmotic backwashing techniques should be combined with chemical cleaning with H_2O_2 to avoid compromising the membrane integrity. Future studies should test the forward osmosis membrane's tolerance to other cleaning agents or wastewater laden with chemicals. Additionally, novel chemical cleaning protocols should be investigated to clean the membrane without compromising integrity.

Sodium docusate was evaluated as a novel cleaning agent for fouled forward osmosis membrane. Although forward osmosis is considered a low fouling process compared to the reverse osmosis, the process is still subjected to irreversible fouling particularly when treating real wastewater with high organic content, such as landfill leachate, for longer durations. Traditional cleaning agents such as alkaline cleaning and acid cleaning, although beneficial, cannot be suitable for all types of membranes or compatible with the types of wastewater. High flux recovery was achieved in the FO

mode with kinetic as well as static cleaning. In the PRO mode, the performance of the docusate was also satisfactory; however, care might be taken as docusate can enhance pore-plugging in the PRO mode, if circulated for a long time. Using static cleaning, a proportion of pumping energy can be saved, bringing long-term benefits for commercial projects using docusate as a cleaning agent.

Future research studies should work on pilot-scale FO applications for wastewater treatment using novel membranes with higher water flux. Unfortunately, current commercial FO membranes have low water flux and therefore have issues in scaling up. CTA membrane is a popular choice for wastewater treatment application due to their high flux recovery and is less prone to fouling than TFC membranes. But the lower flux of CTA membranes is an issue. For the FO process to compete with other processes, novel TFC membranes with high flux, excellent antifouling and chlorine-resistant properties should be investigated in the future for FO wastewater treatment applications.

Future FO studies should also investigate new membranes or modify current ones for particular wastewater such as landfill leachate wastewater where the membrane is tailored to the rejection of contaminants in that particular wastewater such as membrane which has high rejection for heavy metals in landfill leachate. This will ensure more efficiency and probably higher water flux than the current membranes. Finally, future research should investigate treatment of different types of complex wastewater such as mining wastewater using the FO membrane.

References

Abbas, A.A., Jingsong, G., Ping, L.Z., Ya, P.Y. & Al-Rekabi, W.S. 2009, 'Review on LandWll Leachate Treatments', *Journal of Applied Sciences Research*, vol. 5, no. 5, pp. 534-45.

Abdelrasoul, A., Doan, H., Lohi, A. & Cheng, C.-H. 2015, 'Mass transfer mechanisms and transport resistances in membrane separation process', *Mass Transfer-Advancement In Process Modelling*, IntechOpen.

Abejón, R., Garea, A. & Irabien, A. 2013, 'Effective Lifetime Study of Commercial Reverse Osmosis Membranes for Optimal Hydrogen Peroxide Ultrapurification Processes', *Industrial & Engineering Chemistry Research*, vol. 52, no. 48, pp. 17270-84.

Abid, H.S., Johnson, D.J., Hashaikeh, R. & Hilal, N. 2017, 'A review of efforts to reduce membrane fouling by control of feed spacer characteristics', *Desalination*, vol. 420, pp. 384-402.

Abragam, A. & Abragam, A. 1961, *The principles of nuclear magnetism*, Oxford university press.

Achilli, A., Cath, T.Y. & Childress, A.E. 2009, 'Power generation with pressure retarded osmosis: An experimental and theoretical investigation', *Journal of Membrane Science*, vol. 343, no. 1, pp. 42-52.

Achilli, A., Cath, T.Y. & Childress, A.E. 2010, 'Selection of inorganic-based draw solutions for forward osmosis applications', *Journal of Membrane Science*, vol. 364, no. 1-2, pp. 233-41.

Achilli, A., Cath, T.Y., Marchand, E.A. & Childress, A.E. 2009, 'The forward osmosis membrane bioreactor: A low fouling alternative to MBR processes', *Desalination*, vol. 239, no. 1, pp. 10-21.

Aftab, B., Ok, Y.S., Cho, J. & Hur, J. 2019, 'Targeted removal of organic foulants in landfill leachate in forward osmosis system integrated with biochar/activated carbon treatment', *Water Research*, vol. 160, pp. 217-27.

Al-Amoudi, A. & Lovitt, R.W. 2007, 'Fouling strategies and the cleaning system of NF membranes and factors affecting cleaning efficiency', *Journal of Membrane Science*, vol. 303, no. 1, pp. 4-28.

Ali, S.M., Kim, J.E., Phuntsho, S., Jang, A., Choi, J.Y. & Shon, H.K. 2018, 'Forward osmosis system analysis for optimum design and operating conditions', *Water Research*, vol. 145, pp. 429-41.

Alphenaar, P.A., Sleyster, R., De Reuver, P., Ligthart, G.-J. & Lettinga, G. 1993, 'Phosphorus requirement in high-rate anaerobic wastewater treatment', *Water Research*, vol. 27, no. 5, pp. 749-56.

Alsvik, I. & Hägg, M.-B. 2013, 'Pressure retarded osmosis and forward osmosis membranes: materials and methods', *Polymers*, vol. 5, no. 1, pp. 303-27.

Altaee, A., Sharif, A., Zaragoza, G. & Hilal, N. 2014, 'Dual stage PRO process for power generation from different feed resources', *Desalination*, vol. 352, pp. 118-27.

Altaee, A., Zhou, J., Alanezi, A.A. & Zaragoza, G. 2017, 'Pressure retarded osmosis process for power generation: Feasibility, energy balance and controlling parameters', *Applied Energy*, vol. 206, pp. 303-11.

Altaee, A., Zhou, J., Alhathal Alanezi, A. & Zaragoza, G. 2017, 'Pressure retarded osmosis process for power generation: Feasibility, energy balance and controlling parameters', *Applied Energy*, vol. 206, pp. 303-11.

Amin Saad, M. 2004, 'Early discovery of RO membrane fouling and real-time monitoring of plant performance for optimizing cost of water', *Desalination*, vol. 165, pp. 183-91.

Amy, G. 2008a, 'Fundamental understanding of organic matter fouling of membranes', *Desalination*, vol. 231, no. 1, pp. 44-51.

Amy, G. 2008b, 'Fundamental understanding of organic matter fouling of membranes', *Desalination*, vol. 231, no. 1-3, pp. 44-51.

An, Y.H. & Friedman, R.J. 1998, 'Concise review of mechanisms of bacterial adhesion to biomaterial surfaces', *Journal of Biomedical Materials Research*, vol. 43, no. 3, pp. 338-48.

Ansari, A.J., Hai, F.I., Price, W.E., Drewes, J.E. & Nghiem, L.D. 2017, 'Forward osmosis as a platform for resource recovery from municipal wastewater - A critical assessment of the literature', *Journal of Membrane Science*, vol. 529, pp. 195-206.

Ansari, A.J., Hai, F.I., Price, W.E. & Nghiem, L.D. 2016, 'Phosphorus recovery from digested sludge centrate using seawater-driven forward osmosis', *Separation and Purification Technology*, vol. 163, pp. 1-7.

Antony, A., Fudianto, R., Cox, S. & Leslie, G. 2010, 'Assessing the oxidative degradation of polyamide reverse osmosis membrane—Accelerated ageing with hypochlorite exposure', *Journal of Membrane Science*, vol. 347, no. 1, pp. 159-64.

Arkhangelsky, E., Kuzmenko, D., Gitis, N.V., Vinogradov, M., Kuiry, S. & Gitis, V. 2007, 'Hypochlorite Cleaning Causes Degradation of Polymer Membranes', *Tribology Letters*, vol. 28, no. 2, pp. 109-16.

Arkhangelsky, E., Kuzmenko, D. & Gitis, V. 2007, 'Impact of chemical cleaning on properties and functioning of polyethersulfone membranes', *Journal of Membrane Science*, vol. 305, no. 1, pp. 176-84.

Arkhangelsky, E., Wicaksana, F., Chou, S., Al-Rabiah, A.A., Al-Zahrani, S.M. & Wang, R. 2012, 'Effects of scaling and cleaning on the performance of forward osmosis hollow fiber membranes', *Journal of Membrane Science*, vol. 415-416, pp. 101-8.

Armstrong, M.W., Gallego, S. & Chesters, S.P. 2009, 'Cleaning clay from fouled membranes', *Desalination and Water Treatment*, vol. 10, no. 1-3, pp. 108-14.

Atmaca, E. 2009, 'Treatment of landfill leachate by using electro-Fenton method', *Journal of Hazardous Materials*, vol. 163, no. 1, pp. 109-14.

Awad, A.M., Jalab, R., Minier-Matar, J., Adham, S., Nasser, M.S. & Judd, S.J. 2019, 'The status of forward osmosis technology implementation', *Desalination*, vol. 461, pp. 10-21.

Bacchin, P., Aimar, P. & Field, R.W. 2006, 'Critical and sustainable fluxes: Theory, experiments and applications', *Journal of Membrane Science*, vol. 281, no. 1, pp. 42-69.

Bao, X., Wu, Q., Shi, W., Wang, W., Yu, H., Zhu, Z., Zhang, X., Zhang, Z., Zhang, R. & Cui, F. 2019, 'Polyamidoamine dendrimer grafted forward osmosis membrane with superior ammonia selectivity and robust antifouling capacity for domestic wastewater concentration', *Water Research*, vol. 153, pp. 1-10.

Bell, E.A., Holloway, R.W. & Cath, T.Y. 2016, 'Evaluation of forward osmosis membrane performance and fouling during long-term osmotic membrane bioreactor study', *Journal of Membrane Science*, vol. 517, pp. 1-13.

Benavente, J. & Vázquez, M.I. 2004, 'Effect of age and chemical treatments on characteristic parameters for active and porous sublayers of polymeric composite membranes', *Journal of Colloid and Interface Science*, vol. 273, no. 2, pp. 547-55.

Bhol, P., Yadav, S., Altaee, A., Saxena, M., Misra, P.K. & Samal, A.K. 2021, 'Graphene-Based Membranes for Water and Wastewater Treatment: A Review', *ACS Applied Nano Materials*.

Bienert, G.P., Schjoerring, J.K. & Jahn, T.P. 2006, 'Membrane transport of hydrogen peroxide', *Biochimica et Biophysica Acta (BBA)-Biomembranes*, vol. 1758, no. 8, pp. 994-1003.

Blandin, G., Verliefde, A.R.D., Tang, C.Y., Childress, A.E. & Le-Clech, P. 2013, 'Validation of assisted forward osmosis (AFO) process: Impact of hydraulic pressure', *Journal of Membrane Science*, vol. 447, pp. 1-11.

Blandin, G., Vervoort, H., Le-Clech, P. & Verliefde, A.R.D. 2016, 'Fouling and cleaning of high permeability forward osmosis membranes', *Journal of Water Process Engineering*, vol. 9, pp. 161-9.

Blanpain-Avet, P., Doubrovine, N., Lafforgue, C. & Lalande, M. 1999, 'The effect of oscillatory flow on crossflow microfiltration of beer in a tubular mineral membrane system – Membrane fouling resistance decrease and energetic considerations', *Journal of Membrane Science*, vol. 152, no. 2, pp. 151-74.

Blume, T. & Neis, U. 2004, 'Improved wastewater disinfection by ultrasonic pre-treatment', *Ultrasonics Sonochemistry*, vol. 11, no. 5, pp. 333-6.

Bogler, A., Lin, S. & Bar-Zeev, E. 2017, 'Biofouling of membrane distillation, forward osmosis and pressure retarded osmosis: Principles, impacts and future directions', *Journal of Membrane Science*, vol. 542, pp. 378-98.

Boo, C., Elimelech, M. & Hong, S. 2013, 'Fouling control in a forward osmosis process integrating seawater desalination and wastewater reclamation', *Journal of Membrane Science*, vol. 444, pp. 148-56.

Boo, C., Khalil, Y.F. & Elimelech, M. 2015, 'Performance evaluation of trimethylamine–carbon dioxide thermolytic draw solution for engineered osmosis', *Journal of Membrane Science*, vol. 473, pp. 302-9.

Boo, C., Lee, S., Elimelech, M., Meng, Z. & Hong, S. 2012, 'Colloidal fouling in forward osmosis: Role of reverse salt diffusion', *Journal of Membrane Science*, vol. 390-391, pp. 277-84.

Brück, A., McCoy, L.L. & Kilway, K.V. 2000, 'Hydrogen Bonds in Carboxylic Acid−Carboxylate Systems in Solution. 1. In Anhydrous, Aprotic Media', *Organic Letters*, vol. 2, no. 14, pp. 2007-9.

Bucs, S.S., Valladares Linares, R., Vrouwenvelder, J.S. & Picioreanu, C. 2016, 'Biofouling in forward osmosis systems: An experimental and numerical study', *Water Research*, vol. 106, pp. 86-97.

Bui, N.-N., Arena, J.T. & McCutcheon, J.R. 2015, 'Proper accounting of mass transfer resistances in forward osmosis: Improving the accuracy of model predictions of structural parameter', *Journal of Membrane Science*, vol. 492, pp. 289-302.

Bush, J.A., Vanneste, J., Gustafson, E.M., Waechter, C.A., Jassby, D., Turchi, C.S. & Cath, T.Y. 2018, 'Prevention and management of silica scaling in membrane distillation using pH adjustment', *Journal of Membrane Science*, vol. 554, pp. 366-77.

Cai, W., Liu, J., Zhang, X., Ng, W.J. & Liu, Y. 2016, 'Generation of dissolved organic matter and byproducts from activated sludge during contact with sodium hypochlorite and its implications to on-line chemical cleaning in MBR', *Water Research*, vol. 104, pp. 44-52.

Cai, Y. & Hu, X.M. 2016, 'A critical review on draw solutes development for forward osmosis', *Desalination*, vol. 391, pp. 16-29.

Calace, N., Liberatori, A., Petronio, B. & Pietroletti, M. 2001a, 'Characteristics of different molecular weight fractions of organic matter in landfill leachate and their role in soil sorption of heavy metals', *Environmental pollution*, vol. 113, no. 3, pp. 331-9.

Calace, N., Liberatori, A., Petronio, B.M. & Pietroletti, M. 2001b, 'Characteristics of different molecular weight fractions of organic matter in landfill leachate and their role in soil sorption of heavy metals', *Environmental Pollution*, vol. 113, no. 3, pp. 331-9.

Camilleri-Rumbau, M., Masse, L., Dubreuil, J., Mondor, M., Christensen, K.V. & Norddahl, B. 2016, 'Fouling of a spiral-wound reverse osmosis membrane processing swine wastewater: effect of cleaning procedure on fouling resistance', *Environmental technology*, vol. 37, no. 13, pp. 1704-15.

Cath, T., Childress, A. & Elimelech, M. 2006a, 'Forward osmosis: Principles, applications, and recent developments', *Journal of Membrane Science*, vol. 281, no. 1-2, pp. 70-87.

Cath, T.Y., Childress, A.E. & Elimelech, M. 2006b, 'Forward osmosis: Principles, applications, and recent developments', *Journal of Membrane Science*, vol. 281, no. 1, pp. 70-87.

Cen, J., Vukas, M., Barton, G., Kavanagh, J. & Coster, H.G.L. 2015, 'Real time fouling monitoring with Electrical Impedance Spectroscopy', *Journal of Membrane Science*, vol. 484, pp. 133-9.

Chambliss, W.G., Cleary, R.W., Fischer, R., Jones, A.B., Skierkowski, P., Nicholes, W. & Kibbe, A.H. 1981, 'Effect of docusate sodium on drug release from a controlled-release dosage form', *J Pharm Sci*, vol. 70, no. 11, pp. 1248-51.

Chanukya, B.S., Patil, S. & Rastogi, N.K. 2013, 'Influence of concentration polarization on flux behavior in forward osmosis during desalination using ammonium bicarbonate', *Desalination*, vol. 312, pp. 39-44.

Chen, M.-Y., Lee, D.-J., Yang, Z., Peng, X.F. & Lai, J.Y. 2006, 'Fluorecent Staining for Study of Extracellular Polymeric Substances in Membrane Biofouling Layers', *Environmental Science & Technology*, vol. 40, no. 21, pp. 6642-6.

Chiao, Y.-H., Sengupta, A., Chen, S.-T., Huang, S.-H., Hu, C.-C., Hung, W.-S., Chang, Y., Qian, X., Wickramasinghe, S.R., Lee, K.-R. & Lai, J.-Y. 2019, 'Zwitterion augmented polyamide membrane for improved forward osmosis performance with significant antifouling characteristics', *Separation and Purification Technology*, vol. 212, pp. 316-25.

Choi, H.-g., Shah, A.A., Nam, S.-E., Park, Y.-I. & Park, H. 2019, 'Thin-film composite membranes comprising ultrathin hydrophilic polydopamine interlayer with graphene oxide for forward osmosis', *Desalination*, vol. 449, pp. 41-9.

Choi, Y.-J., Kim, S.-H., Jeong, S. & Hwang, T.-M. 2014, 'Application of ultrasound to mitigate calcium sulfate scaling and colloidal fouling', *Desalination*, vol. 336, pp. 153-9.

Choi, Y., Hwang, T.M., Jeong, S. & Lee, S. 2018, 'The use of ultrasound to reduce internal concentration polarization in forward osmosis', *Ultrason Sonochem*, vol. 41, pp. 475-83.

Chou, S., Shi, L., Wang, R., Tang, C.Y., Qiu, C. & Fane, A.G. 2010, 'Characteristics and potential applications of a novel forward osmosis hollow fiber membrane', *Desalination*, vol. 261, no. 3, pp. 365-72.

Chun, Y., Mulcahy, D., Zou, L. & Kim, I.S. 2017, 'A Short Review of Membrane Fouling in Forward Osmosis Processes', *Membranes (Basel)*, vol. 7, no. 2.

Chun, Y., Qing, L., Sun, G., Bilad, M.R., Fane, A.G. & Chong, T.H. 2018, 'Prototype aquaporin-based forward osmosis membrane: Filtration properties and fouling resistance', *Desalination*, vol. 445, pp. 75-84.

Chung, T.-S., Zhang, S., Wang, K.Y., Su, J. & Ling, M.M. 2012, 'Forward osmosis processes: Yesterday, today and tomorrow', *Desalination*, vol. 287, pp. 78-81.

Coday, B.D., Almaraz, N. & Cath, T.Y. 2015, 'Forward osmosis desalination of oil and gas wastewater: Impacts of membrane selection and operating conditions on process performance', *Journal of Membrane Science*, vol. 488, pp. 40-55.

Coday, B.D., Xu, P., Beaudry, E.G., Herron, J., Lampi, K., Hancock, N.T. & Cath, T.Y. 2014, 'The sweet spot of forward osmosis: Treatment of produced water, drilling wastewater, and other complex and difficult liquid streams', *Desalination*, vol. 333, no. 1, pp. 23-35.

Collins, K.D. 1997, 'Charge density-dependent strength of hydration and biological structure', *Biophysical journal*, vol. 72, no. 1, pp. 65-76.

Combe, C., Molis, E., Lucas, P., Riley, R. & Clark, M.M. 1999, 'The effect of CA membrane properties on adsorptive fouling by humic acid', *Journal of Membrane Science*, vol. 154, no. 1, pp. 73-87.

Cornel, P.K., Summers, R.S. & Roberts, P.V. 1986, 'Diffusion of humic acid in dilute aqueous solution', *Journal of Colloid and Interface Science*, vol. 110, no. 1, pp. 149-64.

Cornelissen, E., Harmsen, D., Beerendonk, E., Qin, J., Oo, H., De Korte, K. & Kappelhof, J. 2011, 'The innovative osmotic membrane bioreactor (OMBR) for reuse of wastewater', *Water Science and Technology*, vol. 63, no. 8, pp. 1557-65.

Cornelissen, E., Harmsen, D., De Korte, K., Ruiken, C., Qin, J.-J., Oo, H. & Wessels, L. 2008a, 'Membrane fouling and process performance of forward osmosis membranes on activated sludge', *Journal of Membrane Science*, vol. 319, no. 1-2, pp. 158-68.

Cornelissen, E.R., Harmsen, D., de Korte, K.F., Ruiken, C.J., Qin, J.-J., Oo, H. & Wessels, L.P. 2008b, 'Membrane fouling and process performance of forward osmosis membranes on activated sludge', *Journal of Membrane Science*, vol. 319, no. 1, pp. 158-68.

Cornelissen, E.R., Vrouwenvelder, J.S., Heijman, S.G.J., Viallefont, X.D., Van Der Kooij, D. & Wessels, L.P. 2007, 'Periodic air/water cleaning for control of biofouling in spiral wound membrane elements', *Journal of Membrane Science*, vol. 287, no. 1, pp. 94-101.

Corzo, B., de la Torre, T., Sans, C., Ferrero, E. & Malfeito, J.J. 2017, 'Evaluation of draw solutions and commercially available forward osmosis membrane modules for wastewater reclamation at pilot scale', *Chemical Engineering Journal*, vol. 326, pp. 1-8.

Creber, S.A., Pintelon, T.R.R., Graf von der Schulenburg, D.A.W., Vrouwenvelder, J.S., van Loosdrecht, M.C.M. & Johns, M.L. 2010, 'Magnetic resonance imaging and 3D simulation studies of biofilm accumulation and cleaning on reverse osmosis membranes', *Food and Bioproducts Processing*, vol. 88, no. 4, pp. 401-8.

Croué, J.-P., Benedetti, M., Violleau, D. & Leenheer, J. 2003, 'Characterization and copper binding of humic and nonhumic organic matter isolated from the South Platte River: evidence for the presence of nitrogenous binding site', *Environmental Science & Technology*, vol. 37, no. 2, pp. 328-36.

Cui, Y., Ge, Q., Liu, X.-Y. & Chung, T.-S. 2014, 'Novel forward osmosis process to effectively remove heavy metal ions', *Journal of Membrane Science*, vol. 467, pp. 188-94.

D'Haese, A., Le-Clech, P., Van Nevel, S., Verbeken, K., Cornelissen, E.R., Khan, S.J. & Verliefde, A.R.D. 2013, 'Trace organic solutes in closed-loop forward osmosis applications: Influence of membrane fouling and modeling of solute build-up', *Water Research*, vol. 47, no. 14, pp. 5232-44.

D'souza, N. & Mawson, A. 2005, 'Membrane cleaning in the dairy industry: a review', *Critical reviews in food science and nutrition*, vol. 45, no. 2, pp. 125-34.

Danley-Thomson, A., Worley-Morse, T., Contreras, S.U.J., Herman, S., Brawley, A. & Karcher, K. 2020, 'Determining the effects of Class I landfill leachate on biological nutrient removal in wastewater treatment', *Journal of Environmental Management*, vol. 275, p. 111198.

Dean, J.A. 1999, *Lange's handbook of chemistry*, New york; London: McGraw-Hill, Inc.

Delaunay, D., Rabiller-Baudry, M., Gozálvez-Zafrilla, J.M., Balannec, B., Frappart, M. & Paugam, L. 2008, 'Mapping of protein fouling by FTIR-ATR as experimental tool to study membrane fouling and fluid velocity profile in various geometries and validation by CFD simulation', *Chemical Engineering and Processing: Process Intensification*, vol. 47, no. 7, pp. 1106-17.

Déon, S., Dutournié, P., Fievet, P., Limousy, L. & Bourseau, P. 2013, 'Concentration polarization phenomenon during the nanofiltration of multi-ionic solutions: Influence of the filtrated solution and operating conditions', *Water Research*, vol. 47, no. 7, pp. 2260-72.

Di Bella, G. & Di Trapani, D. 2019, 'A Brief Review on the Resistance-in-Series Model in Membrane Bioreactors (MBRs)', *Membranes*, vol. 9, no. 2, p. 24.

Distefano, T. & Kelly, S. 2017, 'Are we in deep water? Water scarcity and its limits to economic growth', *Ecological Economics*, vol. 142, pp. 130-47.

Dong, Y., Wang, Z., Zhu, C., Wang, Q., Tang, J. & Wu, Z. 2014, 'A forward osmosis membrane system for the post-treatment of MBR-treated landfill leachate', *Journal of Membrane Science*, vol. 471, pp. 192-200.

Du, X., Wang, Y., Qu, F., Li, K., Liu, X., Wang, Z., Li, G. & Liang, H. 2017, 'Impact of bubbly flow in feed channel of forward osmosis for wastewater treatment: Flux performance and biofouling', *Chemical Engineering Journal*, vol. 316, pp. 1047-58.

Dutta, S. & Nath, K. 2018, 'Feasibility of forward osmosis using ultra low pressure RO membrane and Glauber salt as draw solute for wastewater treatment', *Journal of Environmental Chemical Engineering*.

Emadzadeh, D., Lau, W.J., Matsuura, T., Rahbari-Sisakht, M. & Ismail, A.F. 2014, 'A novel thin film composite forward osmosis membrane prepared from PSf–TiO2 nanocomposite substrate for water desalination', *Chemical Engineering Journal*, vol. 237, pp. 70-80.

'<Energy issues in Desalination processes . Critical Review , R. Semiat.pdf>'.

Espinasse, B., Bacchin, P. & Aimar, P. 2002, 'On an experimental method to measure critical flux in ultrafiltration', *Desalination*, vol. 146, no. 1, pp. 91-6.

Fam, W., Phuntsho, S., Lee, J.H. & Shon, H.K. 2013, 'Performance comparison of thin-film composite forward osmosis membranes', *Desalination and Water Treatment*, vol. 51, no. 31-33, pp. 6274-80.

Fan, L., Harris, J.L., Roddick, F.A. & Booker, N.A. 2001, 'Influence of the characteristics of natural organic matter on the fouling of microfiltration membranes', *Water Research*, vol. 35, no. 18, pp. 4455-63.

Fane, T. 2016, 'Inorganic Scaling', in E. Drioli & L. Giorno (eds), *Encyclopedia of Membranes*, Springer Berlin Heidelberg, Berlin, Heidelberg, pp. 1-2.

Farooque, A.M., Al-Amoudi, A. & Numata, K. 1999, 'Degradation study of cellulose triacetate hollow fine-fiber SWRO membranes', *Desalination*, vol. 123, no. 2, pp. 165-71.

Ferraz, F.M., Povinelli, J., Pozzi, E., Vieira, E.M. & Trofino, J.C. 2014, 'Co-treatment of landfill leachate and domestic wastewater using a submerged aerobic biofilter', *Journal of Environmental Management*, vol. 141, pp. 9-15.

Först, C., Stieglitz, L., Roth, W. & Kuhnmünch, S. 1989, 'Quantitative analysis of volatile organic compounds in landfill leachates', *International journal of environmental analytical chemistry*, vol. 37, no. 4, pp. 287-93.

Fortunato, L., Bucs, S., Linares, R.V., Cali, C., Vrouwenvelder, J.S. & Leiknes, T. 2017, 'Spatially-resolved in-situ quantification of biofouling using optical coherence tomography (OCT) and 3D image analysis in a spacer filled channel', *Journal of Membrane Science*, vol. 524, pp. 673-81.

Fridjonsson, E.O., Vogt, S.J., Vrouwenvelder, J.S. & Johns, M.L. 2015, 'Early non-destructive biofouling detection in spiral wound RO membranes using a mobile earth′s field NMR', *Journal of Membrane Science*, vol. 489, pp. 227-36.

Fritzmann, C., Löwenberg, J., Wintgens, T. & Melin, T. 2007, 'State-of-the-art of reverse osmosis desalination', *Desalination*, vol. 216, no. 1-3, pp. 1-76.

Fytianos, K., Voudrias, E. & Raikos, N. 1998, 'Modelling of phosphorus removal from aqueous and wastewater samples using ferric iron', *Environmental Pollution*, vol. 101, no. 1, pp. 123-30.

Gahleitner, B., Loderer, C., Saracino, C., Pum, D. & Fuchs, W. 2014, 'Chemical foam cleaning as an efficient alternative for flux recovery in ultrafiltration processes', *Journal of Membrane Science*, vol. 450, pp. 433-9.

Gai, J.-G. & Gong, X.-L. 2014, 'Zero internal concentration polarization FO membrane: functionalized graphene', *Journal of Materials Chemistry A*, vol. 2, no. 2, pp. 425-9.

Gan, Q., Howell, J., Field, R., England, R., Bird, M. & McKechinie, M. 1999, 'Synergetic cleaning procedure for a ceramic membrane fouled by beer microfiltration', *Journal of membrane Science*, vol. 155, no. 2, pp. 277-89.

Ge, Q., Amy, G.L. & Chung, T.-S. 2017, 'Forward osmosis for oily wastewater reclamation: Multi-charged oxalic acid complexes as draw solutes', *Water Research*, vol. 122, pp. 580-90.

Ge, Q., Wang, P., Wan, C. & Chung, T.-S. 2012, 'Polyelectrolyte-Promoted Forward Osmosis–Membrane Distillation (FO–MD) Hybrid Process for Dye Wastewater Treatment', *Environmental Science & Technology*, vol. 46, no. 11, pp. 6236-43.

Gebreyohannes, A.Y., Curcio, E., Poerio, T., Mazzei, R., Di Profio, G., Drioli, E. & Giorno, L. 2015, 'Treatment of Olive Mill Wastewater by Forward Osmosis', *Separation and Purification Technology*, vol. 147, pp. 292-302.

Ghanbari, F., Wu, J., Khatebasreh, M., Ding, D. & Lin, K.-Y.A. 2020, 'Efficient treatment for landfill leachate through sequential electrocoagulation, electrooxidation and PMS/UV/CuFe2O4 process', *Separation and Purification Technology*, vol. 242, p. 116828.

Gilron, J. 2014, 'Water-energy nexus matching source'.

Gorzalski, A.S. & Coronell, O. 2014, 'Fouling of nanofiltration membranes in full- and bench-scale systems treating groundwater containing silica', *Journal of Membrane Science*, vol. 468, pp. 349-59.

Götz, R. 1986, 'Chlorinated dioxins and dibenzofurans in leachate and sediments of the sanitary landfill in Hamburg-Georgswerder', *Chemosphere*, vol. 15, no. 9, pp. 1981-4.

Goulter, R.M., Gentle, I.R. & Dykes, G.A. 2009, 'Issues in determining factors influencing bacterial attachment: a review using the attachment of Escherichia coli to abiotic surfaces as an example', *Letters in Applied Microbiology*, vol. 49, no. 1, pp. 1-7.

Graf von der Schulenburg, D.A., Vrouwenvelder, J.S., Creber, S.A., van Loosdrecht, M.C.M. & Johns, M.L. 2008, 'Nuclear magnetic resonance microscopy studies of membrane biofouling', *Journal of Membrane Science*, vol. 323, no. 1, pp. 37-44.

Gray, G.T., McCutcheon, J.R. & Elimelech, M. 2006, 'Internal concentration polarization in forward osmosis: role of membrane orientation', *Desalination*, vol. 197, no. 1-3, pp. 1-8.

Gruber, M.F., Johnson, C.J., Tang, C.Y., Jensen, M.H., Yde, L. & Hélix-Nielsen, C. 2011, 'Computational fluid dynamics simulations of flow and concentration polarization in forward osmosis membrane systems', *Journal of Membrane Science*, vol. 379, no. 1, pp. 488-95.

Gu, Y., Wang, Y.-N., Wei, J. & Tang, C.Y. 2013, 'Organic fouling of thin-film composite polyamide and cellulose triacetate forward osmosis membranes by oppositely charged macromolecules', *Water Research*, vol. 47, no. 5, pp. 1867-74.

Guide, W.T. 2007, *Nominal Rejection Characteristics of Thin Film Composite Reverse Osmosis Membranes*, Water Treatment Guide, viewed 24 2020, <https://www.watertreatmentguide.com/Membrane_Rejection.htm#Cellulose%20Triacetate>.

Guo, H., Yao, Z., Wang, J., Yang, Z., Ma, X. & Tang, C.Y. 2018, 'Polydopamine coating on a thin film composite forward osmosis membrane for enhanced mass transport and antifouling performance', *Journal of Membrane Science*, vol. 551, pp. 234-42.

Gwak, G. & Hong, S. 2017, 'New approach for scaling control in forward osmosis (FO) by using an antiscalant-blended draw solution', *Journal of Membrane Science*, vol. 530, pp. 95-103.

Gwak, G., Kim, D.I. & Hong, S. 2018, 'New industrial application of forward osmosis (FO): Precious metal recovery from printed circuit board (PCB) plant wastewater', *Journal of Membrane Science*, vol. 552, pp. 234-42.

Hagmeyer, G. & Gimbel, R. 1998, 'Modelling the salt rejection of nanofiltration membranes for ternary ion mixtures and for single salts at different pH values', *Desalination*, vol. 117, no. 1, pp. 247-56.

Hamdan, M., Sharif, A.O., Derwish, G., Al-Aibi, S. & Altaee, A. 2015, 'Draw solutions for Forward Osmosis process: Osmotic pressure of binary and ternary aqueous solutions of magnesium chloride, sodium chloride, sucrose and maltose', *Journal of Food Engineering*, vol. 155, pp. 10-5.

Han, G., Chung, T.-S., Toriida, M. & Tamai, S. 2012, 'Thin-film composite forward osmosis membranes with novel hydrophilic supports for desalination', *Journal of Membrane Science*, vol. 423-424, pp. 543-55.

Han, G., de Wit, J.S. & Chung, T.-S. 2015, 'Water reclamation from emulsified oily wastewater via effective forward osmosis hollow fiber membranes under the PRO mode', *Water Research*, vol. 81, pp. 54-63.

Han, G., Liang, C.-Z., Chung, T.-S., Weber, M., Staudt, C. & Maletzko, C. 2016, 'Combination of forward osmosis (FO) process with coagulation/flocculation (CF) for potential treatment of textile wastewater', *Water Research*, vol. 91, pp. 361-70.

Hancock, N.T., Black, N.D. & Cath, T.Y. 2012, 'A comparative life cycle assessment of hybrid osmotic dilution desalination and established seawater desalination and wastewater reclamation processes', *Water Research*, vol. 46, no. 4, pp. 1145-54.

Hancock, N.T. & Cath, T.Y. 2009, 'Solute Coupled Diffusion in Osmotically Driven Membrane Processes', *Environmental Science & Technology*, vol. 43, no. 17, pp. 6769-75.

Hancock, N.T., Xu, P., Roby, M.J., Gomez, J.D. & Cath, T.Y. 2013, 'Towards direct potable reuse with forward osmosis: Technical assessment of long-term process performance at the pilot scale', *Journal of Membrane Science*, vol. 445, pp. 34-46.

Hatziantoniou, D. & Howell, J.A. 2002, 'Influence of the properties and characteristics of sugar-beet pulp extract on its fouling and rejection behaviour during membrane filtration', *Desalination*, vol. 148, no. 1, pp. 67-72.

Hausman, R., Gullinkala, T. & Escobar, I.C. 2009, 'Development of low-biofouling polypropylene feedspacers for reverse osmosis', *Journal of applied polymer science*, vol. 114, no. 5, pp. 3068-73.

Hawari, A.H., Al-Qahoumi, A., Ltaief, A., Zaidi, S. & Altaee, A. 2018, 'Dilution of seawater using dewatered construction water in a hybrid forward osmosis system', *Journal of Cleaner Production*, vol. 195, pp. 365-73.

Hawari, A.H., Kamal, N. & Altaee, A. 2016, 'Combined influence of temperature and flow rate of feeds on the performance of forward osmosis', *Desalination*, vol. 398, pp. 98-105.

Heikkinen, J., Kyllönen, H., Järvelä, E., Grönroos, A. & Tang, C.Y. 2017, 'Ultrasound-assisted forward osmosis for mitigating internal concentration polarization', *Journal of Membrane Science*, vol. 528, pp. 147-54.

Hey, T., Bajraktari, N., Davidsson, A., Vogel, J., Madsen, H.T., Helix-Nielsen, C., Jansen, J.C. & Jonsson, K. 2018, 'Evaluation of direct membrane filtration and direct forward osmosis as concepts for compact and energy-positive municipal wastewater treatment', *Environ Technol*, vol. 39, no. 3, pp. 264-76.

Hey, T., Bajraktari, N., Vogel, J., Helix Nielsen, C., la Cour Jansen, J. & Jonsson, K. 2017, 'The effects of physicochemical wastewater treatment operations on forward osmosis', *Environ Technol*, vol. 38, no. 17, pp. 2130-42.

Hickenbottom, K.L., Hancock, N.T., Hutchings, N.R., Appleton, E.W., Beaudry, E.G., Xu, P. & Cath, T.Y. 2013, 'Forward osmosis treatment of drilling mud and fracturing wastewater from oil and gas operations', *Desalination*, vol. 312, pp. 60-6.

Ho, J.S., Sim, L.N., Webster, R.D., Viswanath, B., Coster, H.G. & Fane, A.G. 2017, 'Monitoring fouling behavior of reverse osmosis membranes using electrical impedance spectroscopy: A field trial study', *Desalination*, vol. 407, pp. 75-84.

Hoek, E.M.V. & Elimelech, M. 2003, 'Cake-Enhanced Concentration Polarization: A New Fouling Mechanism for Salt-Rejecting Membranes', *Environmental Science & Technology*, vol. 37, no. 24, pp. 5581-8.

Holloway, R.W., Childress, A.E., Dennett, K.E. & Cath, T.Y. 2007, 'Forward osmosis for concentration of anaerobic digester centrate', *Water Research*, vol. 41, no. 17, pp. 4005-14.

Holloway, R.W., Maltos, R., Vanneste, J. & Cath, T.Y. 2015, 'Mixed draw solutions for improved forward osmosis performance', *Journal of Membrane Science*, vol. 491, pp. 121-31.

Hribar, B., Southall, N.T., Vlachy, V. & Dill, K.A. 2002, 'How ions affect the structure of water', *Journal of the American Chemical Society*, vol. 124, no. 41, pp. 12302-11.

HTI 2011, *Oil wastewater treatment & gas wastewater treatment: lead story*, viewed 7/11/2018 2018, <http://www.htiwater.com/divisions/oil-gas/lead_story.html >.

Hu, Z., Antony, A., Leslie, G. & Le-Clech, P. 2014, 'Real-time monitoring of scale formation in reverse osmosis using electrical impedance spectroscopy', *Journal of membrane science*, vol. 453, pp. 320-7.

Huang, J., Luo, J., Chen, X., Feng, S. & Wan, Y. 2020, 'How Do Chemical Cleaning Agents Act on Polyamide Nanofiltration Membrane and Fouling Layer?', *Industrial & Engineering Chemistry Research*, vol. 59, no. 40, pp. 17653-70.

Ibrahim, A. & Yaser, A.Z. 2019, 'Colour removal from biologically treated landfill leachate with tannin-based coagulant', *Journal of Environmental Chemical Engineering*, vol. 7, no. 6, p. 103483.

Ibrar, I., Altaee, A., Zhou, J.L., Naji, O. & Khanafer, D. 2019, 'Challenges and potentials of forward osmosis process in the treatment of wastewater', *Critical Reviews in Environmental Science and Technology*, pp. 1-45.

Ibrar, I., Naji, O., Sharif, A., Malekizadeh, A., Alhawari, A., Alanezi, A.A. & Altaee, A. 2019, 'A Review of Fouling Mechanisms, Control Strategies and Real-Time Fouling Monitoring Techniques in Forward Osmosis', *Water*, vol. 11, no. 4, p. 695.

Ibrar, I., Yadav, S., Altaee, A., Hawari, A., Nguyen, V. & Zhou, J. 2020, 'A novel empirical method for predicting concentration polarization in forward osmosis for single and multicomponent draw solutions', *Desalination*, vol. 494, p. 114668.

Ibrar, I., Yadav, S., Altaee, A., Samal, A.K., Zhou, J.L., Nguyen, T.V. & Ganbat, N. 2020, 'Treatment of biologically treated landfill leachate with forward osmosis: Investigating membrane performance and cleaning protocols', *Science of The Total Environment*, vol. 744, p. 140901.

Ibrar, I., Yadav, S., Ganbat, N., Samal, A.K., Altaee, A., Zhou, J.L. & Nguyen, T.V. 2021, 'Feasibility of H2O2 cleaning for forward osmosis membrane treating landfill leachate', *Journal of Environmental Management*, vol. 294, p. 113024.

Irvine, G.J., Rajesh, S., Georgiadis, M. & Phillip, W.A. 2013, 'Ion Selective Permeation Through Cellulose Acetate Membranes in Forward Osmosis', *Environmental Science & Technology*, vol. 47, no. 23, pp. 13745-53.

Iskander, S.M., Novak, J.T. & He, Z. 2018, 'Enhancing forward osmosis water recovery from landfill leachate by desalinating brine and recovering ammonia in a microbial desalination cell', *Bioresource Technology*, vol. 255, pp. 76-82.

Iskander, S.M., Novak, J.T. & He, Z. 2019, 'Reduction of reagent requirements and sludge generation in Fenton's oxidation of landfill leachate by synergistically incorporating forward osmosis and humic acid recovery', *Water Research*, vol. 151, pp. 310-7.

Iskander, S.M., Zou, S., Brazil, B., Novak, J.T. & He, Z. 2017, 'Energy consumption by forward osmosis treatment of landfill leachate for water recovery', *Waste Management*, vol. 63, pp. 284-91.

Islam, M.S., Sultana, S., McCutcheon, J.R. & Rahaman, M.S. 2019, 'Treatment of fracking wastewaters via forward osmosis: Evaluation of suitable organic draw solutions', *Desalination*, vol. 452, pp. 149-58.

Jain, G., Satyanarayan, S., Nawghare, P., Kaul, S.N. & Szpyrcowicz, L. 2001, 'Treatment of pharmaceutical wastewater (herbal) by a coagulation/flocculation process', *International Journal of Environmental Studies*, vol. 58, no. 3, pp. 313-30.

Jamil, S., Loganathan, P., Kazner, C. & Vigneswaran, S. 2015, 'Forward osmosis treatment for volume minimisation of reverse osmosis concentrate from a water reclamation plant and removal of organic micropollutants', *Desalination*, vol. 372, pp. 32-8.

Jarusutthirak, C., Amy, G. & Croué, J.-P. 2002, 'Fouling characteristics of wastewater effluent organic matter (EfOM) isolates on NF and UF membranes', *Desalination*, vol. 145, no. 1, pp. 247-55.

Jawad, J., Hawari, A.H. & Zaidi, S. 2020, 'Modeling of forward osmosis process using artificial neural networks (ANN) to predict the permeate flux', *Desalination*, vol. 484, p. 114427.

Jiang, S., Li, Y. & Ladewig, B.P. 2017, 'A review of reverse osmosis membrane fouling and control strategies', *Science of The Total Environment*, vol. 595, pp. 567-83.

Jin, X., She, Q., Ang, X. & Tang, C.Y. 2012, 'Removal of boron and arsenic by forward osmosis membrane: Influence of membrane orientation and organic fouling', *Journal of Membrane Science*, vol. 389, pp. 182-7.

Jin, X., Tang, C.Y., Gu, Y., She, Q. & Qi, S. 2011, 'Boric Acid Permeation in Forward Osmosis Membrane Processes: Modeling, Experiments, and Implications', *Environmental Science & Technology*, vol. 45, no. 6, pp. 2323-30.

Johnson, D.J., Suwaileh, W.A., Mohammed, A.W. & Hilal, N. 2018, 'Osmotic's potential: An overview of draw solutes for forward osmosis', *Desalination*, vol. 434, pp. 100-20.

Jones, K.L. & O'Melia, C.R. 2000, 'Protein and humic acid adsorption onto hydrophilic membrane surfaces: effects of pH and ionic strength', *Journal of Membrane Science*, vol. 165, no. 1, pp. 31-46.

Jung, D.H., Lee, J., Kim, D.Y., Lee, Y.G., Park, M., Lee, S., Yang, D.R. & Kim, J.H. 2011, 'Simulation of forward osmosis membrane process: Effect of membrane orientation and flow direction of feed and draw solutions', *Desalination*, vol. 277, no. 1, pp. 83-91.

Kalafatakis, S., Braekevelt, S., Carlsen, V., Lange, L., Skiadas, I.V. & Gavala, H.N. 2017, 'On a novel strategy for water recovery and recirculation in biorefineries through application of forward osmosis membranes', *Chemical Engineering Journal*, vol. 311, pp. 209-16.

Kang, K.-H., Shin, H.S. & Park, H. 2002, 'Characterization of humic substances present in landfill leachates with different landfill ages and its implications', *Water research*, vol. 36, no. 16, pp. 4023-32.

Karageorgiou, K., Paschalis, M. & Anastassakis, G.N. 2007, 'Removal of phosphate species from solution by adsorption onto calcite used as natural adsorbent', *Journal of Hazardous Materials*, vol. 139, no. 3, pp. 447-52.

Kasahara, S., Maeda, K. & Ishikawa, M. 2004, 'Influence of phosphorus on biofilm accumulation in drinking water distribution systems', *Water science and Technology: water supply*, vol. 4, no. 5-6, pp. 389-98.

Kavanagh, J., Hussain, S., Handelsman, T., Chilcott, T. & Coster, H. 2008, 'Characterisation of Fouled and Cleaned Industrial Reverse Osmosis Membranes by Electrical Impedance Spectroscopy', *Chemeca 2008: Towards a Sustainable Australasia*, p. 202.

Kavanagh, J.M., Hussain, S., Chilcott, T.C. & Coster, H.G.L. 2009, 'Fouling of reverse osmosis membranes using electrical impedance spectroscopy: Measurements and simulations', *Desalination*, vol. 236, no. 1, pp. 187-93.

Kesting, R.E. 1965, 'Semipermeable membranes of cellulose acetate for desalination in the process of reverse osmosis. I. Lyotropic swelling of secondary cellulose acetate', *Journal of Applied Polymer Science*, vol. 9, no. 2, pp. 663-88.

Khorshidi, B., Bhinder, A., Thundat, T., Pernitsky, D. & Sadrzadeh, M. 2016, 'Developing high throughput thin film composite polyamide membranes for forward osmosis treatment of SAGD produced water', *Journal of Membrane Science*, vol. 511, pp. 29-39.

Kim, C.-M., Kim, S.-J., Kim, L.H., Shin, M.S., Yu, H.-W. & Kim, I.S. 2014, 'Effects of phosphate limitation in feed water on biofouling in forward osmosis (FO) process', *Desalination*, vol. 349, pp. 51-9.

Kim, J.E., Phuntsho, S., Lotfi, F. & Shon, H.K. 2015, 'Investigation of pilot-scale 8040 FO membrane module under different operating conditions for brackish water desalination', *Desalination and Water Treatment*, vol. 53, no. 10, pp. 2782-91.

Kim, Y., Elimelech, M., Shon, H.K. & Hong, S. 2014, 'Combined organic and colloidal fouling in forward osmosis: Fouling reversibility and the role of applied pressure', *Journal of Membrane Science*, vol. 460, pp. 206-12.

Kim, Y., Li, S. & Ghaffour, N. 2020, 'Evaluation of different cleaning strategies for different types of forward osmosis membrane fouling and scaling', *Journal of Membrane Science*, vol. 596, p. 117731.

Kochkodan, V., Johnson, D.J. & Hilal, N. 2014, 'Polymeric membranes: Surface modification for minimizing (bio)colloidal fouling', *Advances in Colloid and Interface Science*, vol. 206, pp. 116-40.

Korenak, J., Basu, S., Balakrishnan, M., Hélix-Nielsen, C. & Petrinic, I. 2017, 'Forward Osmosis in Wastewater Treatment Processes', *Acta Chimica Slovenica*, pp. 83-94.

Korenak, J., Hélix-Nielsen, C., Bukšek, H. & Petrinić, I. 2019, 'Efficiency and economic feasibility of forward osmosis in textile wastewater treatment', *Journal of Cleaner Production*, vol. 210, pp. 1483-95.

Kragl, U. 1997, 'Basic Principles of Membrane Technology. (2. Aufl.) Von M. Mulder. Kluwer Academic Publishers, Dordrecht, 1996. 564 S., geb. 174.00 £.—ISBN 0–7923–4247-X', *Angewandte Chemie*, vol. 109, no. 12, pp. 1420-1.

Kumar, R. & Ismail, A.F. 2015, 'Fouling control on microfiltration/ultrafiltration membranes: Effects of morphology, hydrophilicity, and charge', *Journal of Applied Polymer Science*, vol. 132, no. 21.

Kurtoğlu Akkaya, G. & Bilgili, M.S. 2020, 'Evaluating the performance of an electro-membrane bioreactor in treatment of young leachate', *Journal of Environmental Chemical Engineering*, vol. 8, no. 4, p. 104017.

Kwan, S.E., Bar-Zeev, E. & Elimelech, M. 2015, 'Biofouling in forward osmosis and reverse osmosis: Measurements and mechanisms', *Journal of Membrane Science*, vol. 493, pp. 703-8.

Kwon, S.J., Park, S.-H., Park, M.S., Lee, J.S. & Lee, J.-H. 2017, 'Highly permeable and mechanically durable forward osmosis membranes prepared using polyethylene lithium ion battery separators', *Journal of Membrane Science*, vol. 544, pp. 213-20.

Law, J.Y. & Mohammad, A.W. 2017, 'Multiple-solute salts as draw solution for osmotic concentration of succinate feed by forward osmosis', *Journal of Industrial and Engineering Chemistry*, vol. 51, pp. 264-70.

Lay, W.C.L., Zhang, J., Tang, C., Wang, R., Liu, Y. & Fane, A.G. 2012, 'Factors affecting flux performance of forward osmosis systems', *Journal of Membrane Science*, vol. 394-395, pp. 151-68.

Lee, J. & Ghaffour, N. 2019, 'Predicting the performance of large-scale forward osmosis module using spatial variation model: Effect of operating parameters including temperature', *Desalination*, vol. 469, p. 114095.

Lee, K.L., Baker, R.W. & Lonsdale, H.K. 1981, 'Membranes for power generation by pressure-retarded osmosis', *Journal of Membrane Science*, vol. 8, no. 2, pp. 141-71.

Lee, M. & Kim, J. 2009, 'Membrane autopsy to investigate CaCO3 scale formation in pilot-scale, submerged membrane bioreactor treating calcium-rich wastewater', *Journal of Chemical Technology & Biotechnology*, vol. 84, no. 9, pp. 1397-404.

Lee, S., Boo, C., Elimelech, M. & Hong, S. 2010, 'Comparison of fouling behavior in forward osmosis (FO) and reverse osmosis (RO)', *Journal of Membrane Science*, vol. 365, no. 1-2, pp. 34-9.

Lee, S. & Elimelech, M. 2006, 'Relating Organic Fouling of Reverse Osmosis Membranes to Intermolecular Adhesion Forces', *Environmental Science & Technology*, vol. 40, no. 3, pp. 980-7.

Lee , S., Kim, Y., Park, J., Shon, H.K. & Hong, S. 2018, 'Treatment of medical radioactive liquid waste using Forward Osmosis (FO) membrane process', *Journal of Membrane Science*, vol. 556, pp. 238-47.

Lee, S. & Kim, Y.C. 2017, 'Calcium carbonate scaling by reverse draw solute diffusion in a forward osmosis membrane for shale gas wastewater treatment', *Journal of Membrane Science*, vol. 522, pp. 257-66.

Lee, S. & Lee, C.-H. 2000, 'Effect of operating conditions on CaSO4 scale formation mechanism in nanofiltration for water softening', *Water Research*, vol. 34, no. 15, pp. 3854-66.

Lehtola, M.J., Miettinen, I.T., Vartiainen, T., Rantakokko, P., Hirvonen, A. & Martikainen, P.J. 2003, 'Impact of UV disinfection on microbially available phosphorus, organic carbon, and microbial growth in drinking water', *Water Research*, vol. 37, no. 5, pp. 1064-70.

Levitsky, I., Duek, A., Arkhangelsky, E., Pinchev, D., Kadoshian, T., Shetrit, H., Naim, R. & Gitis, V. 2011, 'Understanding the oxidative cleaning of UF membranes', *Journal of Membrane Science*, vol. 377, no. 1, pp. 206-13.

Li, F., Cheng, Q., Tian, Q., Yang, B. & Chen, Q. 2016, 'Biofouling behavior and performance of forward osmosis membranes with bioinspired surface modification in osmotic membrane bioreactor', *Bioresource Technology*, vol. 211, pp. 751-8.

Li, F., Wichmann, K. & Heine, W. 2009, 'Treatment of the methanogenic landfill leachate with thin open channel reverse osmosis membrane modules', *Waste Management*, vol. 29, no. 2, pp. 960-4.

Li, J.-Y., Ni, Z.-Y., Zhou, Z.-Y., Hu, Y.-X., Xu, X.-H. & Cheng, L.-H. 2018, 'Membrane fouling of forward osmosis in dewatering of soluble algal products: Comparison of TFC and CTA membranes', *Journal of Membrane Science*, vol. 552, pp. 213-21.

Li, K., Li, S., Huang, T., Dong, C., Li, J., Zhao, B. & Zhang, S. 2019, 'Chemical Cleaning of Ultrafiltration Membrane Fouled by Humic Substances: Comparison between Hydrogen Peroxide and Sodium Hypochlorite', *International Journal of Environmental Research and Public Health*, vol. 16, no. 14, p. 2568.

Li, M.-N., Sun, X.-F., Wang, L., Wang, S.-Y., Afzal, M.Z., Song, C. & Wang, S.-G. 2018, 'Forward osmosis membranes modified with laminar MoS2 nanosheet to improve desalination performance and antifouling properties', *Desalination*, vol. 436, pp. 107-13.

Li, M., Karanikola, V., Zhang, X., Wang, L. & Elimelech, M. 2018, 'A Self-Standing, Support-Free Membrane for Forward Osmosis with No Internal Concentration Polarization', *Environmental Science & Technology Letters*, vol. 5, no. 5, pp. 266-71.

Li, X., Li, J., Fu, X., Wickramasinghe, R. & Chen, J. 2005, 'Chemical cleaning of PS ultrafilters fouled by the fermentation broth of glutamic acid', *Separation and Purification Technology*, vol. 42, no. 2, pp. 181-7.

Li, Y., Liu, C., Luan, Z., Peng, X., Zhu, C., Chen, Z., Zhang, Z., Fan, J. & Jia, Z. 2006, 'Phosphate removal from aqueous solutions using raw and activated red mud and fly ash', *Journal of Hazardous Materials*, vol. 137, no. 1, pp. 374-83.

Li, Z.-Y., Yangali-Quintanilla, V., Valladares-Linares, R., Li, Q., Zhan, T. & Amy, G. 2012, 'Flux patterns and membrane fouling propensity during desalination of seawater by forward osmosis', *Water Research*, vol. 46, no. 1, pp. 195-204.

Lin, C.-F., Liu, S.-H. & Hao, O.J. 2001, 'Effect of functional groups of humic substances on UF performance', *Water research*, vol. 35, no. 10, pp. 2395-402.

Linares, R.V., Li, Z., Yangali-Quintanilla, V., Li, Q., Vrouwenvelder, J.S., Amy, G.L. & Ghaffour, N. 2016, 'Hybrid SBR–FO system for wastewater treatment and reuse: Operation, fouling and cleaning', *Desalination*, vol. 393, pp. 31-8.

Ling, M.M., Wang, K.Y. & Chung, T.-S. 2010, 'Highly Water-Soluble Magnetic Nanoparticles as Novel Draw Solutes in Forward Osmosis for Water Reuse', *Industrial & Engineering Chemistry Research*, vol. 49, no. 12, pp. 5869-76.

Ling, R., Yu, L., Pham, T.P.T., Shao, J., Chen, J.P. & Reinhard, M. 2017, 'The tolerance of a thin-film composite polyamide reverse osmosis membrane to hydrogen peroxide exposure', *Journal of Membrane Science*, vol. 524, pp. 529-36.

Liu, P., Gao, B., Shon, H.K., Ma, D., Rong, H., Zhao, P., Zhao, S., Yue, Q. & Li, Q. 2014, 'Water flux behavior of blended solutions of ammonium bicarbonate mixed with eight salts respectively as draw solutions in forward osmosis', *Desalination*, vol. 353, pp. 39-47.

Liu, P., Zhang, H., Feng, Y., Shen, C. & Yang, F. 2015, 'Integrating electrochemical oxidation into forward osmosis process for removal of trace antibiotics in wastewater', *J Hazard Mater*, vol. 296, pp. 248-55.

Liu, X. & Ng, H.Y. 2015, 'Fabrication of layered silica–polysulfone mixed matrix substrate membrane for enhancing performance of thin-film composite forward osmosis membrane', *Journal of Membrane Science*, vol. 481, pp. 148-63.

Liu, Y., Chang, S. & Defersha, F.M. 2015, 'Characterization of the proton binding sites of extracellular polymeric substances in an anaerobic membrane bioreactor', *Water Research*, vol. 78, pp. 133-43.

Liu, Y. & Mi, B. 2012, 'Combined fouling of forward osmosis membranes: Synergistic foulant interaction and direct observation of fouling layer formation', *Journal of Membrane Science*, vol. 407-408, pp. 136-44.

Liu, Y. & Mi, B. 2014, 'Effects of organic macromolecular conditioning on gypsum scaling of forward osmosis membranes', *Journal of Membrane Science*, vol. 450, pp. 153-61.

Loeb, S., Titelman, L., Korngold, E. & Freiman, J. 1997, 'Effect of porous support fabric on osmosis through a Loeb-Sourirajan type asymmetric membrane', *Journal of Membrane Science*, vol. 129, no. 2, pp. 243-9.

Lu, P., Liang, S., Zhou, T., Xue, T., Mei, X. & Wang, Q. 2017, 'Layered double hydroxide nanoparticle modified forward osmosis membranes via polydopamine immobilization with significantly enhanced chlorine and fouling resistance', *Desalination*, vol. 421, pp. 99-109.

Luo, W., Xie, M., Hai, F.I., Price, W.E. & Nghiem, L.D. 2016, 'Biodegradation of cellulose triacetate and polyamide forward osmosis membranes in an activated sludge bioreactor: Observations and implications', *Journal of Membrane Science*, vol. 510, pp. 284-92.

Lutchmiah, K., Lauber, L., Roest, K., Harmsen, D.J.H., Post, J.W., Rietveld, L.C., van Lier, J.B. & Cornelissen, E.R. 2014, 'Zwitterions as alternative draw solutions in forward osmosis for application in wastewater reclamation', *Journal of Membrane Science*, vol. 460, pp. 82-90.

Lutchmiah, K., Verliefde, A.R., Roest, K., Rietveld, L.C. & Cornelissen, E.R. 2014, 'Forward osmosis for application in wastewater treatment: a review', *Water Research*, vol. 58, pp. 179-97.

Lv, L., Xu, J., Shan, B. & Gao, C. 2017, 'Concentration performance and cleaning strategy for controlling membrane fouling during forward osmosis concentration of actual oily wastewater', *Journal of Membrane Science*, vol. 523, pp. 15-23.

Madaeni, S.S. & Samieirad, S. 2010, 'Chemical cleaning of reverse osmosis membrane fouled by wastewater', *Desalination*, vol. 257, no. 1, pp. 80-6.

Madsen, H.T., Nissen, S.S., Muff, J. & Søgaard, E.G. 2017, 'Pressure retarded osmosis from hypersaline solutions: investigating commercial FO membranes at high pressures', *Desalination*, vol. 420, pp. 183-90.

Mairal, A.P., Greenberg, A.R., Krantz, W.B. & Bond, L.J. 1999, 'Real-time measurement of inorganic fouling of RO desalination membranes using ultrasonic time-domain reflectometry', *Journal of Membrane Science*, vol. 159, no. 1, pp. 185-96.

Maltos, R.A., Regnery, J., Almaraz, N., Fox, S., Schutter, M., Cath, T.J., Veres, M., Coday, B.D. & Cath, T.Y. 2018, 'Produced water impact on membrane integrity during extended pilot testing of forward osmosis – reverse osmosis treatment', *Desalination*, vol. 440, pp. 99-110.

Mänttäri, M., Martin, H., Nuortila-Jokinen, J. & Nyström, M. 1999, 'Using a spiral wound nanofiltration element for the filtration of paper mill effluents: Pretreatment and fouling', *Advances in Environmental Research*, vol. 3, no. 2, pp. 202-14.

Marañón, E., Castrillón, L., Fernández-Nava, Y., Fernández-Méndez, A. & Fernández-Sánchez, A. 2010, 'Colour, turbidity and COD removal from old landfill leachate by coagulation-flocculation treatment', *Waste management & research*, vol. 28, no. 8, pp. 731-7.

Martinetti, C.R., Childress, A.E. & Cath, T.Y. 2009, 'High recovery of concentrated RO brines using forward osmosis and membrane distillation', *Journal of Membrane Science*, vol. 331, no. 1, pp. 31-9.

Marttinen, S., Kettunen, R., Sormunen, K., Soimasuo, R. & Rintala, J. 2002, 'Screening of physical–chemical methods for removal of organic material, nitrogen and toxicity from low strength landfill leachates', *Chemosphere*, vol. 46, no. 6, pp. 851-8.

Masse, L., Puig-Bargués, J., Mondor, M., Deschênes, L. & Talbot, G. 2015, 'Efficiency of EDTA, SDS, and NaOH solutions to clean RO membranes processing swine wastewater', *Separation Science and Technology*, vol. 50, no. 16, pp. 2509-17.

Matthiasson, E. & Sivik, B. 1980, 'Concentration polarization and fouling', *Desalination*, vol. 35, pp. 59-103.

Mazlan, N.M., Marchetti, P., Maples, H.A., Gu, B., Karan, S., Bismarck, A. & Livingston, A.G. 2016, 'Organic fouling behaviour of structurally and chemically different forward osmosis membranes – A study of cellulose triacetate and thin film composite membranes', *Journal of Membrane Science*, vol. 520, pp. 247-61.

McCutcheon, J.R. & Elimelech, M. 2006a, 'Influence of concentrative and dilutive internal concentration polarization on flux behavior in forward osmosis', *Journal of Membrane Science*, vol. 284, no. 1-2, pp. 237-47.

McCutcheon, J.R. & Elimelech, M. 2006b, 'Influence of concentrative and dilutive internal concentration polarization on flux behavior in forward osmosis', *Journal of Membrane Science*, vol. 284, no. 1, pp. 237-47.

Mccutcheon, J.R. & Elimelech, M. 2007, 'Modeling water flux in forward osmosis: Implications for improved membrane design', *AIChE Journal*, vol. 53, no. 7, pp. 1736-44.

McCutcheon, J.R., McGinnis, R.L. & Elimelech, M. 2005, 'A novel ammonia--carbon dioxide forward (direct) osmosis desalination process ', *Desalination*, vol. 174, pp. 1-11.

McCutcheon, J.R., McGinnis, R.L. & Elimelech, M. 2006a, 'Desalination by ammonia–carbon dioxide forward osmosis: Influence of draw and feed solution concentrations on process performance', *Journal of Membrane Science*, vol. 278, no. 1-2, pp. 114-23.

McCutcheon, J.R., McGinnis, R.L. & Elimelech, M. 2006b, 'Desalination by ammonia–carbon dioxide forward osmosis: Influence of draw and feed solution concentrations on process performance', *Journal of Membrane Science*, vol. 278, no. 1, pp. 114-23.

McGinnis, R.L., Hancock, N.T., Nowosielski-Slepowron, M.S. & McGurgan, G.D. 2013, 'Pilot demonstration of the NH3/CO2 forward osmosis desalination process on high salinity brines', *Desalination*, vol. 312, pp. 67-74.

McGovern, R.K. & Lienhard V, J.H. 2014, 'On the potential of forward osmosis to energetically outperform reverse osmosis desalination', *Journal of Membrane Science*, vol. 469, pp. 245-50.

Medvedev, O. & Shapiro, A. 2005, 'Diffusion coefficients in multicomponent mixtures'.

Meehan, P., Isenhour, J.L., Reeves, R. & Wrenn, K. 2002, 'Ceruminolysis in the pediatric patient: a prospective, double-blinded, randomized controlled trial', *Academic Emergency Medicine*, vol. 9, no. 5, p. 521.

Mi, B. & Elimelech, M. 2008, 'Chemical and physical aspects of organic fouling of forward osmosis membranes', *Journal of Membrane Science*, vol. 320, no. 1-2, pp. 292-302.

Mi, B. & Elimelech, M. 2010a, 'Gypsum Scaling and Cleaning in Forward Osmosis: Measurements and Mechanisms', *Environmental Science & Technology*, vol. 44, no. 6, pp. 2022-8.

Mi, B. & Elimelech, M. 2010b, 'Organic fouling of forward osmosis membranes: Fouling reversibility and cleaning without chemical reagents', *Journal of Membrane Science*, vol. 348, no. 1, pp. 337-45.

Mi, B. & Elimelech, M. 2010c, 'Organic fouling of forward osmosis membranes: fouling reversibility and cleaning without chemical reagents', *Journal of membrane science*, vol. 348, no. 1-2, pp. 337-45.

Mi, B. & Elimelech, M. 2013, 'Silica scaling and scaling reversibility in forward osmosis', *Desalination*, vol. 312, pp. 75-81.

Mohammadi, T., Madaeni, S.S. & Moghadam, M.K. 2003, 'Investigation of membrane fouling', *Desalination*, vol. 153, no. 1, pp. 155-60.

Mondal, S., Field, R.W. & Wu, J.J. 2017, 'Novel approach for sizing forward osmosis membrane systems', *Journal of Membrane Science*, vol. 541, pp. 321-8.

Moody, C.D. & Kessler, J.O. 1976, 'Forward osmosis extractors', *Desalination*, vol. 18, no. 3, pp. 283-95.

Motsa, M.M., Mamba, B.B. & Verliefde, A.R.D. 2018, 'Forward osmosis membrane performance during simulated wastewater reclamation: Fouling mechanisms and fouling layer properties', *Journal of Water Process Engineering*, vol. 23, pp. 109-18.

Mulder, M. & Mulder, J. 1996, *Basic Principles of Membrane Technology*, Springer Science & Business Media.

Myint, A.A., Lee, W., Mun, S., Ahn, C.H., Lee, S. & Yoon, J. 2010, 'Influence of membrane surface properties on the behavior of initial bacterial adhesion and biofilm development onto nanofiltration membranes', *Biofouling*, vol. 26, no. 3, pp. 313-21.

Na, Y., Yang, S. & Lee, S. 2014, 'Evaluation of citrate-coated magnetic nanoparticles as draw solute for forward osmosis', *Desalination*, vol. 347, pp. 34-42.

Nagy, E. 2014, 'A general, resistance-in-series, salt- and water flux models for forward osmosis and pressure-retarded osmosis for energy generation', *Journal of Membrane Science*, vol. 460, pp. 71-81.

Nagy, E., Hegedüs, I., Tow, E.W. & Lienhard V, J.H. 2018, 'Effect of fouling on performance of pressure retarded osmosis (PRO) and forward osmosis (FO)', *Journal of Membrane Science*, vol. 565, pp. 450-62.

Naim, R., Levitsky, I. & Gitis, V. 2012, 'Surfactant cleaning of UF membranes fouled by proteins', *Separation and Purification Technology*, vol. 94, pp. 39-43.

Nataraj, S., Schomäcker, R., Kraume, M., Mishra, I.M. & Drews, A. 2008, 'Analyses of polysaccharide fouling mechanisms during crossflow membrane filtration', *Journal of Membrane Science*, vol. 308, no. 1, pp. 152-61.

Nelson, C. & Ghosh, A. 2011, *Membrane technology for produced water in Lea County*, County Of Lea.

Nguyen, H.T.H. & Min, B. 2020, 'Leachate treatment and electricity generation using an algae-cathode microbial fuel cell with continuous flow through the chambers in series', *Science of The Total Environment*, vol. 723, p. 138054.

Nguyen, N.C., Chen, S.S., Jain, S., Nguyen, H.T., Ray, S.S., Ngo, H.H., Guo, W., Lam, N.T. & Duong, H.C. 2018, 'Exploration of an innovative draw solution for a forward osmosis-membrane distillation desalination process', *Environ Sci Pollut Res Int*, vol. 25, no. 6, pp. 5203-11.

Nguyen, N.C., Duong, H.C., Nguyen, H.T., Chen, S.-S., Le, H.Q., Ngo, H.H., Guo, W., Duong, C.C., Le, N.C. & Bui, X.T. 2020, 'Forward osmosis–membrane distillation hybrid system for desalination using mixed trivalent draw solution', *Journal of Membrane Science*, vol. 603, p. 118029.

Nguyen, N.C., Nguyen, H.T., Ho, S.-T., Chen, S.-S., Ngo, H.H., Guo, W., Ray, S.S. & Hsu, H.-T. 2016, 'Exploring high charge of phosphate as new draw solute in a forward osmosis–

membrane distillation hybrid system for concentrating high-nutrient sludge', *Science of The Total Environment*, vol. 557-558, pp. 44-50.

Nguyen, T.-T., Kook, S., Lee, C., Field, R.W. & Kim, I.S. 2019, 'Critical flux-based membrane fouling control of forward osmosis: Behavior, sustainability, and reversibility', *Journal of Membrane Science*, vol. 570-571, pp. 380-93.

Nguyen, T., Roddick, F.A. & Fan, L. 2012, 'Biofouling of Water Treatment Membranes: A Review of the Underlying Causes, Monitoring Techniques and Control Measures', *Membranes*, vol. 2, no. 4, p. 804.

Ni, T. & Ge, Q. 2018, 'Highly hydrophilic thin-film composition forward osmosis (FO) membranes functionalized with aniline sulfonate/bisulfonate for desalination', *Journal of Membrane Science*, vol. 564, pp. 732-41.

Nicoll, P.G. 2013, 'Forward osmosis—A brief introduction', *Proceedings of the international desalination association world congress on desalination and water reuse, Tianjin, China*, pp. 20-5.

O'Toole, G., Kaplan, H.B. & Kolter, R. 2000, 'Biofilm formation as microbial development', *Annual Reviews in Microbiology*, vol. 54, no. 1, pp. 49-79.

Ochando-Pulido, J.M., Victor-Ortega, M.D. & Martínez-Ferez, A. 2015, 'On the cleaning procedure of a hydrophilic reverse osmosis membrane fouled by secondary-treated olive mill wastewater', *Chemical Engineering Journal*, vol. 260, pp. 142-51.

Ozaki, H., Sharma, K. & Saktaywin, W. 2002, 'Performance of an ultra-low-pressure reverse osmosis membrane (ULPROM) for separating heavy metal: effects of interference parameters', *Desalination*, vol. 144, no. 1, pp. 287-94.

Pan, S.-F., Zhu, M.-P., Chen, J.P., Yuan, Z.-H., Zhong, L.-B. & Zheng, Y.-M. 2015, 'Separation of tetracycline from wastewater using forward osmosis process with thin film composite membrane – Implications for antibiotics recovery', *Separation and Purification Technology*, vol. 153, pp. 76-83.

Parida, V. & Ng, H.Y. 2013, 'Forward osmosis organic fouling: Effects of organic loading, calcium and membrane orientation', *Desalination*, vol. 312, pp. 88-98.

Park, J., Jeong, K., Baek, S., Park, S., Ligaray, M., Chong, T.H. & Cho, K.H. 2019, 'Modeling of NF/RO membrane fouling and flux decline using real-time observations', *Journal of Membrane Science*, vol. 576, pp. 66-77.

Park, J., Jeong, W., Nam, J., Kim, J., Kim, J., Chon, K., Lee, E., Kim, H. & Jang, A. 2014, 'An analysis of the effects of osmotic backwashing on the seawater reverse osmosis process', *Environmental Technology*, vol. 35, no. 12, pp. 1455-61.

Park, M.J., Gonzales, R.R., Abdel-Wahab, A., Phuntsho, S. & Shon, H.K. 2018, 'Hydrophilic polyvinyl alcohol coating on hydrophobic electrospun nanofiber membrane for high performance thin film composite forward osmosis membrane', *Desalination*, vol. 426, pp. 50-9.

Pawley, J.B. 2006, 'Fundamental limits in confocal microscopy', *Handbook of biological confocal microscopy*, Springer, pp. 20-42.

Peng, Y. 2017, 'Perspectives on technology for landfill leachate treatment', *Arabian Journal of Chemistry*, vol. 10, pp. S2567-S74.

Phillip, W.A., Yong, J.S. & Elimelech, M. 2010, 'Reverse Draw Solute Permeation in Forward Osmosis: Modeling and Experiments', *Environmental Science & Technology*, vol. 44, no. 13, pp. 5170-6.

Phuntsho, S., Kim, J.E., Johir, M.A.H., Hong, S., Li, Z., Ghaffour, N., Leiknes, T. & Shon, H.K. 2016, 'Fertiliser drawn forward osmosis process: Pilot-scale desalination of mine impaired water for fertigation', *Journal of Membrane Science*, vol. 508, pp. 22-31.

Phuntsho, S., Sahebi, S., Majeed, T., Lotfi, F., Kim, J.E. & Shon, H.K. 2013, 'Assessing the major factors affecting the performances of forward osmosis and its implications on the desalination process', *Chemical Engineering Journal*, vol. 231, pp. 484-96.

Phuntsho, S., Shon, H.K., Hong, S., Lee, S. & Vigneswaran, S. 2011, 'A novel low energy fertilizer driven forward osmosis desalination for direct fertigation: Evaluating the performance of fertilizer draw solutions', *Journal of Membrane Science*, vol. 375, no. 1-2, pp. 172-81.

Phuntsho, S., Shon, H.K., Majeed, T., El Saliby, I., Vigneswaran, S., Kandasamy, J., Hong, S. & Lee, S. 2012, 'Blended Fertilizers as Draw Solutions for Fertilizer-Drawn Forward Osmosis Desalination', *Environmental Science & Technology*, vol. 46, no. 8, pp. 4567-75.

Pradhan, J., Das, J., Das, S. & Thakur, R.S. 1998, 'Adsorption of Phosphate from Aqueous Solution Using Activated Red Mud', *Journal of Colloid and Interface Science*, vol. 204, no. 1, pp. 169-72.

Puguan, J.M.C., Kim, H.-S., Lee, K.-J. & Kim, H. 2014, 'Low internal concentration polarization in forward osmosis membranes with hydrophilic crosslinked PVA nanofibers as porous support layer', *Desalination*, vol. 336, pp. 24-31.

Qin, J.J., Kekre, K.A., Oo, M.H., Tao, G., Lay, C.L., Lew, C.H., Cornelissen, E.R. & Ruiken, C.J. 2010, 'Preliminary study of osmotic membrane bioreactor: effects of draw solution on water flux and air scouring on fouling', *Water Sci Technol*, vol. 62, no. 6, pp. 1353-60.

Qiu, G. & Ting, Y.-P. 2014, 'Short-term fouling propensity and flux behavior in an osmotic membrane bioreactor for wastewater treatment', *Desalination*, vol. 332, no. 1, pp. 91-9.

Qiu, M. & He, C. 2018, 'Novel zwitterion-silver nanocomposite modified thin-film composite forward osmosis membrane with simultaneous improved water flux and biofouling resistance property', *Applied Surface Science*, vol. 455, pp. 492-501.

Rastgar, M., Bozorg, A., Shakeri, A. & Sadrzadeh, M. 2019, 'Substantially improved antifouling properties in electro-oxidative graphene laminate forward osmosis membrane', *Chemical Engineering Research and Design*, vol. 141, pp. 413-24.

Rautenbach, R. & Mellis, R. 1994, 'Waste water treatment by a combination of bioreactor and nanofiltration', *Desalination*, vol. 95, no. 2, pp. 171-88.

Regula, C., Carretier, E., Wyart, Y., Gésan-Guiziou, G., Vincent, A., Boudot, D. & Moulin, P. 2014, 'Chemical cleaning/disinfection and ageing of organic UF membranes: A review', *Water Research*, vol. 56, pp. 325-65.

Ren, J. & McCutcheon, J.R. 2014, 'A new commercial thin film composite membrane for forward osmosis', *Desalination*, vol. 343, pp. 187-93.

Renou, S., Givaudan, J., Poulain, S., Dirassouyan, F. & Moulin, P. 2008a, 'Landfill leachate treatment: Review and opportunity', *Journal of hazardous materials*, vol. 150, no. 3, pp. 468-93.

Renou, S., Givaudan, J.G., Poulain, S., Dirassouyan, F. & Moulin, P. 2008b, 'Landfill leachate treatment: Review and opportunity', *Journal of Hazardous Materials*, vol. 150, no. 3, pp. 468-93.

Reshadi, M.A.M., Bazargan, A. & McKay, G. 2020, 'A review of the application of adsorbents for landfill leachate treatment: Focus on magnetic adsorption', *Science of The Total Environment*, vol. 731, p. 138863.

Roorda, J.H. 2004, 'Filtration characteristics in dead-end ultrafiltration of wwtp-effluent', TU Delft, Delft University of Technology.

Rose, J., Cho, Y. & Ditri, J. 1992, 'Review of Progress in Quantitative Nondestructive Evaluation, eds. DO Thompson and DE Chimenti', Plenum Press, New York.

Sadri, F., Ramazani, A., Massoudi, A., Khoobi, M., Tarasi, R., Shafiee, A., Azizkhani, V., Dolatyari, L. & Joo, S.W. 2014, 'Green oxidation of alcohols by using hydrogen peroxide in water in the presence of magnetic Fe3O4 nanoparticles as recoverable catalyst', *Green Chemistry Letters and Reviews*, vol. 7, no. 3, pp. 257-64.

Salgot, M. & Folch, M. 2018, 'Wastewater treatment and water reuse', *Current Opinion in Environmental Science & Health*, vol. 2, pp. 64-74.

Sanderson, R., Li, J., Koen, L.J. & Lorenzen, L. 2002, 'Ultrasonic time-domain reflectometry as a non-destructive instrumental visualization technique to monitor inorganic fouling and cleaning on reverse osmosis membranes', *Journal of Membrane Science*, vol. 207, no. 1, pp. 105-17.

Schmitt, J. & Flemming, H.-C. 1998, 'FTIR-spectroscopy in microbial and material analysis', *International Biodeterioration & Biodegradation*, vol. 41, no. 1, pp. 1-11.

Schwarzbauer, J., Heim, S., Brinker, S. & Littke, R. 2002, 'Occurrence and alteration of organic contaminants in seepage and leakage water from a waste deposit landfill', *Water Research*, vol. 36, no. 9, pp. 2275-87.

Setiawan, L., Wang, R., Li, K. & Fane, A.G. 2011, 'Fabrication of novel poly(amide–imide) forward osmosis hollow fiber membranes with a positively charged nanofiltration-like selective layer', *Journal of Membrane Science*, vol. 369, no. 1, pp. 196-205.

Shakeri, A., Salehi, H., Ghorbani, F., Amini, M. & Naslhajian, H. 2019, 'Polyoxometalate based thin film nanocomposite forward osmosis membrane: Superhydrophilic, anti-fouling, and high water permeable', *Journal of Colloid and Interface Science*, vol. 536, pp. 328-38.

Shakeri, A., Salehi, H. & Rastgar, M. 2017, 'Chitosan-based thin active layer membrane for forward osmosis desalination', *Carbohydrate Polymers*, vol. 174, pp. 658-68.

Shannon, M.A., Bohn, P.W., Elimelech, M., Georgiadis, J.G., Mariñas, B.J. & Mayes, A.M. 2008, 'Science and technology for water purification in the coming decades', *Nature*, vol. 452, p. 301.

She, Q., Hou, D., Liu, J., Tan, K.H. & Tang, C.Y. 2013, 'Effect of feed spacer induced membrane deformation on the performance of pressure retarded osmosis (PRO): Implications for PRO process operation', *Journal of Membrane Science*, vol. 445, pp. 170-82.

She, Q., Jin, X., Li, Q. & Tang, C.Y. 2012, 'Relating reverse and forward solute diffusion to membrane fouling in osmotically driven membrane processes', *Water Research*, vol. 46, no. 7, pp. 2478-86.

She, Q., Jin, X. & Tang, C.Y. 2012, 'Osmotic power production from salinity gradient resource by pressure retarded osmosis: Effects of operating conditions and reverse solute diffusion', *Journal of Membrane Science*, vol. 401-402, pp. 262-73.

She, Q., Wang, R., Fane, A.G. & Tang, C.Y. 2016, 'Membrane fouling in osmotically driven membrane processes: A review', *Journal of Membrane Science*, vol. 499, pp. 201-33.

Shon, H.K., Vigneswaran, S., Kim, I.S., Cho, J. & Ngo, H.H. 2006, 'Fouling of ultrafiltration membrane by effluent organic matter: A detailed characterization using different organic fractions in wastewater', *Journal of Membrane Science*, vol. 278, no. 1, pp. 232-8.

Siddiqui, F.A., She, Q., Fane, A.G. & Field, R.W. 2018, 'Exploring the differences between forward osmosis and reverse osmosis fouling', *Journal of Membrane Science*, vol. 565, pp. 241-53.

Silva, L.F., Michel, R.C. & Borges, C.P. 2012, vol. 3.

Sim, L., Wang, Z., Gu, J., Coster, H. & Fane, A. 2013, 'Detection of reverse osmosis membrane fouling with silica, bovine serum albumin and their mixture using in-situ electrical impedance spectroscopy', *Journal of membrane science*, vol. 443, pp. 45-53.

Sim, L.N., Chong, T.H., Taheri, A.H., Sim, S.T.V., Lai, L., Krantz, W.B. & Fane, A.G. 2018, 'A review of fouling indices and monitoring techniques for reverse osmosis', *Desalination*, vol. 434, pp. 169-88.

Sim, S.T.V., Suwarno, S.R., Chong, T.H., Krantz, W.B. & Fane, A.G. 2013, 'Monitoring membrane biofouling via ultrasonic time-domain reflectometry enhanced by silica dosing', *Journal of Membrane Science*, vol. 428, pp. 24-37.

Simon, A., McDonald, J.A., Khan, S.J., Price, W.E. & Nghiem, L.D. 2013, 'Effects of caustic cleaning on pore size of nanofiltration membranes and their rejection of trace organic chemicals', *Journal of Membrane Science*, vol. 447, pp. 153-62.

Simon, A., Price, W.E. & Nghiem, L.D. 2012, 'Effects of chemical cleaning on the nanofiltration of pharmaceutically active compounds (PhACs)', *Separation and Purification Technology*, vol. 88, pp. 208-15.

Singh, G. & Song, L. 2007, 'Experimental correlations of pH and ionic strength effects on the colloidal fouling potential of silica nanoparticles in crossflow ultrafiltration', *Journal of Membrane Science*, vol. 303, no. 1, pp. 112-8.

Singh, N., Petrinic, I., Hélix-Nielsen, C., Basu, S. & Balakrishnan, M. 2018, 'Concentrating molasses distillery wastewater using biomimetic forward osmosis (FO) membranes', *Water Research*, vol. 130, pp. 271-80.

Singh, R. 2006, *Hybrid Membrane Systems for Water Purification: Technology, Systems Design and Operations*, Elsevier.

Slack, R., Gronow, J. & Voulvoulis, N. 2004, 'Hazardous components of household waste', *Critical reviews in environmental science and technology*, vol. 34, no. 5, pp. 419-45.

Song, X., Liu, Z. & Sun, D.D. 2011, 'Nano Gives the Answer: Breaking the Bottleneck of Internal Concentration Polarization with a Nanofiber Composite Forward Osmosis Membrane for a High Water Production Rate', *Advanced Materials*, vol. 23, no. 29, pp. 3256-60.

Straub, A.P., Deshmukh, A. & Elimelech, M. 2016, 'Pressure-retarded osmosis for power generation from salinity gradients: is it viable?', *Energy & Environmental Science*, vol. 9, no. 1, pp. 31-48.

Suarez, S., Lema, J.M. & Omil, F. 2009, 'Pre-treatment of hospital wastewater by coagulation–flocculation and flotation', *Bioresource Technology*, vol. 100, no. 7, pp. 2138-46.

Sun, Y., Tian, J., Song, L., Gao, S., Shi, W. & Cui, F. 2018, 'Dynamic changes of the fouling layer in forward osmosis based membrane processes for municipal wastewater treatment', *Journal of Membrane Science*, vol. 549, pp. 523-32.

Sun, Y., Tian, J., Zhao, Z., Shi, W., Liu, D. & Cui, F. 2016, 'Membrane fouling of forward osmosis (FO) membrane for municipal wastewater treatment: A comparison between direct FO and OMBR', *Water Research*, vol. 104, pp. 330-9.

Sutzkover, I., Hasson, D. & Semiat, R. 2000a, 'Simple technique for measuring the concentration polarization level in a reverse osmosis system', *Desalination*, vol. 131, no. 1-3, pp. 117-27.

Sutzkover, I., Hasson, D. & Semiat, R. 2000b, 'Simple technique for measuring the concentration polarization level in a reverse osmosis system', *Desalination*, vol. 131, no. 1, pp. 117-27.

T. Brunelle, M. 1980, 'Colloidal fouling of reverse osmosis membranes', *Desalination*, vol. 32, pp. 127-35.

Taheri, A.H., Sim, L.N., Chong, T.H., Krantz, W.B. & Fane, A.G. 2015, 'Prediction of reverse osmosis fouling using the feed fouling monitor and salt tracer response technique', *Journal of Membrane Science*, vol. 475, pp. 433-44.

Taheri, A.H., Sim, S.T.V., Sim, L.N., Chong, T.H., Krantz, W.B. & Fane, A.G. 2013, 'Development of a new technique to predict reverse osmosis fouling', *Journal of Membrane Science*, vol. 448, pp. 12-22.

Takahashi, T., Yasukawa, M. & Matsuyama, H. 2016, 'Highly condensed polyvinyl chloride latex production by forward osmosis: Performance and characteristics', *Journal of Membrane Science*, vol. 514, pp. 547-55.

Tan, C.H. & Ng, H.Y. 2008, 'Modified models to predict flux behavior in forward osmosis in consideration of external and internal concentration polarizations', *Journal of Membrane Science*, vol. 324, no. 1, pp. 209-19.

Tan, C.H. & Ng, H.Y. 2013, 'Revised external and internal concentration polarization models to improve flux prediction in forward osmosis process', *Desalination*, vol. 309, pp. 125-40.

Tang, C.Y., She, Q., Lay, W.C.L., Wang, R. & Fane, A.G. 2010a, 'Coupled effects of internal concentration polarization and fouling on flux behavior of forward osmosis membranes during humic acid filtration', *Journal of Membrane Science*, vol. 354, no. 1, pp. 123-33.

Tang, C.Y., She, Q., Lay, W.C.L., Wang, R. & Fane, A.G. 2010b, 'Coupled effects of internal concentration polarization and fouling on flux behavior of forward osmosis membranes during humic acid filtration', *Journal of Membrane Science*, vol. 354, no. 1-2, pp. 123-33.

Tansel, B., Sager, J., Rector, T., Garland, J., Strayer, R.F., Levine, L., Roberts, M., Hummerick, M. & Bauer, J. 2006, 'Significance of hydrated radius and hydration shells on ionic permeability during nanofiltration in dead end and cross flow modes', *Separation and Purification Technology*, vol. 51, no. 1, pp. 40-7.

Thabit, M.S., Hawari, A.H., Ammar, M.H., Zaidi, S., Zaragoza, G. & Altaee, A. 2019, 'Evaluation of forward osmosis as a pretreatment process for multi stage flash seawater desalination', *Desalination*, vol. 461, pp. 22-9.

Thiruvenkatachari, R., Francis, M., Cunnington, M. & Su, S. 2016, 'Application of integrated forward and reverse osmosis for coal mine wastewater desalination', *Separation and Purification Technology*, vol. 163, pp. 181-8.

Thorsen, T. 2004, 'Concentration polarisation by natural organic matter (NOM) in NF and UF', *Journal of Membrane Science*, vol. 233, no. 1-2, pp. 79-91.

Tiraferri, A., Yip, N.Y., Phillip, W.A., Schiffman, J.D. & Elimelech, M. 2011, 'Relating performance of thin-film composite forward osmosis membranes to support layer formation and structure', *Journal of Membrane Science*, vol. 367, no. 1, pp. 340-52.

Tow, E.W., Rencken, M.M. & Lienhard, J.H. 2016, 'In situ visualization of organic fouling and cleaning mechanisms in reverse osmosis and forward osmosis', *Desalination*, vol. 399, pp. 138-47.

Trebouet, D., Schlumpf, J.P., Jaouen, P. & Quemeneur, F. 2001, 'Stabilized landfill leachate treatment by combined physicochemical–nanofiltration processes', *Water Research*, vol. 35, no. 12, pp. 2935-42.

Treybal, R.E. 1980, 'Mass transfer operations', *New York*, vol. 466.

Valladares Linares, R., Bucs, S.S., Li, Z., AbuGhdeeb, M., Amy, G. & Vrouwenvelder, J.S. 2014, 'Impact of spacer thickness on biofouling in forward osmosis', *Water Research*, vol. 57, pp. 223-33.

Valladares Linares, R., Li, Z., Abu-Ghdaib, M., Wei, C.-H., Amy, G. & Vrouwenvelder, J.S. 2013, 'Water harvesting from municipal wastewater via osmotic gradient: An evaluation of process performance', *Journal of Membrane Science*, vol. 447, pp. 50-6.

Valladares Linares, R., Li, Z., Sarp, S., Bucs, S.S., Amy, G. & Vrouwenvelder, J.S. 2014, 'Forward osmosis niches in seawater desalination and wastewater reuse', *Water Res*, vol. 66, pp. 122-39.

Valladares Linares, R., Li, Z., Yangali-Quintanilla, V., Li, Q. & Amy, G. 2013, 'Cleaning protocol for a FO membrane fouled in wastewater reuse', *Desalination and Water Treatment*, vol. 51, no. 25-27, pp. 4821-4.

Valladares Linares, R., Yangali-Quintanilla, V., Li, Z. & Amy, G. 2012, 'NOM and TEP fouling of a forward osmosis (FO) membrane: Foulant identification and cleaning', *Journal of Membrane Science*, vol. 421-422, pp. 217-24.

Van der Bruggen, B., Mänttäri, M. & Nyström, M. 2008, 'Drawbacks of applying nanofiltration and how to avoid them: A review', *Separation and Purification Technology*, vol. 63, no. 2, pp. 251-63.

Vasudevan, S., Sozhan, G., Ravichandran, S., Jayaraj, J., Lakshmi, J. & Sheela, M. 2008, 'Studies on the removal of phosphate from drinking water by electrocoagulation process', *Industrial & Engineering Chemistry Research*, vol. 47, no. 6, pp. 2018-23.

Volpin, F., Fons, E., Chekli, L., Kim, J.E., Jang, A. & Shon, H.K. 2018, 'Hybrid forward osmosis-reverse osmosis for wastewater reuse and seawater desalination: Understanding the optimal feed solution to minimise fouling', *Process Safety and Environmental Protection*, vol. 117, pp. 523-32.

Vrouwenvelder, J.S., Manolarakis, S.A., van der Hoek, J.P., van Paassen, J.A.M., van der Meer, W.G.J., van Agtmaal, J.M.C., Prummel, H.D.M., Kruithof, J.C. & van Loosdrecht, M.C.M. 2008, 'Quantitative biofouling diagnosis in full scale nanofiltration and reverse osmosis installations', *Water Research*, vol. 42, no. 19, pp. 4856-68.

Vu, M.T., Ansari, A.J., Hai, F.I. & Nghiem, L.D. 2018, 'Performance of a seawater-driven forward osmosis process for pre-concentrating digested sludge centrate: Organic enrichment and membrane fouling', *Environmental Science: Water Research & Technology*, vol. 4, no. 7, pp. 1047-56.

Wadekar, S.S., Wang, Y., Lokare, O.R. & Vidic, R.D. 2019, 'Influence of Chemical Cleaning on Physicochemical Characteristics and Ion Rejection by Thin Film Composite Nanofiltration Membranes', *Environmental Science & Technology*, vol. 53, no. 17, pp. 10166-76.

Wait, A.S. 2012, 'Towards potable reuse: assessment of the first pilot-scale hybrid osmotic membrane bioreactor and denitrification system', Colorado School of Mines. Arthur Lakes Library.

Wang, C., Li, Y. & Wang, Y. 2018, 'Treatment of greywater by forward osmosis technology: role of the operating temperature', *Environmental Technology*, pp. 1-10.

Wang, F. & Tarabara, V.V. 2008, 'Pore blocking mechanisms during early stages of membrane fouling by colloids', *Journal of Colloid and Interface Science*, vol. 328, no. 2, pp. 464-9.

Wang, J., Dlamini, D.S., Mishra, A.K., Pendergast, M.T.M., Wong, M.C.Y., Mamba, B.B., Freger, V., Verliefde, A.R.D. & Hoek, E.M.V. 2014, 'A critical review of transport through osmotic membranes', *Journal of Membrane Science*, vol. 454, pp. 516-37.

Wang, K.Y., Ong, R.C. & Chung, T.-S. 2010, 'Double-Skinned Forward Osmosis Membranes for Reducing Internal Concentration Polarization within the Porous Sublayer', *Industrial & Engineering Chemistry Research*, vol. 49, no. 10, pp. 4824-31.

Wang, Q., Zhou, Z., Li, J., Tang, Q. & Hu, Y. 2019, 'Modeling and measurement of temperature and draw solution concentration induced water flux increment efficiencies in the forward osmosis membrane process', *Desalination*, vol. 452, pp. 75-86.

Wang, X.-M. & Li, X.-Y. 2008, 'Accumulation of biopolymer clusters in a submerged membrane bioreactor and its effect on membrane fouling', *Water Research*, vol. 42, no. 4, pp. 855-62.

Wang, X., Chang, V.W.C. & Tang, C.Y. 2016, 'Osmotic membrane bioreactor (OMBR) technology for wastewater treatment and reclamation: Advances, challenges, and prospects for the future', *Journal of Membrane Science*, vol. 504, pp. 113-32.

Wang, X., Hu, T., Wang, Z., Li, X. & Ren, Y. 2017, 'Permeability recovery of fouled forward osmosis membranes by chemical cleaning during a long-term operation of anaerobic osmotic membrane bioreactors treating low-strength wastewater', *Water Research*, vol. 123, pp. 505-12.

Wang, X., Zhao, Y., Yuan, B., Wang, Z., Li, X. & Ren, Y. 2016, 'Comparison of biofouling mechanisms between cellulose triacetate (CTA) and thin-film composite (TFC) polyamide forward osmosis membranes in osmotic membrane bioreactors', *Bioresource Technology*, vol. 202, pp. 50-8.

Wang, Y.-N., Goh, K., Li, X., Setiawan, L. & Wang, R. 2018, 'Membranes and processes for forward osmosis-based desalination: Recent advances and future prospects', *Desalination*, vol. 434, pp. 81-99.

Wang, Y., Duan, W., Wang, W., Di, W., Liu, Y., Liu, Y., Li, Z., Hu, H., Lin, H., Cui, C., Li, D., Dong, H. & Li, C. 2016, 'scAAV9-VEGF prolongs the survival of transgenic ALS mice by promoting activation of M2 microglia and the PI3K/Akt pathway', *Brain Research*, vol. 1648, pp. 1-10.

Wang, Y., Wicaksana, F., Tang, C.Y. & Fane, A.G. 2010, 'Direct Microscopic Observation of Forward Osmosis Membrane Fouling', *Environmental Science & Technology*, vol. 44, no. 18, pp. 7102-9.

Wang, Y., Zhang, M., Liu, Y., Xiao, Q. & Xu, S. 2016, 'Quantitative evaluation of concentration polarization under different operating conditions for forward osmosis process', *Desalination*, vol. 398, pp. 106-13.

Wang, Z., Ding, J., Xie, P., Chen, Y., Wan, Y. & Wang, S. 2018, 'Formation of halogenated by-products during chemical cleaning of humic acid-fouled UF membrane by sodium hypochlorite solution', *Chemical Engineering Journal*, vol. 332, pp. 76-84.

Wang, Z., Tang, J., Zhu, C., Dong, Y., Wang, Q. & Wu, Z. 2015, 'Chemical cleaning protocols for thin film composite (TFC) polyamide forward osmosis membranes used for municipal wastewater treatment', *Journal of Membrane Science*, vol. 475, pp. 184-92.

Wang, Z., Zheng, J., Tang, J., Wang, X. & Wu, Z. 2016, 'A pilot-scale forward osmosis membrane system for concentrating low-strength municipal wastewater: performance and implications', *Scientific Reports*, vol. 6, p. 21653.

Weerasekara, N.A., Choo, K.-H. & Lee, C.-H. 2014, 'Hybridization of physical cleaning and quorum quenching to minimize membrane biofouling and energy consumption in a membrane bioreactor', *Water Research*, vol. 67, pp. 1-10.

Wei, J., Qiu, C., Tang, C.Y., Wang, R. & Fane, A.G. 2011, 'Synthesis and characterization of flat-sheet thin film composite forward osmosis membranes', *Journal of Membrane Science*, vol. 372, no. 1, pp. 292-302.

Wei, X., Wang, Z., Fan, F., Wang, J. & Wang, S. 2010, 'Advanced treatment of a complex pharmaceutical wastewater by nanofiltration: Membrane foulant identification and cleaning', *Desalination*, vol. 251, no. 1, pp. 167-75.

Widjojo, N., Chung, T.-S., Weber, M., Maletzko, C. & Warzelhan, V. 2011, 'The role of sulphonated polymer and macrovoid-free structure in the support layer for thin-film composite (TFC) forward osmosis (FO) membranes', *Journal of Membrane Science*, vol. 383, no. 1, pp. 214-23.

Wong, M.C., Martinez, K., Ramon, G.Z. & Hoek, E.M. 2012a, 'Impacts of operating conditions and solution chemistry on osmotic membrane structure and performance', *Desalination*, vol. 287, pp. 340-9.

Wong, M.C.Y., Martinez, K., Ramon, G.Z. & Hoek, E.M.V. 2012b, 'Impacts of operating conditions and solution chemistry on osmotic membrane structure and performance', *Desalination*, vol. 287, pp. 340-9.

Wu, C.-Y., Mouri, H., Chen, S.-S., Zhang, D.-Z., Koga, M. & Kobayashi, J. 2016, 'Removal of trace-amount mercury from wastewater by forward osmosis', *Journal of Water Process Engineering*, vol. 14, pp. 108-16.

Wu, Z., Zou, S., Zhang, B., Wang, L. & He, Z. 2018, 'Forward osmosis promoted in-situ formation of struvite with simultaneous water recovery from digested swine wastewater', *Chemical Engineering Journal*, vol. 342, pp. 274-80.

WWF 2018, *Water Scarcity*, viewed 13/09 2018, <https://www.worldwildlife.org/threats/water-scarcity>.

Xie, M., Bar-Zeev, E., Hashmi, S.M., Nghiem, L.D. & Elimelech, M. 2015, 'Role of Reverse Divalent Cation Diffusion in Forward Osmosis Biofouling', *Environmental Science & Technology*, vol. 49, no. 22, pp. 13222-9.

Xie, M. & Gray, S.R. 2016, 'Gypsum scaling in forward osmosis: Role of membrane surface chemistry', *Journal of Membrane Science*, vol. 513, pp. 250-9.

Xie, M. & Gray, S.R. 2017, 'Silica scaling in forward osmosis: From solution to membrane interface', *Water Research*, vol. 108, pp. 232-9.

Xie, M., Nghiem, L.D., Price, W.E. & Elimelech, M. 2013a, 'A Forward Osmosis–Membrane Distillation Hybrid Process for Direct Sewer Mining: System Performance and Limitations', *Environmental Science & Technology*, vol. 47, no. 23, pp. 13486-93.

Xie, M., Nghiem, L.D., Price, W.E. & Elimelech, M. 2013b, 'Impact of humic acid fouling on membrane performance and transport of pharmaceutically active compounds in forward osmosis', *Water Research*, vol. 47, no. 13, pp. 4567-75.

Xie, M., Price, W.E., Nghiem, L.D. & Elimelech, M. 2013, 'Effects of feed and draw solution temperature and transmembrane temperature difference on the rejection of trace organic contaminants by forward osmosis', *Journal of Membrane Science*, vol. 438, pp. 57-64.

Xie, M., Tang, C.Y. & Gray, S.R. 2016, 'Spacer-induced forward osmosis membrane integrity loss during gypsum scaling', *Desalination*, vol. 392, pp. 85-90.

Xie, P., de Lannoy, C.-F., Ma, J. & Wiesner, M.R. 2015, 'Chlorination of polyvinyl pyrrolidone–polysulfone membranes: Organic compound release, byproduct formation, and changes in membrane properties', *Journal of Membrane Science*, vol. 489, pp. 28-35.

Xu, W. & Ge, Q. 2018, 'Novel functionalized forward osmosis (FO) membranes for FO desalination: Improved process performance and fouling resistance', *Journal of Membrane Science*, vol. 555, pp. 507-16.

Yadav, S., Ibrar, I., Altaee, A., Déon, S. & Zhou, J. 2020, 'Preparation of novel high permeability and antifouling polysulfone-vanillin membrane', *Desalination*, vol. 496, p. 114759.

Yadav, S., Ibrar, I., Altaee, A., Samal, A.K., Ghobadi, R. & Zhou, J. 2020a, 'Feasibility of brackish water and landfill leachate treatment by GO/MoS2-PVA composite membranes', *Science of The Total Environment*, p. 141088.

Yadav, S., Ibrar, I., Altaee, A., Samal, A.K., Ghobadi, R. & Zhou, J. 2020b, 'Feasibility of brackish water and landfill leachate treatment by GO/MoS2-PVA composite membranes', *Science of The Total Environment*, vol. 745, p. 141088.

Yadav, S., Ibrar, I., Bakly, S., Khanafer, D., Altaee, A., Padmanaban, V., Samal, A.K. & Hawari, A.H. 2020, 'Organic Fouling in Forward Osmosis: A Comprehensive Review', *Water*, vol. 12, no. 5, p. 1505.

Yadav, S., Saleem, H., Ibrar, I., Naji, O., Hawari, A.A., Alanezi, A.A., Zaidi, S.J., Altaee, A. & Zhou, J. 2020, 'Recent developments in forward osmosis membranes using carbon-based nanomaterials', *Desalination*, vol. 482, p. 114375.

Yang, X., Fridjonsson, E.O., Johns, M.L., Wang, R. & Fane, A.G. 2014, 'A non-invasive study of flow dynamics in membrane distillation hollow fiber modules using low-field nuclear magnetic resonance imaging (MRI)', *Journal of Membrane Science*, vol. 451, pp. 46-54.

Yangali-Quintanilla, V., Li, Z., Valladares, R., Li, Q. & Amy, G. 2011, 'Indirect desalination of Red Sea water with forward osmosis and low pressure reverse osmosis for water reuse', *Desalination*, vol. 280, no. 1, pp. 160-6.

Yaroshchuk, A., Bruening, M.L. & Licón Bernal, E.E. 2013, 'Solution-Diffusion–Electro-Migration model and its uses for analysis of nanofiltration, pressure-retarded osmosis and forward osmosis in multi-ionic solutions', *Journal of Membrane Science*, vol. 447, pp. 463-76.

Yip, N.Y. & Elimelech, M. 2011, 'Performance limiting effects in power generation from salinity gradients by pressure retarded osmosis', *Environmental science & technology*, vol. 45, no. 23, pp. 10273-82.

Yip, N.Y., Tiraferri, A., Phillip, W.A., Schiffman, J.D. & Elimelech, M. 2010, 'High Performance Thin-Film Composite Forward Osmosis Membrane', *Environmental Science & Technology*, vol. 44, no. 10, pp. 3812-8.

Yip, N.Y., Tiraferri, A., Phillip, W.A., Schiffman, J.D., Hoover, L.A., Kim, Y.C. & Elimelech, M. 2011, 'Thin-Film Composite Pressure Retarded Osmosis Membranes for Sustainable Power

Generation from Salinity Gradients', *Environmental Science & Technology*, vol. 45, no. 10, pp. 4360-9.

Yoon, H., Baek, Y., Yu, J. & Yoon, J. 2013, 'Biofouling occurrence process and its control in the forward osmosis', *Desalination*, vol. 325, pp. 30-6.

You, S., Lu, J., Tang, C.Y. & Wang, X. 2017, 'Rejection of heavy metals in acidic wastewater by a novel thin-film inorganic forward osmosis membrane', *Chemical Engineering Journal*, vol. 320, pp. 532-8.

Yu, Y., Seo, S., Kim, I.-C. & Lee, S. 2011, 'Nanoporous polyethersulfone (PES) membrane with enhanced flux applied in forward osmosis process', *Journal of Membrane Science*, vol. 375, no. 1, pp. 63-8.

Yuan, B., Wang, X., Tang, C., Li, X. & Yu, G. 2015, 'In situ observation of the growth of biofouling layer in osmotic membrane bioreactors by multiple fluorescence labeling and confocal laser scanning microscopy', *Water Research*, vol. 75, pp. 188-200.

Yuan, W. & Zydney, A.L. 1999, 'Humic acid fouling during microfiltration', *Journal of Membrane Science*, vol. 157, no. 1, pp. 1-12.

Zhang, H., Cheng, S. & Yang, F. 2014, 'Use of a spacer to mitigate concentration polarization during forward osmosis process', *Desalination*, vol. 347, pp. 112-9.

Zhang, H., Jiang, W. & Cui, H. 2017, 'Performance of anaerobic forward osmosis membrane bioreactor coupled with microbial electrolysis cell (AnOMEBR) for energy recovery and membrane fouling alleviation', *Chemical Engineering Journal*, vol. 321, pp. 375-83.

Zhang, H., Li, J., Cui, H., Li, H. & Yang, F. 2015, 'Forward osmosis using electric-responsive polymer hydrogels as draw agents: Influence of freezing–thawing cycles, voltage, feed solutions on process performance', *Chemical Engineering Journal*, vol. 259, pp. 814-9.

Zhang, J., Loong, W.L.C., Chou, S., Tang, C., Wang, R. & Fane, A.G. 2012, 'Membrane biofouling and scaling in forward osmosis membrane bioreactor', *Journal of Membrane Science*, vol. 403-404, pp. 8-14.

Zhang, M., Shan, J. & Tang, C.Y. 2016, 'Gypsum scaling during forward osmosis process—a direct microscopic observation study', *Desalination and Water Treatment*, vol. 57, no. 8, pp. 3317-27.

Zhang, M., She, Q., Yan, X. & Tang, C.Y. 2017, 'Effect of reverse solute diffusion on scaling in forward osmosis: A new control strategy by tailoring draw solution chemistry', *Desalination*, vol. 401, pp. 230-7.

Zhang, S., Wang, K.Y., Chung, T.-S., Chen, H., Jean, Y.C. & Amy, G. 2010, 'Well-constructed cellulose acetate membranes for forward osmosis: Minimized internal concentration polarization with an ultra-thin selective layer', *Journal of Membrane Science*, vol. 360, no. 1, pp. 522-35.

Zhang, W., Ding, L., Jaffrin, M.Y. & Tang, B. 2017, 'Membrane cleaning assisted by high shear stress for restoring ultrafiltration membranes fouled by dairy wastewater', *Chemical Engineering Journal*, vol. 325, pp. 457-65.

Zhang, Y., Pinoy, L., Meesschaert, B. & Van der Bruggen, B. 2013, 'A Natural Driven Membrane Process for Brackish and Wastewater Treatment: Photovoltaic Powered ED and FO Hybrid System', *Environmental Science & Technology*, vol. 47, no. 18, pp. 10548-55.

Zhao, P., Gao, B., Yue, Q., Liu, P. & Shon, H.K. 2016a, 'Fatty acid fouling of forward osmosis membrane: Effects of pH, calcium, membrane orientation, initial permeate flux and foulant composition', *Journal of Environmental Sciences*, vol. 46, pp. 55-62.

Zhao, P., Gao, B., Yue, Q., Liu, S. & Shon, H.K. 2016b, 'The performance of forward osmosis in treating high-salinity wastewater containing heavy metal Ni2+', *Chemical Engineering Journal*, vol. 288, pp. 569-76.

Zhao, S., Zou, L. & Mulcahy, D. 2011, 'Effects of membrane orientation on process performance in forward osmosis applications', *Journal of Membrane Science*, vol. 382, no. 1, pp. 308-15.

Zhao, S., Zou, L., Tang, C.Y. & Mulcahy, D. 2012, 'Recent developments in forward osmosis: Opportunities and challenges', *Journal of Membrane Science*, vol. 396, pp. 1-21.

Zheng, Y., Huang, M.-h., Chen, L., Zheng, W., Xie, P.-k. & Xu, Q. 2015, 'Comparison of tetracycline rejection in reclaimed water by three kinds of forward osmosis membranes', *Desalination*, vol. 359, pp. 113-22.

Zhou, Y., Huang, M., Deng, Q. & Cai, T. 2017, 'Combination and performance of forward osmosis and membrane distillation (FO-MD) for treatment of high salinity landfill leachate', *Desalination*, vol. 420, pp. 99-105.

Zhou, Z., Lee, J.Y. & Chung, T.-S. 2014, 'Thin film composite forward-osmosis membranes with enhanced internal osmotic pressure for internal concentration polarization reduction', *Chemical Engineering Journal*, vol. 249, pp. 236-45.

Zondervan, E. & Roffel, B. 2007, 'Evaluation of different cleaning agents used for cleaning ultra filtration membranes fouled by surface water', *Journal of Membrane Science*, vol. 304, no. 1, pp. 40-9.

Zou, S., Gu, Y., Xiao, D. & Tang, C.Y. 2011, 'The role of physical and chemical parameters on forward osmosis membrane fouling during algae separation', *Journal of Membrane Science*, vol. 366, no. 1, pp. 356-62.

Zou, S. & He, Z. 2016, 'Enhancing wastewater reuse by forward osmosis with self-diluted commercial fertilizers as draw solutes', *Water Res*, vol. 99, pp. 235-43.

Zou, S., Wang, Y.-N., Wicaksana, F., Aung, T., Wong, P.C.Y., Fane, A.G. & Tang, C.Y. 2013, 'Direct microscopic observation of forward osmosis membrane fouling by microalgae: Critical flux and the role of operational conditions', *Journal of Membrane Science*, vol. 436, pp. 174-85.

Zou, S., Yuan, H., Childress, A. & He, Z. 2016, 'Energy Consumption by Recirculation: A Missing Parameter When Evaluating Forward Osmosis', *Environmental Science & Technology*, vol. 50, no. 13, pp. 6827-9.

Zuo, H.-R., Fu, J.-B., Cao, G.-P., Hu, N., Lu, H., Liu, H.-Q., Chen, P.-P. & Yu, J. 2018, 'The effects of surface-charged submicron polystyrene particles on the structure and performance of PSF forward osmosis membrane', *Applied Surface Science*, vol. 436, pp. 1181-92.